

Supporting information

The “Cesium Effect” Magnified: Exceptional Chemoselectivity in Cesium Ion Mediated Nucleophilic Reactions

Soumen Biswas, William B. Hughes, Luca De Angelis, Graham C. Haug, Ramon Trevino, Seth O. Fremin, Hadi D. Arman, Oleg V. Larionov*, and Michael P. Doyle*

Department of Chemistry, The University of Texas at San Antonio, San Antonio, Texas 78249, United States

*Email: oleg.larionov@utsa.edu, michael.doyle@utsa.edu

Table of Contents

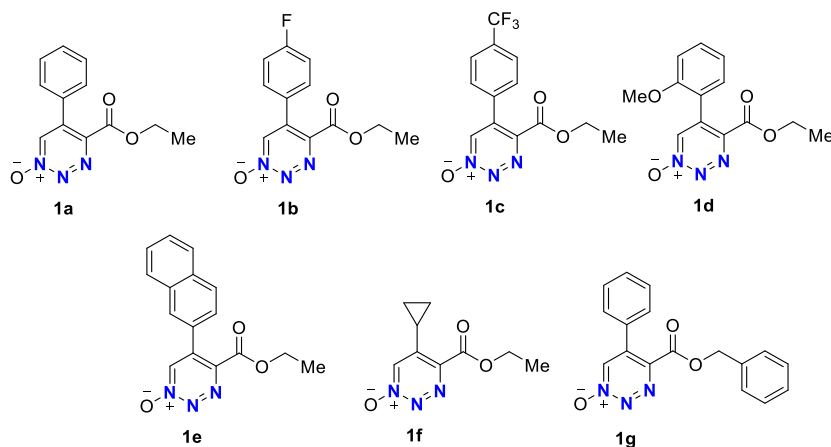
1.	General conditions	S2
2.	Optimization for the reaction conditions for the formation of pyridones	S3
3.	General procedure for the synthesis of 1,2,3-triazine 1-oxide compounds	S4
4.	General procedures for synthesis of pyridone and pyridylpyridone compounds	S5
5.	Analytical and spectral characterization data for products	S6
6.	Preparative scale reaction	S15
7.	Crystallographic data	S15
8.	Computational data	S18
9.	NMR spectra	S85
10.	References	S115

1. General conditions

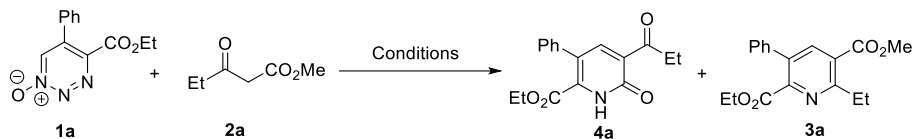
All reactions, unless noted, were performed in oven-dried (150 °C) glassware with magnetic stirring under an atmosphere of air. Analytical thin layer chromatography (TLC) was carried out using EM Science silica gel 60 F254 plates; visualization was accomplished with UV light (254 nm). Column chromatography was performed on CombiFlash® Rf200 and Rf+ purification systems using normal phase disposable columns. NMR spectra were recorded on a Bruker spectrometer (500 MHz and 300 MHz) and calibrated using the resonance signal of the residual undeuterated solvent for ^1H -NMR [$\delta_{\text{H}} = 7.26$ ppm (CDCl_3)] and deuterated solvent for ^{13}C -NMR [$\delta_{\text{C}} = 77.16$ (CDCl_3)] as an internal reference at 298 K. Spectra were reported as follows: chemical shift (δ ppm), multiplicity (Mi), coupling constants (Hz), integration and assignment. The peak information was described as: br = broad, s = singlet, d = doublet, t = triplet, q = quartet, dd = doublet of doublet, m = multiplet, and comp = composite of magnetically non-equivalent protons. ^{13}C -NMR spectra were collected on Bruker instruments (126 MHz and 75 MHz) with complete proton decoupling. High-resolution mass spectra (HRMS) were performed on a Bruker MicroTOFESI mass spectrometer with an ESI resource using CsI or LTQ ESI positive ion calibration solution as the standard. Tetrahydrofuran, dichloromethane, chloroform were purified using a JC-Meyer solvent purification system.

Materials: All β -keto-esters, DBU (1,8-diazabicyclo[5.4.0]undec-7-ene), DABCO (1,4-diazabicyclo[2.2.2]octane), DMAP (4-dimethylaminopyridine), Et_3N (triethylamine), Cs_2CO_3 , CsOH , CsOAc , K_2CO_3 , and Na_2CO_3 were purchased from Sigma Aldrich, TCI, and Alfa Aesar, and they were used without further purification. 1,2,3-Triazine-1-oxides were prepared by the reported literature procedure.^{1,2}

1,2,3-Triazine 1-oxides used in the study



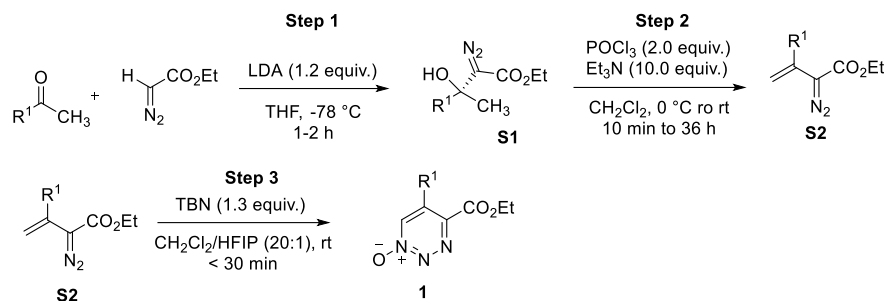
2. Table S1. Optimization for the reaction conditions for the formation of pyridone compounds



Entry	Conditions	Base	Yield of 4a (%) ^a	Yield of 3a (%) ^a
1	CHCl ₃ , 4 h, rt	Cs ₂ CO ₃	76	14
2	CHCl ₃ , 12 h, rt	K ₂ CO ₃	-	81
3	CHCl ₃ , 72 h, rt	Na ₂ CO ₃	-	42
4	CHCl ₃ , 72 h, 60 °C	Na ₂ CO ₃	-	64
9b	CHCl ₃ , 24 h, rt	Ag ₂ CO ₃	-	-
6	THF, 6 h, rt	Cs ₂ CO ₃	53	35
7	DCM, 6 h, rt	Cs ₂ CO ₃	70	20
8	ACN, 6 h, rt	Cs ₂ CO ₃	62	12
9 ^c	CHCl ₃ , 4 h, rt	Cs ₂ CO ₃	64	18
10 ^d	CHCl ₃ , 4 h, rt	Cs ₂ CO ₃	75	15
11 ^e	CHCl ₃ , 18-crown-6, 6 h, rt	Cs ₂ CO ₃	-	72
12	HFIP, rt, 24 h	Cs ₂ CO ₃	-	84
13	CHCl ₃ , 0 °C, 6 h	Cs ₂ CO ₃	64	18
14 ^f	CHCl ₃ , 60 °C, 2 h	Cs ₂ CO ₃	86	<5
15 ^g	CHCl ₃ , 60 °C, 1.5 h	Cs ₂ CO ₃	93 (91)	trace
16 ^h	CHCl ₃ , 6 h	CsF	NR	-
17 ⁱ	CHCl ₃ , 6 h	CsOAc	NR	-
18	CHCl ₃ , 1 h	CsOH	70	trace
19	CHCl ₃ , rt, 24 h	Et ₃ N	-	13
20	CHCl ₃ , rt, 24 h	DMAP	-	95
21	CHCl ₃ , rt, 24 h	DABCO	-	93
22	CHCl ₃ , rt, 10 min	DBU	-	97

Reaction conditions: 1 mL solution of triazine 1-oxide **1a** (0.1 mmol) was added to a stirred solution of ketoester **2a** (0.15 mmol) and base (0.2 mmol) over 30 minutes. ^aNMR yields. Isolated yield in parenthesis. ^b 92% of **1a** was detected. ^c0.5 equiv. of Cs₂CO₃. ^d 1.0 equiv. of Cs₂CO₃. ^e2.0 equiv. of 18-crown-6 was used. ^f triazine 1-oxide **1a** was added at rt and then temperature was increased to 60 °C. ^g triazine 1-oxide **1a** was added to a preheated solution of ketoester **2a** (0.15 mmol) and Cs₂CO₃ at 60 °C. ^h 94% of **1a** was detected. ⁱ93% of **1a** was detected.

3. General procedure for the synthesis of 1,2,3-triazine 1-oxide compounds 1a-1g



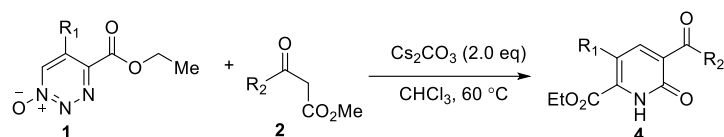
Step 1: Following the reported procedure.¹ To a solution of ketone (10.0 mmol, 1.00 equiv.) and ethyl diazoacetate (10.0 mmol, 1.00 equiv.) in 20 mL of dry THF at -78 °C, was slowly added a solution of freshly prepared LDA (12.0 mmol, 1.20 equiv. 1.0 M in THF) over 30 minutes using a syringe pump. The resulting solution was quenched with water after stirring at -78 °C for 1-2 h. The reaction solution was extracted with ethyl acetate (3 x 15 mL), and the combined organic layer was washed with brine and then dried over anhydrous MgSO₄. After the solvent was evaporated, the crude product was purified by flash chromatography (% hexanes in ethyl acetate = 2%-10%) to give the β -hydroxy diazo **S1** compounds in 45%-83% yield. These compounds are stable at 0 °C and could be stored for months.

Step 2: Following the reported procedure.¹ To a solution of the **S1** compound (1.0 mmol, 1.0 equiv.) and Et₃N (1.4 mL, 10 mmol, 10 equiv.) in 10 mL CH₂Cl₂ at 0 °C was slowly added a solution of POCl₃ (300 mg, 2.0 mmol, 2 equiv.) in 4 mL of CH₂Cl₂ over 5 min. The reaction solution was warmed to room temperature, and the progress of the reaction was followed by TLC until consumption of the β -hydroxy diazo compound was complete. The reaction solution was quenched with water and extracted with ethyl acetate (3 x 10 mL), and the combined organic layer was dried over anhydrous MgSO₄. After the solvent was evaporated, the crude product was purified by flash chromatography (% ethyl acetate in hexanes = 2%-5%) to give the vinyl diazo **S2** compound in 50%-90% yield. These compounds are not stable, slowly undergoing intramolecular cycloaddition to pyrazoles, and were used immediately following their preparation.

Step 3: Following the reported procedure,² ^tBuONO (1.3 mmol, 1.3 equiv.) was added to 10 mL solution containing 20:1 v/v DCM:HFIPA (HFIPA = hexafluoroisopropyl alcohol), and the vinyl diazo compound **S2** (1.0 mmol, 1.0 equiv., 0.10 M in DCM) was added dropwise to the solution over 5 minutes. The reaction solution was stirred at room temperature under air for 1 h. After the solvent was evaporated, the crude product was purified by flash chromatography (% ethyl acetate in hexanes = 20%-50%) to give the 1,2,3-triazine 1-oxide **1** in 80%-99% yields. These compounds are bench stable and could be stored for months.

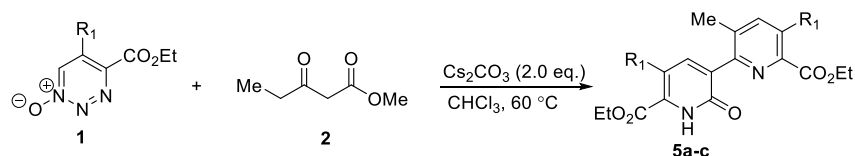
4. General procedures for synthesis of pyridone and pyridylpyridone compounds

Synthesis of pyridone compounds from 1,2,3-triazine 1-oxides and β -ketoesters.



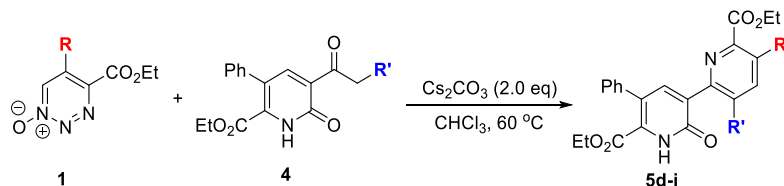
A chloroform solution (1.0 mL) of 1,2,3-triazine 1-oxide derivative **1** (0.1 mmol, 1 equiv.) was added dropwise over 30 minutes to a 1.0 mL solution of CHCl_3 containing β -keto ester **2** (0.15 mmol, 1.5 equiv.) and a Cs_2CO_3 (0.2 mmol, 65.2 mg) at 60°C . The reaction was continued for 30-90 minutes at same temperature. After the completion of the reaction (monitored by TLC), the reaction mixture was cooled to room temperature, then diluted with 5.0 mL of dichloromethane. The organic layer was washed with saturated ammonium chloride solution (5.0 mL) followed by water and brine solution, then dried over anhydrous MgSO_4 , filtered, and the solvent was evaporated under reduced pressure. The product mixture was purified by flash chromatography (ethyl acetate in hexanes = 20-60%) to give the pyridone compound **4** with yields of 80-94%.

Synthesis of symmetrical pyridylpyridones compounds from 1,2,3-triazine 1-oxides and β -ketoesters.



A chloroform solution (1.0 mL) of 1,2,3-triazine 1-oxide derivative **1** (0.1 mmol, 1 equiv.) was added dropwise over 30 minutes to a 0.5 mL solution of CHCl_3 containing β -keto ester **2** (0.05 mmol, 0.5 equiv.) and a Cs_2CO_3 (0.1 mmol, 32.5 mg) at 60°C . The reaction was continued for 4-6 h at same temperature. After the completion of the reaction (monitored by TLC), the reaction mixture was cooled to room temperature, then diluted with 5.0 mL of dichloromethane. The organic layer was washed with saturated ammonium chloride solution (5.0 mL) followed by water and brine solution, then dried over anhydrous MgSO_4 , filtered, and the solvent was evaporated under reduced pressure. The product mixture was purified by flash chromatography (ethyl acetate in hexanes = 30-70%) to give 2-pyridyl-3-pyridones **9a-c** with yields of 86-90%.

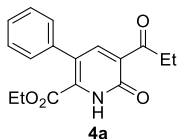
Synthesis of unsymmetrical pyridylpyridones compounds from 1,2,3-triazine 1-oxides and pyridones.



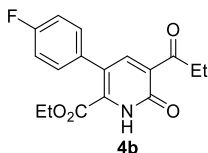
1,2,3-Triazine 1-oxide derivative **1** (0.1 mmol, 1.0 equiv.) was added all at once to a 1.0 mL solution of CHCl_3 containing pyridone **4** (0.1 mmol, 1.0 equiv.) and Cs_2CO_3 (0.2 mmol, 65.2 mg) at 60°C . The reaction was continued for 4-12 h at same temperature. After the completion of the reaction (monitored by TLC), the reaction mixture was cooled to room temperature, then diluted with 5.0 mL of dichloromethane. The organic layer was washed with saturated ammonium chloride

solution (5.0 mL) followed by water and brine solution, then dried over anhydrous MgSO_4 , filtered, and the solvent was evaporated under reduced pressure. The product mixture was purified by flash chromatography (ethyl acetate in hexanes = 30-70%) to give 2-pyridyl-3-pyridones **9d-i** with yields of 72-90%.

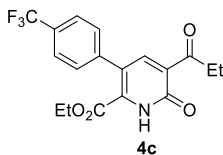
5. Analytical and spectral characterization data for products



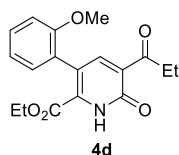
Ethyl 6-Oxo-3-phenyl-5-propionyl-1,6-dihydropyridine-2-carboxylate, 4a: White solid (27.2 mg, 91% yield) 0.1 mmol scale reaction. Flash column chromatography conditions: hexane:ethyl acetate = 1:1. Mp 108-110 °C. $^1\text{H NMR}$ (500 MHz, CDCl_3) δ 10.02 (br s, 1H), 8.15 (s, 1H), 7.48-7.37 (comp, 3H), 7.28 (d, $J = 7.5$ Hz, 2H), 4.19 (q, $J = 7.2$ Hz, 2H), 3.21 (q, $J = 7.2$ Hz, 2H), 1.21 (t, $J = 7.2$ Hz, 3H), 1.05 (t, $J = 7.2$ Hz, 3H). $^{13}\text{C NMR}$ (126 MHz, CDCl_3) δ 201.2, 162.1, 160.6, 146.2, 137.5, 136.7, 129.0, 128.9, 128.4, 128.3, 125.4, 62.9, 35.6, 13.59, 8.0. **HRMS** (ESI) m/z : $[\text{M} + \text{H}]^+$ Calcd for $\text{C}_{17}\text{H}_{17}\text{NO}_4$ 300.1230; Found: 300.1229.



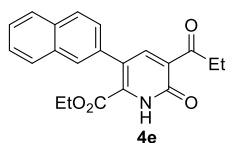
Ethyl 3-(4-Fluorophenyl)-6-oxo-5-propionyl-1,6-dihydropyridine-2-carboxylate, 4b: White solid (26.9 mg, 85% yield) 0.1 mmol scale reaction. Flash column chromatography conditions: hexane:ethyl acetate = 1:1. Mp 142-144 °C. $^1\text{H NMR}$ (500 MHz, CDCl_3) δ 9.95 (br s, 1H), 8.08 (s, 1H), 7.23 (d, $J = 8.4$ Hz, 2H), 7.10 (d, $J = 8.4$ Hz, 2H), 4.20 (q, $J = 7.1$ Hz, 2H), 3.19 (q, $J = 7.2$ Hz, 2H), 1.19 (t, $J = 7.2$ Hz, 3H), 1.08 (t, $J = 7.1$ Hz, 3H). $^{13}\text{C NMR}$ (126 MHz, CDCl_3) δ 201.0, 162.8 (d, $J_{\text{C-F}} = 240$ Hz), 161.9, 160.4, 146.1, 132.7, 132.6, 130.8, 130.7 (d, $J_{\text{C-F}} = 8$ Hz), 124.3, 115.4 (d, $J_{\text{C-F}} = 21$ Hz), 63.1, 35.8, 13.7, 8.0. $^{19}\text{F NMR}$ (471 MHz, CDCl_3) δ -113.5. **HRMS** (ESI) m/z : $[\text{M} + \text{H}]^+$ Calcd for $\text{C}_{17}\text{H}_{16}\text{FNO}_4$ 318.1136; Found: 318.1134.



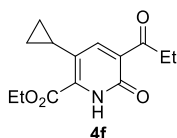
Ethyl 6-Oxo-5-propionyl-3-(4-trifluoromethylphenyl)-1,6-dihydropyridine-2-carboxylate, 4c: White solid (30.8 mg, 84% yield) 0.1 mmol scale reaction. Flash column chromatography conditions: hexane:ethyl acetate = 1:1. Mp 165-167 °C. $^1\text{H NMR}$ (500 MHz, CDCl_3) δ 10.31 (br s, 1H), 8.09 (s, 1H), 7.67 (d, $J = 7.9$ Hz, 2H), 7.39 (d, $J = 7.9$ Hz, 2H), 4.19 (q, $J = 7.1$ Hz, 2H), 3.19 (q, $J = 7.1$ Hz, 2H), 1.19 (t, $J = 7.1$ Hz, 3H), 1.03 (t, $J = 7.1$ Hz, 3H). $^{13}\text{C NMR}$ (126 MHz, CDCl_3) δ 200.8, 161.5, 160.5, 145.7, 140.5, 130.5 (q, $J_{\text{C-F}} = 32$ Hz), 129.4, 125.4 (q, $J_{\text{C-F}} = 3$ Hz), 125.2, 123.7, 123.4 (q, $J_{\text{C-F}} = 289$ Hz), 123.0, 63.2, 35.8, 13.5, 8.0. $^{19}\text{F NMR}$ (471 MHz, CDCl_3) δ -62.7. **HRMS** (ESI) m/z : $[\text{M} + \text{H}]^+$ Calcd for $\text{C}_{18}\text{H}_{16}\text{F}_3\text{NO}_4$ 368.1104; Found: 368.1102.



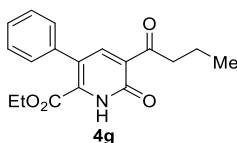
Ethyl 3-(2-Methoxyphenyl)-6-oxo-5-propionyl-1,6-dihydropyridine-2-carboxylate, 4d; White solid (29.6 mg, 90% yield) 0.1 mmol scale reaction. Flash column chromatography conditions: hexane:ethyl acetate = 1:1. Mp 140-142 °C. **¹H NMR** (500 MHz, CDCl₃) δ 10.27 (br s, 1H), 8.15 (s, 1H), 7.33 (t, *J* = 7.5 Hz, 1H), 6.95 (comp, 1H), 6.89-6.78 (comp, 2H), 4.21 (q, *J* = 7.1 Hz, 2H), 3.84 (s, 3H), 3.20 (q, *J* = 7.1 Hz, 2H), 1.21 (t, *J* = 7.1 Hz, 3H), 1.08 (t, *J* = 7.1 Hz, 3H). **¹³C NMR** (126 MHz, CDCl₃) δ 201.3, 162.2, 160.7, 159.6, 146.0, 145.9, 137.9, 129.5, 129.4, 125.2, 121.3, 114.6, 113.7, 62.9, 55.5, 35.6, 13.6, 8.0. **HRMS** (ESI) *m/z*: [M + H]⁺ Calcd for C₁₈H₁₉NO₅ 330.1336; Found: 330.1334.



Ethyl 3-(Naphthalen-2-yl)-6-oxo-5-propionyl-1,6-dihydropyridine-2-carboxylate, 4e; White solid (32.1 mg, 92% yield) 0.1 mmol scale reaction. Flash column chromatography conditions: hexane:ethyl acetate = 1:1. Mp 155-157 °C. **¹H NMR** (500 MHz, CDCl₃) δ 10.41 (br s, 1H), 8.23 (s, 1H), 7.89-7.83 (comp, 3H), 7.74 (s, 1H), 7.55-7.51 (comp, 2H), 7.36 (d, *J* = 8.3 Hz, 1H), 4.15 (q, *J* = 7.1 Hz, 2H), 3.21 (q, *J* = 7.2 Hz, 2H), 1.20 (t, *J* = 7.1 Hz, 3H), 0.93 (t, *J* = 7.2 Hz, 3H). **¹³C NMR** (126 MHz, CDCl₃) δ 201.2, 162.0, 160.6, 146.4, 134.1, 133.1, 132.9, 128.1, 128.0, 127.9, 127.9, 127.8, 127.0, 126.9, 126.7, 126.7, 125.3, 63.0, 35.8, 13.6, 8.0. **HRMS** (ESI) *m/z*: [M + H]⁺ Calcd for C₂₁H₁₉NO₄ 350.1387; Found: 350.1385.

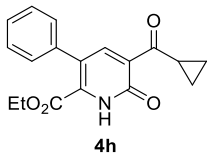


Ethyl 3-Cyclopropyl-6-oxo-5-propionyl-1,6-dihydropyridine-2-carboxylate, 4f; White solid (21.0 mg, 80% yield) 0.1 mmol scale reaction. Flash column chromatography conditions: hexane:ethyl acetate = 1:1. Mp 98-100 °C. **¹H NMR** (500 MHz, CDCl₃) δ 9.93 (br s, 1H), 7.79 (s, 1H), 4.46 (q, *J* = 7.1 Hz, 2H), 3.16 (q, *J* = 7.1 Hz, 2H), 2.56 (tt, *J* = 8.6, 4.4 Hz, 1H), 1.43 (t, *J* = 7.1 Hz, 3H), 1.15 (t, *J* = 7.1 Hz, 3H), 1.08- 0.97 (comp, 2H), 0.72-0.70 (comp, 2H). **¹³C NMR** (126 MHz, CDCl₃) δ 200.7, 161.4, 159.6, 142.8, 127.9, 126.8, 126.5, 63.2, 36.2, 14.3, 11.2, 8.1, 7.9. **HRMS** (ESI) *m/z*: [M + H]⁺ Calcd for C₁₄H₁₇NO₄ 264.1230; Found: 264.1227.

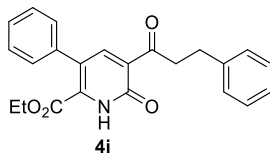


Ethyl 5-Butyl-6-oxo-3-phenyl-1,6-dihydropyridine-2-carboxylate, 4g; White solid (29.4 mg, 94% yield) 0.1 mmol scale reaction. Flash column chromatography conditions: hexane:ethyl

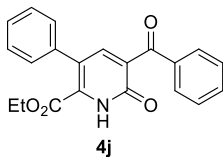
acetate = 2:1. Mp 128-130 °C. **¹H NMR** (500 MHz, CDCl₃) δ 10.46 (br s, 1H), 8.14 (s, 1H), 7.51-7.33 (comp, 3H), 7.28 (dd, *J* = 6.7, 2.5 Hz, 2H), 4.19 (q, *J* = 7.1 Hz, 2H), 3.16 (t, *J* = 7.1 Hz, 2H), 1.77-1.73 (comp, 2H), 1.06 (t, *J* = 7.1 Hz, 3H), 1.00 (t, *J* = 7.2 Hz, 3H). **¹³C NMR** (126 MHz, CDCl₃) δ 200.8, 162.2, 160.7, 146.1, 136.7, 128.8, 128.7, 128.5, 128.4, 128.3, 125.4, 62.9, 44.0, 17.4, 13.9, 13.6. **HRMS** (ESI) *m/z*: [M + H]⁺ Calcd for C₁₈H₁₉NO₄ 314.1387; Found: 314.1385.



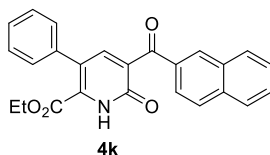
Ethyl 5-(Cyclopropanecarbonyl)-6-oxo-3-phenyl-1,6-dihydropyridine-2-carboxylate, 4h; White solid (27.7 mg, 89% yield) 0.1 mmol scale reaction. Flash column chromatography conditions: hexane:ethyl acetate = 1:1. Mp 136-138 °C. **¹H NMR** (500 MHz, CDCl₃) δ 10.74 (br s, 1H), 8.14 (s, 1H), 7.43-7.40 (comp, 3H), 7.34-7.24 (comp, 2H), 4.19 (q, *J* = 7.1 Hz, 2H), 3.26-3.23 (m, 1H), 1.30-1.28 (comp, 2H), 1.15-1.12 (comp, 2H), 1.05 (t, *J* = 7.1 Hz, 3H). **¹³C NMR** (126 MHz, CDCl₃) δ 201.0, 162.3, 161.1, 145.7, 145.6, 136.7, 128.8, 128.4, 128.3, 128.2, 125.5, 62.8, 19.6, 13.7, 13.6. **HRMS** (ESI) *m/z*: [M + H]⁺ Calcd for C₁₈H₁₇NO₄ 312.1230; Found: 312.1229.



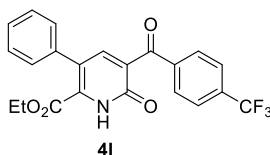
Ethyl 6-Oxo-3-phenyl-5-(3-phenylpropanoyl)-1,6-dihydropyridine-2-carboxylate, 4i; White solid (34.9 mg, 93% yield) 0.1 mmol scale reaction. Flash column chromatography conditions: hexane:ethyl acetate = 1:1. Mp 148-150 °C. **¹H NMR** (500 MHz, CDCl₃) δ 10.10 (br s, 1H), 8.13 (s, 1H), 7.45 – 7.38 (comp, 3H), 7.32 – 7.23 (comp, 6H), 7.21 (dd, *J* = 6.7, 2.1 Hz, 1H), 4.16 (q, *J* = 7.1 Hz, 2H), 3.53 (t, *J* = 7.5 Hz, 2H), 3.06 (t, *J* = 7.5 Hz, 2H), 1.03 (t, *J* = 7.1 Hz, 3H). **¹³C NMR** (126 MHz, CDCl₃) δ 199.3, 161.7, 160.2, 146.6, 141.0, 136.5, 129.2, 128.7, 128.7, 128.6, 128.4, 128.3, 128.2, 126.0, 125.0, 62.9, 43.9, 29.9, 13.4. **HRMS** (ESI) *m/z*: [M + H]⁺ Calcd for C₂₃H₂₁NO₄ 376.1543; Found: 376.1542.



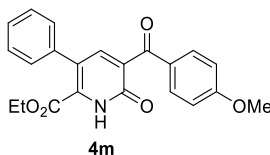
Ethyl 5-Benzoyl-6-oxo-3-phenyl-1,6-dihydropyridine-2-carboxylate, 4j; White solid (32.7 mg, 94% yield) 0.1 mmol scale reaction. Flash column chromatography conditions: hexane:ethyl acetate = 1:1. Mp 140-142 °C. **¹H NMR** (500 MHz, CDCl₃) δ 10.81 (br s, 1H), 7.91 (d, *J* = 7.6 Hz, 2H), 7.76 (s, 1H), 7.62 (t, *J* = 7.6 Hz, 1H), 7.50 (t, *J* = 7.6 Hz, 2H), 7.42-7.40 (comp, 3H), 7.34 – 7.25 (comp, 2H), 4.14 (q, *J* = 7.1 Hz, 2H), 1.03 (t, *J* = 7.1 Hz, 3H). **¹³C NMR** (126 MHz, CDCl₃) δ 193.9, 161.6, 160.0, 145.4, 136.6, 136.4, 135.4, 133.7, 132.5, 129.8, 128.8, 128.7, 128.4, 128.3, 124.9, 62.9, 13.6. **HRMS** (ESI) *m/z*: [M + H]⁺ Calcd for C₂₁H₁₇NO₄ 348.1230; Found: 348.1228.



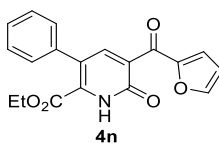
Ethyl 5-(2-Naphthoyl)-6-oxo-3-phenyl-1,6-dihydropyridine-2-carboxylate, 4k; White solid (34.1 mg, 86% yield) 0.1 mmol scale reaction. Flash column chromatography conditions: hexane:ethyl acetate = 1:1. Mp 163-165 °C. ¹H NMR (500 MHz, CDCl₃) δ 10.61 (br s, 1H), 8.39 (s, 1H), 8.04 – 7.87 (comp, 4H), 7.82 (s, 1H), 7.62-7.58 (comp, 2H), 7.43-7.38 (comp, 3H), 7.35 – 7.25 (comp, 2H), 4.13 (q, *J* = 7.1 Hz, 2H), 1.02 (t, *J* = 7.1 Hz, 3H). ¹³C NMR (126 MHz, CDCl₃) δ 193.7, 161.5, 160.0, 145.4, 136.5, 136.0, 135.0, 133.8, 133.2, 132.5, 132.1, 129.8, 128.9, 128.8, 128.5, 128.4, 128.3, 127.9, 126.9, 124.8, 62.9, 13.5. HRMS (ESI) *m/z*: [M + H]⁺ Calcd for C₂₅H₁₉NO₄ 398.1387; Found: 398.1387.



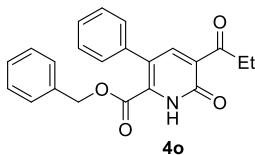
Ethyl 6-Oxo-3-phenyl-5-(4-(trifluoromethyl)benzoyl)-1,6-dihydropyridine-2-carboxylate, 4l; White solid (37.3 mg, 90% yield) 0.1 mmol scale reaction. Flash column chromatography conditions: hexane:ethyl acetate = 1:1. Mp 176-178 °C. ¹H NMR (500 MHz, CDCl₃) δ 10.68 (br s, 1H), 8.01 (d, *J* = 8.0 Hz, 2H), 7.85 (s, 1H), 7.76 (d, *J* = 8.0 Hz, 2H), 7.43-7.41 (comp, 3H), 7.32 – 7.26 (comp, 2H), 4.14 (q, *J* = 7.2 Hz, 2H), 1.01 (t, *J* = 7.2 Hz, 3H). ¹³C NMR (126 MHz, CDCl₃) δ 192.7, 161.3, 159.6, 146.7, 139.4, 136.3, 135.0, 138.8, 134.6, 132.5, 129.9, 128.9, 128.5, 125.6 (q, *J*_{C-F} = 4 Hz), 124.7, 123.5 (q, *J*_{C-F} = 260 Hz), 63.1, 13.5. HRMS (ESI) *m/z*: [M + H]⁺ Calcd for C₂₂H₁₆F₃NO₄ 416.1104; Found: 416.1102.



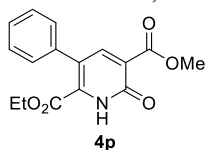
Ethyl 5-(4-Methoxybenzoyl)-6-oxo-3-phenyl-1,6-dihydropyridine-2-carboxylate, 4m; White solid (34.3, 91% yield) 0.1 mmol scale reaction. Flash column chromatography conditions: hexane:ethyl acetate = 1:1. Mp 168-170 °C. ¹H NMR (500 MHz, CDCl₃) δ 10.40 (br s, 1H), 7.91 (d, *J* = 8.4 Hz, 2H), 7.71 (s, 1H), 7.46 – 7.37 (comp, 3H), 7.34 – 7.26 (comp, 2H), 6.97 (d, *J* = 8.4 Hz, 2H), 4.17 (q, *J* = 7.1 Hz, 2H), 3.90 (s, 3H), 1.04 (t, *J* = 7.1 Hz, 3H). ¹³C NMR (126 MHz, CDCl₃) δ 192.0, 164.3, 161.6, 159.7, 144.9, 136.7, 134.2, 133.6, 132.4, 129.3, 128.9, 128.4, 128.3, 125.0, 114.0, 77.4, 62.9, 55.7, 13.6. HRMS (ESI) *m/z*: [M + H]⁺ Calcd for C₂₂H₂₀NO₅ 378.1336; Found: 378.1334.



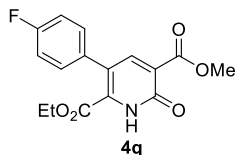
Ethyl 5-(furan-2-carbonyl)-6-oxo-3-phenyl-1,6-dihydropyridine-2-carboxylate, 4n; White solid (27.3 mg, 81% yield) 0.1 mmol scale reaction,. Flash column chromatography conditions: hexane:ethyl acetate = 1:1. Mp 102-104 °C. ¹H NMR (500 MHz, CDCl₃) δ 10.19 (br s, 1H), 7.98 (s, 1H), 7.68 (s, 1H), 7.41-7.31 (comp, 4H), 7.29-7.27 (comp, 2H), 6.60 (d, *J* = 4.3 Hz, 1H), 4.18 (q, *J* = 7.2 Hz, 2H), 1.03 (t, *J* = 7.2 Hz, 3H). ¹³C NMR (126 MHz, CDCl₃) δ 179.8, 161.9, 159.8, 152.1, 147.9, 145.5, 136.7, 131.1, 129.1, 128.9, 128.5, 128.5, 125.3, 121.3, 112.9, 63.0, 13.6. HRMS (ESI) *m/z*: [M + H]⁺ Calcd for C₁₉H₁₆NO₅ 338.1023; Found: 338.1022.



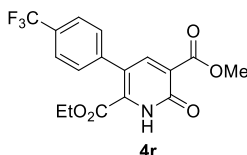
Benzyl 6-oxo-3-phenyl-5-propionyl-1,6-dihydropyridine-2-carboxylate, 4o; White solid (31.4 mg, 87% yield) 0.1 mmol scale reaction. Flash column chromatography conditions: hexane:ethyl acetate = 1:1. Mp 158-160 °C. ¹H NMR (500 MHz, CDCl₃) δ 9.82 (br s, 1H), 8.10 (s, 1H), 7.38 – 7.25 (comp, 6H), 7.21 (d, *J* = 7.1 Hz, 2H), 6.99 (d, *J* = 7.1 Hz, 2H), 5.14 (s, 2H), 3.17 (q, *J* = 7.2 Hz, 2H), 1.19 (t, *J* = 7.2 Hz, 3H). ¹³C NMR (126 MHz, CDCl₃) δ 201.2, 162.2, 160.8, 146.1, 146.0, 136.5, 133.9, 128.8, 128.7, 128.6, 128.6, 128.5, 128.4, 128.3, 125.5, 68.6, 35.6, 8.0. HRMS (ESI) *m/z*: [M + H]⁺ Calcd for C₂₂H₂₀NO₄ 362.1387; Found: 362.1387.



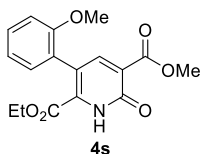
2-Ethyl 5-methyl 6-oxo-3-phenyl-1,6-dihydropyridine-2,5-dicarboxylate, 4p; White solid, (25.3 mg, 84% yield), 0.1 mmol scale reaction,. Flash column chromatography conditions: hexane:ethyl acetate = 1:1. mp 103-105 °C. ¹H NMR (500 MHz, CDCl₃) δ 10.77 (br s, 1H), 8.25 (s, 1H), 7.48 – 7.38 (comp, 3H), 7.32-7.29 (comp, 2H), 4.21 (q, *J* = 7.1 Hz, 2H), 3.99 (s, 3H), 1.09 (t, *J* = 7.1 Hz, 3H). ¹³C NMR (126 MHz, CDCl₃) δ 166.9, 163.6, 161.3, 145.3, 136.6, 128.7, 128.6, 128.5, 128.5, 128.3, 127.0, 62.6, 53.1, 13.7. HRMS (ESI) *m/z*: [M + H]⁺ Calcd for C₁₆H₁₅NO₄ 302.1023; Found: 302.1021.



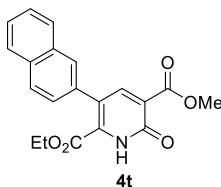
2-Ethyl 5-methyl 3-(4-Fluorophenyl)-6-oxo-1,6-dihydropyridine-2,5-dicarboxylate, 4q; White solid, (25.8 mg, 81% yield), 0.1 mmol scale reaction, Flash column chromatography conditions: hexane:ethyl acetate = 1:1. mp 145-147 °C. ¹H NMR (500 MHz, CDCl₃) δ 10.73 (br s, 1H), 8.22 (s, 1H), 7.27-7.29 (comp, 2H), 7.14-7.12 (comp, 2H), 4.23 (q, *J* = 7.2 Hz, 2H), 4.00 (s, 3H), 1.14 (t, *J* = 7.2 Hz, 3H). ¹³C NMR (126 MHz, CDCl₃) δ. 166.9, 163.4, 162.7 (d, *J*_{C-F} = 220 Hz), 161.3, 145.0, 132.6, 132.5, 130.5, 130.4, (d, *J*_{C-F} = 4 Hz), 126.0, 115.5 (d, *J*_{C-F} = 21 Hz), 62.6, 53.1, 13.7. ¹⁹F NMR (471 MHz, CDCl₃) δ -113.9. HRMS (ESI) *m/z*: [M + H]⁺ Calcd for C₁₆H₁₄FNO₅ 320.0929; Found: 320.0928.



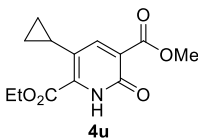
2-Ethyl 5-methyl 6-oxo-3-(4-(Trifluoromethyl)phenyl)-1,6-dihydropyridine-2,5-dicarboxylate, 4r; White solid, (29.5 mg, 80% yield), 0.1 mmol scale reaction,. Flash column chromatography conditions: hexane:ethyl acetate = 1:1. mp 162-164 °C. $^1\text{H NMR}$ (500 MHz, CDCl_3) δ 10.84 (br s, 1H), 8.23 (s, 1H), 7.71 (d, J = 8.0 Hz, 2H), 7.45 (d, J = 8.0 Hz, 2H), 4.24 (q, J = 7.2 Hz, 2H), 4.01 (s, 3H), 1.12 (t, J = 7.2 Hz, 3H). $^{13}\text{C NMR}$ (126 MHz, CDCl_3) δ 166.8, 163.2, 161.6, 144.7, 131.0, 130.4 (q, $J_{\text{C-F}}$ = 37 Hz), 129.1, 125.4 (q, $J_{\text{C-F}}$ = 7.2 Hz), 135.4, 123.5 (q, $J_{\text{C-F}}$ = 7.2 Hz), 123.0 (q, $J_{\text{C-F}}$ = 272 Hz), 120.7, 62.7, 53.2, 13.6. $^{19}\text{F NMR}$ (471 MHz, CDCl_3) δ -63.1. **HRMS** (ESI) m/z : $[\text{M} + \text{H}]^+$ Calcd for $\text{C}_{17}\text{H}_{14}\text{F}_3\text{NO}_5$ 370.0897; Found: 370.0895.



2-Ethyl 5-methyl 3-(2-Methoxyphenyl)-6-oxo-1,6-dihydropyridine-2,5-dicarboxylate, 4s; White solid, (28.1 mg, 85% yield), 0.1 mmol scale reaction, following procedure 2. Flash column chromatography conditions: hexane:ethyl acetate = 1:1. mp 94-96 °C. $^1\text{H NMR}$ (500 MHz, CDCl_3) δ 10.54 (br s, 1H), 8.17 (s, 1H), 7.37-7.25 (m, 1H), 7.18-7.16 (m, 1H), 7.01 (t, J = 7.4 Hz, 1H), 6.90 (d, J = 8.2 Hz, 1H), 4.17 (q, J = 7.1 Hz, 2H), 3.94 (s, 3H), 3.73 (s, 3H), 1.06 (t, J = 7.1 Hz, 3H). $^{13}\text{C NMR}$ (126 MHz, CDCl_3) δ 166.5, 162.8, 160.5, 156.4, 147.3, 132.3, 130.0, 129.9, 125.8, 122.2, 120.8, 120.3, 110.5, 62.4, 55.4, 53.0, 13.7. **HRMS** (ESI) m/z : $[\text{M} + \text{H}]^+$ Calcd for $\text{C}_{17}\text{H}_{17}\text{NO}_6$ 332.1129; Found: 332.1130.

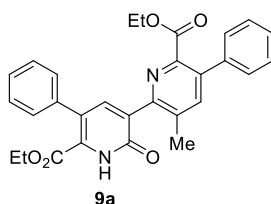


2-Ethyl 5-methyl 3-(Naphthalen-2-yl)-6-oxo-1,6-dihydropyridine-2,5-dicarboxylate, 4t; White solid, (28.8 mg, 82% yield), 0.1 mmol scale reaction, Flash column chromatography conditions: hexane:ethyl acetate = 1:1. mp 156-158 °C. $^1\text{H NMR}$ (500 MHz, CDCl_3) δ 10.71 (br s, 1H), 8.24 (s, 1H), 7.90 (d, J = 8.3 Hz, 2H), 7.53-7.43 (comp, 4H), 7.32 (d, J = 7.0 Hz, 1H), 3.93 (s, 3H), 3.90 (t, J = 7.1 Hz, 2H), 0.59 (t, J = 7.1 Hz, 3H). $^{13}\text{C NMR}$ (126 MHz, CDCl_3) δ 166.1, 162.2, 160.4, 147.2, 134.3, 133.4, 131.9, 128.7, 128.7, 128.7, 128.4, 126.8, 126.6, 126.1, 125.1, 124.8, 123.9, 62.4, 52.9, 13.0. **HRMS** (ESI) m/z : $[\text{M} + \text{H}]^+$ Calcd for $\text{C}_{20}\text{H}_{17}\text{NO}_5$ 352.1179; Found: 352.1177.

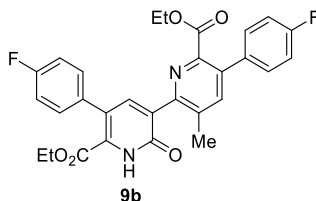


2-Ethyl 5-methyl 3-cyclopropyl-6-oxo-1,6-dihydropyridine-2,5-dicarboxylate, 4u; White solid, (19.6 mg, 74% yield), 0.1 mmol scale reaction,. Flash column chromatography conditions: hexane:ethyl acetate = 1:1. mp 130-132 °C. $^1\text{H NMR}$ (500 MHz, CDCl_3) δ 10.29 (br s, 1H), 7.86

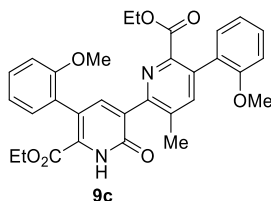
(s, 1H), 4.45 (q, $J = 7.1$ Hz, 2H), 3.94 (s, 3H), 2.47-2.45 (m, 1H), 1.42 (t, $J = 7.1$ Hz, 3H), 1.01 (comp, 2H), 0.67 (comp, 2H). ^{13}C NMR (126 MHz, CDCl_3) δ 166.5, 162.7, 159.7, 142.8, 142.0, 142.0, 127.5, 62.8, 53.0, 14.3, 11.2, 8.1, 8.0. **HRMS** (ESI) m/z : $[\text{M} + \text{H}]^+$ Calcd for $\text{C}_{13}\text{H}_{15}\text{NO}_5$ 266.1023; Found: 266.1021.



Diethyl 3-methyl-2'-oxo-5,5'-diphenyl-1',2'-dihydro-[2,3'-bipyridine]-6,6'-dicarboxylate, 9a; White solid (26.8 mg, 90% yield) 0.05 mmol scale reaction. Flash column chromatography conditions: hexane:ethyl acetate = 1:2. Mp 142-144 °C. ^1H NMR (500 MHz, CDCl_3) δ 10.01 (br s, 1H), 7.78 (s, 1H), 7.66 (s, 1H), 7.45 – 7.35 (comp, 8H), 7.33 (dd, $J = 6.3, 2.6$ Hz, 2H), 4.20 (q, $J = 7.1$ Hz, 2H), 4.14 (q, $J = 7.1$ Hz, 2H), 2.48 (s, 3H), 1.05 (t, $J = 7.1$ Hz, 3H), 1.01 (t, $J = 7.1$ Hz, 3H). ^{13}C NMR (126 MHz, CDCl_3) δ 167.0, 161.3, 159.3, 151.9, 146.7, 145.4, 140.2, 138.2, 137.0, 136.8, 136.5, 135.4, 130.3, 129.0, 128.4, 128.3, 128.2, 128.0, 129.9, 125.5, 62.7, 61.5, 19.0, 13.6, 13.4. **HRMS** (ESI) m/z : $[\text{M} + \text{H}]^+$ Calcd for $\text{C}_{29}\text{H}_{26}\text{N}_2\text{O}_5$ 483.1914; Found: 483.1918.

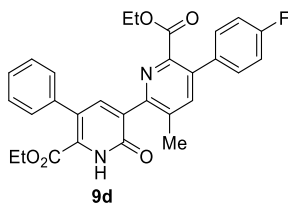


Diethyl 5,5'-bis(4-Fluorophenyl)-3-methyl-2'-oxo-1',2'-dihydro-[2,3'-bipyridine]-6,6'-dicarboxylate, 9b; White solid (22.3 mg, 86% yield) 0.05 mmol scale reaction. Flash column chromatography conditions: hexane:ethyl acetate = 1:2. Mp 162-164 °C. ^1H NMR (500 MHz, CDCl_3) δ 10.06 (br s, 1H), 7.73 (s, 1H), 7.63 (s, 1H), 7.35-7.29 (comp, 4H), 7.15-7.09 (comp, 4H), 4.24 – 4.14 (comp, 4H), 2.48 (s, 3H), 1.10-1.04 (comp, 6H). ^{13}C NMR (126 MHz, CDCl_3) δ 166.8, 162.7 (d, $J_{\text{C-F}} = 252$ Hz), 162.6 (d, $J_{\text{C-F}} = 250$ Hz), 161.1, 159.3, 152.0, 146.6, 145.2, 140.3, 136.5, 135.9, 135.6, 134.2 (d, $J_{\text{C-F}} = 4$ Hz), 132.9 (d, $J_{\text{C-F}} = 4$ Hz), 130.8 (d, $J_{\text{C-F}} = 8$ Hz), 130.6, 130.0 (d, $J_{\text{C-F}} = 8$ Hz), 124.3, 115.4 (d, $J_{\text{C-F}} = 22$ Hz), 115.0 (d, $J_{\text{C-F}} = 22$ Hz), 62.8, 61.6, 19.0, 13.7, 13.5. ^{19}F NMR (471 MHz, CDCl_3) δ -113.8, -114.0. **HRMS** (ESI) m/z : $[\text{M} + \text{H}]^+$ Calcd for $\text{C}_{29}\text{H}_{24}\text{F}_2\text{N}_2\text{O}_5$ 519.1726; Found: 519.1728.

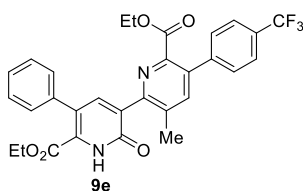


Diethyl 5,5'-bis(2-Methoxyphenyl)-3-methyl-2'-oxo-1',2'-dihydro-[2,3'-bipyridine]-6,6'-dicarboxylate, 9c; White solid (23.9 mg, 88% yield) 0.05 mmol scale reaction. Flash column chromatography conditions: hexane:ethyl acetate = 1:2. Mp 149-151 °C. ^1H NMR (500 MHz, CDCl_3) δ 10.03 (br s, 1H), 7.76 (s, 1H), 7.60 (s, 1H), 7.39-7.34 (comp, 2H), 7.28 – 7.23 (comp, 2H), 7.08-6.99 (comp, 2H), 6.92 (d, $J = 8.2$ Hz, 2H), 4.19-4.10 (comp, 4H), 3.77 (s, 3H), 3.74 (s,

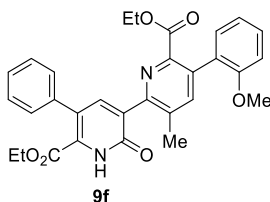
3H), 2.48 (s, 3H), 1.09-1.04 (comp, 6H). **¹³C NMR** (126 MHz, CDCl₃) δ 166.4, 161.7, 159.5, 156.4, 156.1, 151.8, 146.9, 146.0, 141.2, 136.2, 135.7, 133.8, 131.7, 130.3, 130.2, 130.00, 129.5, 129.4, 127.9, 126.1, 120.8, 120.4, 110.3, 110.1, 62.3, 61.0, 55.4, 55.1, 19.1, 13.7, 13.5. **HRMS** (ESI) m/z: [M + H]⁺ Calcd for C₃₁H₃₀N₂O₇ 543.2126; Found: 543.2132.



Diethyl 5-(4-Fluorophenyl)-3-methyl-2'-oxo-5'-phenyl-1',2'-dihydro-[2,3'-bipyridine]-6,6'-dicarboxylate, 9d; White solid (43.5 mg, 87% yield) 0.1 mmol scale reaction. Flash column chromatography conditions: hexane:ethyl acetate = 1:2. Mp 154-156 °C. **¹H NMR** (500 MHz, CDCl₃) δ 9.95 (br s, 1H), 7.77 (s, 1H), 7.63 (s, 1H), 7.42-7.39 (comp, 3H), 7.35-7.31 (comp, 4H), 7.14 (t, *J* = 8.4 Hz, 2H), 4.18 (comp, 4H), 2.48 (s, 3H), 1.05 (comp, 6H). **¹³C NMR** (126 MHz, CDCl₃) δ 166.8, 162.7 (d, *J*_{C-F} = 252 Hz), 161.4, 159.3, 152.2, 146.6, 145.4, 140.2, 137.0, 136.4, 135.8, 135.5, 134.2 (d, *J*_{C-F} = 4 Hz), 130.4, 130.0 (d, *J*_{C-F} = 9 Hz), 129.0, 128.0, 128.0, 125.4, 115.4 (d, *J*_{C-F} = 25 Hz), 62.7, 61.6, 19.0, 13.7, 13.4. **¹⁹F NMR** (471 MHz, CDCl₃) δ -114.0. **HRMS** (ESI) m/z: [M + H]⁺ Calcd for C₂₉H₂₅FN₂O₅ 501.1820; Found: 501.1823.

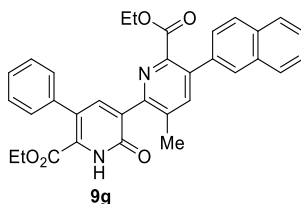


Diethyl 3-Methyl-2'-oxo-5'-phenyl-5-(4-(Trifluoromethyl)phenyl)-1',2'-dihydro-[2,3'-bipyridine]-6,6'-dicarboxylate, 9e; White solid (49.5 mg, 90% yield) 0.1 mmol scale reaction. Flash column chromatography conditions: hexane:ethyl acetate = 1:2. Mp 168-170 °C. **¹H NMR** (500 MHz, CDCl₃) δ 9.99 (br s, 1H), 7.78 (s, 1H), 7.71 (d, *J* = 8.0 Hz, 2H), 7.64 (s, 1H), 7.49 (d, *J* = 8.0 Hz, 2H), 7.44 – 7.39 (comp, 3H), 7.34-7.31 (comp, 2H), 4.23 – 4.13 (comp, 4H), 2.50 (s, 3H), 1.07 – 0.99 (comp, 6H). **¹³C NMR** (126 MHz, CDCl₃) δ 166.3, 161.3, 159.2, 152.8, 146.2, 145.4, 142.1, 140.2, 136.6, 136.2, 135.9, 135.8, 130.5, 130.2 (q, *J*_{C-F} = 32 Hz), 129.0, 128.7, 128.1, 128.0, 125.5, 125.3 (q, *J*_{C-F} = 4 Hz), 124.1 (q, *J*_{C-F} = 272 Hz), 62.7, 61.7, 19.1, 13.6, 13.4. **¹⁹F NMR** (471 MHz, CDCl₃) δ -62.6. **HRMS** (ESI) m/z: [M + H]⁺ Calcd for C₃₀H₂₅F₃N₂O₅ 551.1788; Found: 551.1793.

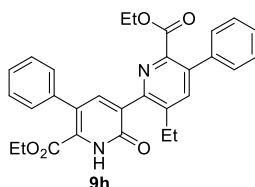


Diethyl 5-(2-Methoxyphenyl)-3-methyl-2'-oxo-5'-phenyl-1',2'-dihydro-[2,3'-bipyridine]-6,6'-dicarboxylate, 9f; White solid (45.6 mg, 89% yield) 0.1 mmol scale reaction. Flash column chromatography conditions: hexane:ethyl acetate = 1:2. Mp 150-152 °C. **¹H NMR** (500 MHz, CDCl₃) δ 10.01 (br s, 1H), 7.81 (s, 1H), 7.61 (s, 1H), 7.42-7.36 (comp, 4H), 7.35 – 7.31 (comp, 2H), 7.28-7.26 (comp, 1H), 7.07 (t, *J* = 8.2 Hz, 1H), 6.93 (d, *J* = 8.2 Hz, 1H), 4.19 (q, *J* = 7.5 Hz,

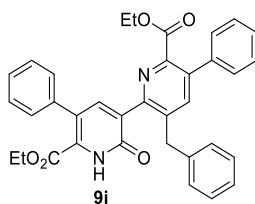
2H), 4.13 (q, $J = 7.1$ Hz, 2H), 3.74 (s, 3H), 2.47 (s, 3H), 1.06-1.01 (comp, 6H). ^{13}C NMR (126 MHz, CDCl_3) δ 166.3, 161.5, 159.4, 156.1, 151.5, 146.9, 145.3, 141.3, 137.1, 136.6, 135.7, 134.0, 130.4, 130.0, 129.5, 129.0, 128.0, 127.9, 127.8, 125.6, 120.8, 110.1, 62.6, 61.1, 55.1, 19.1, 13.7, 13.5. **HRMS** (ESI) m/z : $[\text{M} + \text{H}]^+$ Calcd for $\text{C}_{30}\text{H}_{28}\text{N}_2\text{O}_6$ 513.2020; Found: 513.2022.



Diethyl 3-Methyl-5-(naphthalen-2-yl)-2'-oxo-5'-phenyl-1',2'-dihydro-[2,3'-bipyridine]-6,6'-dicarboxylate, 9g; White solid (45.8 mg, 86% yield) 0.1 mmol scale reaction. Flash column chromatography conditions: hexane:ethyl acetate = 1:2. Mp 172-174 °C. ^1H NMR (500 MHz, CDCl_3) δ 9.87 (br s, 1H), 7.89 (d, $J = 8.3$ Hz, 2H), 7.84 (s, 1H), 7.69 (s, 1H), 7.57 (d, $J = 8.3$ Hz, 1H), 7.54 – 7.46 (comp, 2H), 7.45 – 7.37 (comp, 4H), 7.35-7.32 (comp, 3H), 4.19 (q, $J = 7.1$ Hz, 2H), 3.80 (q, $J = 7.1$ Hz, 2H), 2.49 (s, 3H), 1.03 (t, $J = 7.1$ Hz, 3H), 0.53 (t, $J = 7.1$ Hz, 3H). ^{13}C NMR (126 MHz, CDCl_3) δ 166.0, 161.4, 159.3, 152.6, 147.1, 145.6, 141.7, 137.0, 136.6, 136.4, 136.0, 135.8, 133.3, 131.8, 130.4, 129.0, 128.2, 128.2, 128.1, 128.0, 127.9, 126.4, 126.3, 126.0, 125.5, 125.1, 62.7, 61.1, 19.1, 13.4, 13.1. **HRMS** (ESI) m/z : $[\text{M} + \text{H}]^+$ Calcd for $\text{C}_{33}\text{H}_{28}\text{N}_2\text{O}_5$ 533.2071; Found: 533.2076.



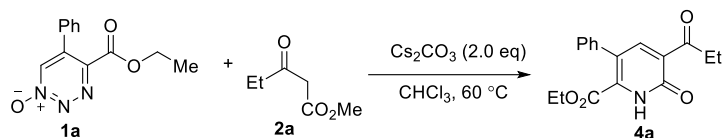
Diethyl 3-Ethyl-2'-oxo-5,5'-diphenyl-1',2'-dihydro-[2,3'-bipyridine]-6,6'-dicarboxylate, 9h; White solid (38.7 mg, 78% yield) 0.1 mmol scale reaction. Flash column chromatography conditions: hexane:ethyl acetate = 1:2. Mp 145-147 °C. ^1H NMR (500 MHz, CDCl_3) δ 9.86 (br s, 1H), 7.73 (s, 1H), 7.71 (s, 1H), 7.44-7.36 (comp, 8H), 7.34-7.30 (comp, 2H), 4.20 (q, $J = 7.1$, 2H), 4.15 (q, $J = 7.1$, 2H), 2.83 (q, $J = 7.1$ Hz, 2H), 1.26 (t, $J = 7.1$ Hz, 3H), 1.05 (t, $J = 7.1$ Hz, 3H), 1.01 (t, $J = 7.1$ Hz, 3H). ^{13}C NMR (126 MHz, CDCl_3) δ 167.0, 161.3, 159.6, 151.6, 146.7, 145.3, 140.9, 138.4, 138.3, 137.1, 137.0, 136.7, 136.7, 130.1, 129.0, 128.4, 128.3, 128.0, 127.9, 125.5, 62.7, 61.5, 25.1, 14.1, 13.6, 13.5. **HRMS** (ESI) m/z : $[\text{M} + \text{H}]^+$ Calcd for $\text{C}_{30}\text{H}_{28}\text{N}_2\text{O}_5$ 497.2071; Found: 497.2070.



Diethyl 3-Benzyl-2'-oxo-5,5'-diphenyl-1',2'-dihydro-[2,3'-bipyridine]-6,6'-dicarboxylate, 9i; White solid (40.2 mg, 72% yield) 0.1 mmol scale reaction. Flash column chromatography conditions: hexane:ethyl acetate = 1:2. Mp 160-162 °C. ^1H NMR (500 MHz, CDCl_3) δ 9.85 (br s, 1H), 7.62 (s, 1H), 7.49 (s, 1H), 7.46 – 7.31 (comp, 8H), 7.26 – 7.12 (comp, 5H), 7.07 (d, $J = 7.3$ Hz, 2H), 4.23 (s, 2H), 4.19-4.15 (comp, 4H), 1.04-0.98 (comp, 6H). ^{13}C NMR (126 MHz, CDCl_3) δ 167.0, 161.3, 159.6, 152.1, 147.2, 145.5, 139.9, 139.2, 138.7, 138.0, 136.9, 136.7, 136.5, 130.1,

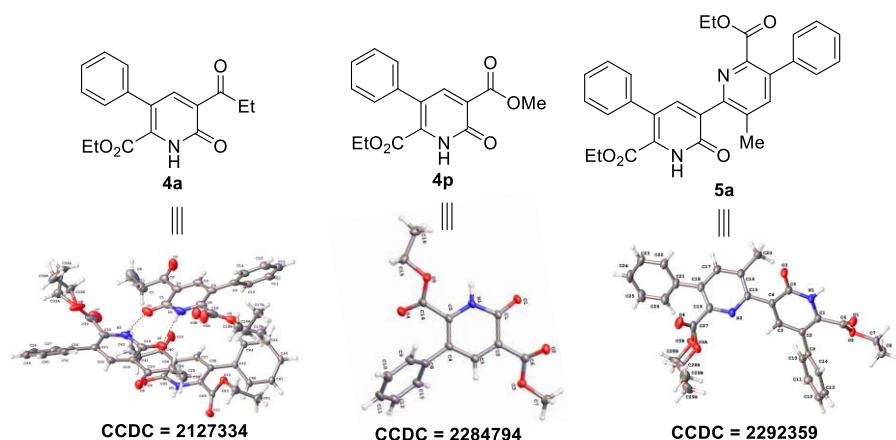
129.1, 128.9, 128.5, 128.4, 128.3, 128.0, 127.9, 127.8, 126.4, 125.4, 62.7, 61.6, 38.6, 13.6, 13.4.
HRMS (ESI) *m/z*: [M + H]⁺ Calcd for C₃₅H₃₀N₂O₅ 559.2227; Found: 559.2231.

6. 1 mmol scale reaction: Procedure for the synthesis of pyridineone compound **4a** from 1,2,3-triazine 1-oxide and ketoester



A chloroform solution (10.0 mL) of 1,2,3-triazine 1-oxide derivative **1a** (1.0 mmol, 1 equiv.) was added dropwise over 30 minutes to a 10.0 mL solution of CHCl₃ containing β-keto ester **2a** (1.5 mmol, 1.5 equiv.) and a Cs₂CO₃ (20 mmol, 652 mg) at 60 °C. The reaction was continued for 1 h at same temperature. After completion of the reaction (monitored by TLC), the reaction mixture was cooled to room temperature and diluted with 50.0 mL of dichloromethane. The organic layer was washed with saturated ammonium chloride solution (50.0 mL) followed by water and brine solution, then dried over anhydrous MgSO₄, filtered, and the solvent was evaporated under reduced pressure. Pure pyridone compound **4a** was obtained from DCM/hexane solvent (5:1) mixture by crystallization in 92% yield (275 mg).

7. Crystallographic data



Single crystals of C₁₇H₁₇NO₄ (**4a**) were prepared by slow evaporation of a dichloromethane:hexane (1:10) solution. A suitable colorless plate-like crystal, with dimensions of 0.140 mm × 0.088 mm × 0.074 mm, was mounted in paratone oil onto a nylon loop. Single crystals of C₁₆H₁₅NO₅ (**4p**) were prepared by slow evaporation of a ethyl acetate:hexane (10:1) solution. A suitable colorless plate-like crystal of **4p**, with dimensions of 0.152 mm × 0.112 mm × 0.096 mm, was mounted in paratone oil onto a nylon loop. Single crystals of C₂₉H₂₆N₂O₅ (**9a**) were prepared by slow evaporation of a dichloromethane:hexane (1:10) solution. A suitable colorless plate-like crystal, with dimensions of 0.152 mm × 0.112 mm × 0.096 mm, was mounted in paratone oil onto a nylon loop. All data were collected at 298(1) K and 298(1) K for compounds

4a, **4p** and **9a** respectively, using a XtaLAB Synergy/ Dualflex, HyPix fitted with CuK α radiation ($\lambda = 1.54184$ Å). Data collection and unit cell refinement were performed using *CrysAlisPro* software.^[1] The total number of data were measured in the $6.2^\circ < 2\theta < 153.2^\circ$, $6.6^\circ < 2\theta < 153.0^\circ$ and $9^\circ < 2\theta < 152.2^\circ$ for compounds **4a**, **4p** and **9a** respectively, using ω scans. Data processing and absorption correction, giving minimum and maximum transmission factors (0.653, 1.000 for compound (**4a**)/ 0.621, 1.00 for compound (**4p**)/ 0.487, 1.00 for compound (**9a**)) were accomplished with *CrysAlisPro*³ and *SCALE3 ABSPACK*⁴, respectively. The structure, using Olex2⁵, was solved with the ShelXT⁶ structure solution program using direct methods and refined (on F^2) with the ShelXL⁷ refinement package using full-matrix, least-squares techniques. All non-hydrogen atoms were refined with anisotropic displacement parameters. All hydrogen atom positions were determined by geometry and refined by a riding model.

Compound number	4a	4p	9a
Identification code	Hpd462(1)	Hpd614(2)	Hpd750
Empirical formula	C ₁₇ H ₁₇ NO ₄	C ₁₆ H ₁₅ NO ₅	C ₂₉ H ₂₆ N ₂ O ₅
Formula weight	299.31	301.29	482.52
Crystal system	Triclinic	Monoclinic	Monoclinic
Space group	<i>P</i> - <i>I</i>	<i>P</i> 2 ₁ / <i>n</i>	<i>P</i> 2 ₁ / <i>c</i>
<i>a</i> (Å)	12.5967(2)	15.6843(2)	13.83436(15)
<i>b</i> (Å)	12.8747(2)	6.33089(7)	11.10289(10)
<i>c</i> (Å)	15.6198(3)	15.8937(2)	20.5729(2)
α (°)	72.566(2)	90	90
β (°)	69.811(1)	114.758(2)	109.0934(12)
γ (°)	75.602(1)	90	90
Volume (Å ³)	2238.30(7)	1433.11(3)	2986.18(6)
Z	6	4	4
ρ (calc.)	1.332	1.396	1.073
λ	1.54184	1.54184	1.54184
Temp. (K)	100.0(1)	298(1)	100(1)

F(000)	948	632	1016
μ (mm ⁻¹)	0.785	0.877	0.601
T _{min} , T _{max}	0.653, 1.000	0.621, 1.000	0.487, 1.000
2 θ _{range} (°)	6.2 to 153.2	6.6, 153.0	6.76 to 152.8
Reflections collected	42637	30584	29239
Independent reflections	9064 [R(int) = 0.0360]	2921 [R(int) = 0.0329]	5984 [R(int) = 0.0315]
Completeness	99.8%	99.9%	99.9%
Data / restraints / parameters	9064 / 44 / 624	2921 / 0 / 204	5384 / 0 / 359
Observed data [I > 2 σ (I)]	8008	2657	5338
$wR(F^2$ all data)	0.1031	0.0943	0.1291
$R(F$ obsd data)	0.0430	0.0351	0.0443
Goodness-of-fit on F^2	0.89	1.06	1.05
largest diff. peak and hole (e Å ⁻³)	0.38 / -0.46	0.20 / -0.21	0.20 / -0.32

$$wR_2 = \{ \Sigma [w(F_o^2 - F_c^2)^2] / \Sigma [w(F_o^2)^2] \}^{1/2}$$

$$R_1 = \Sigma ||F_o| - |F_c|| / \Sigma |F_o|$$

8. Computational data

Software

Quantum chemical calculations were performed using the Lonestar6 supercomputer at the Texas Advanced Computing Center (TACC) hosted by the University of Texas in Austin, Texas, and Bridges-2 supercomputer hosted by the Pittsburgh Supercomputing Center (PSC) and supported by Advanced Cyberinfrastructure Coordination Ecosystem: Services & Support (ACCESS) program. DFT geometry optimization, vibrational frequency, and IRC calculations were conducted using Gaussian 16 (rA.03).⁸ The CREST utility of the xTB software suite⁹ was used to locate initial starting geometries for optimization via DFT. Final images of minima and transition state structure geometries were rendered using CYLview (v1.0.600)¹⁰ and VMD (v1.9.4a53).¹¹ Routine visualization and monitoring of calculations was performed with Chemcraft (v1.8-622b).¹²

Details of Computational Methods

Gaussian 16 DFT calculations

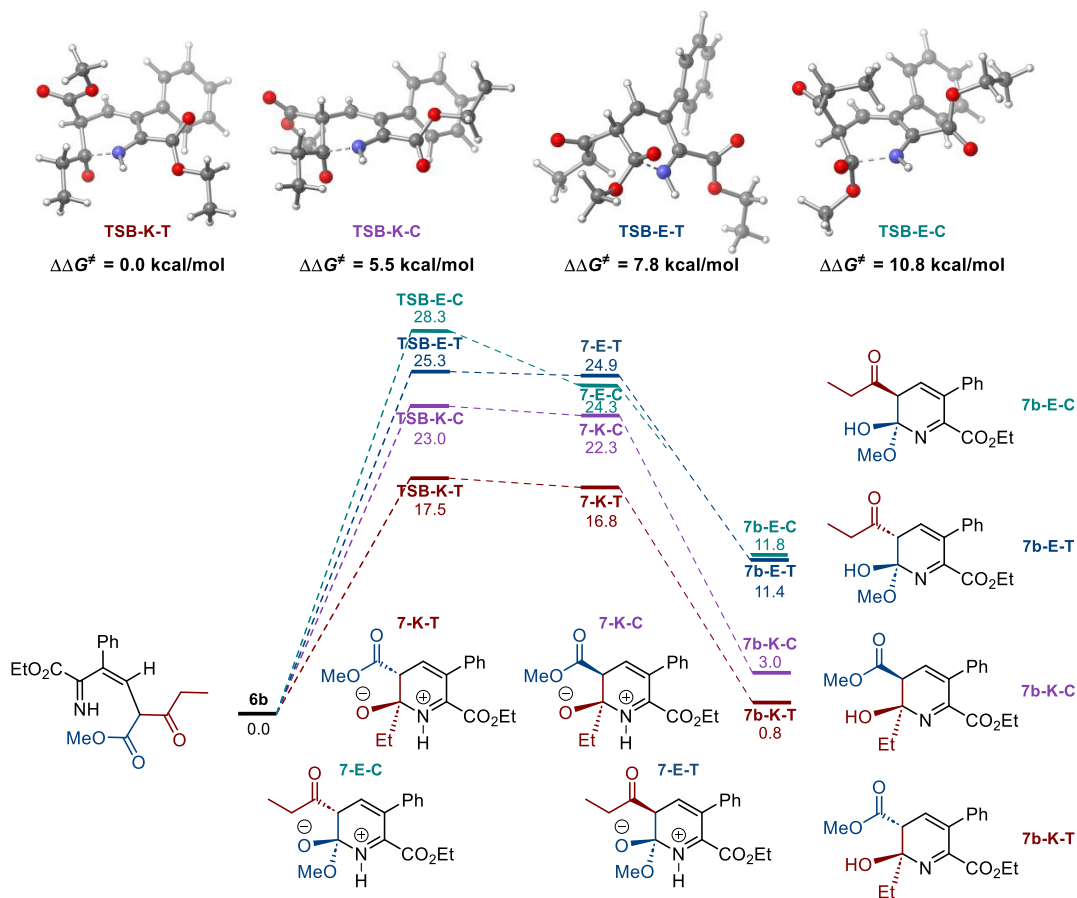
Geometries of ground state minima and transition state structures were optimized without constraints using MN15 density functional approximation and the def2-TZVP basis set in dichloromethane solvent using the SMD solvation model. Calculations were set to “tight” convergence criteria with an ultrafine grid. Frequency calculations at the same level of theory were used to confirm the nature of the isolated stationary points. Geometries with zero imaginary frequencies were deemed minima whereas those with exactly one imaginary frequency along the chemical path of interest were deemed transition state structures. Intrinsic reaction coordinate (IRC) calculations were performed to further corroborate that the located transition state structures connected reactants to products. The quasi-harmonic approximation at 1M concentration was applied via GoodVibes¹³ to all structures to correct for potential errors associated with low magnitude vibrational frequencies using a cut-off frequency of 50 cm⁻¹. Single point corrections of the above geometries were calculated using PW6B95-D3(BJ) in dichloromethane solvent under the SMD solvation model. The def2-TZVPPD basis set was used by appending diffuse functions obtained from the EMSL BSE¹⁴ to the G16-available def2-TZVPP basis set. This level of theory provided the final electronic component to the reported free energies.

Boltzmann Ensemble Averaging

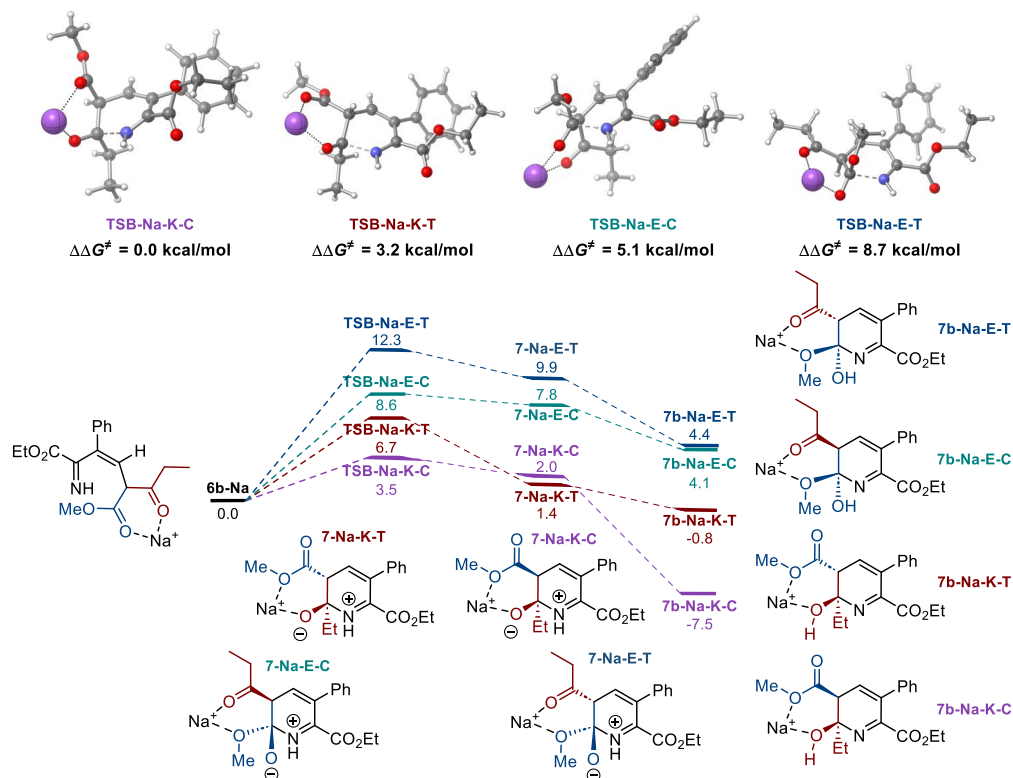
To improve the accuracy of the DFT computational analysis of the reaction pathway, ensemble averaging was applied across the obtained structurally distinct conformers of each structure, as previously described.¹⁵

Diastereomeric Energy Diagrams

Cyclization transition state **TSB** resulted in cis and trans diastereomeric reaction pathways for structures **TSB**, **7**, and **7b**, with the pathways recombining at the final products, **8-E** and **8-K**. The metal-free pathway shows kinetic preference for trans configuration in the addition of the imine nitrogen to both the keto and the ester groups. The sodium- and cesium-mediated pathways show kinetic preference for cis configuration in the addition of the imine nitrogen to both the keto and ester groups. Energy difference between the most favorable and second most favorable transition states for each pathway (metal-free, $\Delta\Delta G^\ddagger = 5.5$ kcal/mol; sodium-mediated, $\Delta\Delta G^\ddagger = 3.2$ kcal/mol; cesium mediated, $\Delta\Delta G^\ddagger = 3.3$ kcal/mol) suggest substantial kinetic preference for the lowest energy transition state over all other diastereomeric pathways.



Scheme S1. Computed Gibbs free energy profile of metal ion-free cyclization pathways, ΔG , kcal/mol.



Scheme S2. Computed Gibbs free energy profile of the sodium-mediated cyclization pathways, ΔG , kcal/mol.

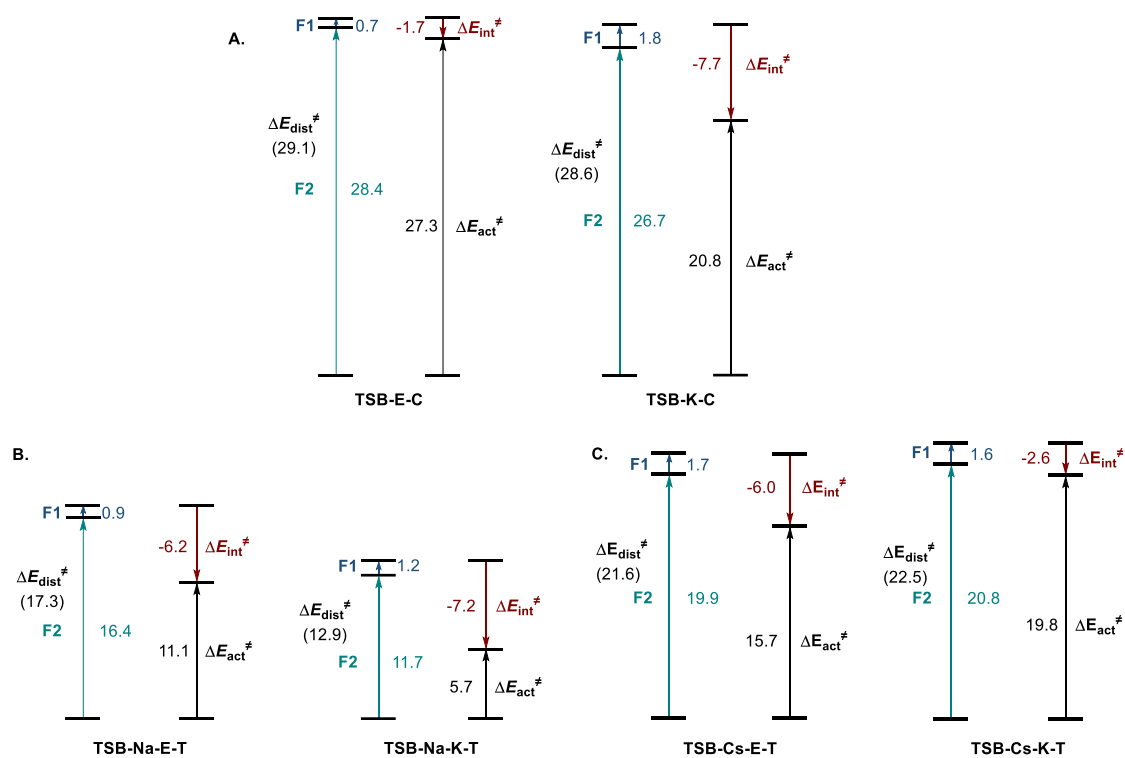


Figure S2. Distortion/Interaction analysis of the disfavored diastereomeric cyclization transition states. **A.** The cyclization process in the absence of metal ions (cis pathway). **B.** The sodium-mediated trans pathway. **C.** The cesium-mediated trans pathway. ΔE , kcal/mol.

**Conformational Analysis and Tables of Thermodynamic Values by Structure –
PW6B95(D3BJ) / def2-TZVPPD / SMD (DCM)**

5

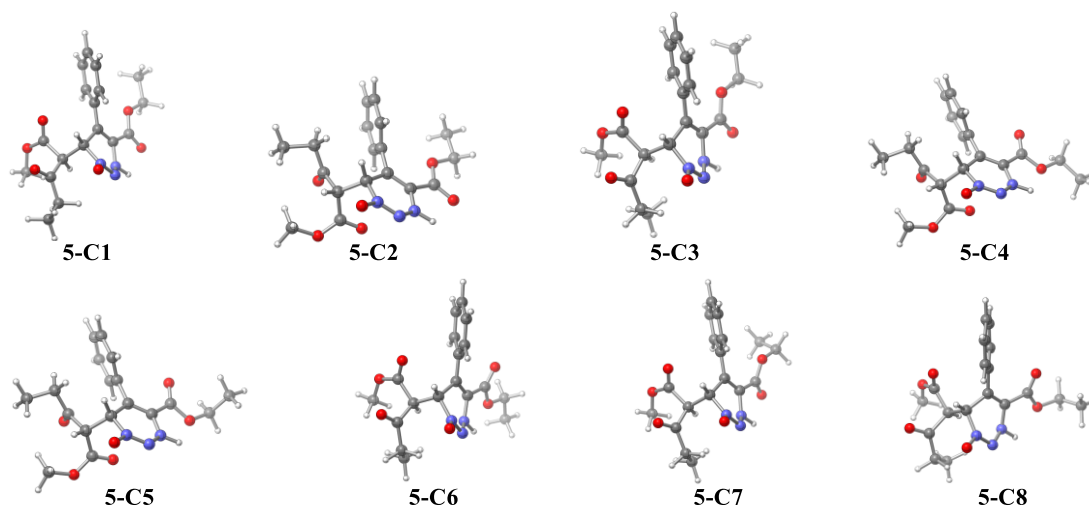


Figure S3. Conformers of addition intermediate **5**.

Table S2. Energies of conformers of addition intermediate **5**.^a

Structure	ΔE	ΔH	ΔG	ΔG (GV50)	$\Delta\Delta G$
5-C1	-1316.242973	-1315.833191	-1315.918831	-1315.915303	0.00
5-C2	-1316.242367	-1315.832843	-1315.917799	-1315.914949	0.22
5-C3	-1316.240997	-1315.831176	-1315.916271	-1315.912885	1.52
5-C4	-1316.240446	-1315.83067	-1315.915392	-1315.912628	1.68
5-C5	-1316.23976	-1315.829803	-1315.914298	-1315.911359	2.47
5-C6	-1316.239083	-1315.829015	-1315.914742	-1315.911135	2.62
5-C7	-1316.240261	-1315.830115	-1315.914123	-1315.9111	2.64
5-C8	-1316.238423	-1315.828428	-1315.914413	-1315.910414	3.07

^aEnergies were obtained as single points at the PW6B95(D3BJ) / def2-TZVPPD / SMD (DCM) level of theory based on structures optimized at the MN15 / def2-TZVP / SMD (DCM) level of theory. ΔE , ΔH , ΔG , and ΔG (GV50), hartree; $\Delta\Delta G$, kcal/mol.

TSA

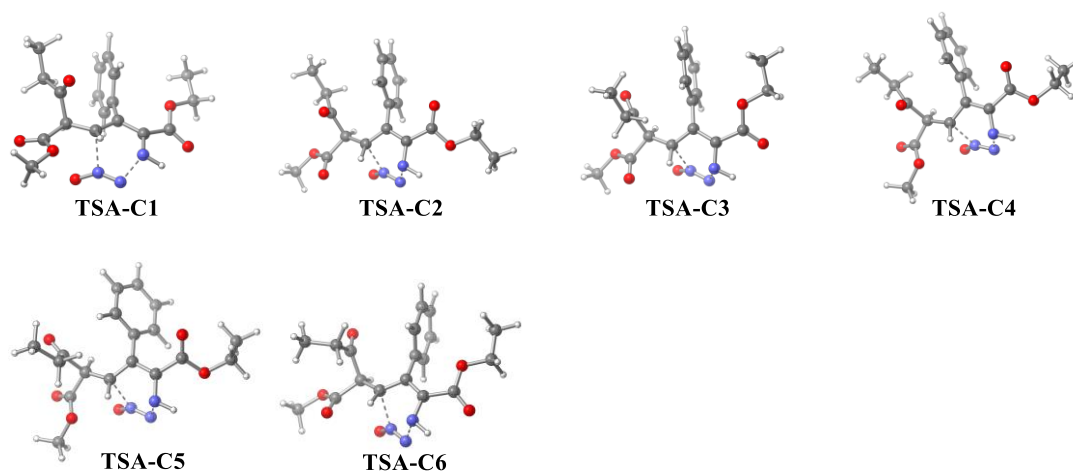


Figure S4. Conformers of N₂O extrusion transition state **TSA**.

Table S3. Energies of conformers of N₂O extrusion transition state **TSA**.^a

Structure	ΔE	ΔH	ΔG	ΔG (GV50)	$\Delta\Delta G$
TSA-C1	-1316.199217	-1315.794156	-1315.880713	-1315.878142	0.00
TSA-C2	-1316.198488	-1315.793513	-1315.880669	-1315.877761	0.24
TSA-C3	-1316.19751	-1315.792557	-1315.88	-1315.876821	0.83
TSA-C4	-1316.196803	-1315.791721	-1315.879333	-1315.875928	1.39
TSA-C5	-1316.194997	-1315.789916	-1315.876806	-1315.873672	2.80
TSA-C6	-1316.194386	-1315.789174	-1315.876952	-1315.873606	2.85

^aEnergies were obtained as single points at the PW6B95(D3BJ) / def2-TZVPPD / SMD (DCM) level of theory based on structures optimized at the MN15 / def2-TZVP / SMD (DCM) level of theory. ΔE , ΔH , ΔG , and ΔG (GV50), hartree; $\Delta\Delta G$, kcal/mol.

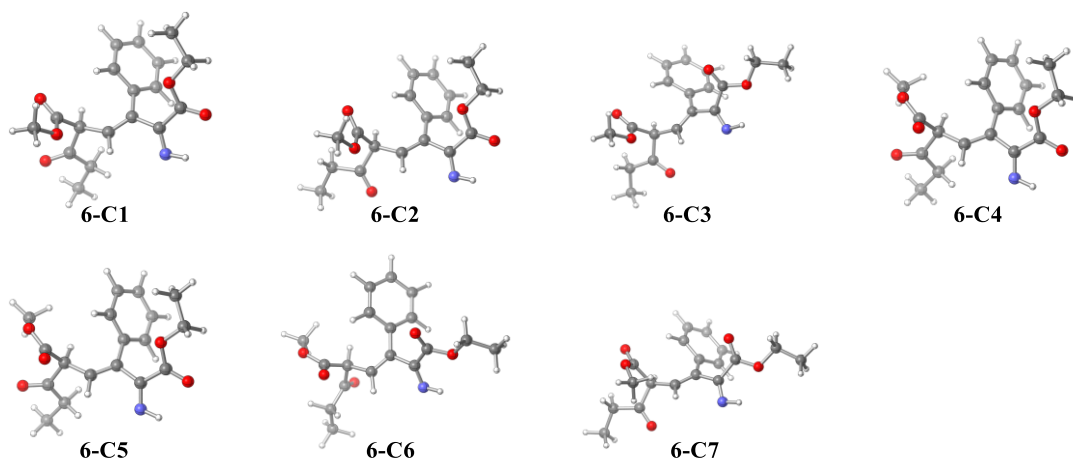


Figure S5. Conformers of extrusion intermediate **6**.

Table S4. Energies of conformers of extrusion intermediate **6**.^a

Structure	ΔE	ΔH	ΔG	ΔG (GV50)	$\Delta\Delta G$
6-C1	-1131.318146	-1130.927426	-1131.012624	-1131.008106	0.00
6-C2	-1131.316676	-1130.92589	-1131.011364	-1131.006838	0.80
6-C3	-1131.315077	-1130.924267	-1131.009997	-1131.005449	1.67
6-C4	-1131.310984	-1130.920123	-1131.004303	-1130.999982	5.10
6-C5	-1131.309155	-1130.918342	-1131.002077	-1130.998225	6.20
6-C6	-1131.306818	-1130.915871	-1130.999743	-1130.995827	7.71
6-C7	-1131.30445	-1130.913581	-1130.997096	-1130.993318	9.28

^aEnergies were obtained as single points at the PW6B95(D3BJ) / def2-TZVPPD / SMD (DCM) level of theory based on structures optimized at the MN15 / def2-TZVP / SMD (DCM) level of theory. ΔE , ΔH , ΔG , and ΔG (GV50), hartree; $\Delta\Delta G$, kcal/mol.

6b

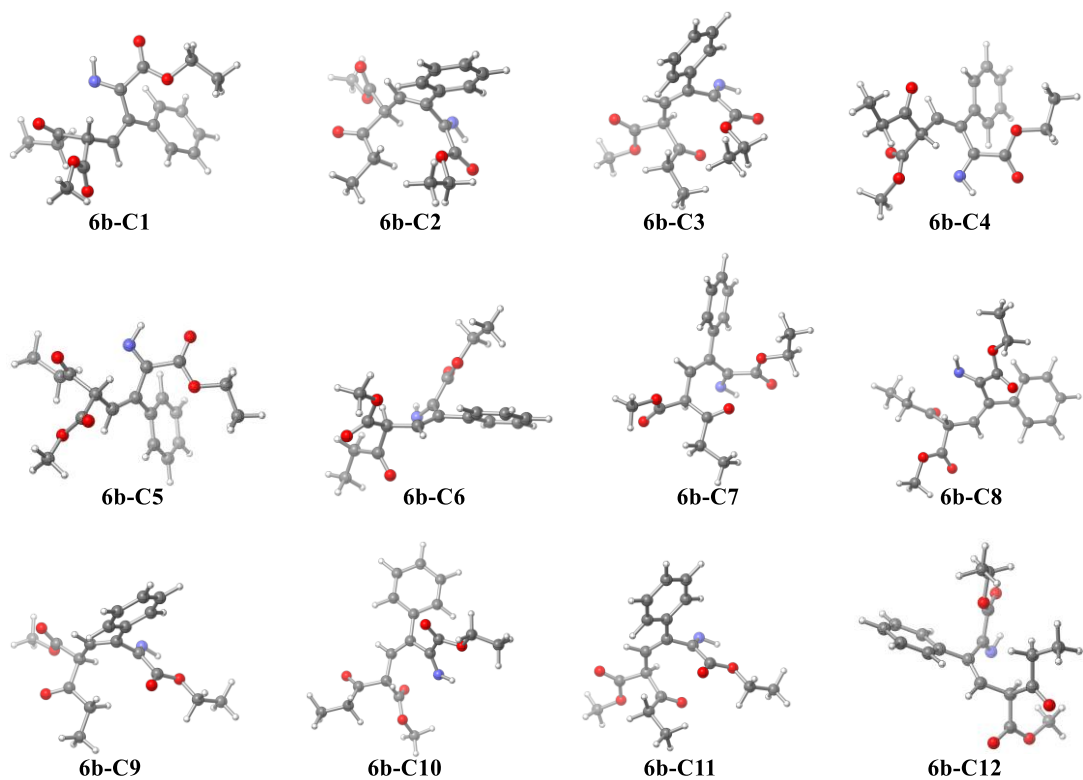


Figure S6. Conformers of isomerized intermediate **6b**.

Table S5. Energies of conformers of isomerized intermediate **6b**. ^a

Structure	ΔE	ΔH	ΔG	ΔG (GV50)	$\Delta\Delta G$
6b-C1	-1131.318958	-1130.928391	-1131.012545	-1131.0086	0.00
6b-C2	-1131.319154	-1130.928385	-1131.011964	-1131.008373	0.14
6b-C3	-1131.318089	-1130.927608	-1131.011613	-1131.007463	0.71
6b-C4	-1131.318157	-1130.927512	-1131.01067	-1131.007352	0.78
6b-C5	-1131.317976	-1130.927188	-1131.010913	-1131.0072	0.88
6b-C6	-1131.317632	-1130.926819	-1131.010577	-1131.006855	1.10
6b-C7	-1131.31655	-1130.926088	-1131.010651	-1131.006476	1.33
6b-C8	-1131.316878	-1130.926017	-1131.010281	-1131.00635	1.41
6b-C9	-1131.316688	-1130.925877	-1131.00989	-1131.006274	1.46
6b-C10	-1131.316339	-1130.925536	-1131.010182	-1131.006098	1.57
6b-C11	-1131.315391	-1130.924678	-1131.008922	-1131.004985	2.27
6b-C12	-1131.311704	-1130.9208	-1131.00364	-1131.000063	5.36

^aEnergies were obtained as single points at the PW6B95(D3BJ) / def2-TZVPPD / SMD (DCM) level of theory based on structures optimized at the MN15 / def2-TZVP / SMD (DCM) level of theory. ΔE , ΔH , ΔG , and ΔG (GV50), hartree; $\Delta\Delta G$, kcal/mol.

6b-Cs

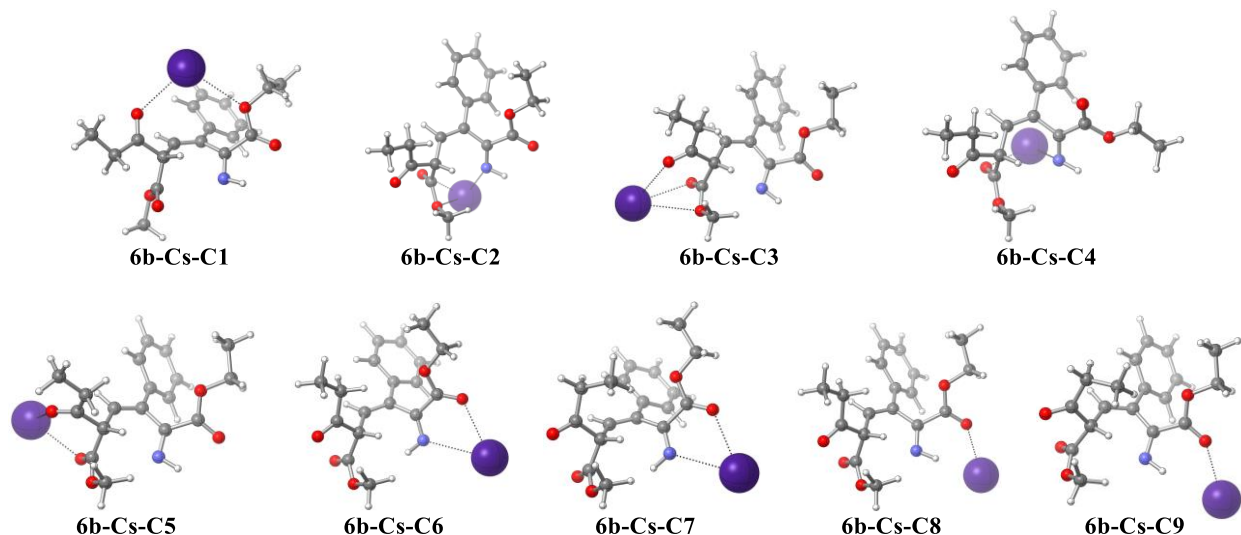


Figure S7. Conformers of cesium-coordinated isomerized intermediate **6b-Cs**.

Table S6. Energies of conformers of cesium-coordinated isomerized intermediate **6b-Cs**. ^a

Structure	ΔE	ΔH	ΔG	ΔG (GV50)	$\Delta\Delta G$
6b-Cs-C1	-1151.417318	-1151.023362	-1151.112575	-1151.108624	0.00
6b-Cs-C2	-1151.413913	-1151.019832	-1151.109166	-1151.10531	2.08
6b-Cs-C3	-1151.413084	-1151.019122	-1151.10913	-1151.104901	2.34
6b-Cs-C4	-1151.412111	-1151.018228	-1151.108677	-1151.104181	2.79
6b-Cs-C5	-1151.41269	-1151.018355	-1151.108971	-1151.104054	2.87
6b-Cs-C6	-1151.409636	-1151.015048	-1151.105093	-1151.100573	5.05
6b-Cs-C7	-1151.408912	-1151.01428	-1151.10385	-1151.099553	5.69
6b-Cs-C8	-1151.406531	-1151.012377	-1151.102211	-1151.097999	6.67
6b-Cs-C9	-1151.405714	-1151.011444	-1151.102591	-1151.097247	7.14

^aEnergies were obtained as single points at the PW6B95(D3BJ) / def2-TZVPPD / SMD (DCM) level of theory based on structures optimized at the MN15 / def2-TZVP / SMD (DCM) level of theory. ΔE , ΔH , ΔG , and ΔG (GV50), hartree; $\Delta\Delta G$, kcal/mol.

6b-Na

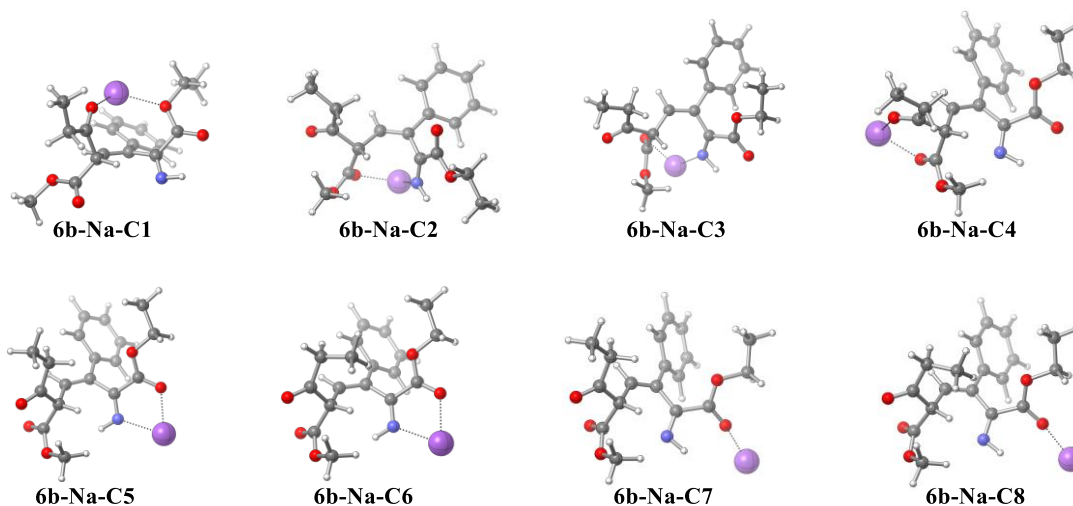


Figure S8. Conformers of sodium-coordinated isomerized intermediate **6b-Na**.

Table S7. Energies of conformers of sodium-coordinated isomerized intermediate **6b-Na**.^a

Structure	ΔE	ΔH	ΔG	ΔG (GV50)	$\Delta\Delta G$
6b-Na-C1	-1293.708364	-1293.31402	-1293.399133	-1293.396588	0.00
6b-Na-C2	-1293.704391	-1293.309956	-1293.397078	-1293.393529	1.92
6b-Na-C3	-1293.703664	-1293.309525	-1293.396133	-1293.392842	2.35
6b-Na-C4	-1293.70428	-1293.309604	-1293.395373	-1293.392165	2.78
6b-Na-C5	-1293.702677	-1293.307711	-1293.394156	-1293.390357	3.91
6b-Na-C6	-1293.702336	-1293.30707	-1293.392202	-1293.389118	4.69
6b-Na-C7	-1293.686625	-1293.292733	-1293.381195	-1293.377066	12.25
6b-Na-C8	-1293.686112	-1293.291793	-1293.379874	-1293.375435	13.27

^aEnergies were obtained as single points at the PW6B95(D3BJ) / def2-TZVPPD / SMD (DCM) level of theory based on structures optimized at the MN15 / def2-TZVP / SMD (DCM) level of theory. ΔE , ΔH , ΔG , and ΔG (GV50), hartree; $\Delta\Delta G$, kcal/mol.

TSB-E-T

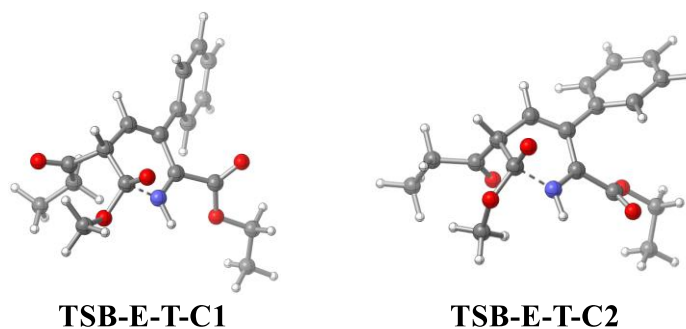


Figure S9. Conformers of ester cyclization trans transition state **TSB-E-T**.

Table S8. Energies of conformers of ester cyclization trans transition state **TSB-E-T**.^a

Structure	ΔE	ΔH	ΔG	ΔG (GV50)	$\Delta\Delta G$
TSB-E-T-C1	-1131.279933	-1130.891491	-1130.972814	-1130.969288	0.00
TSB-E-T-C2	-1131.276121	-1130.887405	-1130.965681	-1130.962761	4.10

^aEnergies were obtained as single points at the PW6B95(D3BJ) / def2-TZVPPD / SMD (DCM) level of theory based on structures optimized at the MN15 / def2-TZVP / SMD (DCM) level of theory. ΔE , ΔH , ΔG , and ΔG (GV50), hartree; $\Delta\Delta G$, kcal/mol.

TSB-E-C

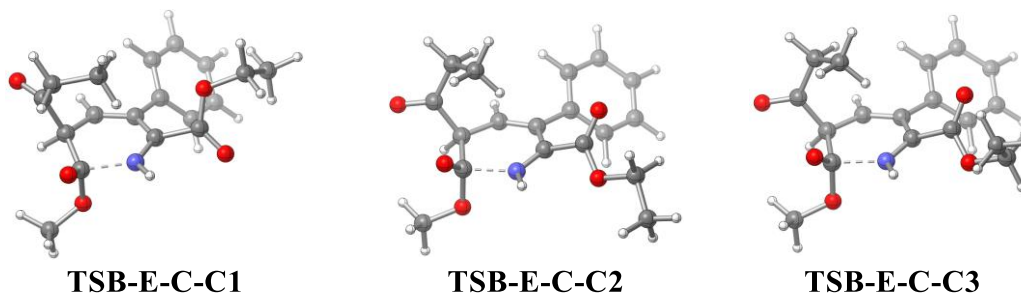


Figure S10. Conformers of ester cyclization cis transition state **TSB-E-C**.

Table S9. Energies of conformers of ester cyclization cis transition state **TSB-E-C**.^a

Structure	ΔE	ΔH	ΔG	ΔG (GV50)	$\Delta\Delta G$
TSB-E-C-C1	-1131.273262	-1130.884655	-1130.96559	-1130.961959	0.00
TSB-E-C-C2	-1131.273182	-1130.884249	-1130.964461	-1130.961458	0.31
TSB-E-C-C3	-1131.272725	-1130.883765	-1130.963504	-1130.960582	0.86

^aEnergies were obtained as single points at the PW6B95(D3BJ) / def2-TZVPPD / SMD (DCM) level of theory based on structures optimized at the MN15 / def2-TZVP / SMD (DCM) level of theory. ΔE , ΔH , ΔG , and ΔG (GV50), hartree; $\Delta\Delta G$, kcal/mol.

TSB-K-T

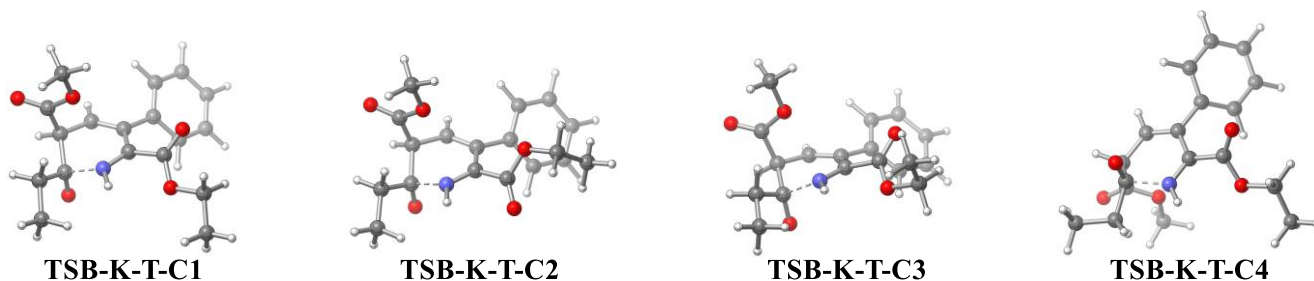


Figure S11. Conformers of ketone cyclization trans transition state **TSB-K-T**.

Table S10. Energies of conformers of ketone cyclization trans transition state **TSB-K-T**.^a

Structure	ΔE	ΔH	ΔG	ΔG (GV50)	$\Delta\Delta G$
TSB-K-T-C1	-1131.292553	-1130.903029	-1130.981893	-1130.979408	0.00
TSB-K-T-C2	-1131.292844	-1130.903409	-1130.981448	-1130.979066	0.21
TSB-K-T-C3	-1131.292053	-1130.90243	-1130.98105	-1130.978576	0.52
TSB-K-T-C4	-1131.290316	-1130.900729	-1130.979539	-1130.976878	1.59

^aEnergies were obtained as single points at the PW6B95(D3BJ) / def2-TZVPPD / SMD (DCM) level of theory based on structures optimized at the MN15 / def2-TZVP / SMD (DCM) level of theory. ΔE , ΔH , ΔG , and ΔG (GV50), hartree; $\Delta\Delta G$, kcal/mol.

TSB-K-C

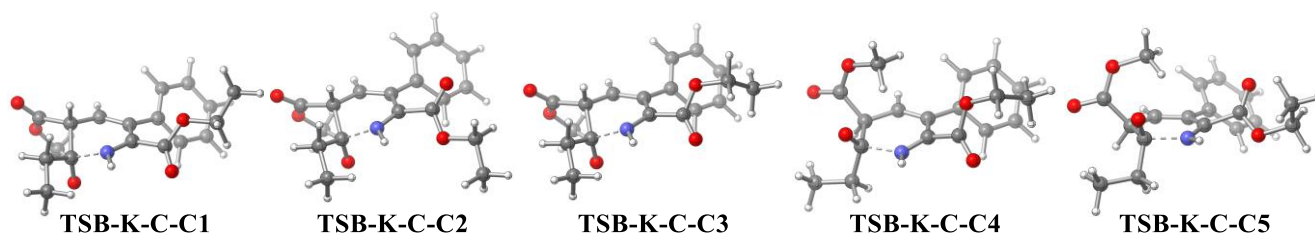


Figure S12. Conformers of ketone cyclization cis transition state **TSB-K-C**.

Table S11. Energies of conformers of ketone cyclization cis transition state **TSB-K-C**.^a

Structure	ΔE	ΔH	ΔG	ΔG (GV50)	$\Delta\Delta G$
TSB-K-C-C1	-1131.286239	-1130.897009	-1130.975863	-1130.973218	0.00
TSB-K-C-C2	-1131.285099	-1130.895775	-1130.974477	-1130.971894	0.83
TSB-K-C-C3	-1131.2855	-1130.896156	-1130.974216	-1130.971655	0.98
TSB-K-C-C4	-1131.280099	-1130.890806	-1130.968652	-1130.966269	4.36
TSB-K-C-C5	-1131.279246	-1130.889622	-1130.967568	-1130.9651	5.09

^aEnergies were obtained as single points at the PW6B95(D3BJ) / def2-TZVPPD / SMD (DCM) level of theory based on structures optimized at the MN15 / def2-TZVP / SMD (DCM) level of theory. ΔE , ΔH , ΔG , and ΔG (GV50), hartree; $\Delta\Delta G$, kcal/mol.

TSB-Cs-E-T

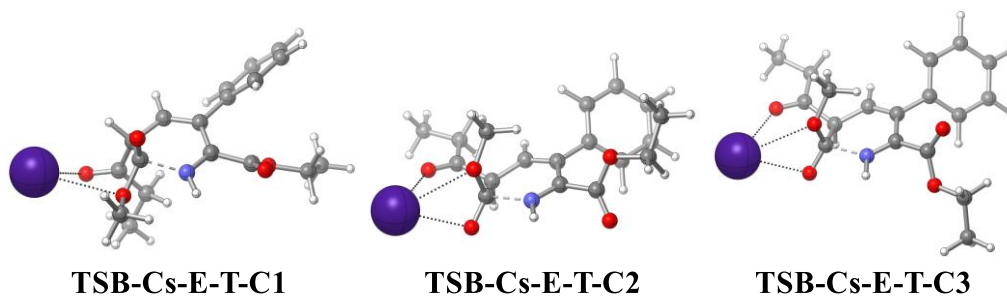


Figure S13. Conformers of cesium-coordinated ester cyclization trans transition state **TSB-Cs-E-T**.

Table S12. Energies of conformers of cesium-coordinated ester cyclization trans transition state **TSB-Cs-E-T**.^a

Structure	ΔE	ΔH	ΔG	ΔG (GV50)	$\Delta\Delta G$
TSB-Cs-E-T-C1	-1151.387739	-1150.995819	-1151.081755	-1151.078507	0.00

TSB-Cs-E-T-C2	-1151.385208	-1150.993566	-1151.078861	-1151.075213	2.07
TSB-Cs-E-T-C3	-1151.384459	-1150.992772	-1151.077911	-1151.074508	2.51

^aEnergies were obtained as single points at the PW6B95(D3BJ) / def2-TZVPPD / SMD (DCM) level of theory based on structures optimized at the MN15 / def2-TZVP / SMD (DCM) level of theory. ΔE , ΔH , ΔG , and ΔG (GV50), hartree; $\Delta\Delta G$, kcal/mol.

TSB-Cs-E-C

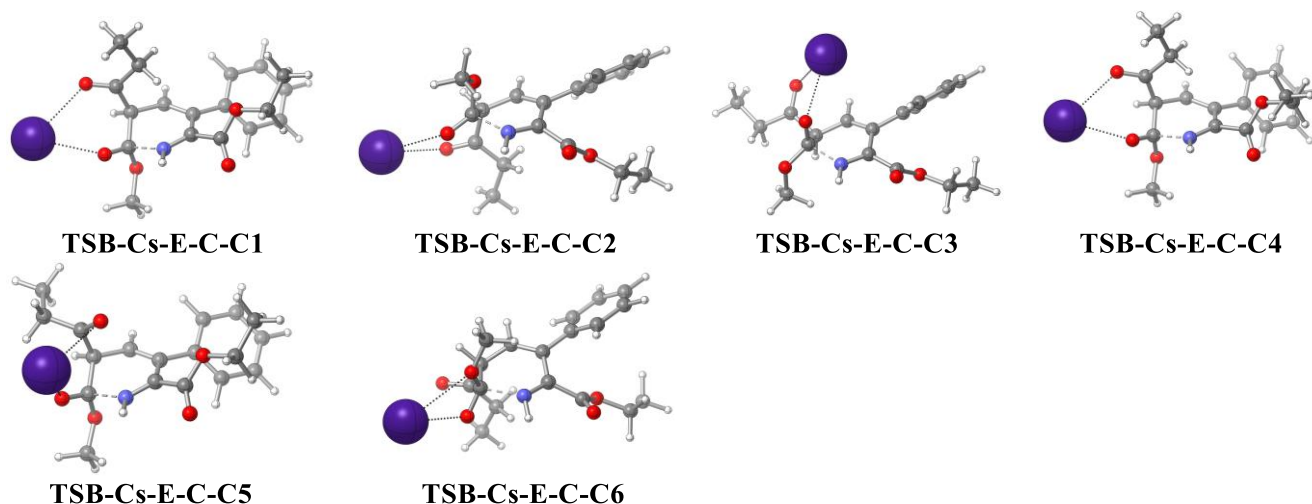


Figure S14. Conformers of cesium-coordinated ester cyclization cis transition state **TSB-Cs-E-C**.

Table S13. Energies of conformers of cesium-coordinated ester cyclization cis transition state **TSB-Cs-E-C**. ^a

Structure	ΔE	ΔH	ΔG	ΔG (GV50)	$\Delta\Delta G$
TSB-Cs-E-C-C1	-1151.391698	-1151.000171	-1151.088019	-1151.083789	0.00
TSB-Cs-E-C-C2	-1151.391724	-1151.000243	-1151.086938	-1151.083121	0.42
TSB-Cs-E-C-C3	-1151.392381	-1151.000711	-1151.086222	-1151.082758	0.65
TSB-Cs-E-C-C4	-1151.39051	-1150.99878	-1151.086447	-1151.082228	0.98
TSB-Cs-E-C-C5	-1151.389591	-1150.997665	-1151.084742	-1151.081116	1.68
TSB-Cs-E-C-C6	-1151.387921	-1150.99624	-1151.084619	-1151.079629	2.61

^aEnergies were obtained as single points at the PW6B95(D3BJ) / def2-TZVPPD / SMD (DCM) level of theory based on structures optimized at the MN15 / def2-TZVP / SMD (DCM) level of theory. ΔE , ΔH , ΔG , and ΔG (GV50), hartree; $\Delta\Delta G$, kcal/mol.

TSB-Cs-K-T

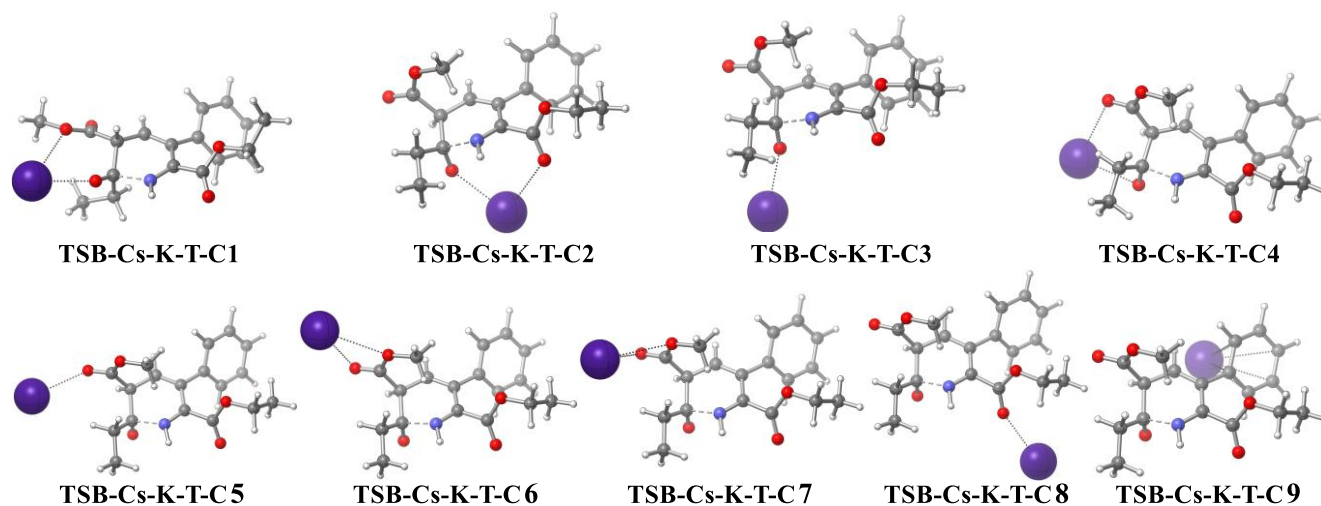


Figure S15. Conformers of cesium-coordinated ketone cyclization trans transition state **TSB-Cs-K-T**.

Table S14. Energies of conformers of cesium-coordinated ketone cyclization trans transition state **TSB-Cs-K-T**.^a

Structure	ΔE	ΔH	ΔG	ΔG (GV50)	$\Delta\Delta G$
TSB-Cs-K-T-C1	-1151.398956	-1151.00674	-1151.09289	-1151.089481	0.00
TSB-Cs-K-T-C2	-1151.382226	-1150.98941	-1151.074884	-1151.071333	11.39
TSB-Cs-K-T-C3	-1151.381473	-1150.988697	-1151.075356	-1151.071226	11.46
TSB-Cs-K-T-C4	-1151.379695	-1150.986665	-1151.072798	-1151.069043	12.83
TSB-Cs-K-T-C5	-1151.376443	-1150.983668	-1151.070114	-1151.066033	14.71
TSB-Cs-K-T-C6	-1151.375989	-1150.983253	-1151.069218	-1151.065563	15.01
TSB-Cs-K-T-C7	-1151.376068	-1150.983208	-1151.067824	-1151.064618	15.60
TSB-Cs-K-T-C8	-1151.373221	-1150.980386	-1151.0651	-1151.061769	17.39
TSB-Cs-K-T-C9	-1151.373216	-1150.980227	-1151.063851	-1151.06134	17.66

^aEnergies were obtained as single points at the PW6B95(D3BJ) / def2-TZVPPD / SMD (DCM) level of theory based on structures optimized at the MN15 / def2-TZVP / SMD (DCM) level of theory. ΔE , ΔH , ΔG , and ΔG (GV50), hartree; $\Delta\Delta G$, kcal/mol.

TSB-Cs-K-C

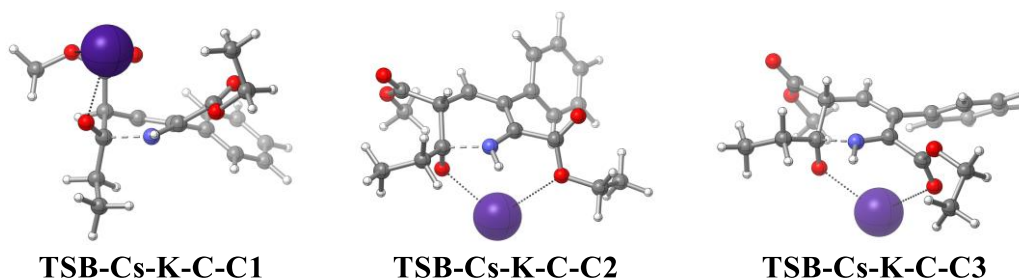


Figure S16. Conformers of cesium-coordinated ketone cyclization cis transition state **TSB-Cs-K-C**.

Table S15. Energies of conformers of cesium-coordinated ketone cyclization cis transition state **TSB-Cs-K-C**.^a

Structure	ΔE	ΔH	ΔG	ΔG (GV50)	$\Delta\Delta G$
TSB-Cs-K-C-C1	-1151.3932	-1151.000009	-1151.083425	-1151.080735	0.00
TSB-Cs-K-C-C2	-1151.385587	-1150.99305	-1151.078693	-1151.075312	3.40
TSB-Cs-K-C-C3	-1151.385812	-1150.992722	-1151.076855	-1151.074354	4.00

^aEnergies were obtained as single points at the PW6B95(D3BJ) / def2-TZVPPD / SMD (DCM) level of theory based on structures optimized at the MN15 / def2-TZVP / SMD (DCM) level of theory. ΔE , ΔH , ΔG , and ΔG (GV50), hartree; $\Delta\Delta G$, kcal/mol.

TSB-Na-E-T

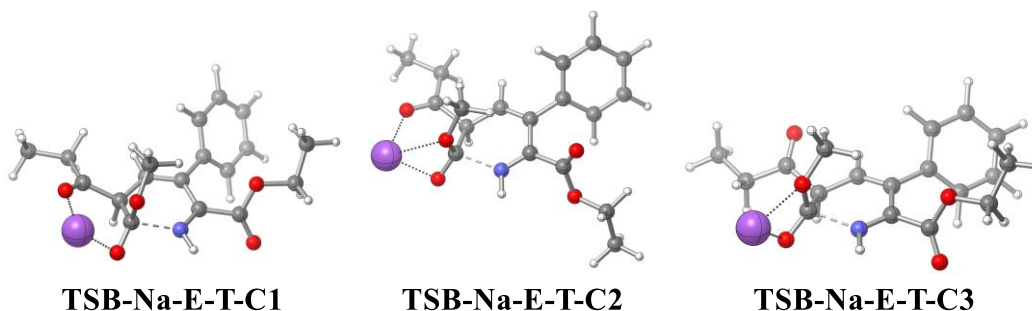


Figure S17. Conformers of sodium-coordinated ester cyclization trans transition state **TSB-Na-E-T**.

Table S16. Energies of conformers of sodium-coordinated ester cyclization trans transition state **TSB-Na-E-T**.^a

Structure	ΔE	ΔH	ΔG	ΔG (GV50)	$\Delta\Delta G$
-----------	------------	------------	------------	-------------------	------------------

TSB-Na-E-T-C1	-1293.68462	-1293.292346	-1293.374027	-1293.371183	0.000
TSB-Na-E-T-C2	-1293.684077	-1293.291849	-1293.373488	-1293.370828	0.222
TSB-Na-E-T-C3	-1293.676163	-1293.284265	-1293.367953	-1293.364818	3.994

^aEnergies were obtained as single points at the PW6B95(D3BJ) / def2-TZVPPD / SMD (DCM) level of theory based on structures optimized at the MN15 / def2-TZVP / SMD (DCM) level of theory. ΔE , ΔH , ΔG , and ΔG (GV50), hartree; $\Delta\Delta G$, kcal/mol.

TSB-Na-E-C

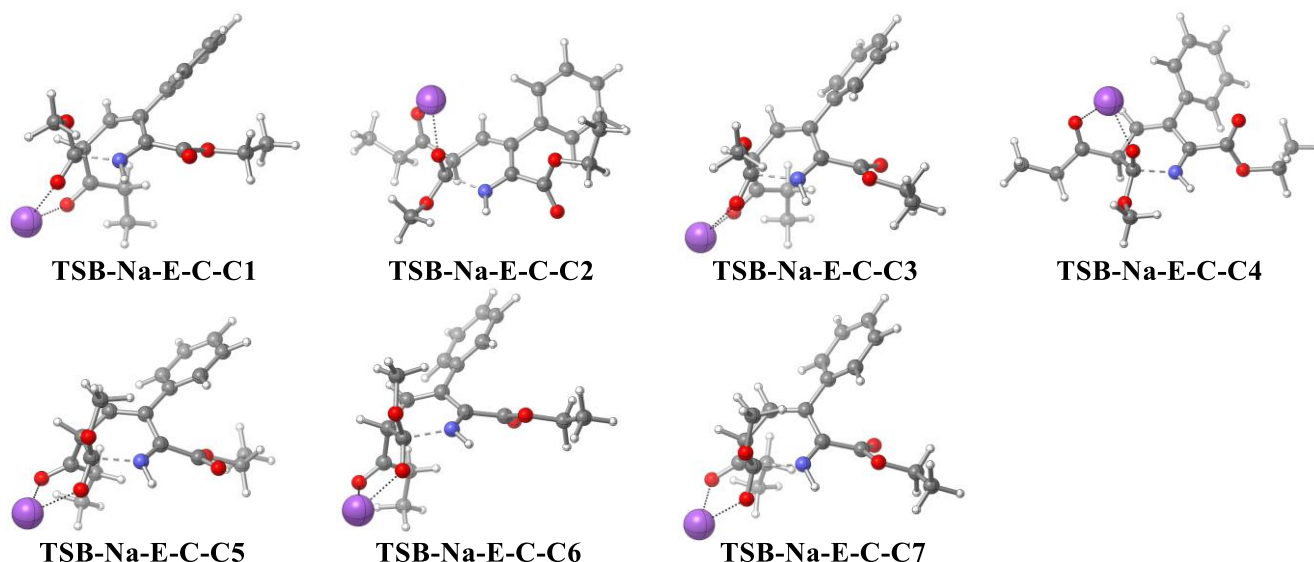


Figure S18. Conformers of sodium-coordinated ester cyclization cis transition state **TSB-Na-E-C**.

Table S17. Energies of conformers of sodium-coordinated ester cyclization cis transition state **TSB-Na-E-C**.^a

Structure	ΔE	ΔH	ΔG	ΔG (GV50)	$\Delta\Delta G$
TSB-Na-E-C-C1	-1293.690002	-1293.29828	-1293.382565	-1293.378835	0.00
TSB-Na-E-C-C2	-1293.688877	-1293.296999	-1293.38188	-1293.378059	0.49
TSB-Na-E-C-C3	-1293.688891	-1293.296945	-1293.381539	-1293.378026	0.51
TSB-Na-E-C-C4	-1293.688349	-1293.296011	-1293.379802	-1293.376652	1.37
TSB-Na-E-C-C5	-1293.683539	-1293.29155	-1293.37443	-1293.371119	4.84

TSB-Na-E-C-C6	-1293.682551	-1293.29057	-1293.374349	-1293.37067	5.12
TSB-Na-E-C-C7	-1293.682682	-1293.290246	-1293.372822	-1293.36958	5.81

^aEnergies were obtained as single points at the PW6B95(D3BJ) / def2-TZVPPD / SMD (DCM) level of theory based on structures optimized at the MN15 / def2-TZVP / SMD (DCM) level of theory. ΔE , ΔH , ΔG , and ΔG (GV50), hartree; $\Delta\Delta G$, kcal/mol.

TSB-Na-K-T

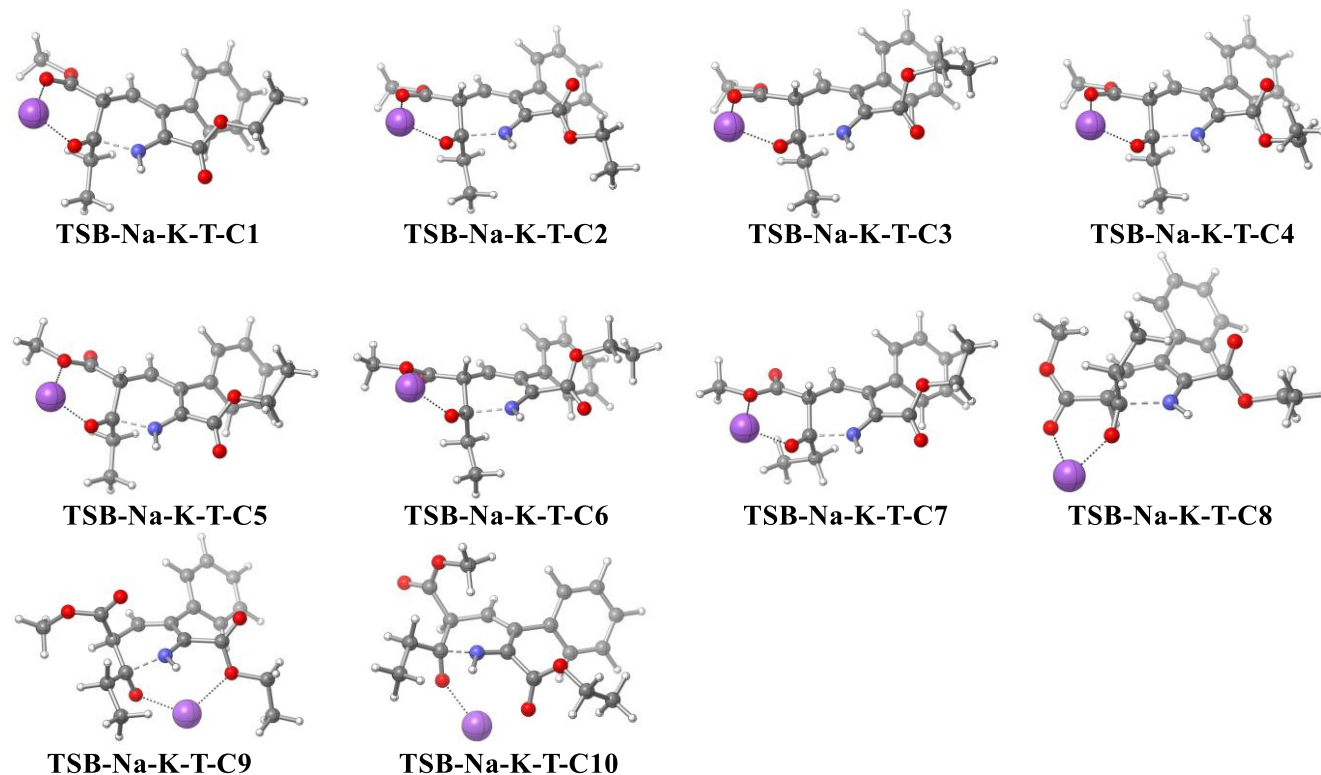


Figure S19. Conformers of sodium-coordinated ketone cyclization trans transition state **TSB-Na-K-T**.

Table S18. Energies of conformers of sodium-coordinated ketone cyclization trans transition state **TSB-Na-K-T**.^a

Structure	ΔE	ΔH	ΔG	ΔG (GV50)	$\Delta\Delta G$
TSB-Na-K-T-C1	-1293.700428	-1293.307574	-1293.390604	-1293.38811	0.00
TSB-Na-K-T-C2	-1293.699101	-1293.306369	-1293.39101	-1293.387474	0.40
TSB-Na-K-T-C3	-1293.699767	-1293.306802	-1293.389036	-1293.386596	0.95
TSB-Na-K-T-C4	-1293.698636	-1293.305451	-1293.388818	-1293.38578	1.46

TSB-Na-K-T-C5	-1293.69505	-1293.302329	-1293.385406	-1293.382821	3.32
TSB-Na-K-T-C6	-1293.694404	-1293.301477	-1293.383684	-1293.38136	4.24
TSB-Na-K-T-C7	-1293.693882	-1293.301042	-1293.383172	-1293.380893	4.53
TSB-Na-K-T-C8	-1293.675437	-1293.282229	-1293.363737	-1293.361179	16.90
TSB-Na-K-T-C9	-1293.675612	-1293.282179	-1293.362555	-1293.361088	16.96
TSB-Na-K-T-C10	-1293.674443	-1293.281039	-1293.363346	-1293.360422	17.37

^aEnergies were obtained as single points at the PW6B95(D3BJ) / def2-TZVPPD / SMD (DCM) level of theory based on structures optimized at the MN15 / def2-TZVP / SMD (DCM) level of theory. ΔE , ΔH , ΔG , and ΔG (GV50), hartree; $\Delta\Delta G$, kcal/mol.

TSB-Na-K-C

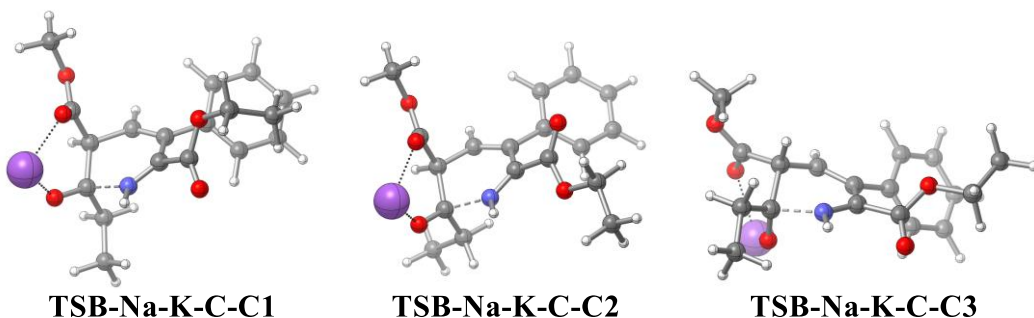


Figure S20. Conformers of sodium-coordinated ketone cyclization cis transition state **TSB-Na-K-C**

Table S19. Energies of conformers of sodium-coordinated ketone cyclization cis transition state **TSB-Na-K-C**.^a

Structure	ΔE	ΔH	ΔG	ΔG (GV50)	$\Delta\Delta G$
TSB-Na-K-C-C1	-1293.696895	-1293.303979	-1293.388198	-1293.384486	0.00
TSB-Na-K-C-C2	-1293.695116	-1293.302311	-1293.387276	-1293.383284	0.75
TSB-Na-K-C-C3	-1293.69421	-1293.301267	-1293.38352	-1293.380796	2.32

^aEnergies were obtained as single points at the PW6B95(D3BJ) / def2-TZVPPD / SMD (DCM) level of theory based on structures optimized at the MN15 / def2-TZVP / SMD (DCM) level of theory. ΔE , ΔH , ΔG , and ΔG (GV50), hartree; $\Delta\Delta G$, kcal/mol.

7-E-T

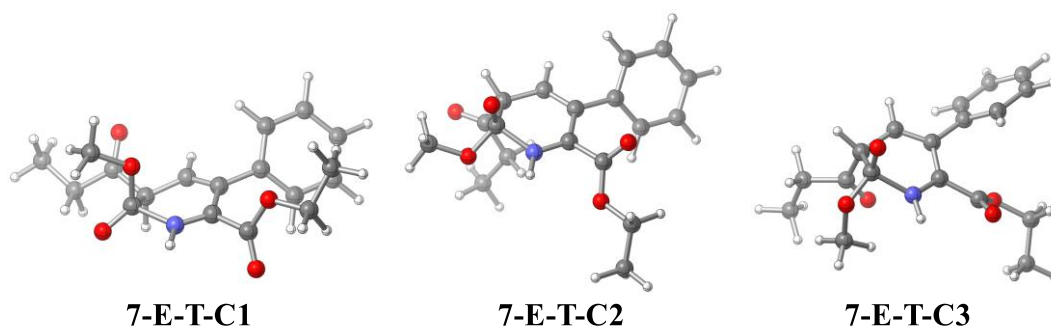


Figure S21. Conformers of the ester cyclization trans zwitterion **7-E-T**

Table S20. Energies of conformers of ester cyclization trans zwitterion **7-E-T**^a

Structure	ΔE	ΔH	ΔG	ΔG (GV50)	$\Delta\Delta G$
7-E-T-C1	-1131.27941	-1130.890415	-1130.971763	-1130.968923	0.00
7-E-T-C2	-1131.280776	-1130.890868	-1130.971201	-1130.968187	0.46
7-E-T-C3	-1131.276098	-1130.886372	-1130.966041	-1130.963103	3.65

^aEnergies were obtained as single points at the PW6B95(D3BJ) / def2-TZVPPD / SMD (DCM) level of theory based on structures optimized at the MN15 / def2-TZVP / SMD (DCM) level of theory. ΔE , ΔH , ΔG , and ΔG (GV50), hartree; $\Delta\Delta G$, kcal/mol.

7-E-C

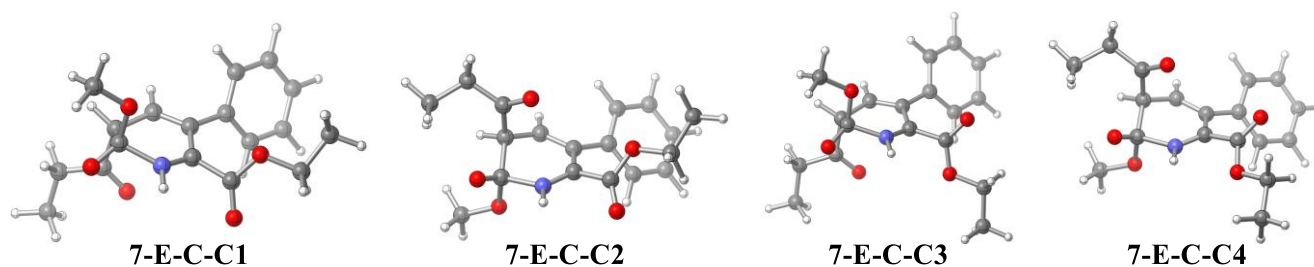


Figure S22. Conformers of the ester cyclization cis zwitterion **7-E-C**

Table S21. Energies of conformers of ester cyclization cis zwitterion **7-E-C**^a

Structure	ΔE	ΔH	ΔG	ΔG (GV50)	$\Delta\Delta G$
7-E-C-C1	-1131.280029	-1130.890687	-1130.97235	-1130.968938	0.00

7-E-C-C2	-1131.279698	-1130.889941	-1130.971489	-1130.968166	0.48
7-E-C-C3	-1131.279599	-1130.889997	-1130.97129	-1130.968049	0.56
7-E-C-C4	-1131.278432	-1130.888163	-1130.967698	-1130.965334	2.26

^aEnergies were obtained as single points at the PW6B95(D3BJ) / def2-TZVPPD / SMD (DCM) level of theory based on structures optimized at the MN15 / def2-TZVP / SMD (DCM) level of theory. ΔE , ΔH , ΔG , and ΔG (GV50), hartree; $\Delta\Delta G$, kcal/mol.

7-K-T

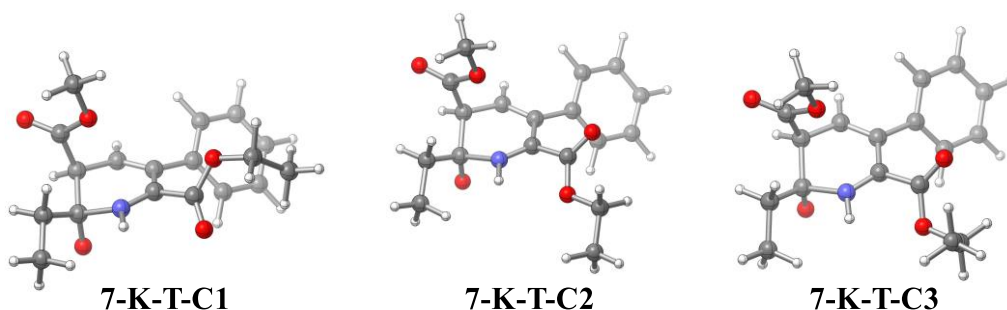


Figure S23. Conformers of the ketone cyclization trans zwitterion **7-K-T**

Table S22. Energies of conformers of ketone cyclization trans zwitterion **7-K-T**^a

Structure	ΔE	ΔH	ΔG	ΔG (GV50)	$\Delta\Delta G$
7-K-T-C1	-1131.292882	-1130.902452	-1130.983396	-1130.979933	0.00
7-K-T-C2	-1131.292506	-1130.901975	-1130.98232	-1130.979719	0.13
7-K-T-C3	-1131.292007	-1130.901402	-1130.981582	-1130.978962	0.61

^aEnergies were obtained as single points at the PW6B95(D3BJ) / def2-TZVPPD / SMD (DCM) level of theory based on structures optimized at the MN15 / def2-TZVP / SMD (DCM) level of theory. ΔE , ΔH , ΔG , and ΔG (GV50), hartree; $\Delta\Delta G$, kcal/mol.

7-K-C

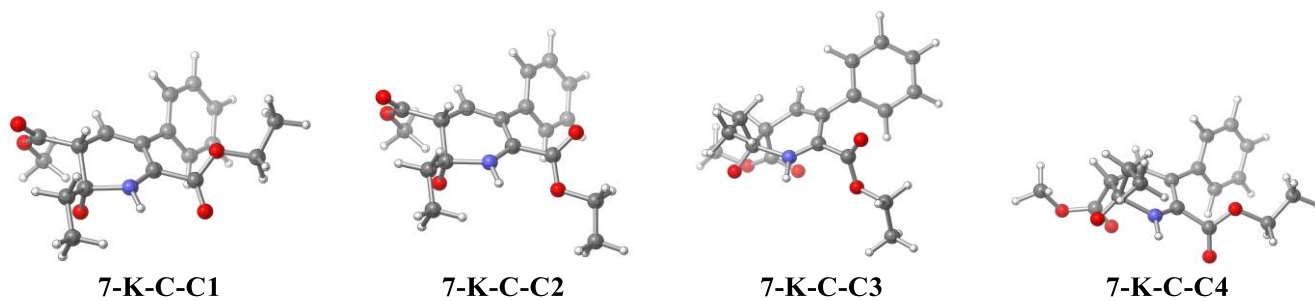


Figure S24. Conformers of the ketone cyclization cis zwitterion **7-K-C**

Table S23. Energies of conformers of ketone cyclization cis zwitterion **7-K-C**^a

Structure	ΔE	ΔH	ΔG	ΔG (GV50)	$\Delta\Delta G$
7-K-C-C1	-1131.286255	-1130.895797	-1130.974614	-1130.9723	0.00
7-K-C-C2	-1131.284978	-1130.894603	-1130.974559	-1130.971751	0.34
7-K-C-C3	-1131.282596	-1130.892263	-1130.972633	-1130.969883	1.52
7-K-C-C4	-1131.282558	-1130.892213	-1130.971671	-1130.969331	1.86

^aEnergies were obtained as single points at the PW6B95(D3BJ) / def2-TZVPPD / SMD (DCM) level of theory based on structures optimized at the MN15 / def2-TZVP / SMD (DCM) level of theory. ΔE , ΔH , ΔG , and ΔG (GV50), hartree; $\Delta\Delta G$, kcal/mol.

7-Cs-E-T

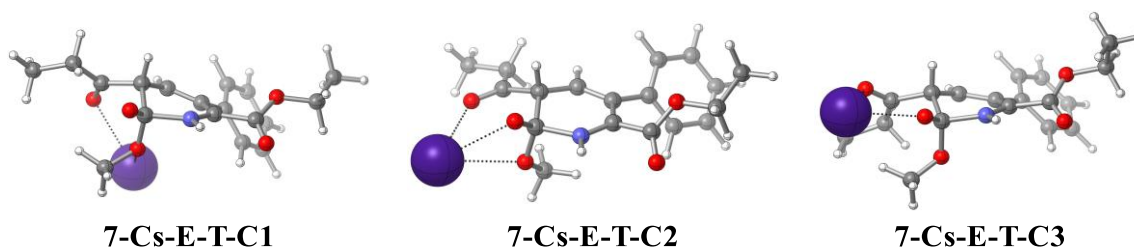


Figure S25. Conformers of cesium-coordinated ester cyclization trans zwitterion **7-Cs-E-T**

Table S24. Energies of conformers of cesium-coordinated ester cyclization trans zwitterion **7-Cs-E-T**^a

Structure	ΔE	ΔH	ΔG	ΔG (GV50)	$\Delta\Delta G$
7-Cs-E-T-C1	-1151.387009	-1150.994511	-1151.083205	-1151.078839	0.00

7-Cs-E-T-C2	-1151.387394	-1150.994779	-1151.081461	-1151.077577	0.79
7-Cs-E-T-C3	-1151.387523	-1150.994716	-1151.081012	-1151.077543	0.81

^aEnergies were obtained as single points at the PW6B95(D3BJ) / def2-TZVPPD / SMD (DCM) level of theory based on structures optimized at the MN15 / def2-TZVP / SMD (DCM) level of theory. ΔE , ΔH , ΔG , and ΔG (GV50), hartree; $\Delta\Delta G$, kcal/mol.

7-Cs-E-C

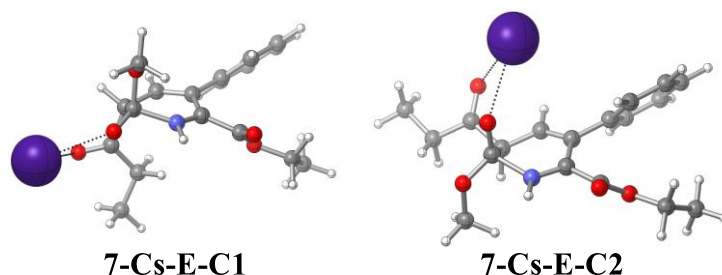


Figure S26. Conformers of cesium-coordinated ester cyclization cis zwitterion **7-Cs-E-C**

Table S25. Energies of conformers of cesium-coordinated ester cyclization cis zwitterion **7-Cs-E-C**^a

Structure	ΔE	ΔH	ΔG	ΔG (GV50)	$\Delta\Delta G$
7-Cs-E-C-C1	-1151.3915	-1150.998894	-1151.088153	-1151.083507	0.00
7-Cs-E-C-C2	-1151.392287	-1150.999742	-1151.087399	-1151.083429	0.05

^aEnergies were obtained as single points at the PW6B95(D3BJ) / def2-TZVPPD / SMD (DCM) level of theory based on structures optimized at the MN15 / def2-TZVP / SMD (DCM) level of theory. ΔE , ΔH , ΔG , and ΔG (GV50), hartree; $\Delta\Delta G$, kcal/mol.

7-Cs-K-T

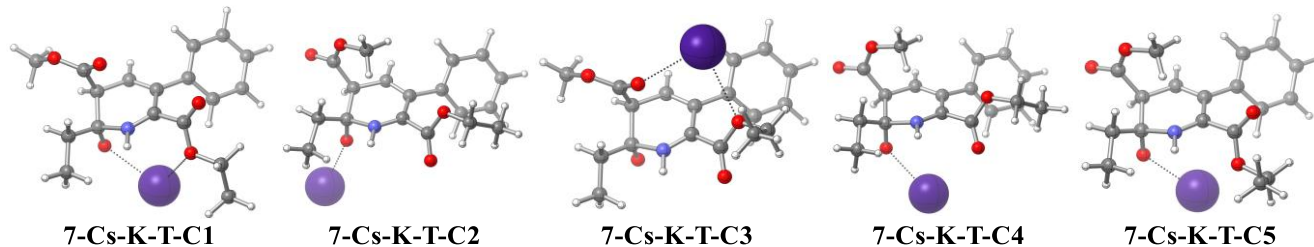
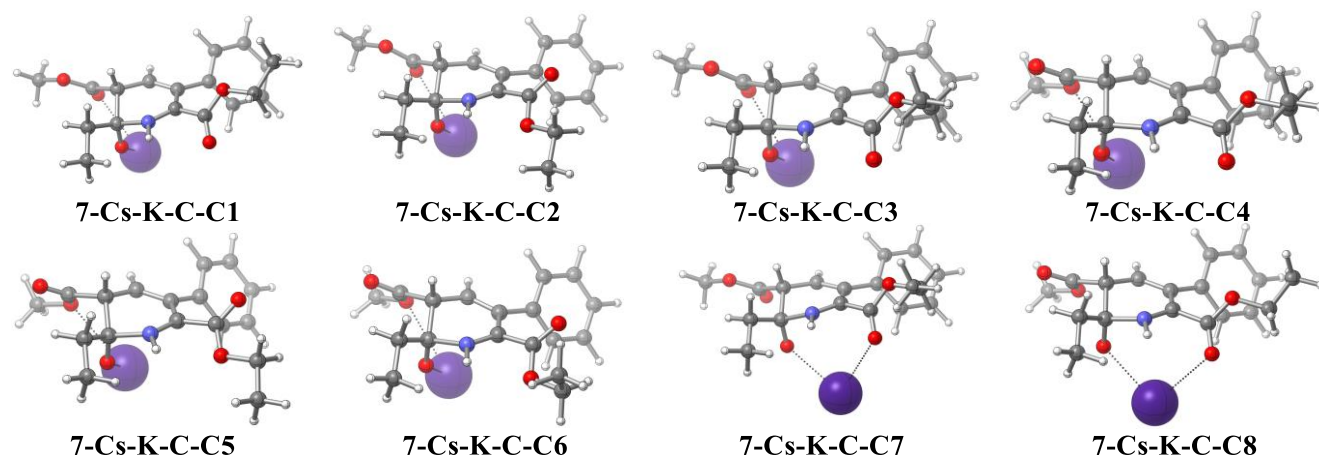


Figure S27. Conformers of cesium-coordinated ketone cyclization trans zwitterion **7-Cs-K-T**

Table S26. Energies of conformers of cesium-coordinated ketone cyclization trans zwitterion **7-Cs-K-T^a**

Structure	ΔE	ΔH	ΔG	ΔG (GV50)	$\Delta\Delta G$
7-Cs-K-T-C1	-1151.38841	-1150.993995	-1151.077868	-1151.075694	0.00
7-Cs-K-T-C2	-1151.384137	-1150.9897	-1151.0764	-1151.072137	2.23
7-Cs-K-T-C3	-1151.38519	-1150.990722	-1151.074451	-1151.072063	2.28
7-Cs-K-T-C4	-1151.383714	-1150.989291	-1151.073753	-1151.070826	3.05
7-Cs-K-T-C5	-1151.381412	-1150.98702	-1151.071301	-1151.068553	4.48

7-Cs-K-C**Figure S28.** Conformers of cesium-coordinated ketone cyclization cis zwitterion **7-Cs-K-C****Table S27.** Energies of conformers of cesium-coordinated ketone cyclization cis zwitterion **7-Cs-K-C^a**

Structure	ΔE	ΔH	ΔG	ΔG (GV50)	$\Delta\Delta G$
7-Cs-K-C-C1	-1151.405361	-1151.011357	-1151.098298	-1151.094438	0.00
7-Cs-K-C-C2	-1151.403936	-1151.009852	-1151.097115	-1151.093215	0.77
7-Cs-K-C-C3	-1151.404194	-1151.010077	-1151.097222	-1151.093118	0.83
7-Cs-K-C-C4	-1151.401705	-1151.007492	-1151.094033	-1151.090405	2.53
7-Cs-K-C-C5	-1151.4011	-1151.007184	-1151.092999	-1151.090201	2.66
7-Cs-K-C-C6	-1151.400965	-1151.006688	-1151.092327	-1151.089188	3.29
7-Cs-K-C-C7	-1151.39901	-1151.005086	-1151.09353	-1151.08904	3.39

7-Cs-K-C-C8	-1151.399391	-1151.00554	-1151.092655	-1151.088706	3.60
--------------------	--------------	-------------	--------------	--------------	------

^aEnergies were obtained as single points at the PW6B95(D3BJ) / def2-TZVPPD / SMD (DCM) level of theory based on structures optimized at the MN15 / def2-TZVP / SMD (DCM) level of theory. ΔE , ΔH , ΔG , and ΔG (GV50), hartree; $\Delta\Delta G$, kcal/mol.

7-Na-E-T

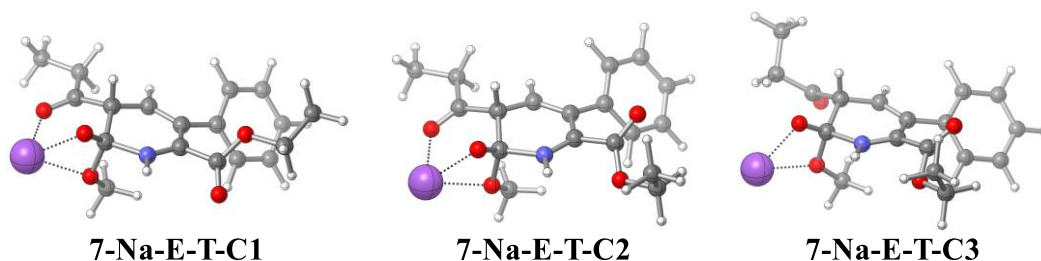


Figure S29. Conformers of sodium-coordinated ester cyclization trans zwitterion **7-Na-E-T**

Table S28. Energies of conformers of sodium-coordinated ester cyclization trans zwitterion **7-Na-E-T**^a

Structure	ΔE	ΔH	ΔG	ΔG (GV50)	$\Delta\Delta G$
7-Na-E-T-C1	-1293.690763	-1293.297521	-1293.380594	-1293.377208	0.00
7-Na-E-T-C2	-1293.688945	-1293.295473	-1293.37647	-1293.374172	1.90
7-Na-E-T-C3	-1293.67976	-1293.286083	-1293.370204	-1293.366713	6.59

^aEnergies were obtained as single points at the PW6B95(D3BJ) / def2-TZVPPD / SMD (DCM) level of theory based on structures optimized at the MN15 / def2-TZVP / SMD (DCM) level of theory. ΔE , ΔH , ΔG , and ΔG (GV50), hartree; $\Delta\Delta G$, kcal/mol.

7-Na-E-C

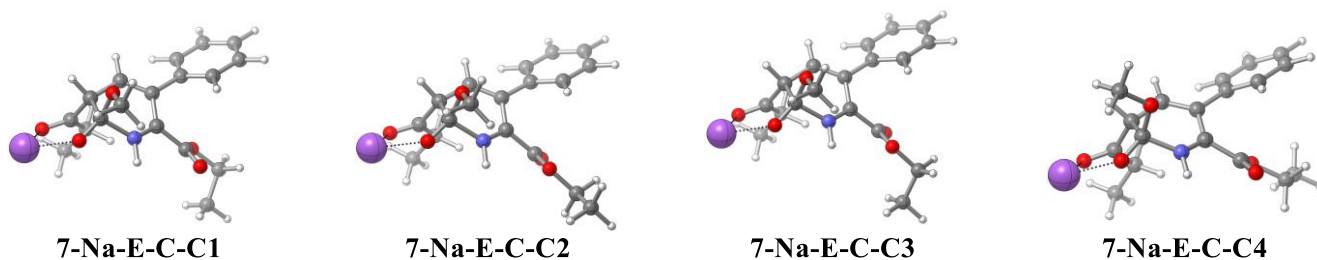
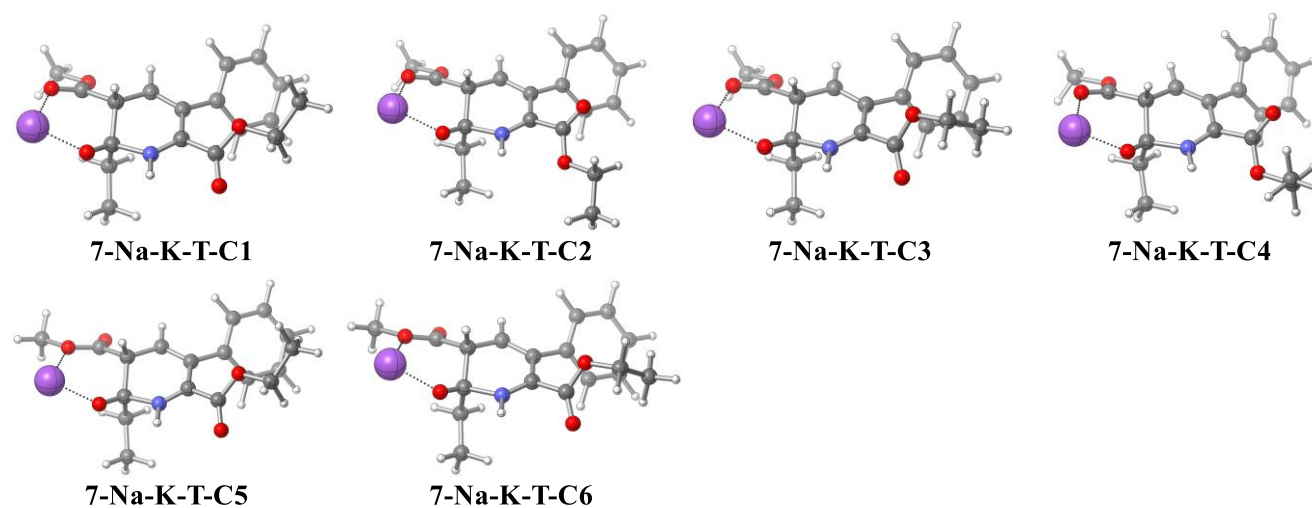


Figure S30. Conformers of sodium-coordinated ester cyclization cis zwitterion **7-Na-E-C**

Table S29. Energies of conformers of sodium-coordinated ester cyclization cis zwitterion **7-Na-E-C**^a

Structure	ΔE	ΔH	ΔG	ΔG (GV50)	$\Delta\Delta G$
7-Na-E-C-C1	-1293.689303	-1293.296063	-1293.379956	-1293.376738	0.00
7-Na-E-C-C2	-1293.689222	-1293.296017	-1293.379457	-1293.376619	0.07
7-Na-E-C-C3	-1293.688758	-1293.295534	-1293.378991	-1293.376066	0.42
7-Na-E-C-C4	-1293.687808	-1293.294649	-1293.378254	-1293.375061	1.05

^aEnergies were obtained as single points at the PW6B95(D3BJ) / def2-TZVPPD / SMD (DCM) level of theory based on structures optimized at the MN15 / def2-TZVP / SMD (DCM) level of theory. ΔE , ΔH , ΔG , and ΔG (GV50), hartree; $\Delta\Delta G$, kcal/mol.

7-Na-K-T**Figure S31.** Conformers of sodium-coordinated ketone cyclization trans zwitterion **7-Na-K-T****Table S30.** Energies of conformers of sodium-coordinated ketone cyclization trans zwitterion **7-Na-K-T**^a

Structure	ΔE	ΔH	ΔG	ΔG (GV50)	$\Delta\Delta G$
7-Na-K-T-C1	-1293.702579	-1293.308272	-1293.392141	-1293.389103	0.00
7-Na-K-T-C2	-1293.701098	-1293.306942	-1293.391318	-1293.388068	0.65
7-Na-K-T-C3	-1293.701874	-1293.30756	-1293.390868	-1293.388011	0.69
7-Na-K-T-C4	-1293.70072	-1293.306273	-1293.389534	-1293.386776	1.46
7-Na-K-T-C5	-1293.697157	-1293.302892	-1293.386388	-1293.383571	3.47

7-Na-K-T-C6	-1293.696394	-1293.302099	-1293.384749	-1293.382255	4.30
--------------------	--------------	--------------	--------------	--------------	------

^aEnergies were obtained as single points at the PW6B95(D3BJ) / def2-TZVPPD / SMD (DCM) level of theory based on structures optimized at the MN15 / def2-TZVP / SMD (DCM) level of theory. ΔE , ΔH , ΔG , and ΔG (GV50), hartree; $\Delta\Delta G$, kcal/mol.

7-Na-K-C

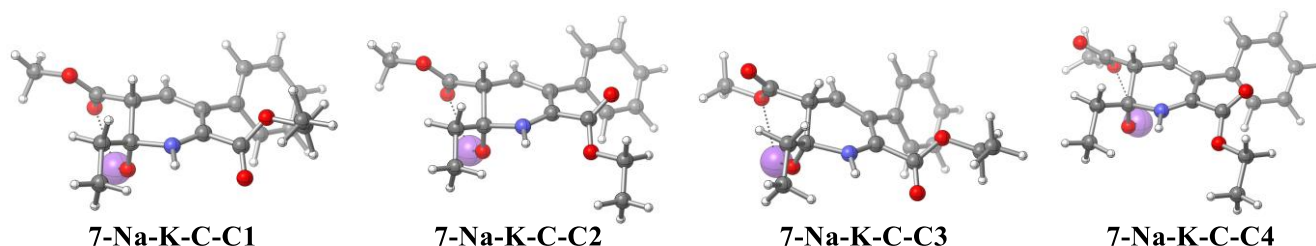


Figure S32. Conformers of sodium-coordinated ketone cyclization cis zwitterion **7-Na-K-C**

Table S31. Energies of conformers of sodium-coordinated ketone cyclization cis zwitterion **7-Na-K-C^a**

Structure	ΔE	ΔH	ΔG	ΔG (GV50)	$\Delta\Delta G$
7-Na-K-C-C1	-1293.702982	-1293.308205	-1293.391529	-1293.388466	0.00
7-Na-K-C-C2	-1293.702844	-1293.307994	-1293.390561	-1293.387995	0.30
7-Na-K-C-C3	-1293.696666	-1293.302098	-1293.384951	-1293.382424	3.79
7-Na-K-C-C4	-1293.696511	-1293.301949	-1293.384419	-1293.382145	3.97

^aEnergies were obtained as single points at the PW6B95(D3BJ) / def2-TZVPPD / SMD (DCM) level of theory based on structures optimized at the MN15 / def2-TZVP / SMD (DCM) level of theory. ΔE , ΔH , ΔG , and ΔG (GV50), hartree; $\Delta\Delta G$, kcal/mol.

7b-E-T

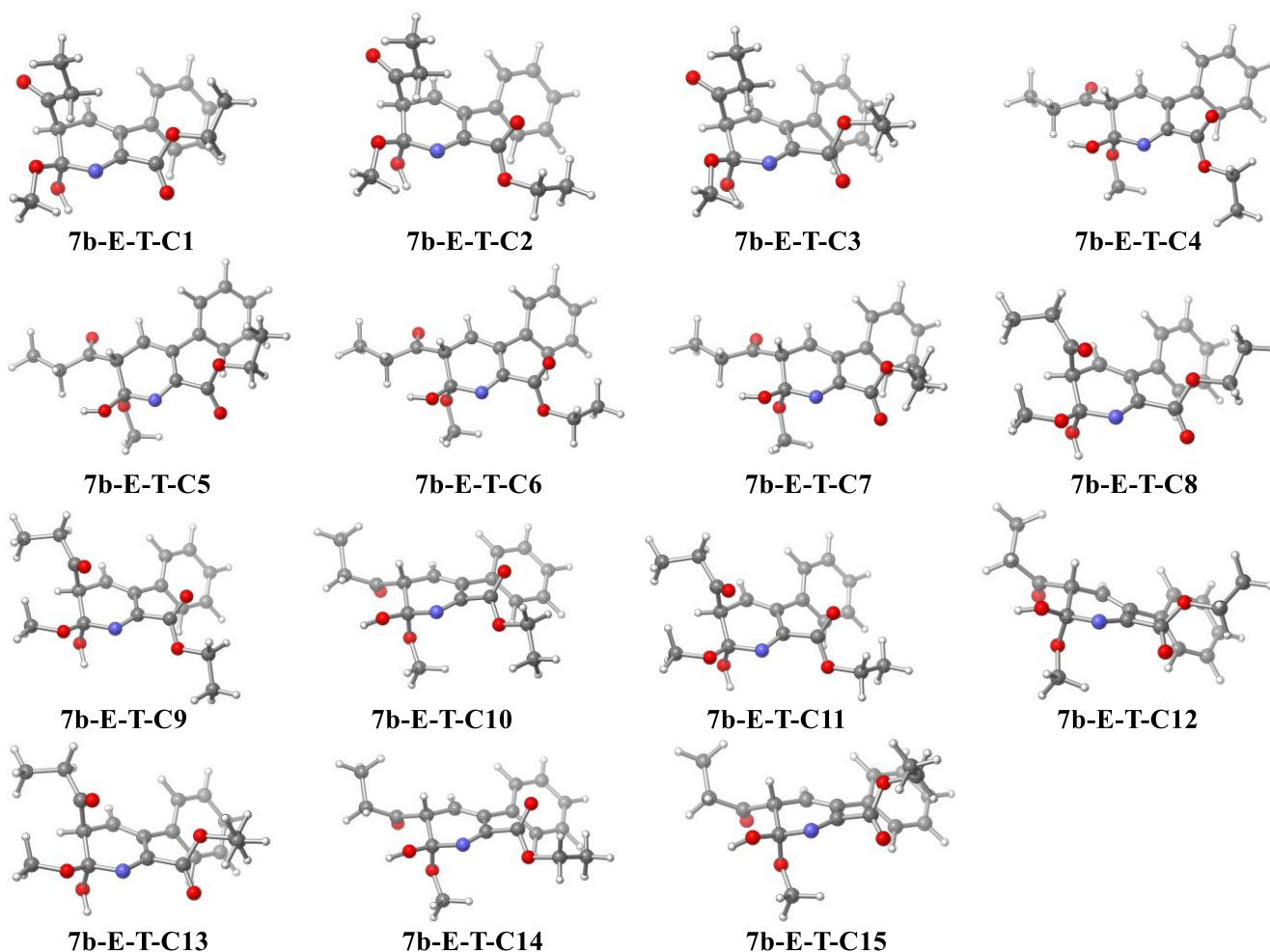


Figure S33. Conformers of ester cyclization trans intermediate **7b-E-T**.

Table S32. Energies of conformers of ester cyclization trans intermediate **7b-E-T**. ^a

Structure	ΔE	ΔH	ΔG	ΔG (GV50)	$\Delta\Delta G$
7b-E-T-C1	-1131.307293	-1130.916683	-1130.996557	-1130.993753	0.00
7b-E-T-C2	-1131.306542	-1130.915885	-1130.995522	-1130.992876	0.55
7b-E-T-C3	-1131.30617	-1130.915425	-1130.995073	-1130.99241	0.84
7b-E-T-C4	-1131.302129	-1130.911645	-1130.992008	-1130.989077	2.93
7b-E-T-C5	-1131.302403	-1130.911847	-1130.991695	-1130.988891	3.05
7b-E-T-C6	-1131.301914	-1130.911358	-1130.990935	-1130.988308	3.42
7b-E-T-C7	-1131.301228	-1130.910491	-1130.990297	-1130.987478	3.94

7b-E-T-C8	-1131.301607	-1130.910899	-1130.989902	-1130.98733	4.03
7b-E-T-C9	-1131.301051	-1130.910474	-1130.989755	-1130.98728	4.06
7b-E-T-C10	-1131.29982	-1130.909024	-1130.989393	-1130.986583	4.50
7b-E-T-C11	-1131.3008	-1130.910074	-1130.988384	-1130.98628	4.69
7b-E-T-C12	-1131.300078	-1130.909299	-1130.988727	-1130.986248	4.71
7b-E-T-C13	-1131.300399	-1130.909594	-1130.988441	-1130.985939	4.90
7b-E-T-C14	-1131.299619	-1130.908811	-1130.988076	-1130.985675	5.07
7b-E-T-C15	-1131.29884	-1130.908034	-1130.988451	-1130.985277	5.32

^aEnergies were obtained as single points at the PW6B95(D3BJ) / def2-TZVPPD / SMD (DCM) level of theory based on structures optimized at the MN15 / def2-TZVP / SMD (DCM) level of theory. ΔE , ΔH , ΔG , and ΔG (GV50), hartree; $\Delta\Delta G$, kcal/mol.

7b-E-C

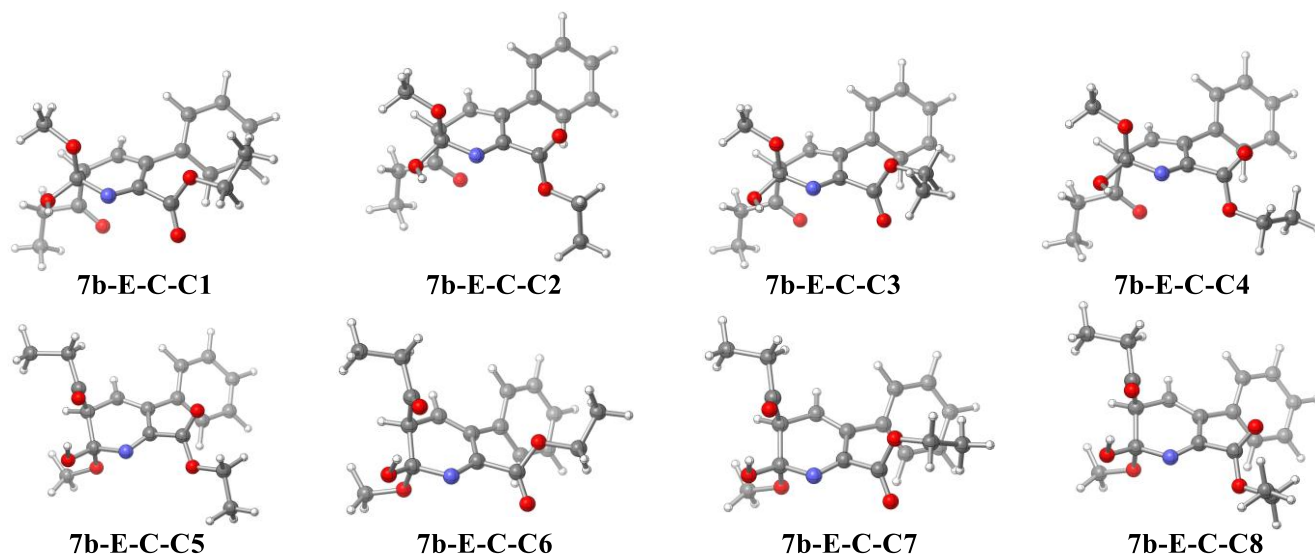


Figure S34. Conformers of ester cyclization cis intermediate **7b-E-C**.

Table S33. Energies of conformers of ester cyclization cis intermediate **7b-E-C**. ^a

Structure	ΔE	ΔH	ΔG	ΔG (GV50)	$\Delta\Delta G$
7b-E-C-C1	-1131.30287	-1130.912383	-1130.992676	-1130.989573	0.00
7b-E-C-C2	-1131.302691	-1130.911955	-1130.991872	-1130.988916	0.41

7b-E-C-C3	-1131.301856	-1130.911192	-1130.991422	-1130.988345	0.77
7b-E-C-C4	-1131.302487	-1130.911712	-1130.99088	-1130.98817	0.88
7b-E-C-C5	-1131.300679	-1130.909622	-1130.989712	-1130.986772	1.76
7b-E-C-C6	-1131.300834	-1130.909761	-1130.989626	-1130.986527	1.91
7b-E-C-C7	-1131.300525	-1130.909562	-1130.988869	-1130.985894	2.31
7b-E-C-C8	-1131.300079	-1130.908941	-1130.988878	-1130.985821	2.35

^aEnergies were obtained as single points at the PW6B95(D3BJ) / def2-TZVPPD / SMD (DCM) level of theory based on structures optimized at the MN15 / def2-TZVP / SMD (DCM) level of theory. ΔE , ΔH , ΔG , and ΔG (GV50), hartree; $\Delta\Delta G$, kcal/mol.

7b-K-T

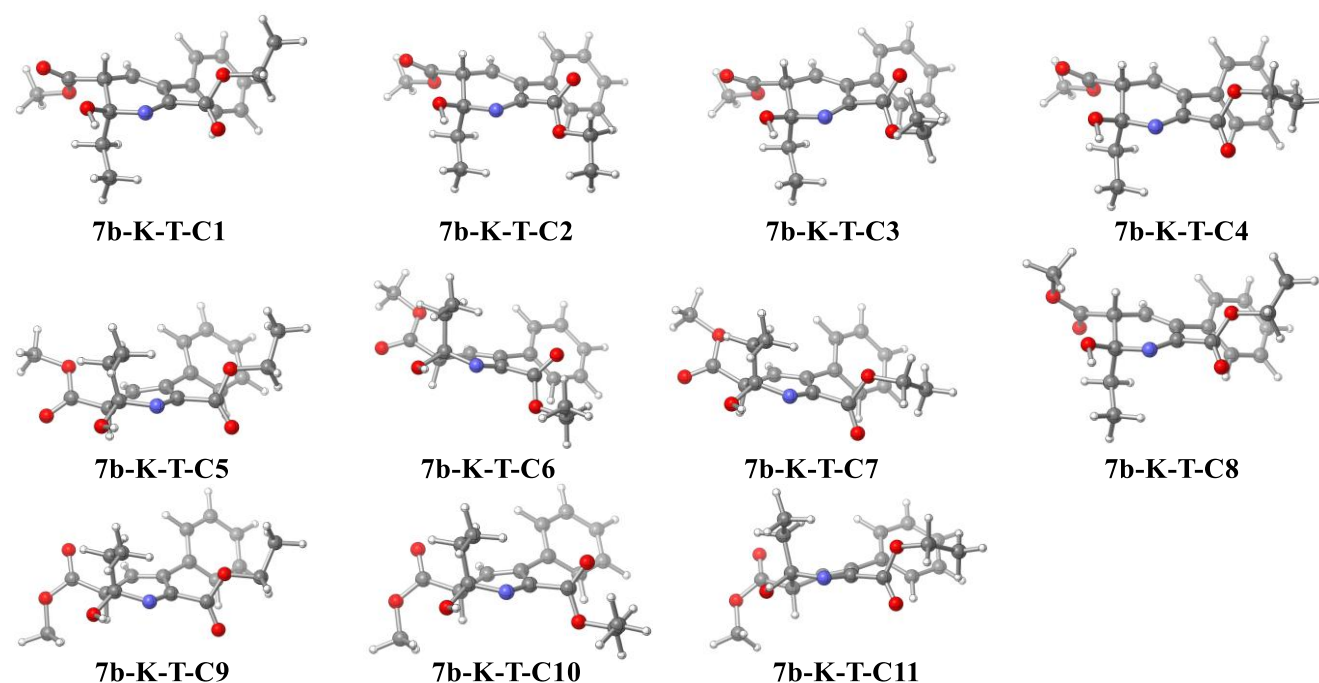


Figure S35. Conformers of ketone cyclization trans intermediate **7b-K-T**.

Table S34. Energies of conformers of ketone cyclization trans intermediate **7b-K-T**.^a

Structure	ΔE	ΔH	ΔG	ΔG (GV50)	$\Delta\Delta G$
7b-K-T-C1	-1131.324063	-1130.932801	-1131.012585	-1131.010013	0.00
7b-K-T-C2	-1131.323542	-1130.9323	-1131.012369	-1131.0097	0.20

7b-K-T-C3	-1131.322876	-1130.931579	-1131.011849	-1131.008929	0.68
7b-K-T-C4	-1131.323612	-1130.932264	-1131.011088	-1131.008926	0.68
7b-K-T-C5	-1131.320677	-1130.929699	-1131.010148	-1131.007291	1.71
7b-K-T-C6	-1131.319884	-1130.928558	-1131.008495	-1131.005735	2.68
7b-K-T-C7	-1131.320005	-1130.928734	-1131.008239	-1131.00559	2.78
7b-K-T-C8	-1131.317387	-1130.926038	-1131.004712	-1131.002681	4.60
7b-K-T-C9	-1131.31374	-1130.922602	-1131.002495	-1130.999853	6.38
7b-K-T-C10	-1131.312726	-1130.9214	-1131.002179	-1130.998984	6.92
7b-K-T-C11	-1131.313067	-1130.921708	-1131.001315	-1130.998545	7.20

^aEnergies were obtained as single points at the PW6B95(D3BJ) / def2-TZVPPD / SMD (DCM) level of theory based on structures optimized at the MN15 / def2-TZVP / SMD (DCM) level of theory. ΔE , ΔH , ΔG , and ΔG (GV50), hartree; $\Delta\Delta G$, kcal/mol.

7b-K-C

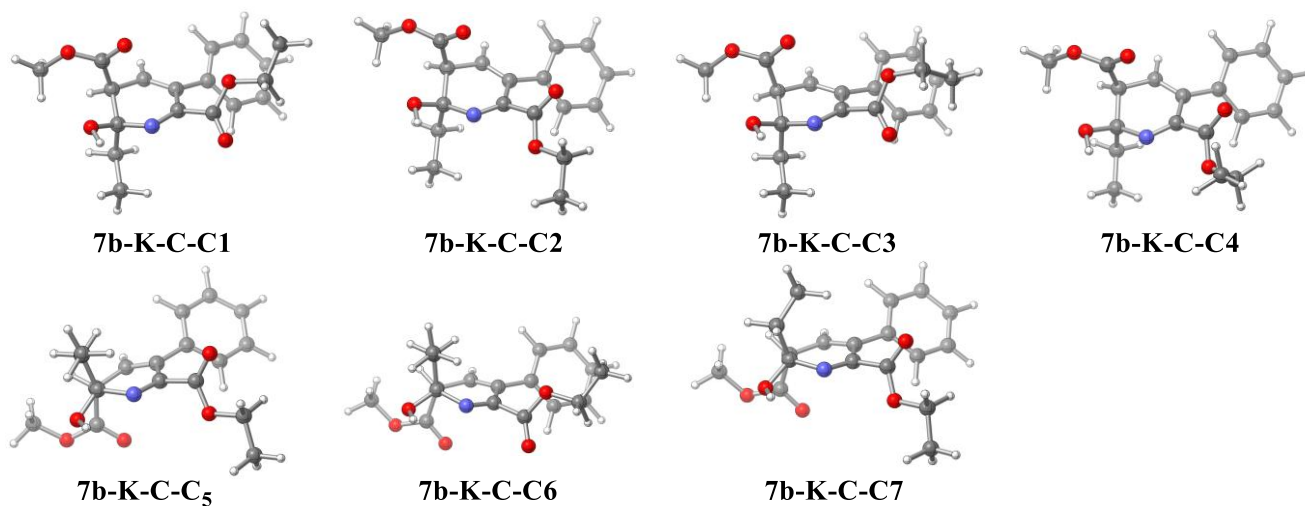


Figure S36. Conformers of ketone cyclization cis intermediate **7b-K-C**.

Table S35. Energies of conformers of ketone cyclization cis intermediate **7b-K-C**.^a

Structure	ΔE	ΔH	ΔG	ΔG (GV50)	$\Delta\Delta G$
7b-K-C-C1	-1131.318139	-1130.926748	-1131.006283	-1131.003659	0.00
7b-K-C-C2	-1131.317236	-1130.925845	-1131.005333	-1131.002849	0.51

7b-K-C-C3	-1131.317632	-1130.926213	-1131.005063	-1131.00276	0.56
7b-K-C-C4	-1131.316644	-1130.925136	-1131.004291	-1131.001865	1.13
7b-K-C-C5	-1131.314503	-1130.923161	-1131.00325	-1131.000344	2.08
7b-K-C-C6	-1131.314515	-1130.923328	-1131.002632	-1131.000216	2.16
7b-K-C-C7	-1131.314822	-1130.923425	-1131.002202	-1130.999593	2.55

^aEnergies were obtained as single points at the PW6B95(D3BJ) / def2-TZVPPD / SMD (DCM) level of theory based on structures optimized at the MN15 / def2-TZVP / SMD (DCM) level of theory. ΔE , ΔH , ΔG , and ΔG (GV50), hartree; $\Delta\Delta G$, kcal/mol.

7b-Cs-E-T

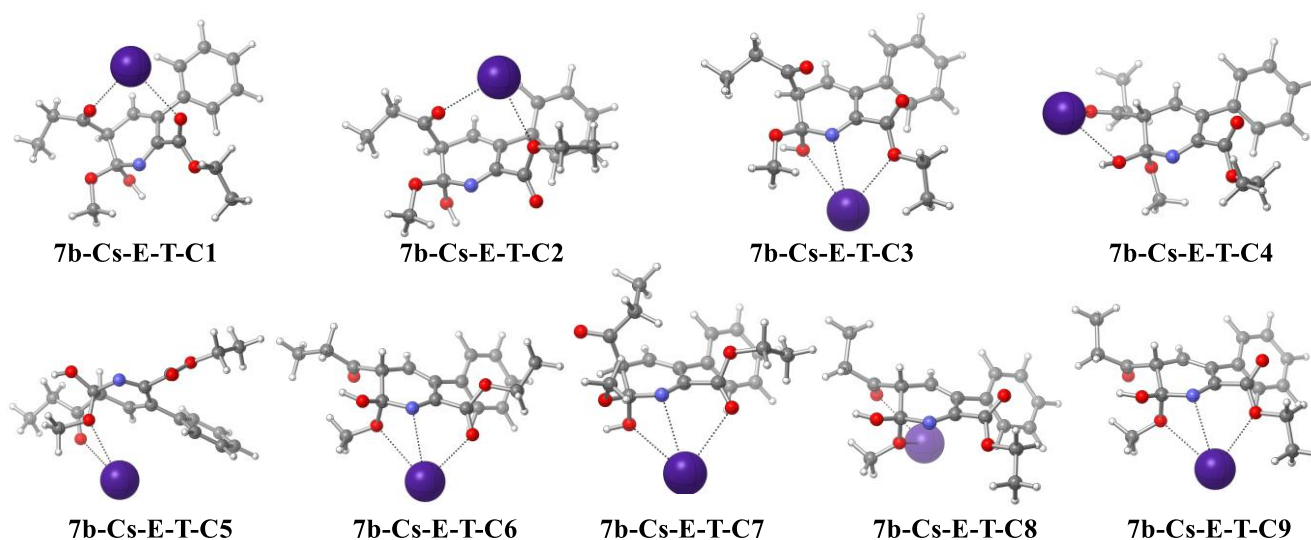


Figure S37. Conformers of cesium-coordinated ester cyclization trans intermediate **7b-Cs-E-T**.

Table S36. Energies of conformers of cesium-coordinated ester cyclization trans intermediate **7b-Cs-E-T**.^a

Structure	ΔE	ΔH	ΔG	ΔG (GV50)	$\Delta\Delta G$
7b-Cs-E-T-C1	-1151.408106	-1151.014243	-1151.101014	-1151.097741	0.00
7b-Cs-E-T-C2	-1151.405469	-1151.011552	-1151.096958	-1151.094135	2.26
7b-Cs-E-T-C3	-1151.404135	-1151.010165	-1151.095909	-1151.092836	3.08
7b-Cs-E-T-C4	-1151.400011	-1151.005953	-1151.093706	-1151.089887	4.93
7b-Cs-E-T-C5	-1151.399802	-1151.006218	-1151.090792	-1151.087885	6.18

7b-Cs-E-T-C6	-1151.398933	-1151.005312	-1151.090542	-1151.087701	6.30
7b-Cs-E-T-C7	-1151.399249	-1151.006569	-1151.089864	-1151.087603	6.36
7b-Cs-E-T-C8	-1151.397494	-1151.003751	-1151.090256	-1151.086766	6.89
7b-Cs-E-T-C9	-1151.39588	-1151.001861	-1151.086728	-1151.084545	8.28

^aEnergies were obtained as single points at the PW6B95(D3BJ) / def2-TZVPPD / SMD (DCM) level of theory based on structures optimized at the MN15 / def2-TZVP / SMD (DCM) level of theory. ΔE , ΔH , ΔG , and ΔG (GV50), hartree; $\Delta\Delta G$, kcal/mol.

7b-Cs-E-C

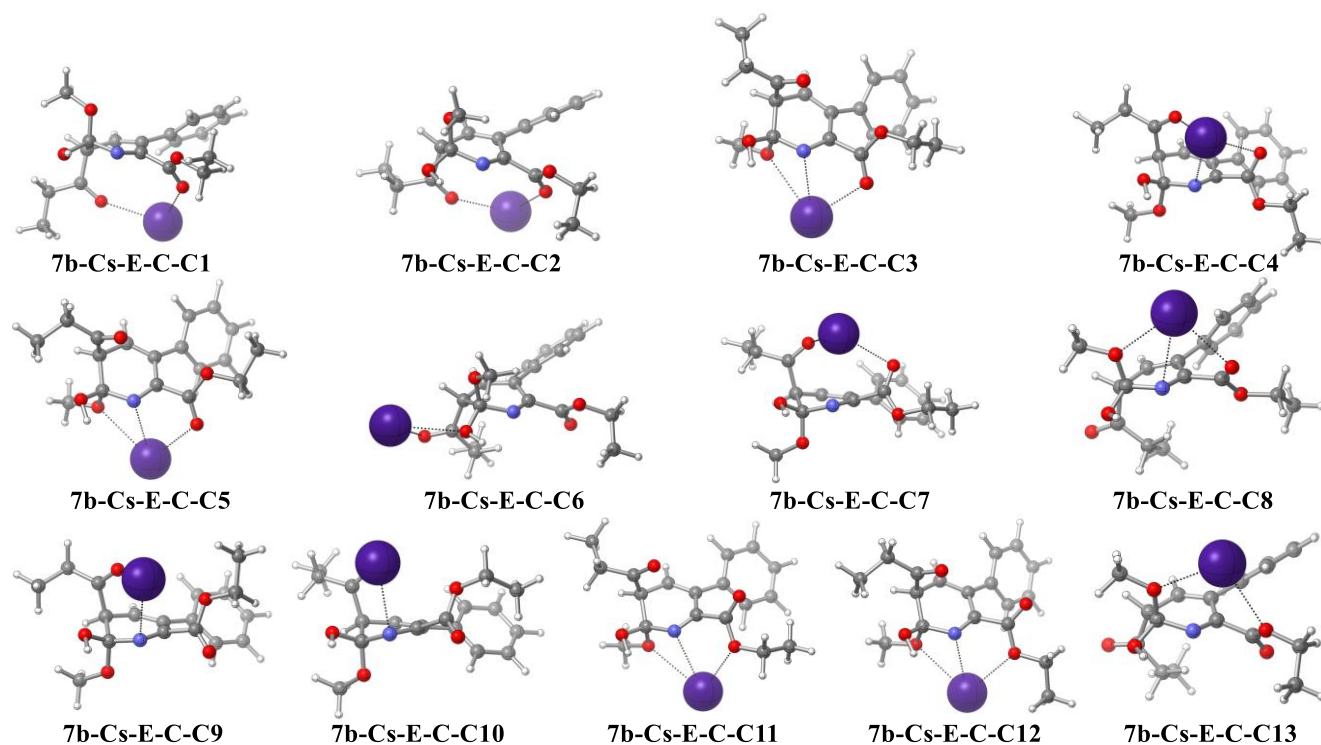


Figure S38. Conformers of cesium-coordinated ester cyclization cis intermediate **7b-Cs-E-C**.

Table S37. Energies of conformers of cesium-coordinated ester cyclization cis intermediate **7b-Cs-E-C**.^a

Structure	ΔE	ΔH	ΔG	ΔG (GV50)	$\Delta\Delta G$
7b-Cs-E-C-C1	-1151.410611	-1151.016717	-1151.103733	-1151.099996	0.00
7b-Cs-E-C-C2	-1151.40865	-1151.014482	-1151.102141	-1151.098273	1.08
7b-Cs-E-C-C3	-1151.406214	-1151.011933	-1151.097577	-1151.094794	3.26

7b-Cs-E-C-C4	-1151.405165	-1151.011058	-1151.098361	-1151.094493	3.45
7b-Cs-E-C-C5	-1151.40533	-1151.011152	-1151.097165	-1151.094162	3.66
7b-Cs-E-C-C6	-1151.404505	-1151.010382	-1151.097517	-1151.093956	3.79
7b-Cs-E-C-C7	-1151.405399	-1151.010938	-1151.097472	-1151.093778	3.90
7b-Cs-E-C-C8	-1151.40516	-1151.010764	-1151.09678	-1151.093666	3.97
7b-Cs-E-C-C9	-1151.404489	-1151.010328	-1151.096346	-1151.093289	4.21
7b-Cs-E-C-C10	-1151.405261	-1151.010858	-1151.095715	-1151.093046	4.36
7b-Cs-E-C-C11	-1151.403552	-1151.009252	-1151.095432	-1151.092217	4.88
7b-Cs-E-C-C12	-1151.403297	-1151.009092	-1151.094906	-1151.092135	4.93
7b-Cs-E-C-C13	-1151.402292	-1151.00806	-1151.094983	-1151.091417	5.38

^aEnergies were obtained as single points at the PW6B95(D3BJ) / def2-TZVPPD / SMD (DCM) level of theory based on structures optimized at the MN15 / def2-TZVP / SMD (DCM) level of theory. ΔE , ΔH , ΔG , and ΔG (GV50), hartree; $\Delta\Delta G$, kcal/mol.

7b-Cs-K-T

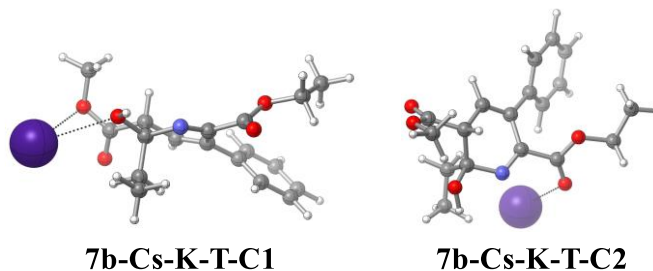


Figure S39. Conformers of cesium-coordinated ketone cyclization trans intermediate **7b-Cs-K-T**.

Table S38. Energies of conformers of cesium-coordinated ketone cyclization trans intermediate **7b-Cs-K-T**.^a

Structure	ΔE	ΔH	ΔG	ΔG (GV50)	$\Delta\Delta G$
7b-Cs-K-T-C1	-1151.416007	-1151.021834	-1151.109092	-1151.105355	0.00
7b-Cs-K-T-C2	-1151.41427	-1151.019559	-1151.105332	-1151.102053	2.07

^aEnergies were obtained as single points at the PW6B95(D3BJ) / def2-TZVPPD / SMD (DCM) level of theory based on structures optimized at the MN15 / def2-TZVP / SMD (DCM) level of theory. ΔE , ΔH , ΔG , and ΔG (GV50), hartree; $\Delta\Delta G$, kcal/mol.

7b-Cs-K-C

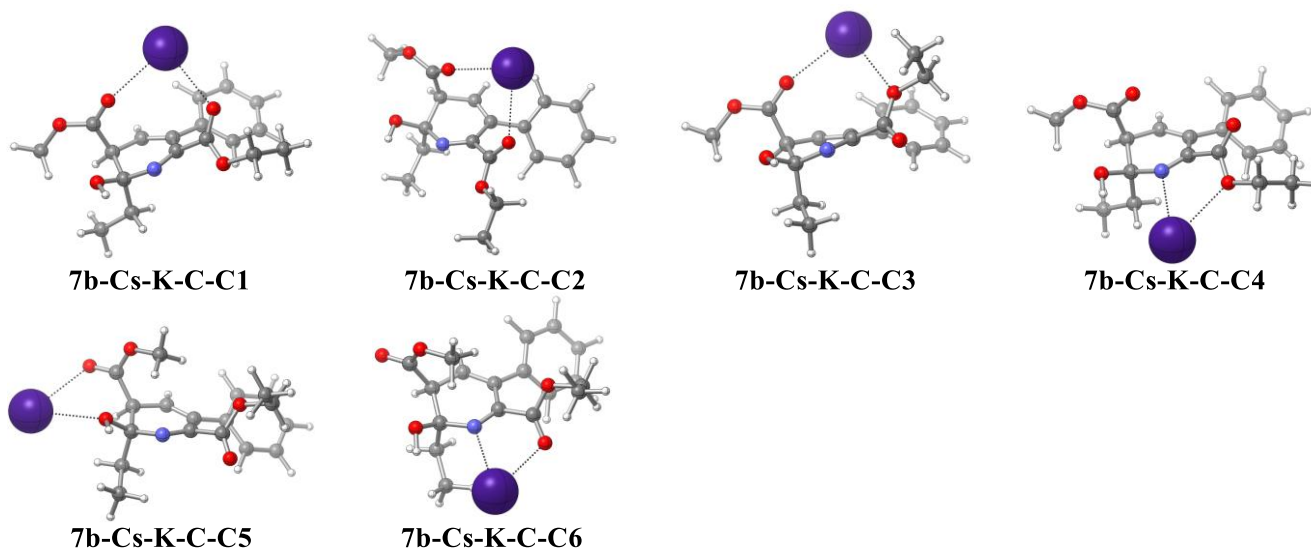


Figure S40. Conformers of cesium-coordinated ketone cyclization cis intermediate **7b-Cs-K-C**.

Table S39. Energies of conformers of cesium-coordinated ketone cyclization cis intermediate **7b-Cs-K-C**.^a

Structure	ΔE	ΔH	ΔG	ΔG (GV50)	$\Delta\Delta G$
7b-Cs-K-C-C1	-1151.423624	-1151.028927	-1151.114179	-1151.111496	0.00
7b-Cs-K-C-C2	-1151.423408	-1151.028722	-1151.114443	-1151.11142	0.05
7b-Cs-K-C-C3	-1151.420259	-1151.025543	-1151.110093	-1151.107469	2.53
7b-Cs-K-C-C4	-1151.414741	-1151.019973	-1151.105694	-1151.102788	5.46
7b-Cs-K-C-C5	-1151.413019	-1151.018234	-1151.104039	-1151.100872	6.67
7b-Cs-K-C-C6	-1151.412621	-1151.017725	-1151.102629	-1151.099637	7.44

^aEnergies were obtained as single points at the PW6B95(D3BJ) / def2-TZVPPD / SMD (DCM) level of theory based on structures optimized at the MN15 / def2-TZVP / SMD (DCM) level of theory. ΔE , ΔH , ΔG , and ΔG (GV50), hartree; $\Delta\Delta G$, kcal/mol.

7b-Na-E-T

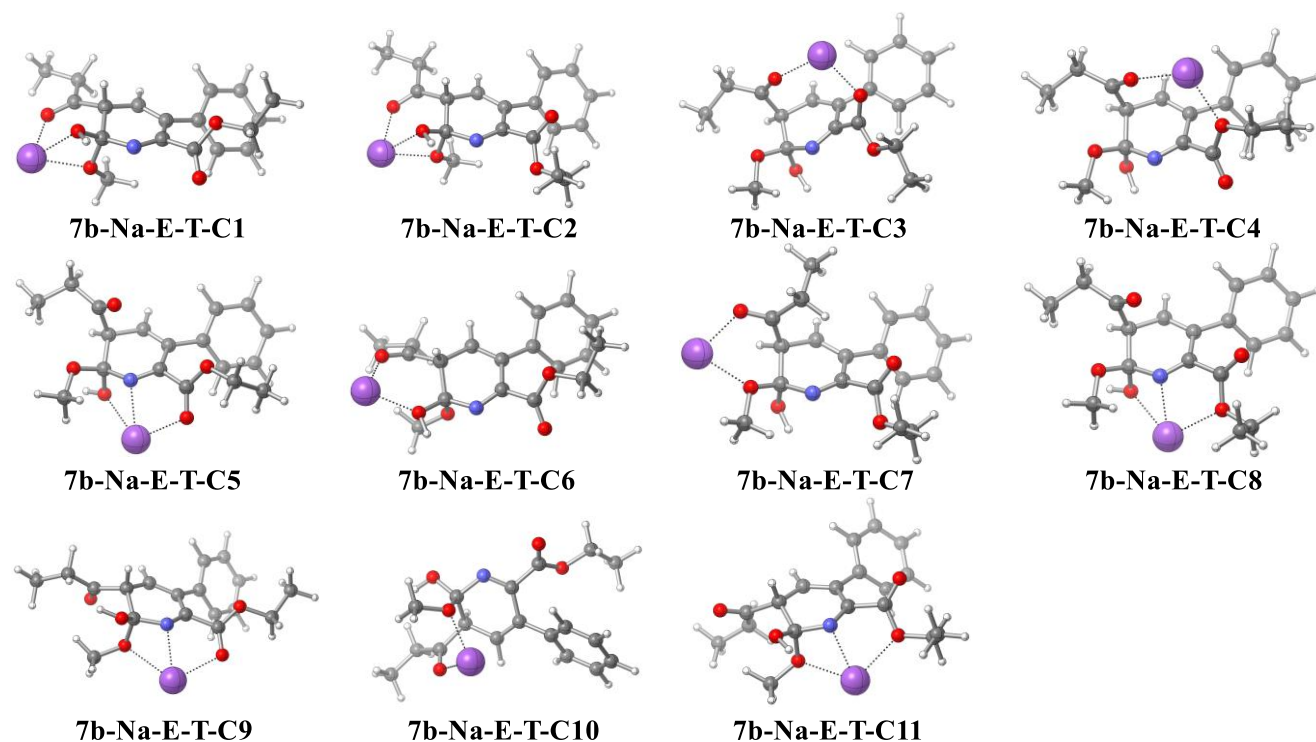


Figure S41. Conformers of sodium-coordinated ester cyclization trans intermediate **7b-Na-E-T**.

Table S40. Energies of conformers of sodium-coordinated ester cyclization trans intermediate **7b-Na-E-T**.^a

Structure	ΔE	ΔH	ΔG	ΔG (GV50)	$\Delta\Delta G$
7b-Na-E-T-C1	-1293.704301	-1293.310743	-1293.392234	-1293.3899	0.00
7b-Na-E-T-C2	-1293.703559	-1293.309746	-1293.391551	-1293.388892	0.63
7b-Na-E-T-C3	-1293.700853	-1293.306582	-1293.390343	-1293.387541	1.48
7b-Na-E-T-C4	-1293.695294	-1293.301481	-1293.383779	-1293.38172	5.13
7b-Na-E-T-C5	-1293.695113	-1293.300898	-1293.383297	-1293.381276	5.41
7b-Na-E-T-C6	-1293.694318	-1293.300526	-1293.38244	-1293.380374	5.98
7b-Na-E-T-C7	-1293.693394	-1293.299145	-1293.383041	-1293.38026	6.05
7b-Na-E-T-C8	-1293.690765	-1293.29675	-1293.380648	-1293.377966	7.49
7b-Na-E-T-C9	-1293.690821	-1293.296856	-1293.379276	-1293.377038	8.07
7b-Na-E-T-C10	-1293.689561	-1293.295775	-1293.37766	-1293.375597	8.98

7b-Na-E-T-C11	-1293.688103	-1293.294384	-1293.377299	-1293.374812	9.47
----------------------	--------------	--------------	--------------	--------------	------

^aEnergies were obtained as single points at the PW6B95(D3BJ) / def2-TZVPPD / SMD (DCM) level of theory based on structures optimized at the MN15 / def2-TZVP / SMD (DCM) level of theory. ΔE , ΔH , ΔG , and ΔG (GV50), hartree; $\Delta\Delta G$, kcal/mol.

7b-Na-E-C

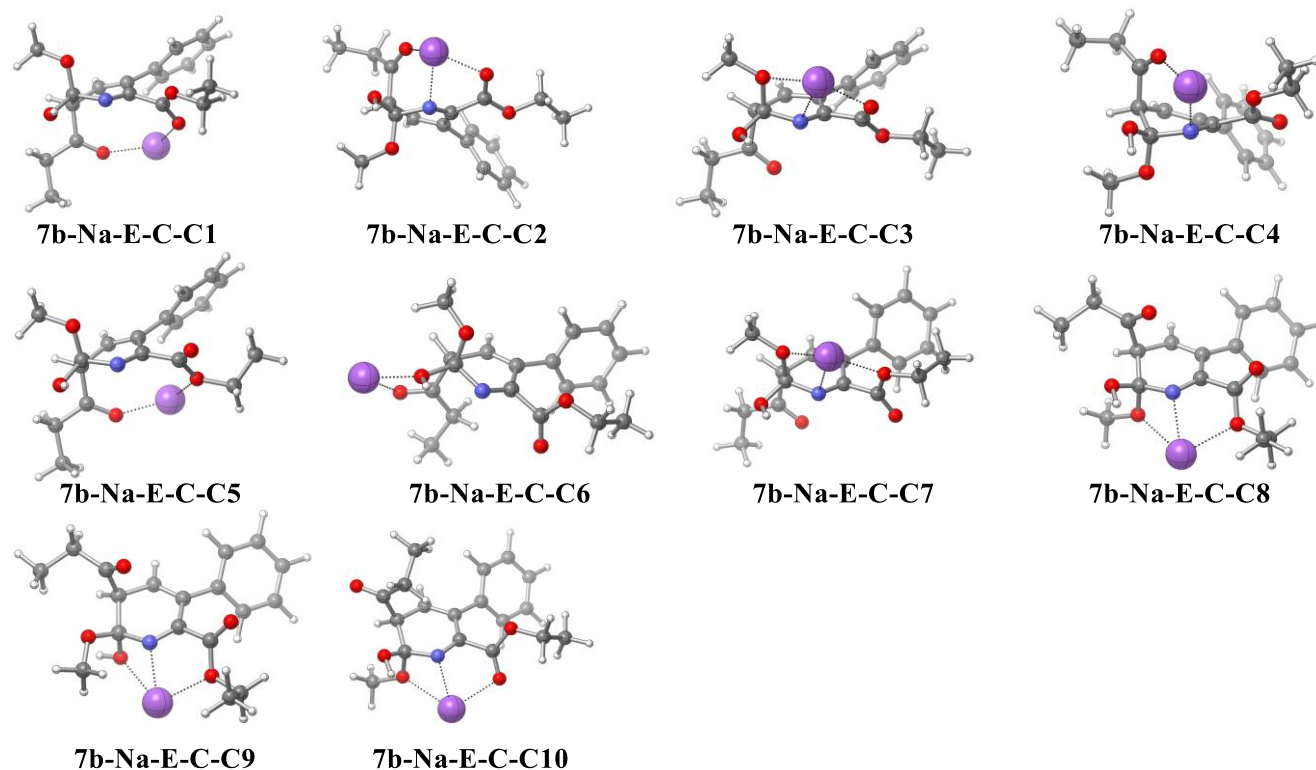


Figure S42. Conformers of sodium-coordinated ester cyclization cis intermediate **7b-Na-E-C**.

Table S41. Energies of conformers of sodium-coordinated ester cyclization cis intermediate **7b-Na-E-C**.^a

Structure	ΔE	ΔH	ΔG	ΔG (GV50)	$\Delta\Delta G$
7b-Na-E-C-C1	-1293.704417	-1293.310235	-1293.393168	-1293.390573	0.00
7b-Na-E-C-C2	-1293.702937	-1293.308389	-1293.391014	-1293.388526	1.28
7b-Na-E-C-C3	-1293.699282	-1293.305349	-1293.388848	-1293.386264	2.70
7b-Na-E-C-C4	-1293.700302	-1293.305633	-1293.387141	-1293.384931	3.54
7b-Na-E-C-C5	-1293.698217	-1293.30441	-1293.387178	-1293.384565	3.77
7b-Na-E-C-C6	-1293.691847	-1293.298136	-1293.381742	-1293.378702	7.45

7b-Na-E-C-C7	-1293.691442	-1293.297529	-1293.381299	-1293.378389	7.65
7b-Na-E-C-C8	-1293.691639	-1293.29746	-1293.380819	-1293.378351	7.67
7b-Na-E-C-C9	-1293.696171	-1293.300418	-1293.379064	-1293.377694	8.08
7b-Na-E-C-C10	-1293.683815	-1293.289548	-1293.373034	-1293.370215	12.78

^aEnergies were obtained as single points at the PW6B95(D3BJ) / def2-TZVPPD / SMD (DCM) level of theory based on structures optimized at the MN15 / def2-TZVP / SMD (DCM) level of theory. ΔE , ΔH , ΔG , and ΔG (GV50), hartree; $\Delta\Delta G$, kcal/mol.

7b-Na-K-T

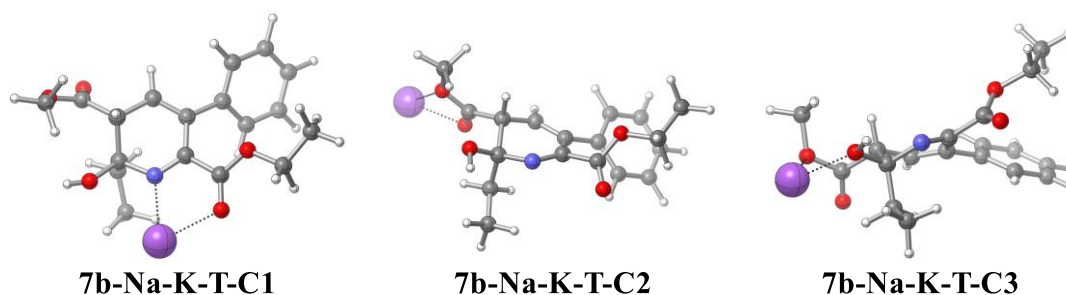


Figure S43. Conformers of sodium-coordinated ketone cyclization trans intermediate **7b-Na-K-T**.

Table S42. Energies of conformers sodium-coordinated ketone cyclization trans intermediate **7b-Na-K-T**.^a

Structure	ΔE	ΔH	ΔG	ΔG (GV50)	$\Delta\Delta G$
7b-Na-K-T-C1	-1293.710722	-1293.315948	-1293.399878	-1293.396803	0.00
7b-Na-K-T-C2	-1293.700964	-1293.306366	-1293.390166	-1293.387645	5.75
7b-Na-K-T-C3	-1293.698312	-1293.303819	-1293.387019	-1293.384412	7.78

^aEnergies were obtained as single points at the PW6B95(D3BJ) / def2-TZVPPD / SMD (DCM) level of theory based on structures optimized at the MN15 / def2-TZVP / SMD (DCM) level of theory. ΔE , ΔH , ΔG , and ΔG (GV50), hartree; $\Delta\Delta G$, kcal/mol.

7b-Na-K-C

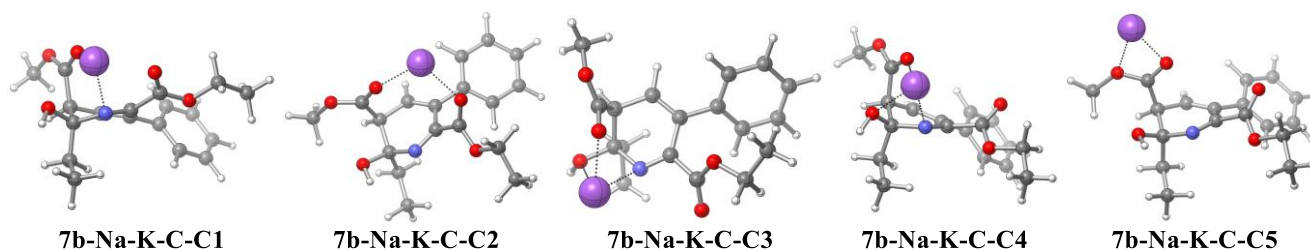


Figure S44. Conformers of sodium-coordinated ketone cyclization cis intermediate **7b-Na-K-C**.

Table S43. Energies of conformers sodium-coordinated ketone cyclization cis intermediate **7b-Na-K-C**.^a

Structure	ΔE	ΔH	ΔG	ΔG (GV50)	$\Delta\Delta G$
7b-Na-K-C-C1	-1293.719304	-1293.324572	-1293.408179	-1293.405272	0.00
7b-Na-K-C-C2	-1293.717835	-1293.322756	-1293.404913	-1293.402775	1.57
7b-Na-K-C-C3	-1293.717533	-1293.322484	-1293.40504	-1293.402618	1.67
7b-Na-K-C-C4	-1293.717183	-1293.322023	-1293.404056	-1293.401724	2.23
7b-Na-K-C-C5	-1293.70273	-1293.307912	-1293.392152	-1293.389087	10.16

^aEnergies were obtained as single points at the PW6B95(D3BJ) / def2-TZVPPD / SMD (DCM) level of theory based on structures optimized at the MN15 / def2-TZVP / SMD (DCM) level of theory. ΔE , ΔH , ΔG , and ΔG (GV50), hartree; $\Delta\Delta G$, kcal/mol.

8-E

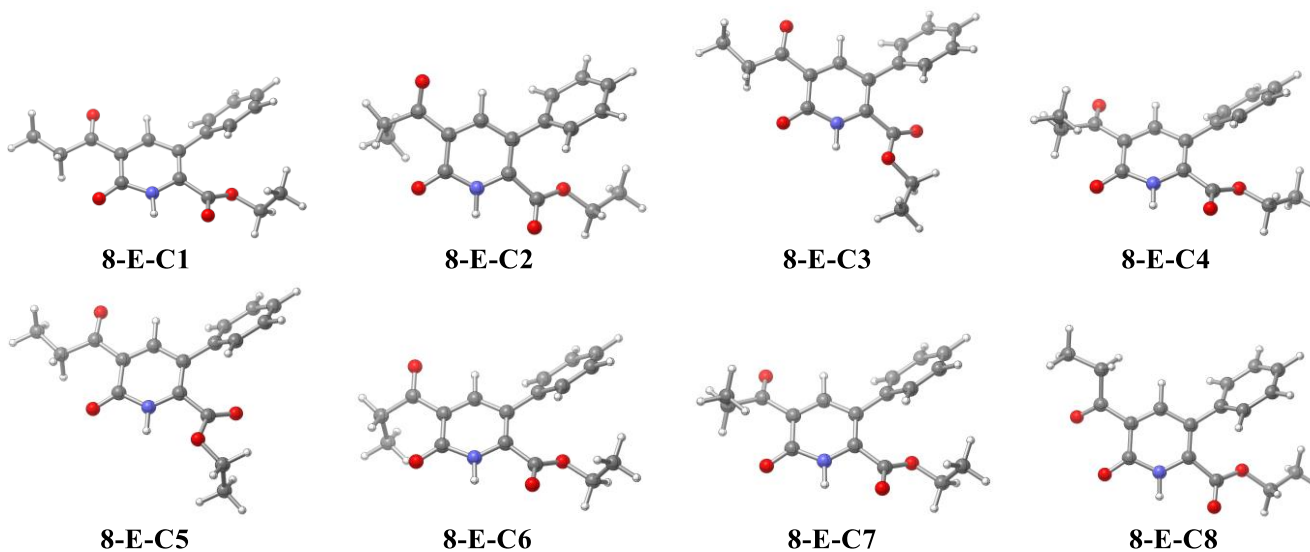


Figure S45. Conformers of pyridone product **8-E**.

Table S44. Energies of conformers of pyridone product **8-E**.^a

Structure	ΔE	ΔH	ΔG	ΔG (GV50)	$\Delta\Delta G$
8-E-C1	-1015.439527	-1015.106237	-1015.178984	-1015.176366	0.00
8-E-C2	-1015.438641	-1015.105285	-1015.178905	-1015.175911	0.29
8-E-C3	-1015.438417	-1015.105192	-1015.178854	-1015.175872	0.31
8-E-C4	-1015.438703	-1015.10526	-1015.17859	-1015.175789	0.36
8-E-C5	-1015.437812	-1015.104461	-1015.177084	-1015.174549	1.14
8-E-C6	-1015.437904	-1015.104371	-1015.176596	-1015.174302	1.30
8-E-C7	-1015.437945	-1015.104363	-1015.17649	-1015.174217	1.35
8-E-C8	-1015.435252	-1015.101952	-1015.175419	-1015.172856	2.20

^a Energies were obtained as single points at the PW6B95(D3BJ) / def2-TZVPPD / SMD (DCM) level of theory based on structures optimized at the MN15 / def2-TZVP / SMD (DCM) level of theory. ΔE , ΔH , ΔG , and ΔG (GV50), hartree; $\Delta\Delta G$, kcal/mol.

8-K

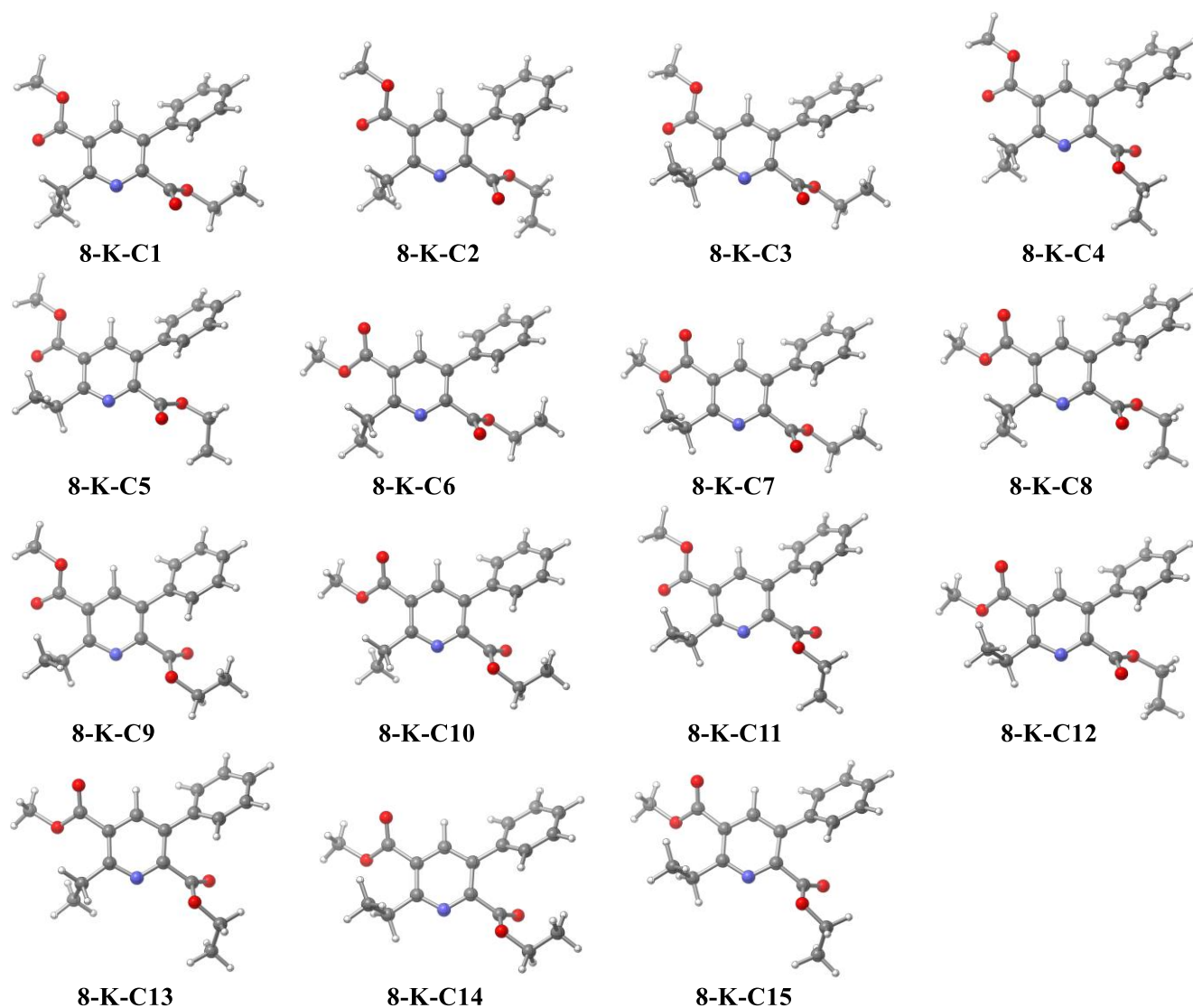


Figure S46. Conformers of pyridine product **8-K**.

Table S45. Energies of conformers of pyridine product **8-K**.^a

Structure	ΔE	ΔH	ΔG	ΔG (GV50)	$\Delta\Delta G$
8-K-C1	-1054.809355	-1054.445911	-1054.521945	-1054.519291	0.00
8-K-C2	-1054.808921	-1054.445435	-1054.521905	-1054.519148	0.09
8-K-C3	-1054.808898	-1054.445482	-1054.522044	-1054.518983	0.19
8-K-C4	-1054.808631	-1054.445091	-1054.521331	-1054.518709	0.37
8-K-C5	-1054.808457	-1054.444926	-1054.521898	-1054.518679	0.38

8-K-C6	-1054.808693	-1054.445217	-1054.521092	-1054.518479	0.51
8-K-C7	-1054.808474	-1054.445058	-1054.520796	-1054.518423	0.54
8-K-C8	-1054.808207	-1054.44468	-1054.521064	-1054.518371	0.58
8-K-C9	-1054.808431	-1054.444952	-1054.520964	-1054.51833	0.60
8-K-C10	-1054.808195	-1054.44473	-1054.520783	-1054.518274	0.64
8-K-C11	-1054.808143	-1054.444595	-1054.521143	-1054.518243	0.66
8-K-C12	-1054.80804	-1054.444531	-1054.520725	-1054.51817	0.70
8-K-C13	-1054.807908	-1054.444377	-1054.521045	-1054.518153	0.71
8-K-C14	-1054.807987	-1054.444587	-1054.520528	-1054.518118	0.74
8-K-C15	-1054.807679	-1054.444196	-1054.520725	-1054.51797	0.83

^aEnergies were obtained as single points at the PW6B95(D3BJ) / def2-TZVPPD / SMD (DCM) level of theory based on structures optimized at the MN15 / def2-TZVP / SMD (DCM) level of theory. ΔE , ΔH , ΔG , and ΔG (GV50), hartree; $\Delta\Delta G$, kcal/mol.

Table S46. Energies of other structures.^a

Structure	ΔE	ΔH	ΔG	ΔG (GV50)
N ₂ O	-184.9544308	-184.9393862	-184.9642602	-184.9642602
H ₂ O	-76.55366451	-76.52870578	-76.55079278	-76.55079278
MeOH	-115.9109426	-115.8554341	-115.8826501	-115.8826511
Cs ⁺	-20.08973125	-20.08737107	-20.10664507	-20.10664507
Na ⁺	-162.3547732	-162.3524127	-162.3692017	-162.3692017

^aEnergies were obtained as single points at the PW6B95(D3BJ) / def2-TZVPPD / SMD (DCM) level of theory based on structures optimized at the MN15 / def2-TZVP / SMD (DCM) level of theory. ΔE , ΔH , ΔG , and ΔG (GV50), hartree; $\Delta\Delta G$, kcal/mol.

**Distortion/Interaction-Activation Strain Fragments and Electronic Energy by Structure –
MN15 / def2-TZVP / SMD (DCM)**

6b Fragment F1

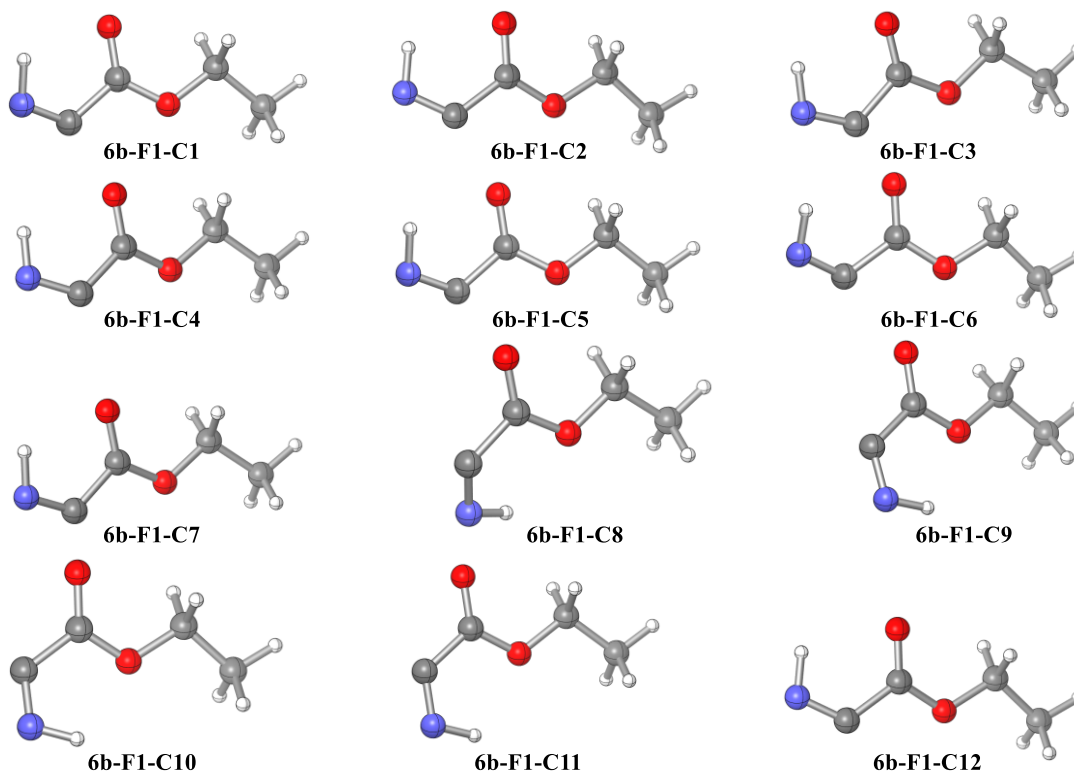


Figure S47. Conformers of fragment **F1** for intermediate **6b**.

Table S47. Energies of conformers of fragment **F1** for intermediate **6b**. ^a

Structure	ΔE
6b-C3	-360.890759
6b-C2	-360.8901045
6b-C12	-360.8900083
6b-C7	-360.8898753
6b-C5	-360.8895681
6b-C1	-360.8895596
6b-C6	-360.8892895
6b-C4	-360.8892737
6b-C11	-360.8886553

6b-C9	-360.888134
6b-C8	-360.8879095
6b-C10	-360.8878114

^aEnergies were obtained as single points at the MN15 / def2-TZVP / SMD (DCM) level of theory based on structures optimized at the same level of theory. ΔE , hartree.

6b Fragment F2

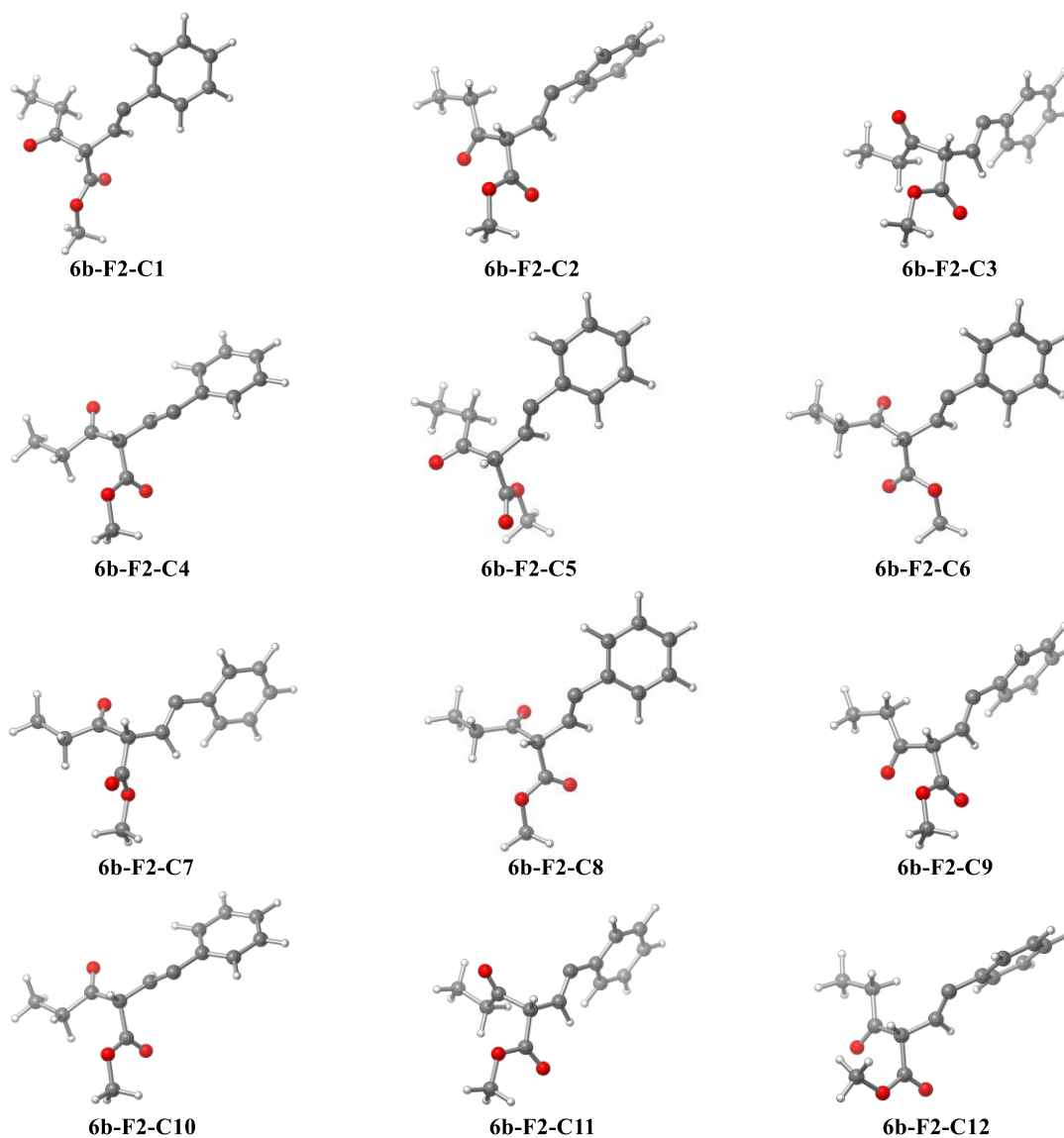


Figure S48. Conformers of fragment **F2** for intermediate **6b**.

Table S48. Energies of conformers of fragment **F2** for intermediate **6b**.^a

Structure	ΔE
6b-C2	-767.5050699
6b-C9	-767.5047208
6b-C11	-767.5040672
6b-C3	-767.5038929
6b-C8	-767.5023681
6b-C4	-767.5023488
6b-C10	-767.5023311
6b-C1	-767.5021559
6b-C6	-767.501702
6b-C7	-767.501279
6b-C5	-767.5010874
6b-C12	-767.4973661

^aEnergies were obtained as single points at the MN15 / def2-TZVP / SMD (DCM) level of theory based on structures optimized at the same level of theory. ΔE , hartree.

6b-Cs Fragment F1

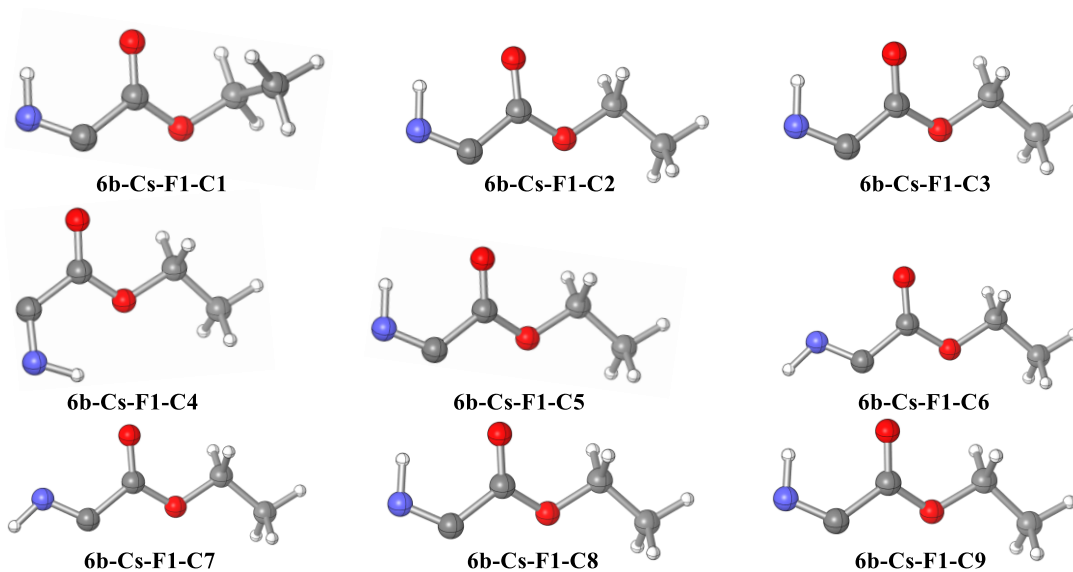


Figure S49. Conformers of fragment **F1** for intermediate **6b-Cs**.

Table S49. Energies of conformers of fragment **F1** for intermediate **6b-Cs**.^a

Structure	ΔE
6b-Cs-C6	-360.8949175
6b-Cs-C7	-360.8943334
6b-Cs-C1	-360.88957
6b-Cs-C5	-360.8894261
6b-Cs-C9	-360.8893931
6b-Cs-C8	-360.8892505
6b-Cs-C3	-360.8892505
6b-Cs-C2	-360.888974
6b-Cs-C4	-360.8882698

^aEnergies were obtained as single points at the MN15 / def2-TZVP / SMD (DCM) level of theory based on structures optimized at the same level of theory. ΔE , hartree.

6b-Cs Fragment F2

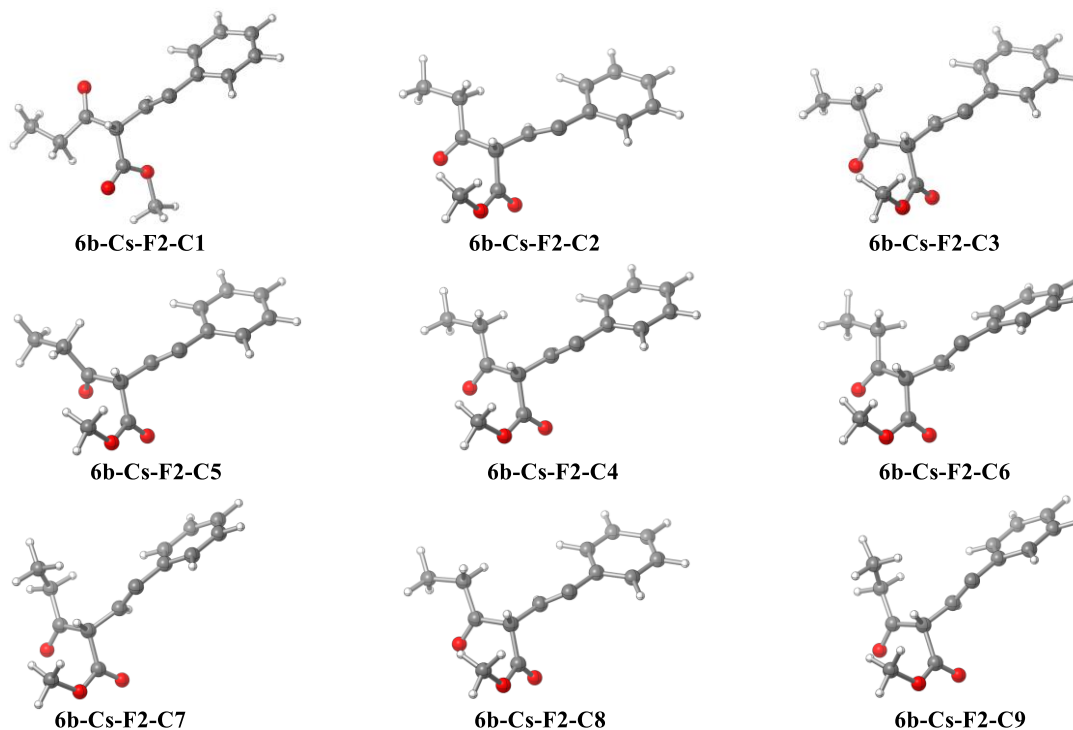


Figure S50. Conformers of fragment **F2** for intermediate **6b-Cs**.

Table S50. Energies of conformers of fragment **F2** for intermediate **6b-Cs**.^a

Structure	ΔE
6b-Cs-C1	-767.5017852
6b-Cs-C6	-767.4974734
6b-Cs-C7	-767.495785
6b-Cs-C4	-767.495432
6b-Cs-C9	-767.4949094
6b-Cs-C2	-767.4943543
6b-Cs-C8	-767.4935853
6b-Cs-C3	-767.4935853
6b-Cs-C5	-767.4919119

^aEnergies were obtained as single points at the MN15 / def2-TZVP / SMD (DCM) level of theory based on structures optimized at the same level of theory. ΔE , hartree.

6b-Na Fragment F1

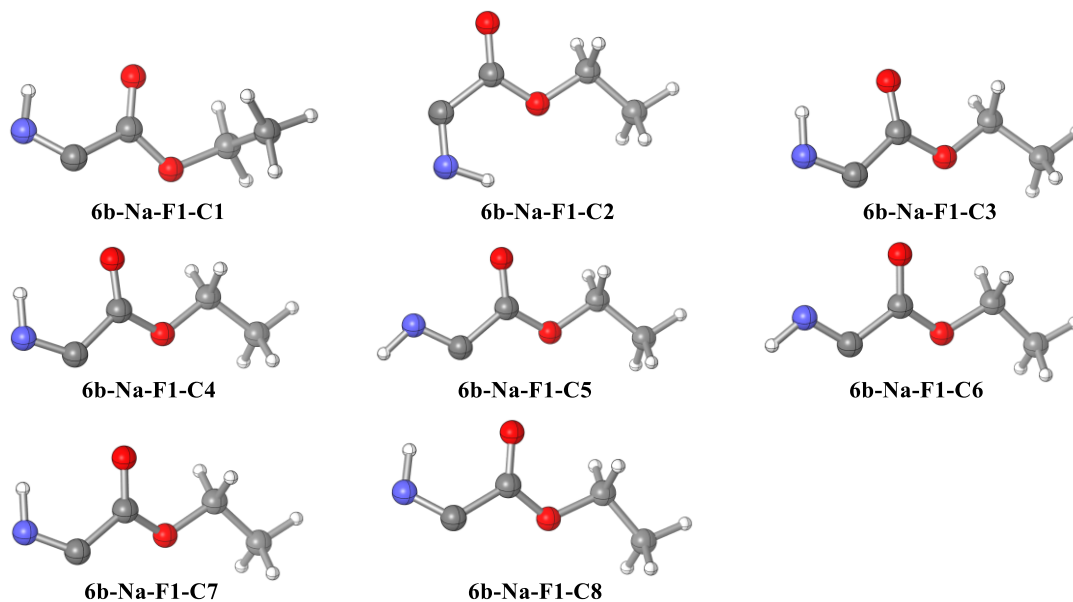


Figure S51. Conformers of fragment **F1** for intermediate **6b-Na**.

Table S51. Energies of conformers of fragment **F1** for intermediate **6b-Na**.^a

Structure	ΔE
6b-Na-C5	-360.8931161
6b-Na-C6	-360.8929365
6b-Na-C4	-360.8898244
6b-Na-C8	-360.889313
6b-Na-C1	-360.8891442
6b-Na-C7	-360.8887943
6b-Na-C2	-360.8885236
6b-Na-C3	-360.8883351

^aEnergies were obtained as single points at the MN15 / def2-TZVP / SMD (DCM) level of theory based on structures optimized at the same level of theory. ΔE , hartree.

6b-Na Fragment F2

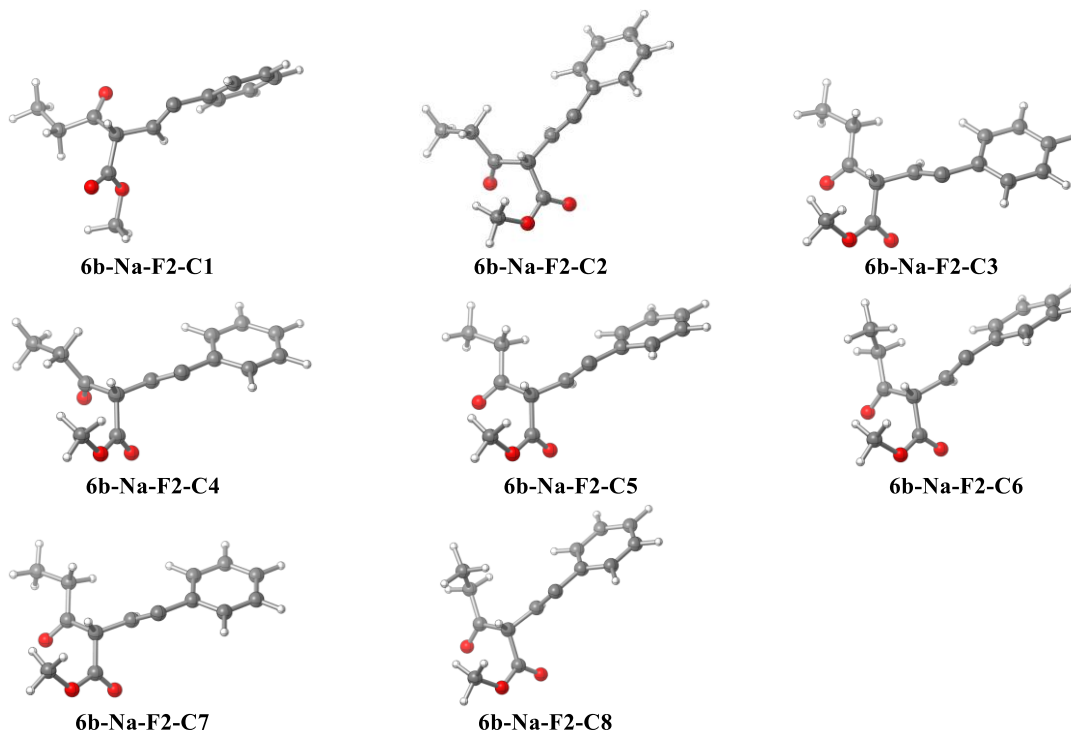


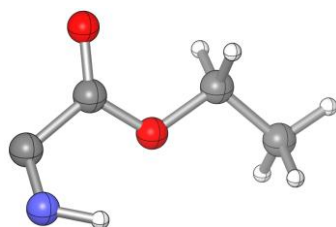
Figure S52. Conformers of fragment **F2** for intermediate **6b-Na**.

Table S52. Energies of conformers fragment **F2** for intermediate **6b-Na**. ^a

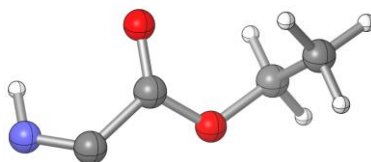
Structure	ΔE
6b-Na-C1	-767.5020854
6b-Na-C5	-767.4974223
6b-Na-C6	-767.4959084
6b-Na-C2	-767.4951958
6b-Na-C8	-767.4948013
6b-Na-C7	-767.4941417
6b-Na-C3	-767.4929534
6b-Na-C4	-767.4896099

^aEnergies were obtained as single points at the MN15 / def2-TZVP / SMD (DCM) level of theory based on structures optimized at the same level of theory. ΔE , hartree.

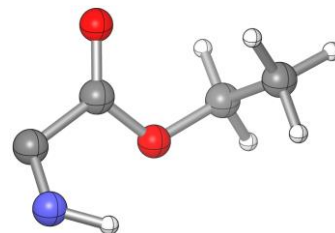
TSB-K-T Fragment F1



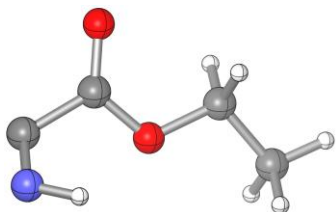
TSB-K-T-F1-C1



TSB-K-T-F1-C2



TSB-K-T-F1-C3



TSB-K-T-F1-C4

Figure S53. Conformers of fragment **F1** for transition state **TSB-K-T**.

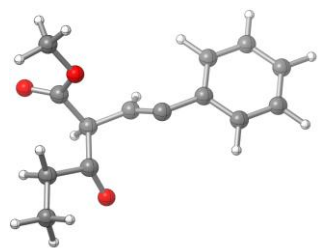
Table S53. Energies of conformers of fragment **F1** for transition state **TSB-K-T**. ^a

Structure	ΔE
TSB-K-T-C2	-360.8870855
TSB-K-T-C1	-360.8853292

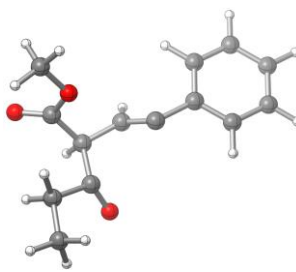
TSB-K-T-C4	-360.8852605
TSB-K-T-C3	-360.8850094

^aEnergies were obtained as single points at the MN15 / def2-TZVP / SMD (DCM) level of theory based on structures optimized at the same level of theory. ΔE , hartree.

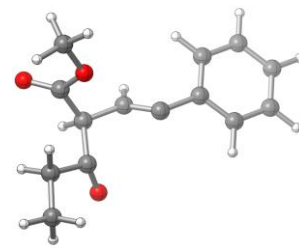
TSB-K-T Fragment F2



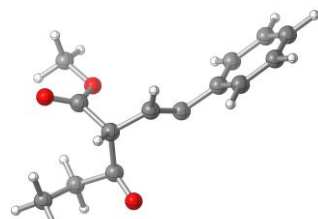
TSB-K-T-F2-C1



TSB-K-T-F2-C2



TSB-K-T-F2-C3



TSB-K-T-F2-C4

Figure S54. Conformers of fragment **F2** for transition state **TSB-K-T**.

Table S54. Energies of conformers of fragment **F2** for transition state **TSB-K-T**.^a

Structure	ΔE
TSB-K-T-C4	-767.4693553
TSB-K-T-C3	-767.4692234
TSB-K-T-C1	-767.4690992
TSB-K-T-C2	-767.468291

^aEnergies were obtained as single points at the MN15 / def2-TZVP / SMD (DCM) level of theory based on structures optimized at the same level of theory. ΔE , hartree.

TSB-K-C Fragment F1

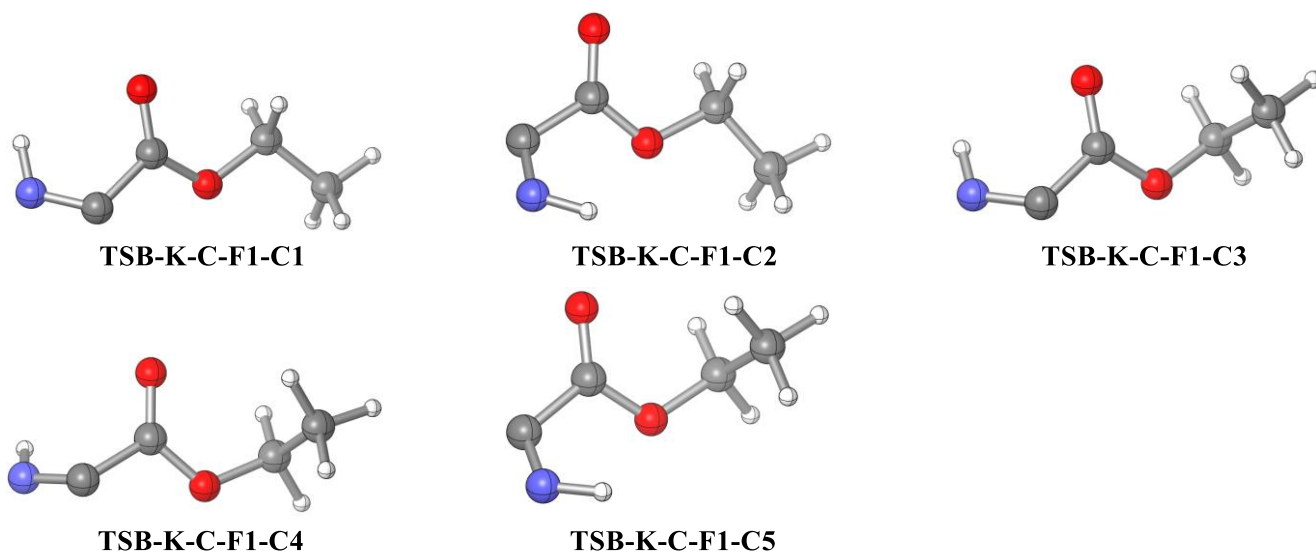


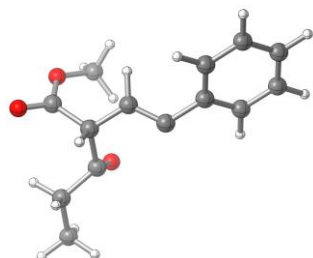
Figure S55. Conformers of fragment **F1** for transition state **TSB-K-C**.

Table S55. Energies of conformers of fragment **F1** for transition state **TSB-K-C**.^a

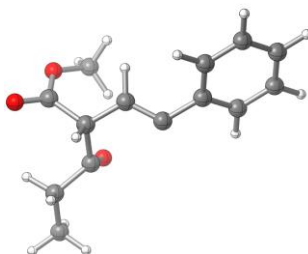
Structure	ΔE
TSB-K-C-C4	-360.888161
TSB-K-C-C3	-360.8866489
TSB-K-C-C1	-360.8861748
TSB-K-C-C5	-360.8858119
TSB-K-C-C2	-360.8849229

^aEnergies were obtained as single points at the MN15 / def2-TZVP / SMD (DCM) level of theory based on structures optimized at the same level of theory. ΔE , hartree.

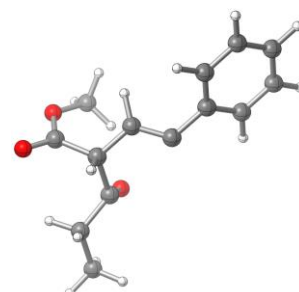
TSB-K-C Fragment F2



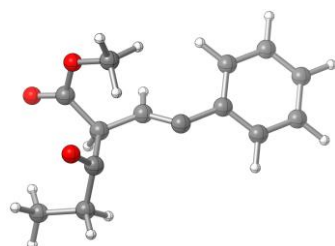
TSB-K-C-F2-C1



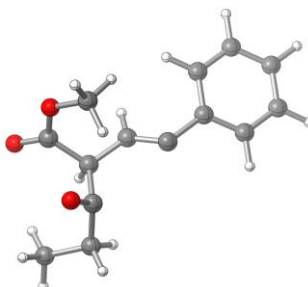
TSB-K-C-F2-C2



TSB-K-C-F2-C3



TSB-K-C-F2-C4



TSB-K-C-F2-C5

Figure S56. Conformers of fragment **F2** for transition state **TSB-K-C**.

Table S56. Energies of conformers of fragment **F2** for transition state **TSB-K-C**.^a

Structure	ΔE
TSB-K-C-C5	-767.4609139
TSB-K-C-C4	-767.46032
TSB-K-C-C1	-767.4594254
TSB-K-C-C3	-767.4592898
TSB-K-C-C2	-767.4588573

^aEnergies were obtained as single points at the MN15 / def2-TZVP / SMD (DCM) level of theory based on structures optimized at the same level of theory. ΔE , hartree.

TSB-E-T Fragment F1

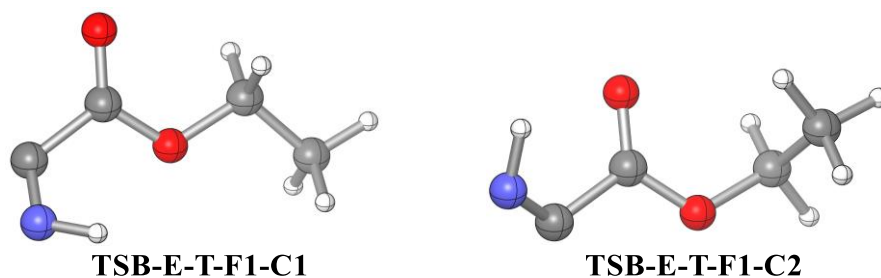


Figure S57. Conformers of fragment **F1** for transition state **TSB-E-T**.

Table S57. Energies of conformers of fragment **F1** for transition state **TSB-E-T**.^a

Structure	ΔE
TSB-E-T-C1	-360.8866259
TSB-E-T-C2	-360.8863391

^aEnergies were obtained as single points at the MN15 / def2-TZVP / SMD (DCM) level of theory based on structures optimized at the same level of theory. ΔE , hartree.

TSB-E-T Fragment F2

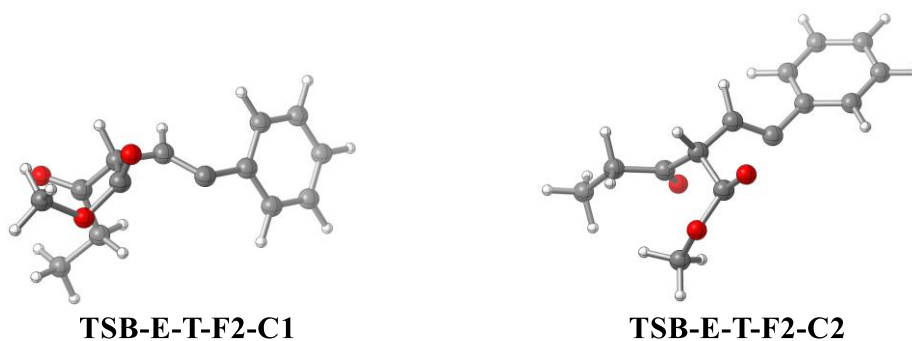


Figure S58. Conformers of fragment **F2** for transition state **TSB-E-T**.

Table S58. Energies of conformers of fragment **F2** for transition state **TSB-E-T**.^a

Structure	ΔE
TSB-E-T-C1	-767.4618329
TSB-E-T-C2	-767.4522743

^aEnergies were obtained as single points at the MN15 / def2-TZVP / SMD (DCM) level of theory based on structures optimized at the same level of theory. ΔE , hartree.

TSB-E-C Fragment F1

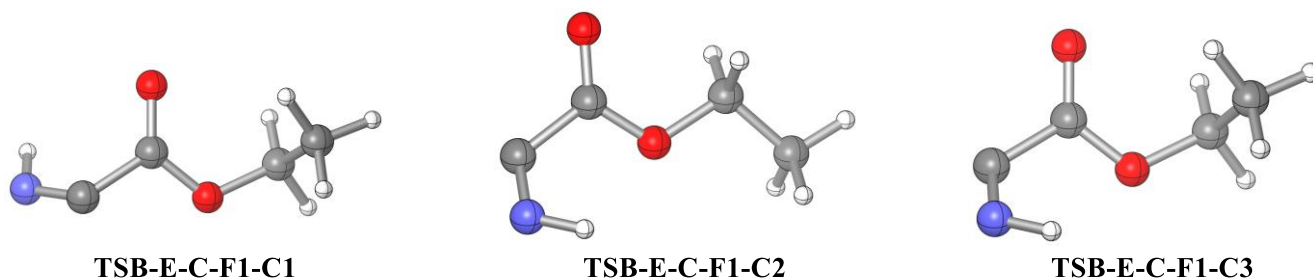


Figure S59. Conformers of fragment **F1** for transition state **TSB-E-C**.

Table S59. Energies of conformers of fragment **F1** for transition state **TSB-E-C**. ^a

Structure	ΔE
TSB-E-C-C1	-360.8894664
TSB-E-C-C2	-360.8876299
TSB-E-C-C3	-360.8873482

^aEnergies were obtained as single points at the MN15 / def2-TZVP / SMD (DCM) level of theory based on structures optimized at the same level of theory. ΔE , hartree.

TSB-E-C Fragment F2

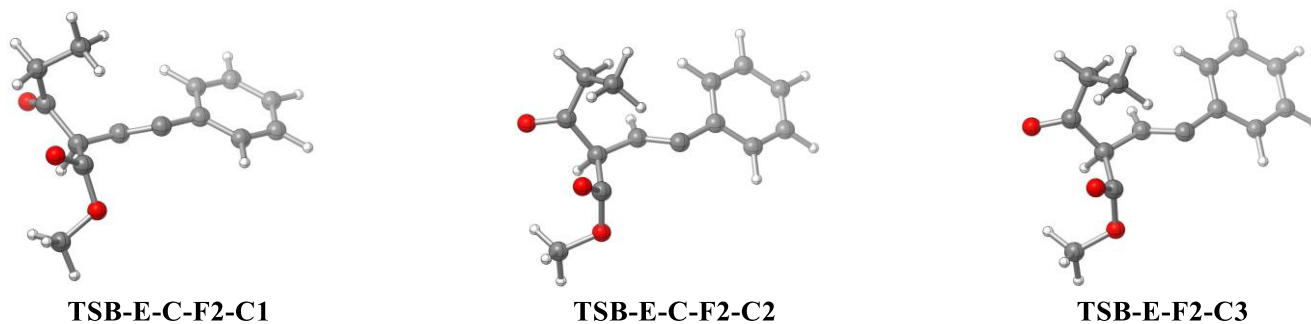


Figure S60. Conformers of fragment **F2** for transition state **TSB-E-C**.

Table S60. Energies of conformers of fragment **F2** for transition state **TSB-E-C**. ^a

Structure	ΔE
TSB-E-C-C3	-767.457268
TSB-E-C-C2	-767.4572525
TSB-E-C-C1	-767.4569468

^aEnergies were obtained as single points at the MN15 / def2-TZVP / SMD (DCM) level of theory based on structures optimized at the same level of theory. ΔE , hartree.

TSB-Cs-K-T Fragment F1

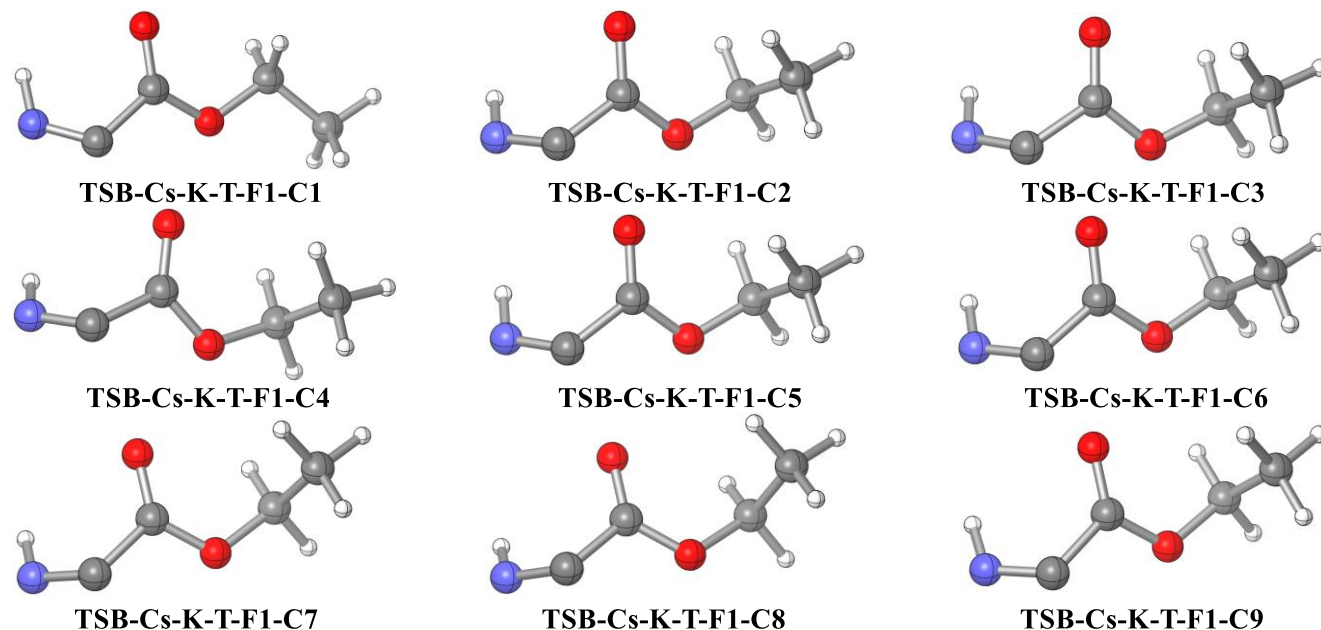


Figure S61. Conformers of fragment **F1** for transition state **TSB-Cs-K-T**.

Table S61. Energies of conformers of fragment **F1** for transition state **TSB-Cs-K-T**.^a

Structure	ΔE
TSB-Cs-K-T-C1	-360.8890472
TSB-Cs-K-T-C4	-360.8884158
TSB-Cs-K-T-C3	-360.8882955
TSB-Cs-K-T-C5	-360.8876659
TSB-Cs-K-T-C2	-360.8876348
TSB-Cs-K-T-C9	-360.8875916
TSB-Cs-K-T-C6	-360.887549
TSB-Cs-K-T-C7	-360.8870643
TSB-Cs-K-T-C8	-360.8866972

^aEnergies were obtained as single points at the MN15 / def2-TZVP / SMD (DCM) level of theory based on structures optimized at the same level of theory. ΔE , hartree.

TSB-Cs-K-T Fragment F2

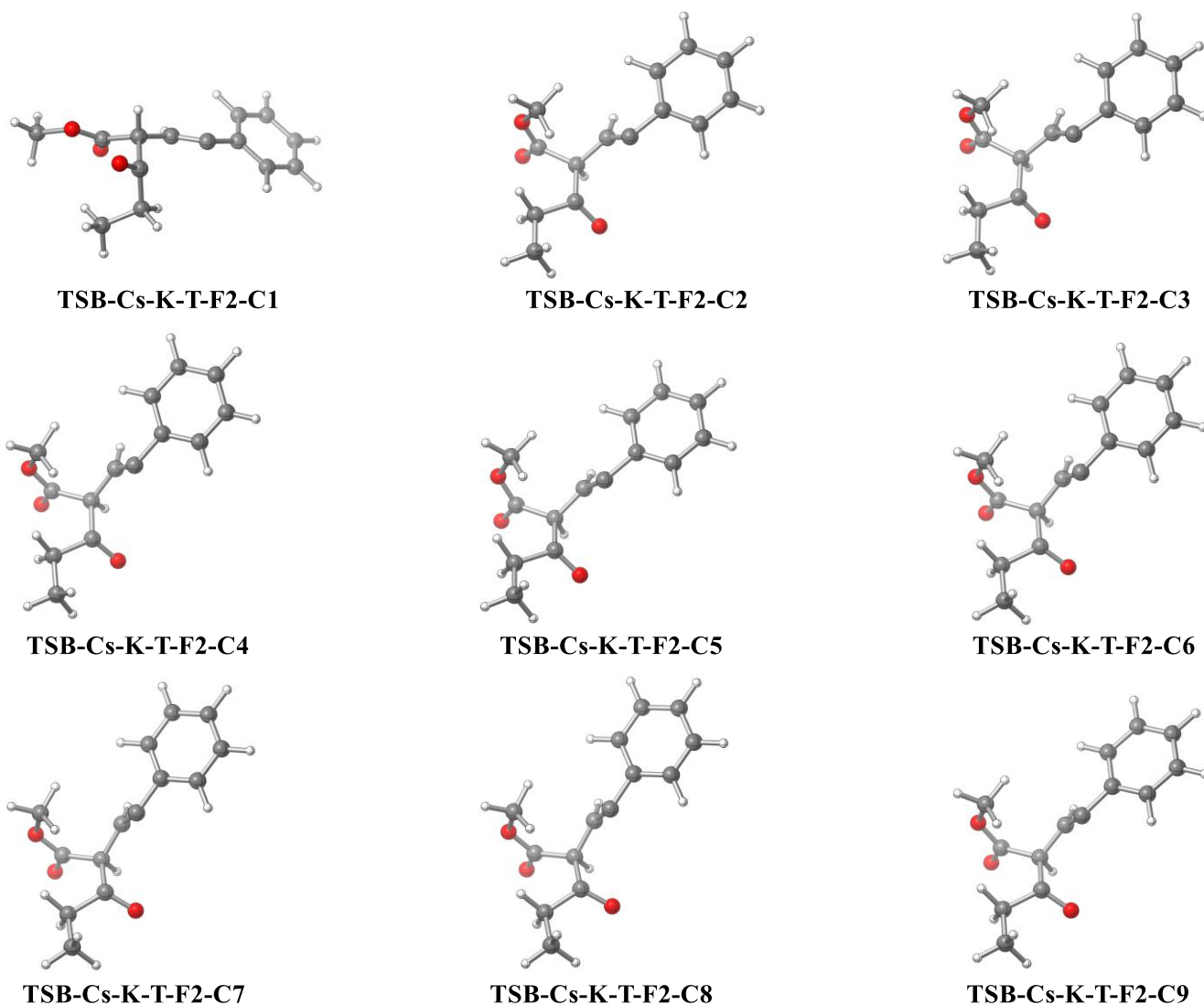


Figure S62. Conformers of fragment **F2** for transition state **TSB-Cs-K-T**.

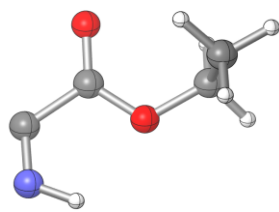
Table S62. Energies of conformers of fragment **F2** for transition state **TSB-Cs-K-T**.^a

Structure	ΔE
TSB-Cs-K-T-C1	-767.4793681
TSB-Cs-K-T-C3	-767.4641035
TSB-Cs-K-T-C2	-767.4625831
TSB-Cs-K-T-C4	-767.4610787
TSB-Cs-K-T-C5	-767.459925

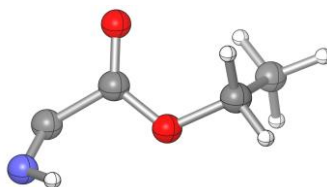
TSB-Cs-K-T-C7	-767.4593369
TSB-Cs-K-T-C6	-767.4590215
TSB-Cs-K-T-C8	-767.457707
TSB-Cs-K-T-C9	-767.4565832

^aEnergies were obtained as single points at the MN15 / def2-TZVP / SMD (DCM) level of theory based on structures optimized at the same level of theory. ΔE , hartree.

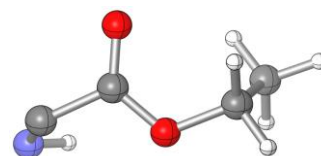
TSB-Cs-K-C Fragment F1



TSB-Cs-K-C-F1-C1



TSB-Cs-K-C-F1-C2



TSB-Cs-K-C-F1-C3

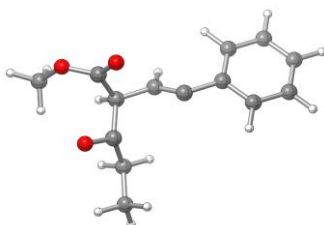
Figure S63. Conformers of fragment **F1** for transition state **TSB-Cs-K-C**.

Table S63. Energies of conformers of fragment **F1** for transition state **TSB-Cs-K-C**.^a

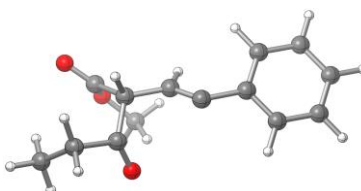
Structure	ΔE
TSB-Cs-K-C-C2	-360.8858021
TSB-Cs-K-C-C1	-360.8854029
TSB-Cs-K-C-C3	-360.8853893

^aEnergies were obtained as single points at the MN15 / def2-TZVP / SMD (DCM) level of theory based on structures optimized at the same level of theory. ΔE , hartree.

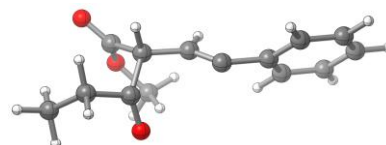
TSB-Cs-K-C Fragment F2



TSB-Cs-K-C-F2-C1



TSB-Cs-K-C-F2-C2



TSB-Cs-K-C-F2-C3

Figure S64. Conformers of fragment **F2** for transition state **TSB-Cs-K-C**.

Table S64. Energies of conformers of fragment **F2** for transition state **TSB-Cs-K-C**.^a

Structure	ΔE
TSB-Cs-K-C-C1	-767.4654485
TSB-Cs-K-C-C2	-767.4651693
TSB-Cs-K-C-C3	-767.4621897

^aEnergies were obtained as single points at the MN15 / def2-TZVP / SMD (DCM) level of theory based on structures optimized at the same level of theory. ΔE , hartree.

TSB-Cs-E-T Fragment F1

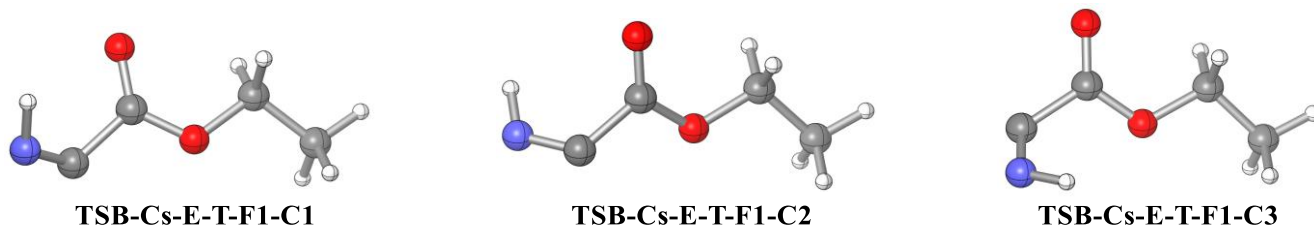


Figure S65. Conformers of fragment **F1** for transition state **TSB-Cs-E-T**.

Table S65. Energies of conformers of fragment **F1** for transition state **TSB-Cs-E-T**.^a

Structure	ΔE
TSB-Cs-E-T-C2	-360.8881578
TSB-Cs-E-T-C1	-360.8878187
TSB-Cs-E-T-C3	-360.8868463

^aEnergies were obtained as single points at the MN15 / def2-TZVP / SMD (DCM) level of theory based on structures optimized at the same level of theory. ΔE , hartree.

TSB-Cs-E-T Fragment F2

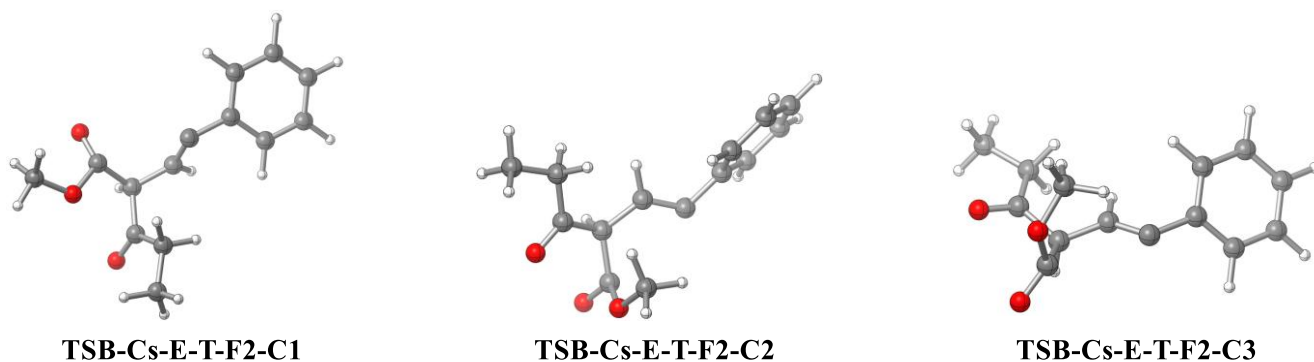


Figure S66. Conformers of fragment **F2** for transition state **TSB-Cs-E-T**.

Table S66. Energies of conformers of fragment **F2** for transition state **TSB-Cs-E-T**.^a

Structure	ΔE
TSB-Cs-E-T-C1	-767.4677878
TSB-Cs-E-T-C3	-767.4618319
TSB-Cs-E-T-C2	-767.4615093

^aEnergies were obtained as single points at the MN15 / def2-TZVP / SMD (DCM) level of theory based on structures optimized at the same level of theory. ΔE , hartree.

TSB-Cs-E-C Fragment F1

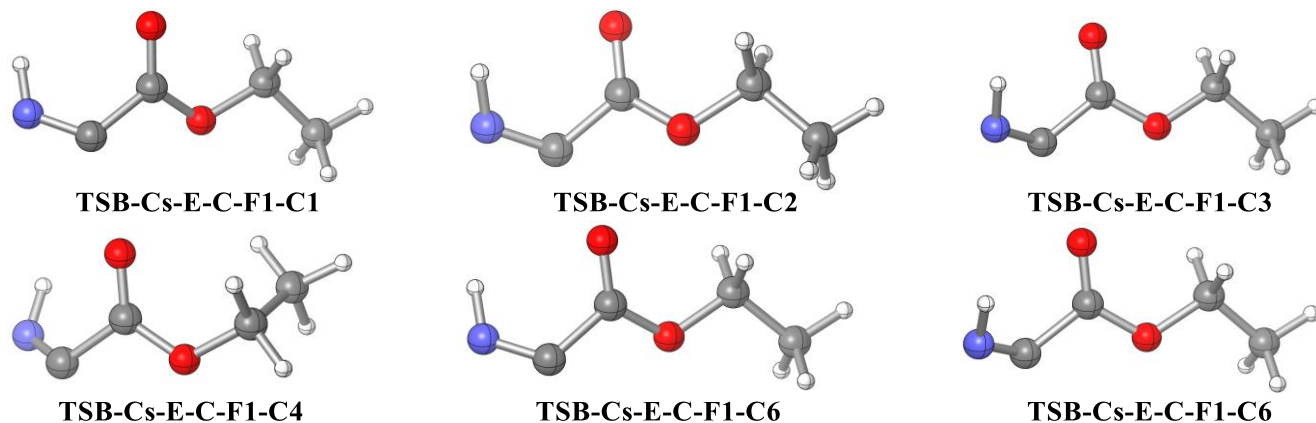


Figure S67. Conformers of fragment **F1** for transition state **TSB-Cs-E-C**.

Table S67. Energies of conformers of fragment **F1** for transition state **TSB-Cs-E-C**.^a

Structure	ΔE
TSB-Cs-E-C-C6	-360.8885666
TSB-Cs-E-C-C1	-360.8878381
TSB-Cs-E-C-C4	-360.8877311
TSB-Cs-E-C-C5	-360.8877224
TSB-Cs-E-C-C2	-360.8875087

^aEnergies were obtained as single points at the MN15 / def2-TZVP / SMD (DCM) level of theory based on structures optimized at the same level of theory. ΔE , hartree.

TSB-Cs-E-C Fragment F2

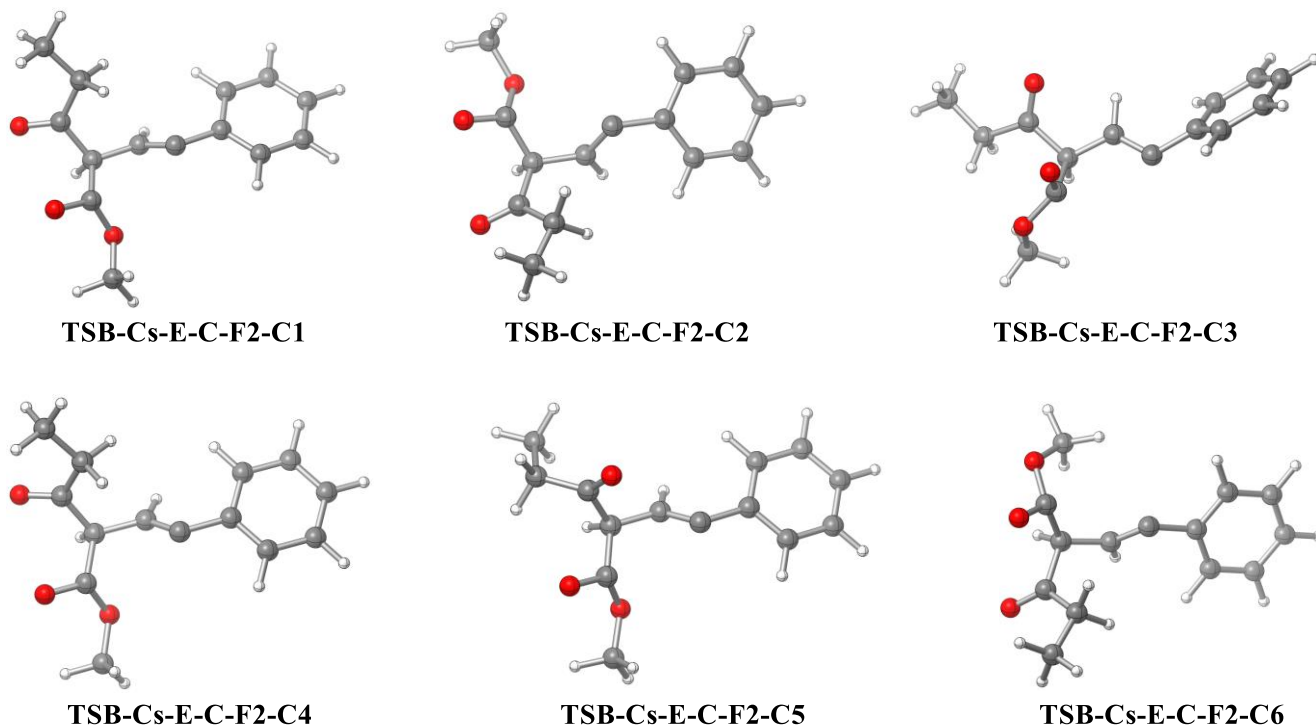


Figure S68. Conformers of fragment **F2** for transition state **TSB-Cs-E-C**.

Table S68. Energies of conformers of fragment **F2** for transition state **TSB-Cs-E-C**.^a

Structure	ΔE
TSB-Cs-E-C-C6	-767.466413
TSB-Cs-E-C-C5	-767.4637485

TSB-Cs-E-C-C4	-767.4635251
TSB-Cs-E-C-C1	-767.4628295
TSB-Cs-E-C-C2	-767.4626709

^aEnergies were obtained as single points at the MN15 / def2-TZVP / SMD (DCM) level of theory based on structures optimized at the same level of theory. ΔE , hartree.

TSB-Na-K-T Fragment F1

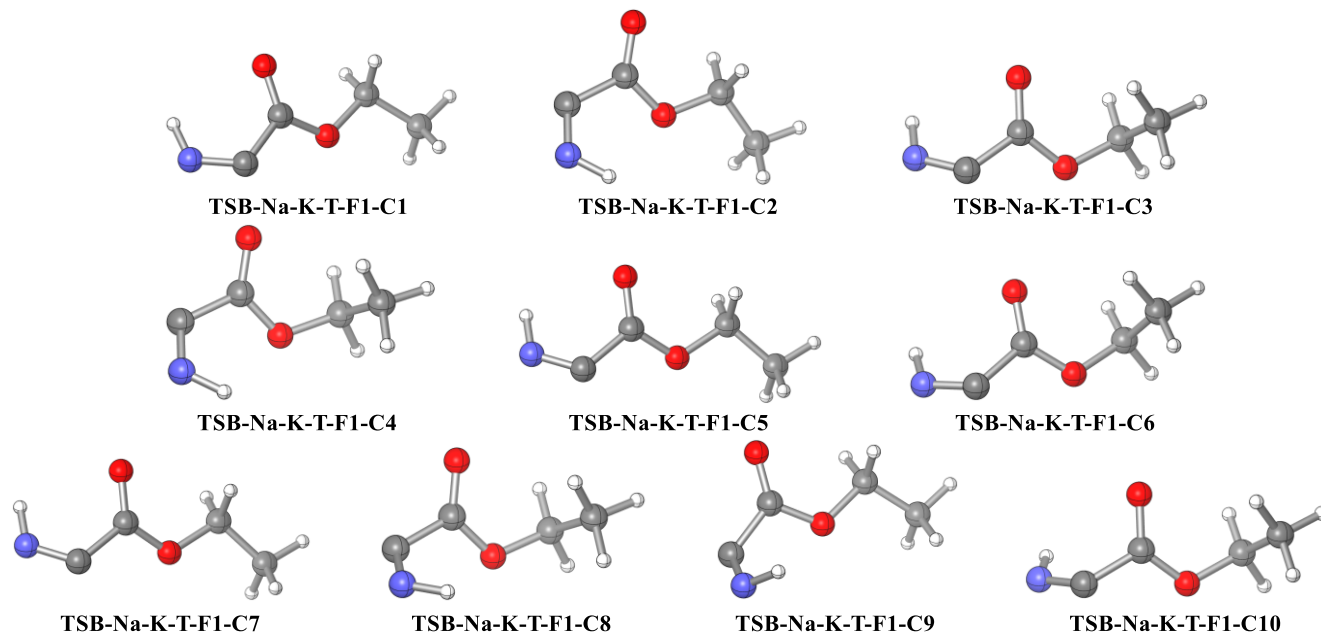


Figure S69. Conformers of fragment **F1** for transition state **TSB-Na-K-T**.

Table S69. Energies of conformers of fragment **F1** for transition state **TSB-Na-K-T**.^a

Structure	ΔE
TSB-Na-K-T-C3	-360.8898057
TSB-Na-K-T-C6	-360.8897817
TSB-Na-K-T-C7	-360.889501
TSB-Na-K-T-C5	-360.8892917
TSB-Na-K-T-C1	-360.8892682
TSB-Na-K-T-C2	-360.8876763
TSB-Na-K-T-C4	-360.8874357
TSB-Na-K-T-C8	-360.8867019

TSB-Na-K-T-C9	-360.8858274
TSB-Na-K-T-C10	-360.885262

^aEnergies were obtained as single points at the MN15 / def2-TZVP / SMD (DCM) level of theory based on structures optimized at the same level of theory. ΔE , hartree.

TSB-Na-K-T Fragment F2

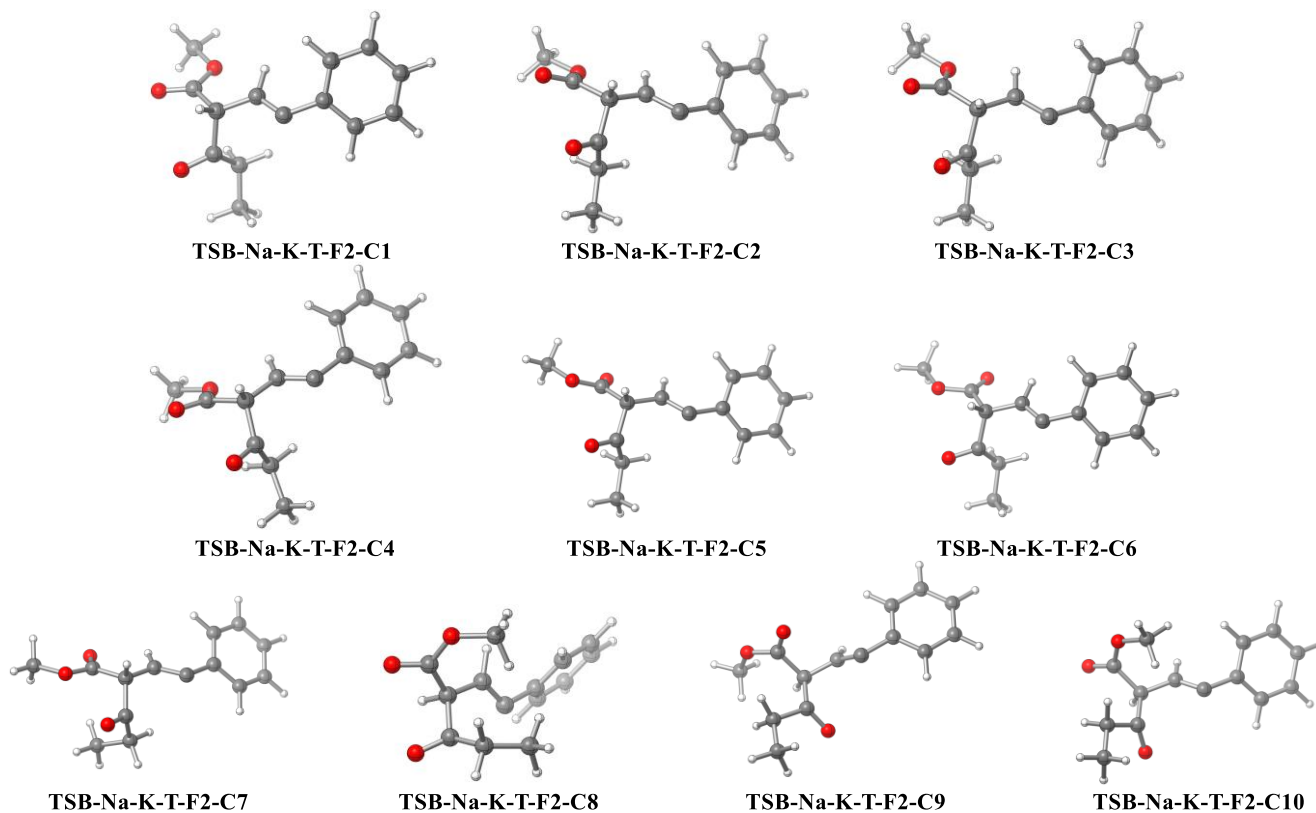


Figure S70. Conformers of fragment **F2** for transition state **TSB-Na-K-T**.

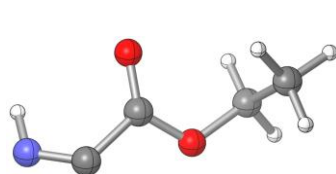
Table S70. Energies of conformers of fragment **F2** for transition state **TSB-Na-K-T**.^a

Structure	ΔE
TSB-Na-K-T-C7	-767.483619
TSB-Na-K-T-C6	-767.4829992
TSB-Na-K-T-C5	-767.4825825
TSB-Na-K-T-C3	-767.4807686
TSB-Na-K-T-C4	-767.4804792
TSB-Na-K-T-C2	-767.4800816

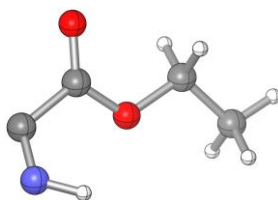
TSB-Na-K-T-C1	-767.4800435
TSB-Na-K-T-C9	-767.4712748
TSB-Na-K-T-C10	-767.4634094
TSB-Na-K-T-C8	-767.4605217

^aEnergies were obtained as single points at the MN15 / def2-TZVP / SMD (DCM) level of theory based on structures optimized at the same level of theory. ΔE , hartree.

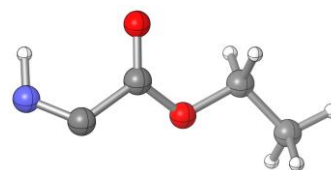
TSB-Na-K-C Fragment F1



TSB-Na-K-C-F1-C1



TSB-Na-K-C-F1-C2



TSB-Na-K-C-F1-C3

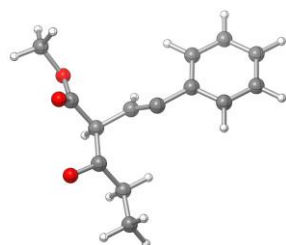
Figure S71. Conformers of fragment **F1** for transition state **TSB-Na-K-C**.

Table S71. Energies of conformers of fragment **F1** for transition state **TSB-Na-K-C**.^a

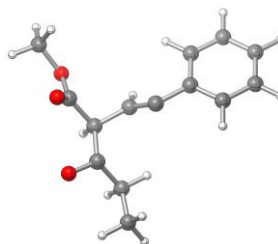
Structure	ΔE
TSB-Na-K-C-C1	-360.8893736
TSB-Na-K-C-C3	-360.8885053
TSB-Na-K-C-C2	-360.8879021

^aEnergies were obtained as single points at the MN15 / def2-TZVP / SMD (DCM) level of theory based on structures optimized at the same level of theory. ΔE , hartree.

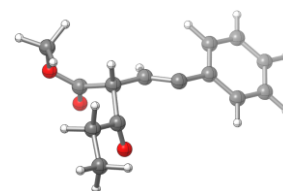
TSB-Na-K-C Fragment F2



TSB-Na-K-C-F2-C1



TSB-Na-K-C-F2-C2



TSB-Na-K-C-F2-C3

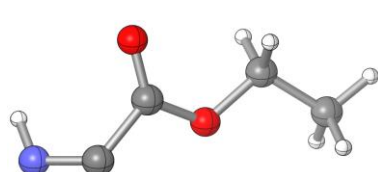
Figure S72. Conformers of fragment **F2** for transition state **TSB-Na-K-C**.

Table S72. Energies of conformers of fragment **F2** for transition state **TSB-Na-K-C**.^a

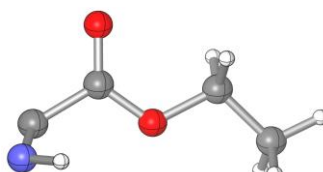
Structure	ΔE
TSB-Na-K-C-C2	-767.4757391
TSB-Na-K-C-C1	-767.4755163
TSB-Na-K-C-C3	-767.4701713

^aEnergies were obtained as single points at the MN15 / def2-TZVP / SMD (DCM) level of theory based on structures optimized at the same level of theory. ΔE , hartree.

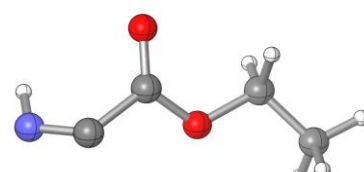
TSB-Na-E-T Fragment F1



TSB-Na-E-T-F1-C1



TSB-Na-E-T-F1-C2



TSB-Na-E-T-F1-C3

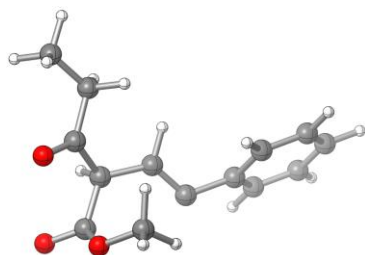
Figure S73. Conformers of fragment **F1** for transition state **TSB-Na-E-T**.

Table S73. Energies of conformers of fragment **F1** for transition state **TSB-Na-E-T**.^a

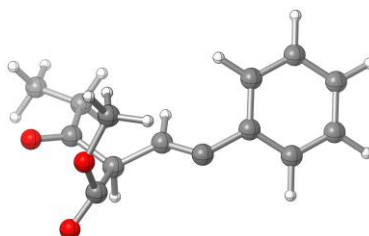
Structure	ΔE
TSB-Na-E-T-C1	-360.8888639
TSB-Na-E-T-C3	-360.8886144
TSB-Na-E-T-C2	-360.8882133

^aEnergies were obtained as single points at the MN15 / def2-TZVP / SMD (DCM) level of theory based on structures optimized at the same level of theory. ΔE , hartree.

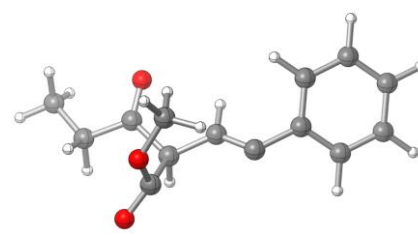
TSB-Na-E-T Fragment F2



TSB-Na-E-T-F2-C1



TSB-Na-E-T-F2-C2



TSB-Na-E-T-F2-C3

Figure S74. Conformers of fragment **F2** for transition state **TSB-Na-E-T**.

Table S74. Energies of conformers of fragment **F2** for transition state **TSB-Na-E-T**.^a

Structure	ΔE
TSB-Na-E-T-C3	-767.4717853
TSB-Na-E-T-C2	-767.4678667
TSB-Na-E-T-C1	-767.4676947

^aEnergies were obtained as single points at the MN15 / def2-TZVP / SMD (DCM) level of theory based on structures optimized at the same level of theory. ΔE , hartree.

TSB-Na-E-C Fragment F1

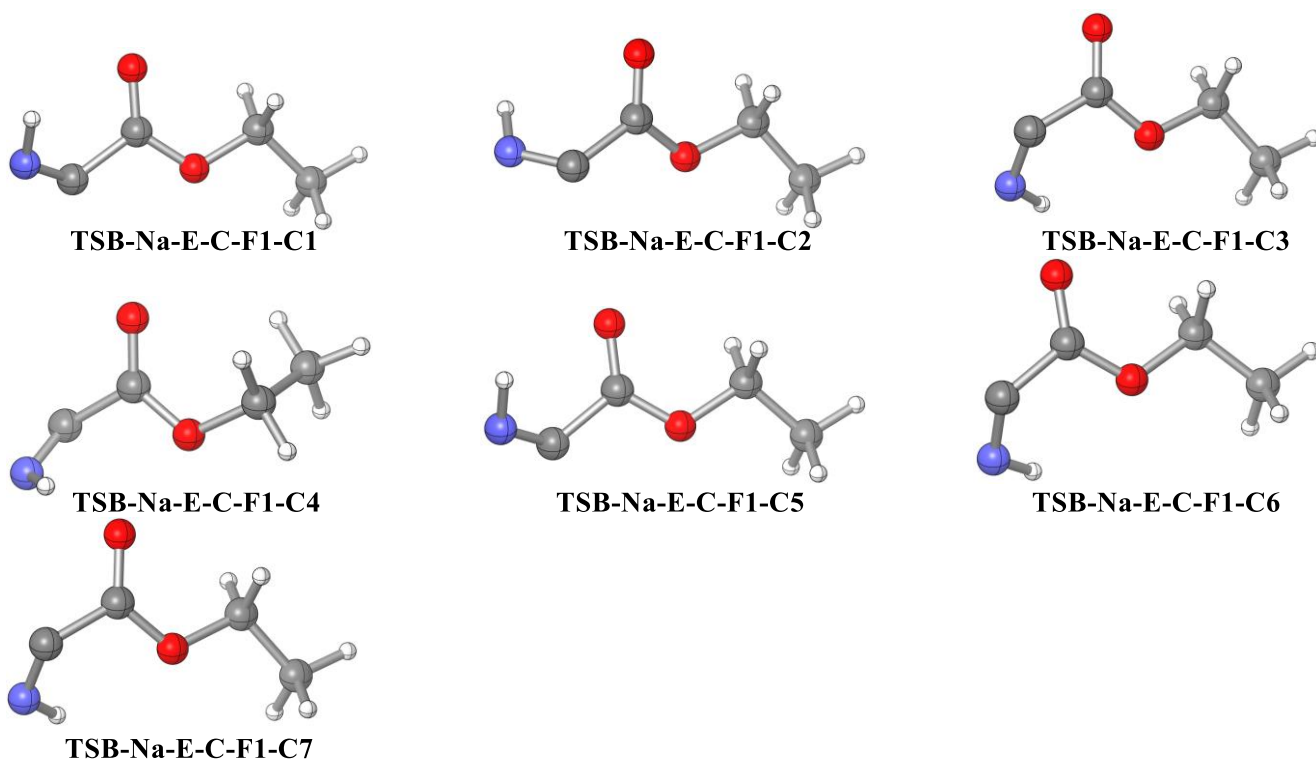


Figure S75. Conformers of fragment **F1** for transition state **TSB-Na-E-C**.

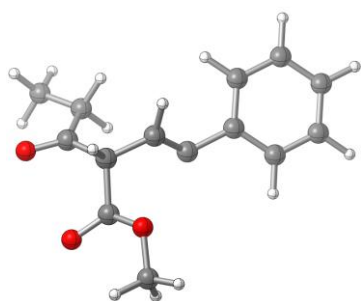
Table S75. Energies of conformers of fragment **F1** for transition state **TSB-Na-E-C**.^a

Structure	ΔE
TSB-Na-E-C5	-360.8893635
TSB-Na-E-C1	-360.8881534

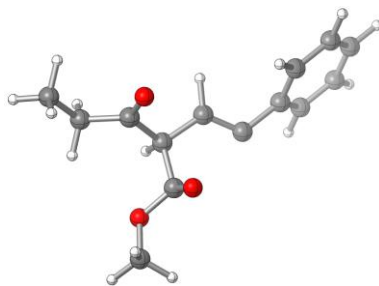
TSB-Na-E-C2	-360.8879725
TSB-Na-E-C7	-360.8878785
TSB-Na-E-C6	-360.8876561
TSB-Na-E-C3	-360.8869037
TSB-Na-E-C4	-360.8864558

^aEnergies were obtained as single points at the MN15 / def2-TZVP / SMD (DCM) level of theory based on structures optimized at the same level of theory. ΔE , hartree.

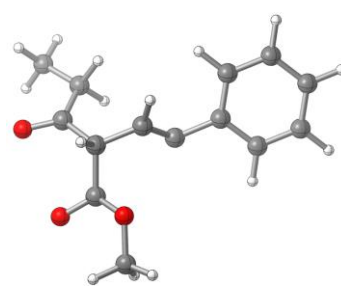
TSB-Na-E-C Fragment F2



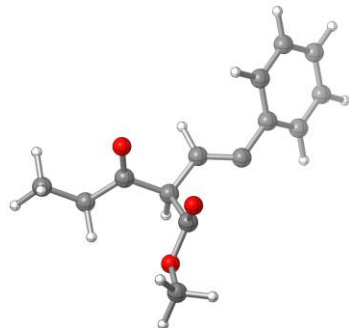
TSB-Na-E-C-F2-C1



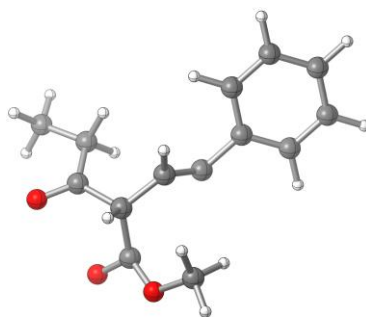
TSB-Na-E-C-F2-C2



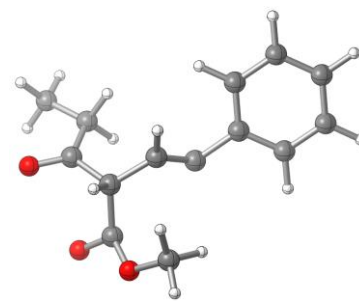
TSB-Na-E-C-F2-C3



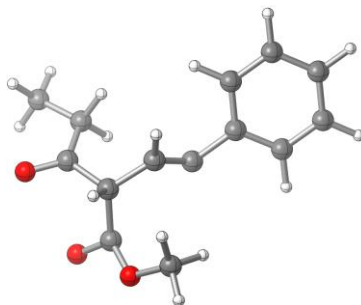
TSB-Na-E-C-F2-C4



TSB-Na-E-C-F2-C5



TSB-Na-E-C-F2-C6



TSB-Na-E-C-F2-C7

Figure S76. Conformers of fragment **F2** for transition state **TSB-Na-E-C**.

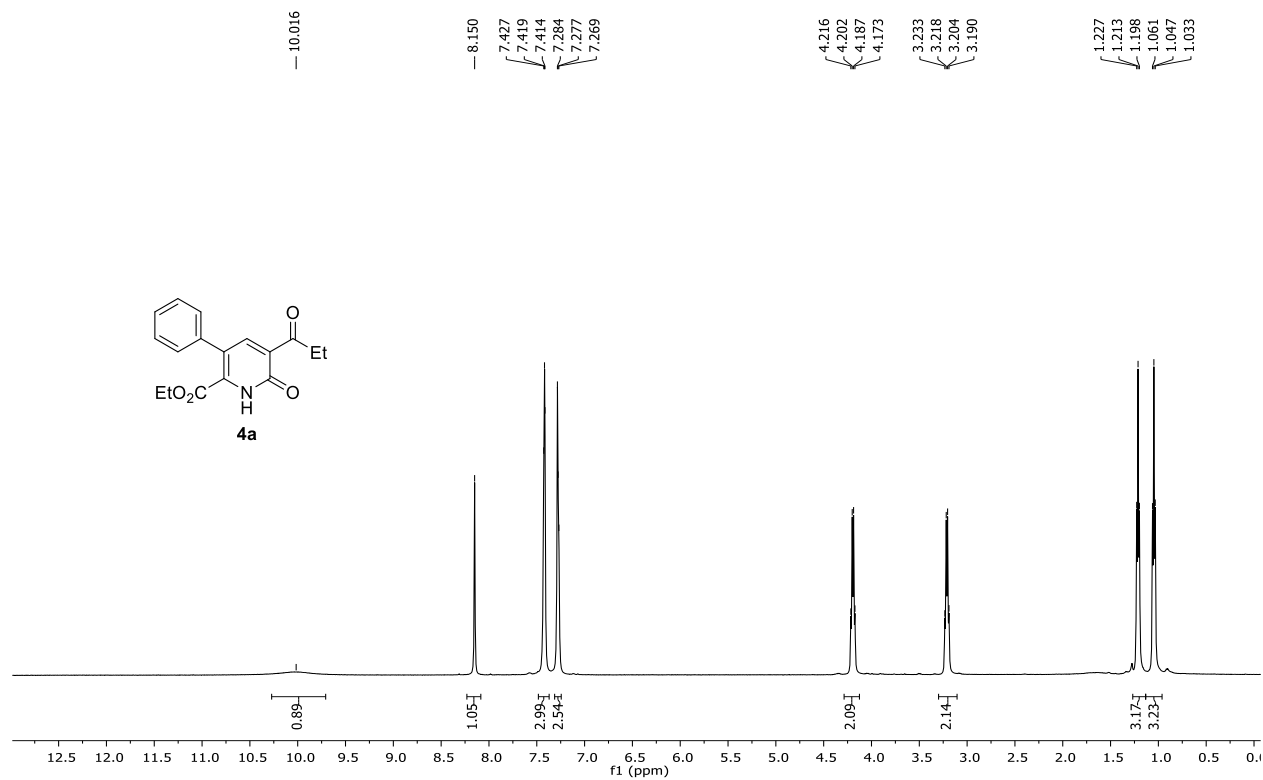
Table S76. Energies of conformers of fragment **F2** for transition state **TSB-Na-E-C**.^a

Structure	ΔE
TSB-Na-E-C4	-767.4713784
TSB-Na-E-C2	-767.4710121
TSB-Na-E-C1	-767.4682315
TSB-Na-E-C3	-767.4678666
TSB-Na-E-C6	-767.4673483
TSB-Na-E-C7	-767.4672787
TSB-Na-E-C5	-767.4669896

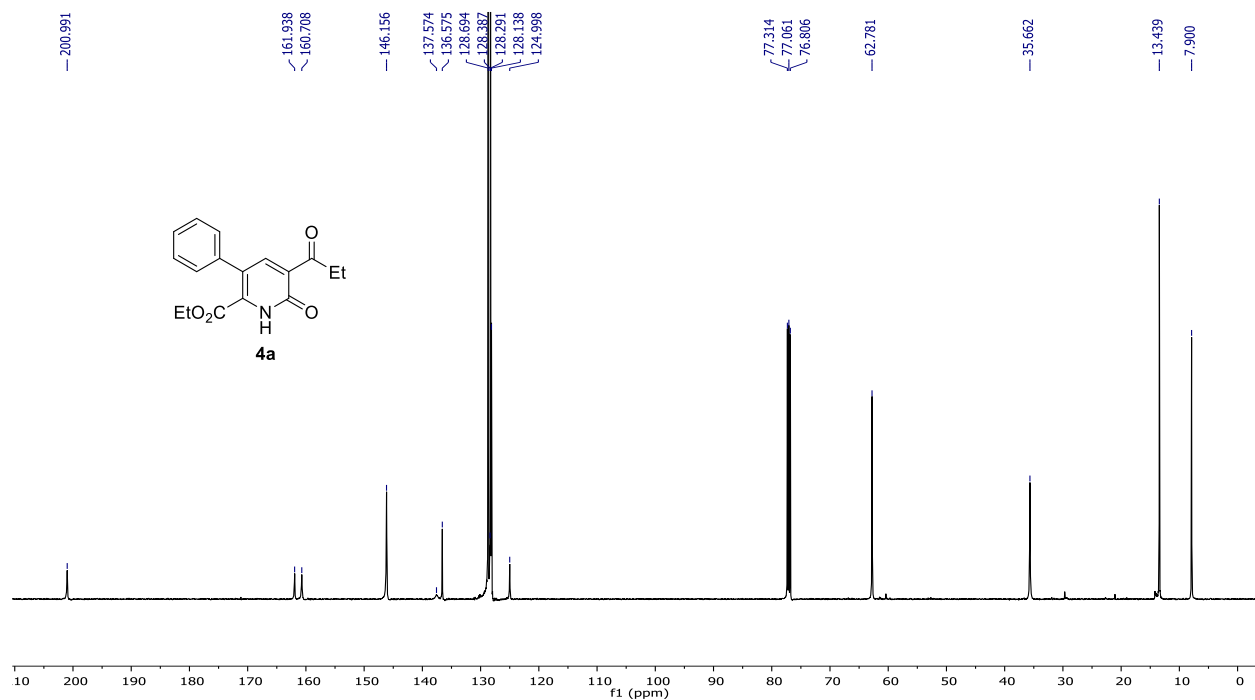
^aEnergies were obtained as single points at the MN15 / def2-TZVP / SMD (DCM) level of theory based on structures optimized at the same level of theory. ΔE , hartree.

9. NMR spectra

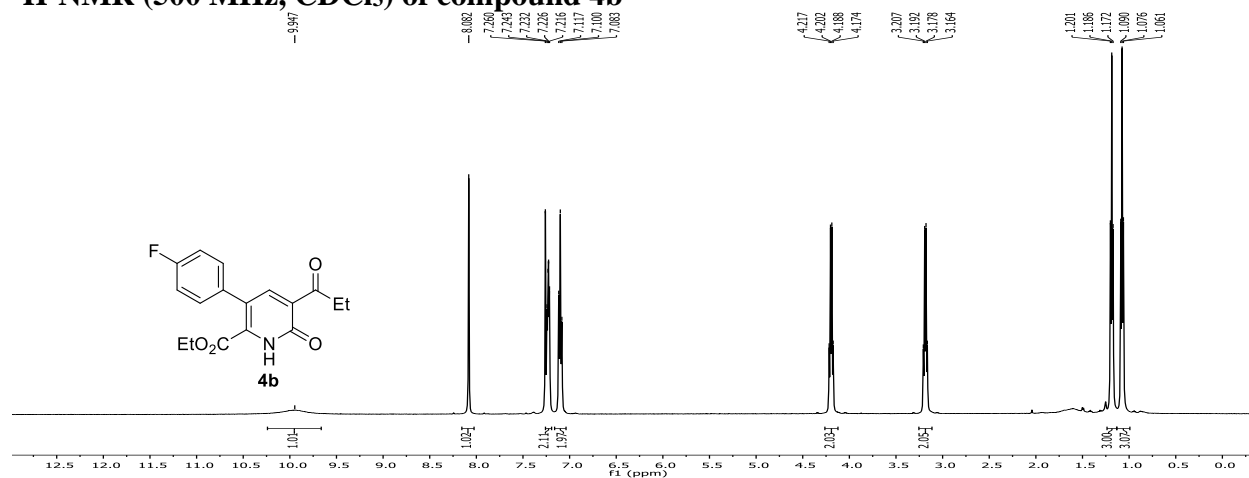
^1H -NMR (500 MHz, CDCl_3) of compound 4a



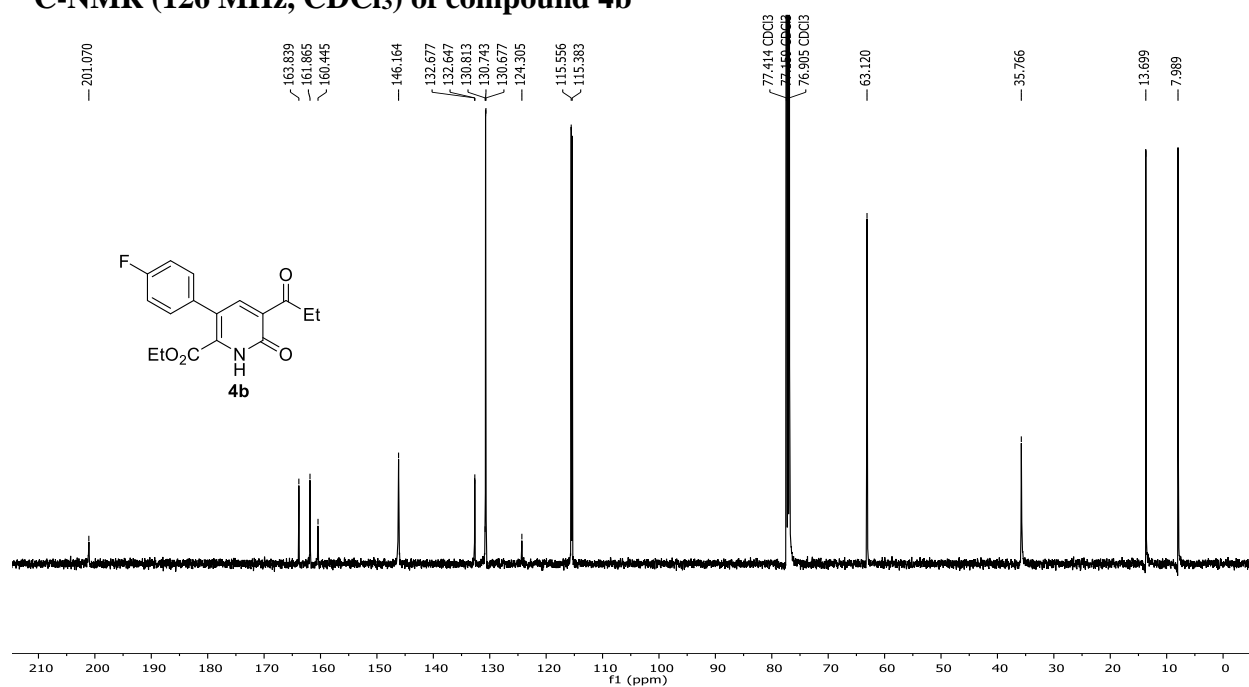
^{13}C -NMR (126 MHz, CDCl_3) of compound 4a



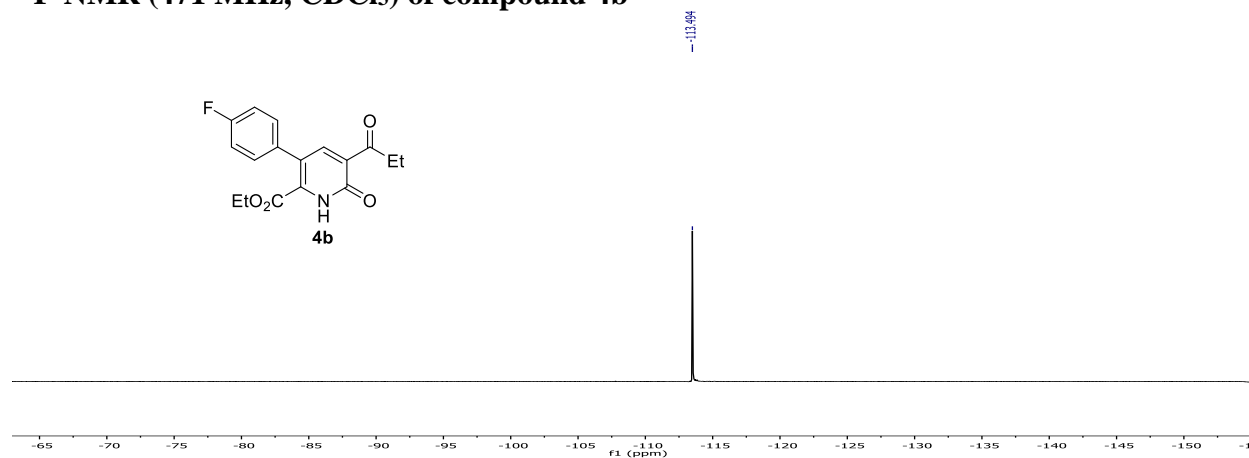
^1H -NMR (500 MHz, CDCl_3) of compound 4b



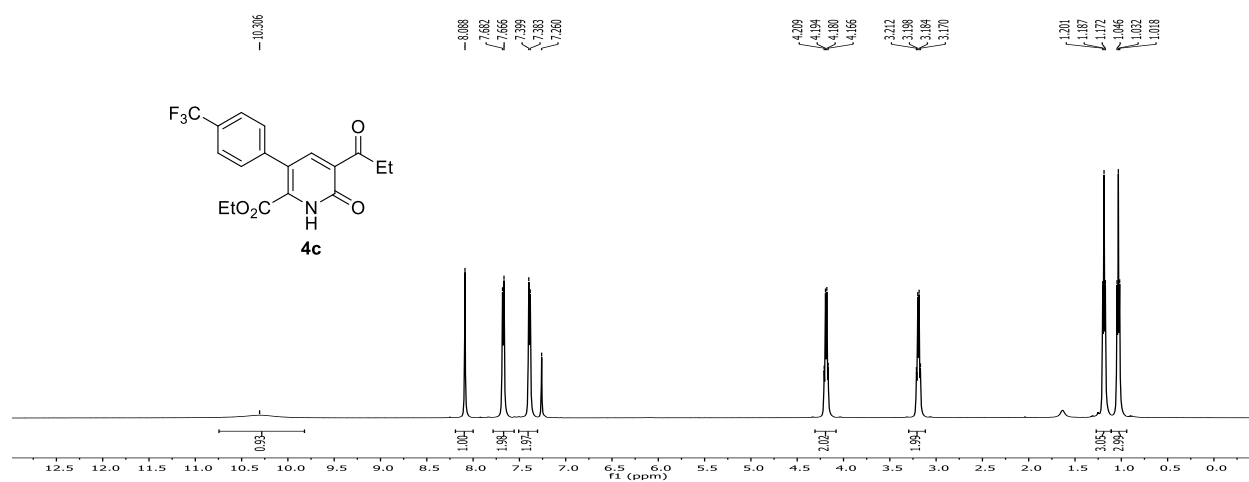
^{13}C -NMR (126 MHz, CDCl_3) of compound 4b



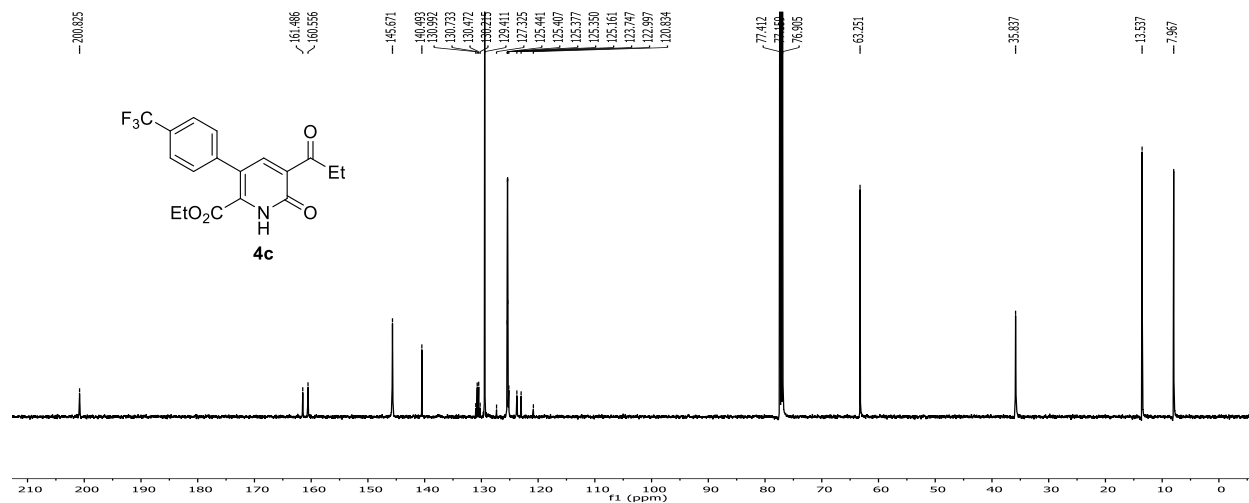
^{19}F -NMR (471 MHz, CDCl_3) of compound 4b



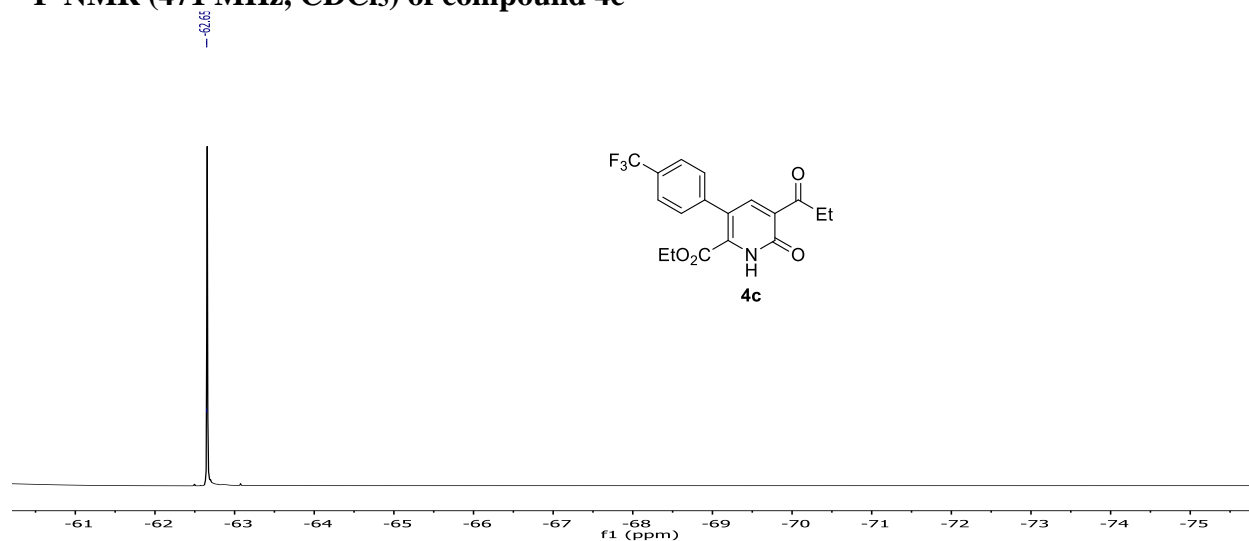
^1H -NMR (500 MHz, CDCl_3) of compound **4c**



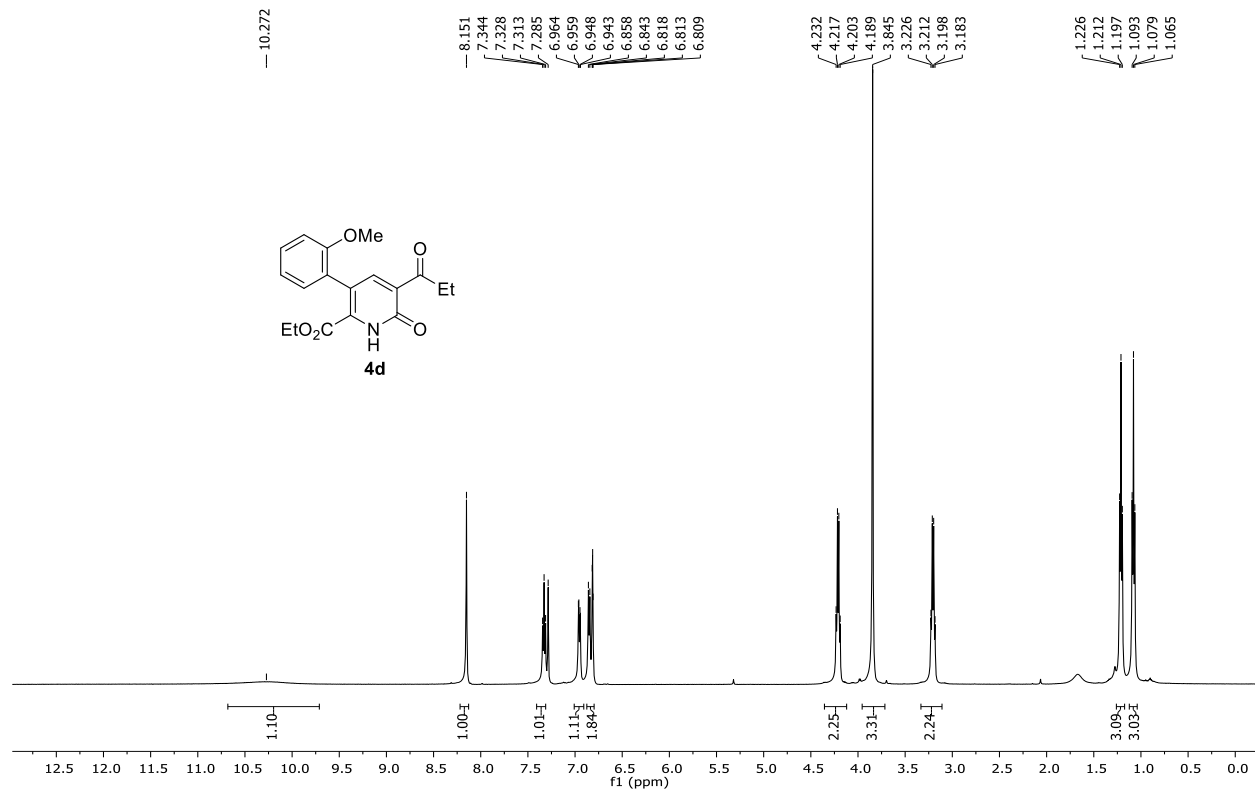
^{13}C -NMR (126 MHz, CDCl_3) of compound **4c**



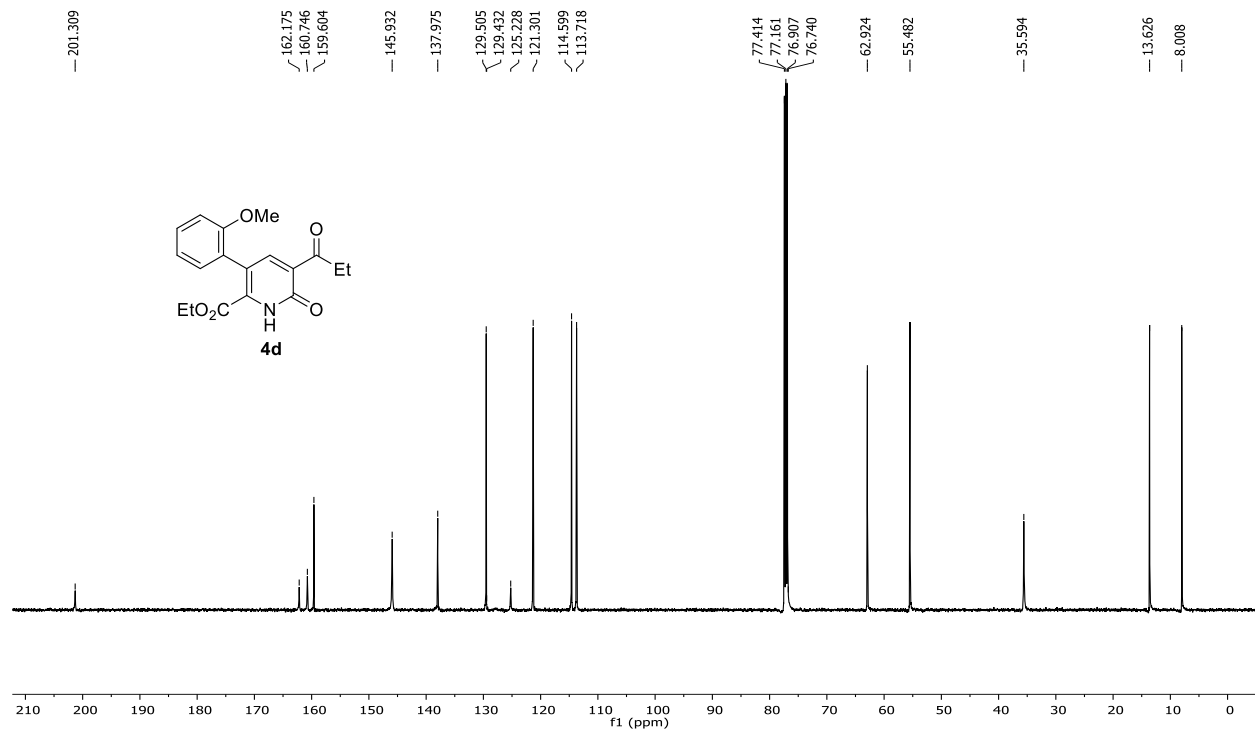
^{19}F -NMR (471 MHz, CDCl_3) of compound **4c**



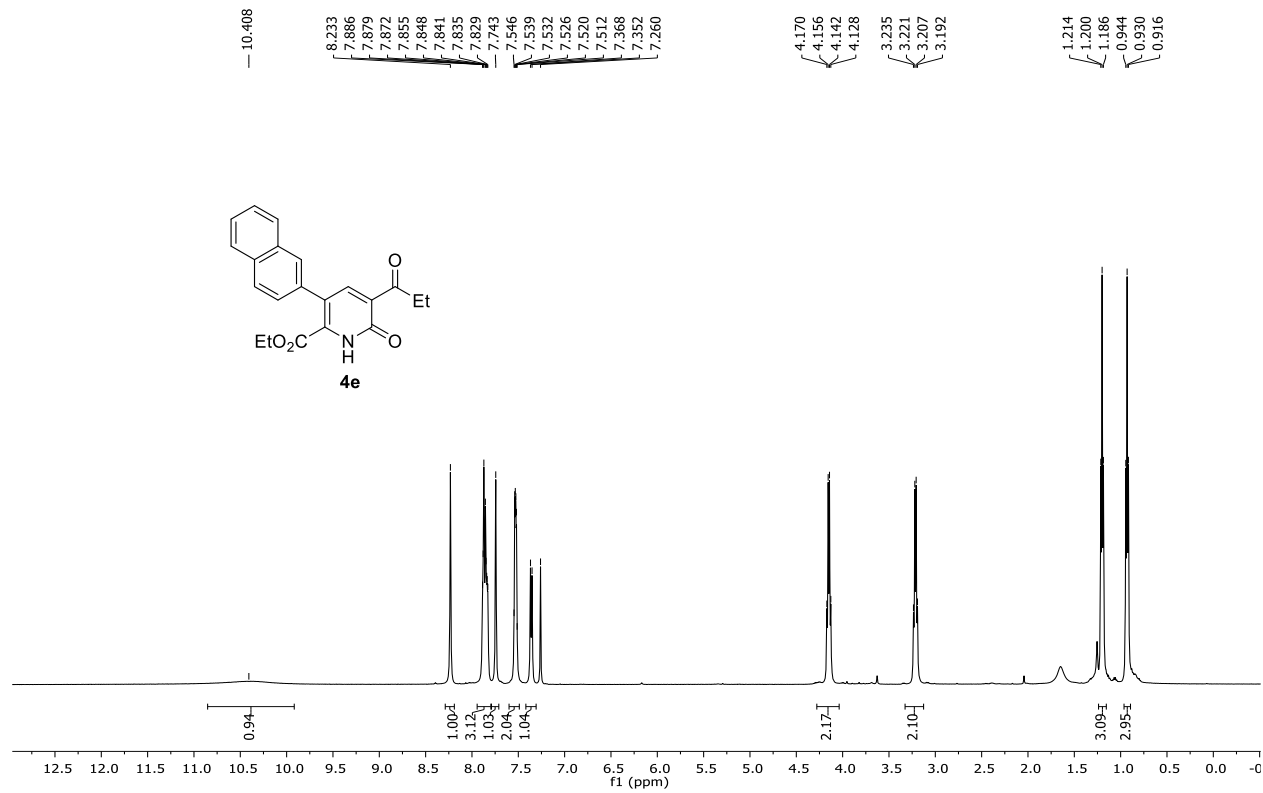
^1H -NMR (500 MHz, CDCl_3) of compound 4d



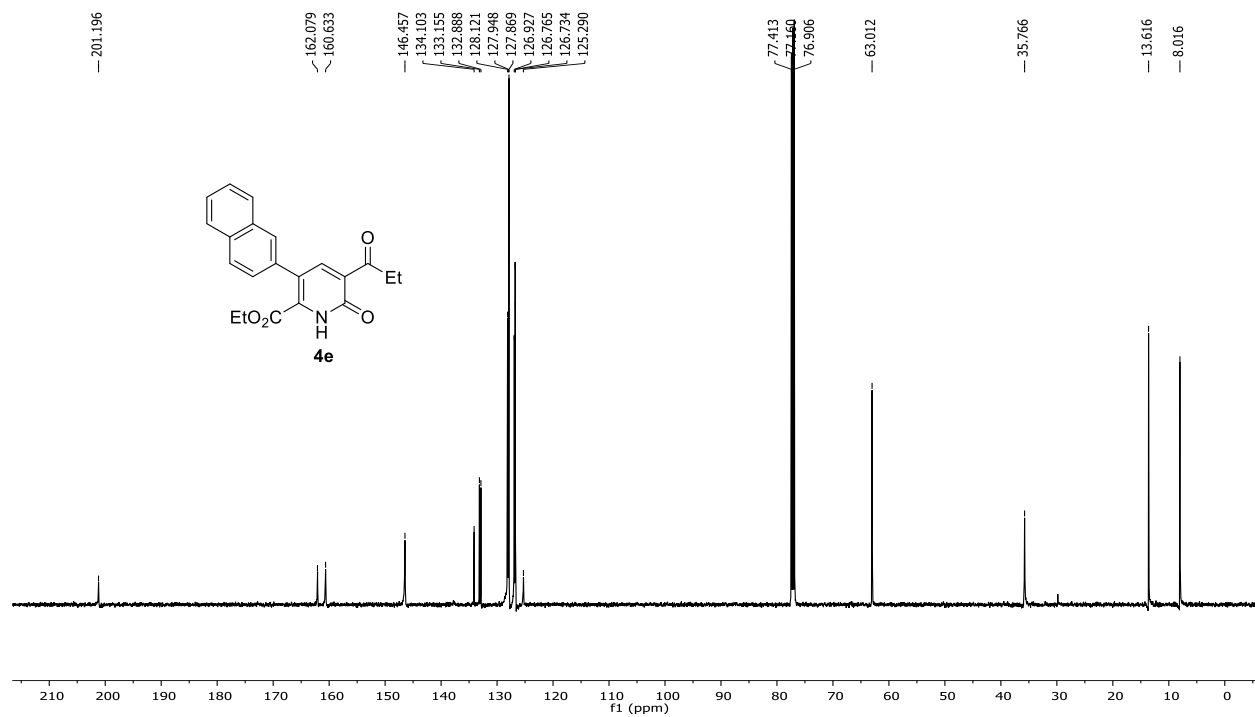
^{13}C -NMR (126 MHz, CDCl_3) of compound 4d



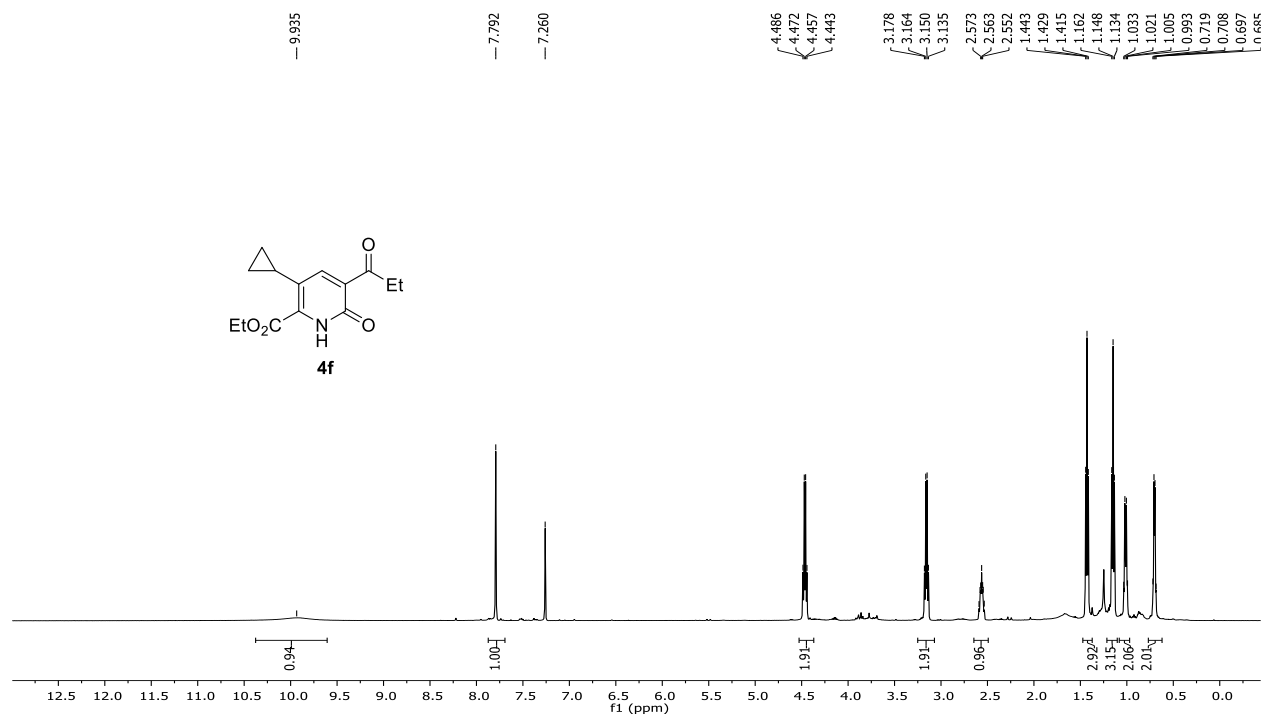
^1H -NMR (500 MHz, CDCl_3) of compound **4e**



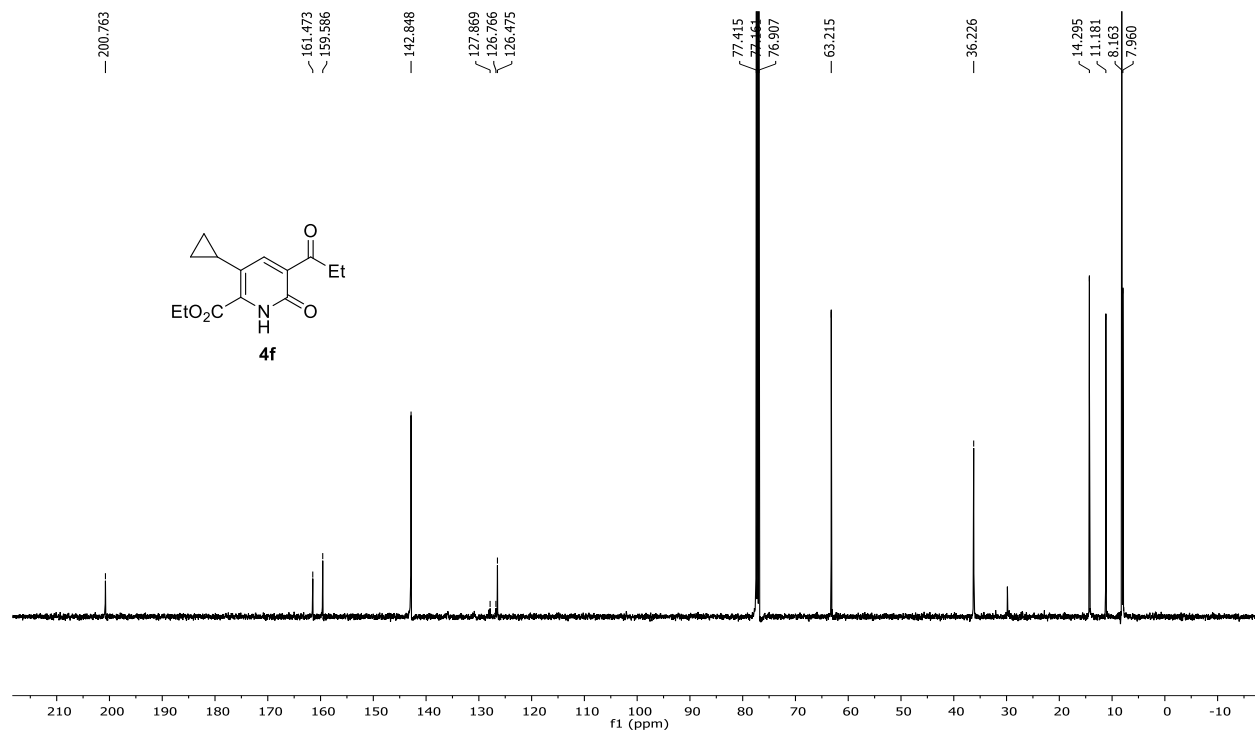
^{13}C -NMR (126 MHz, CDCl_3) of compound **4e**



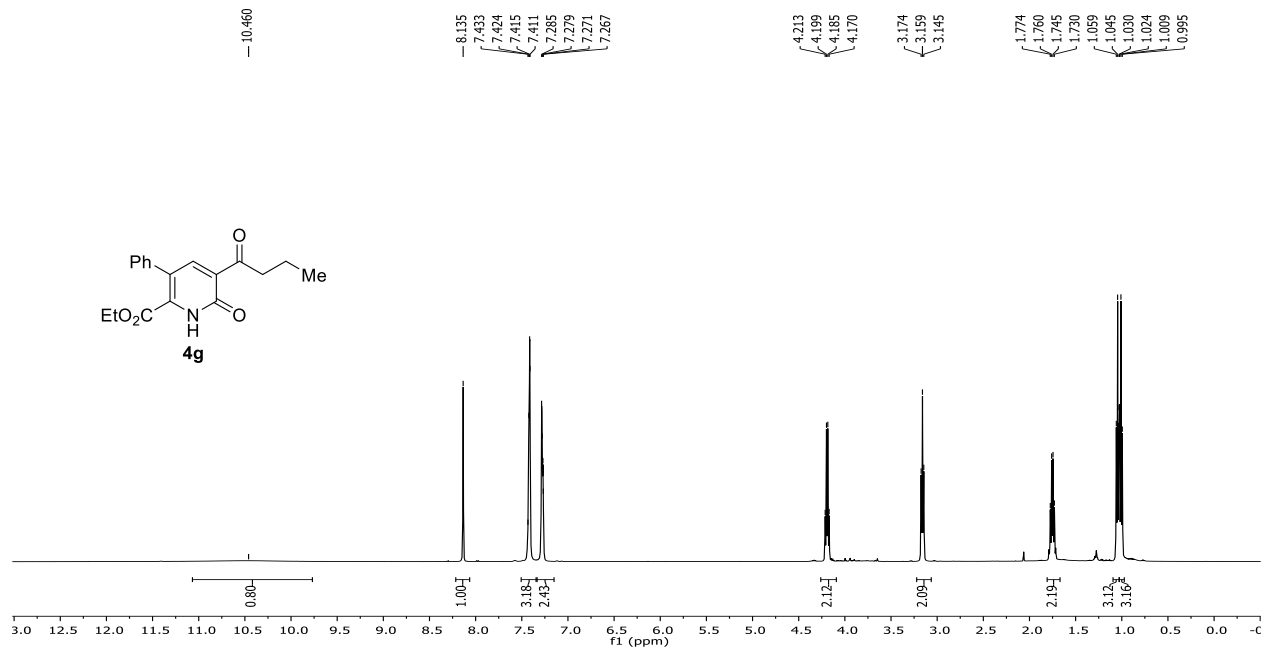
^1H -NMR (500 MHz, CDCl_3) of compound **4f**



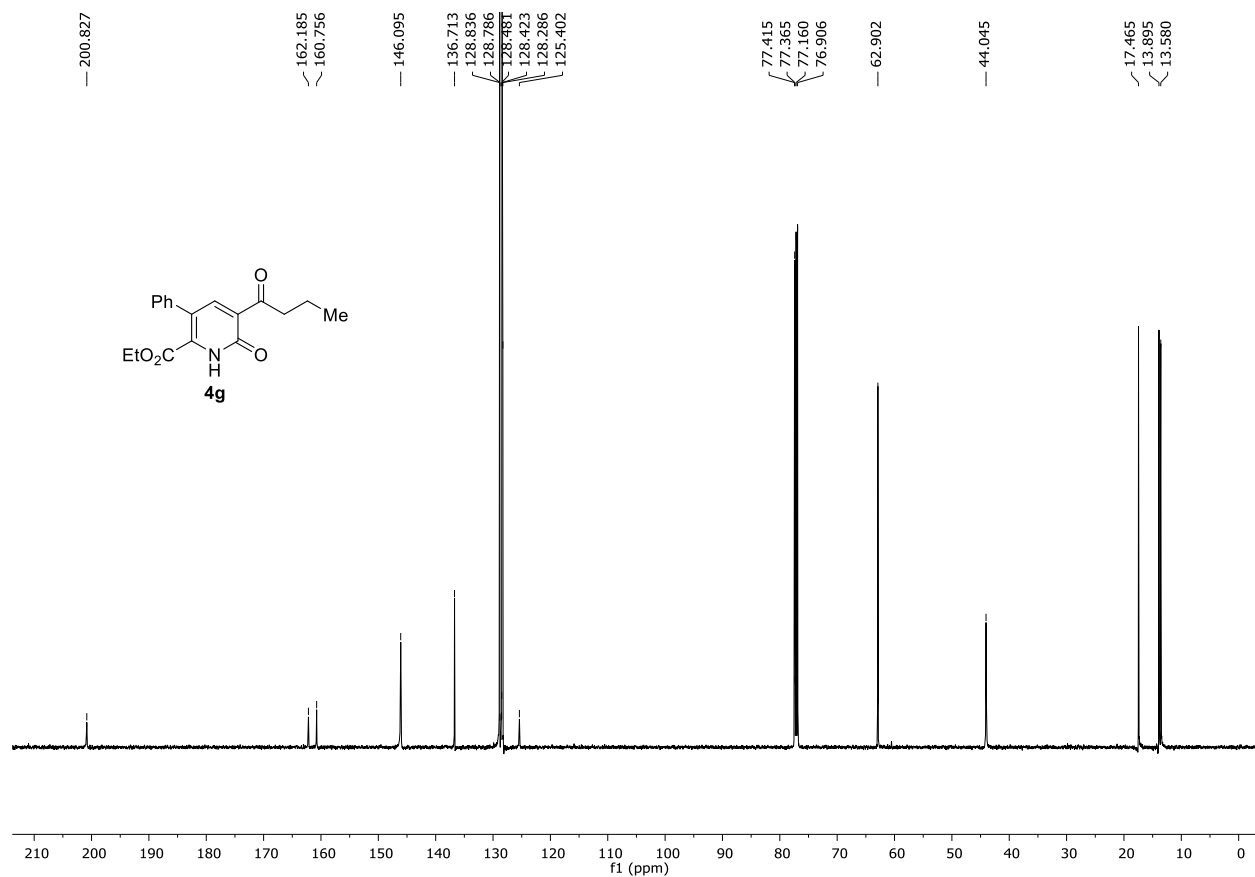
^{13}C -NMR (126 MHz, CDCl_3) of compound **4f**



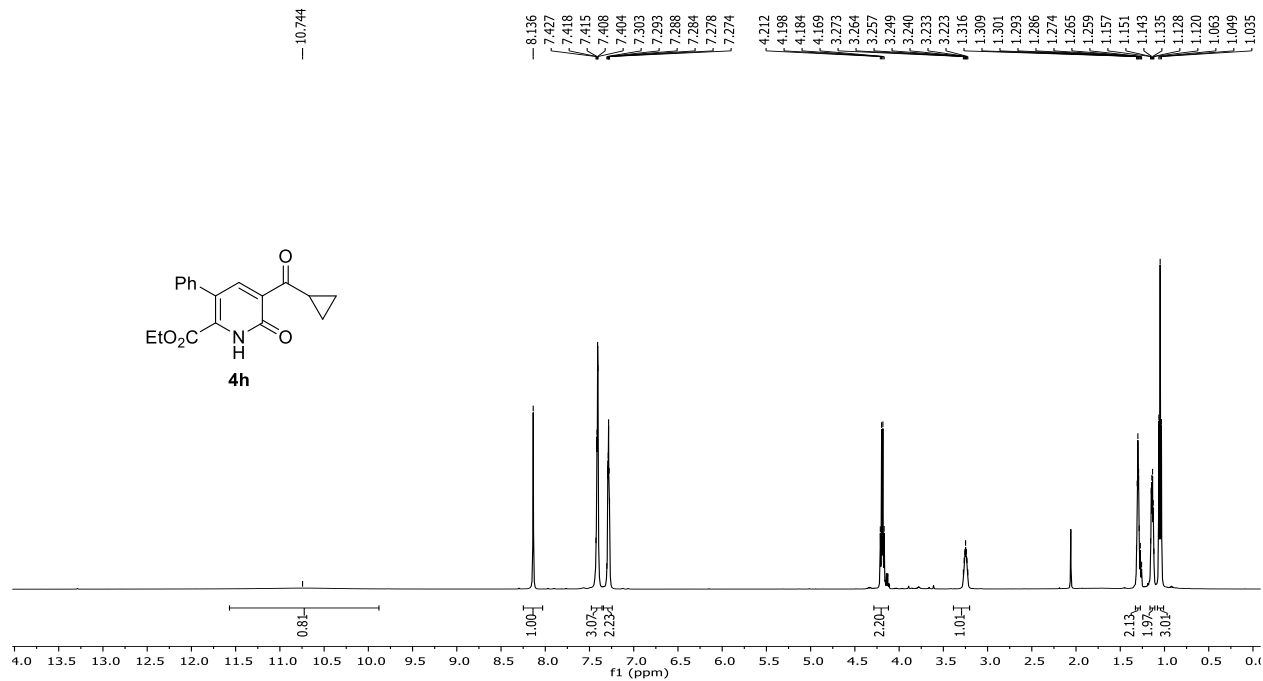
^1H -NMR (500 MHz, CDCl_3) of compound **4g**



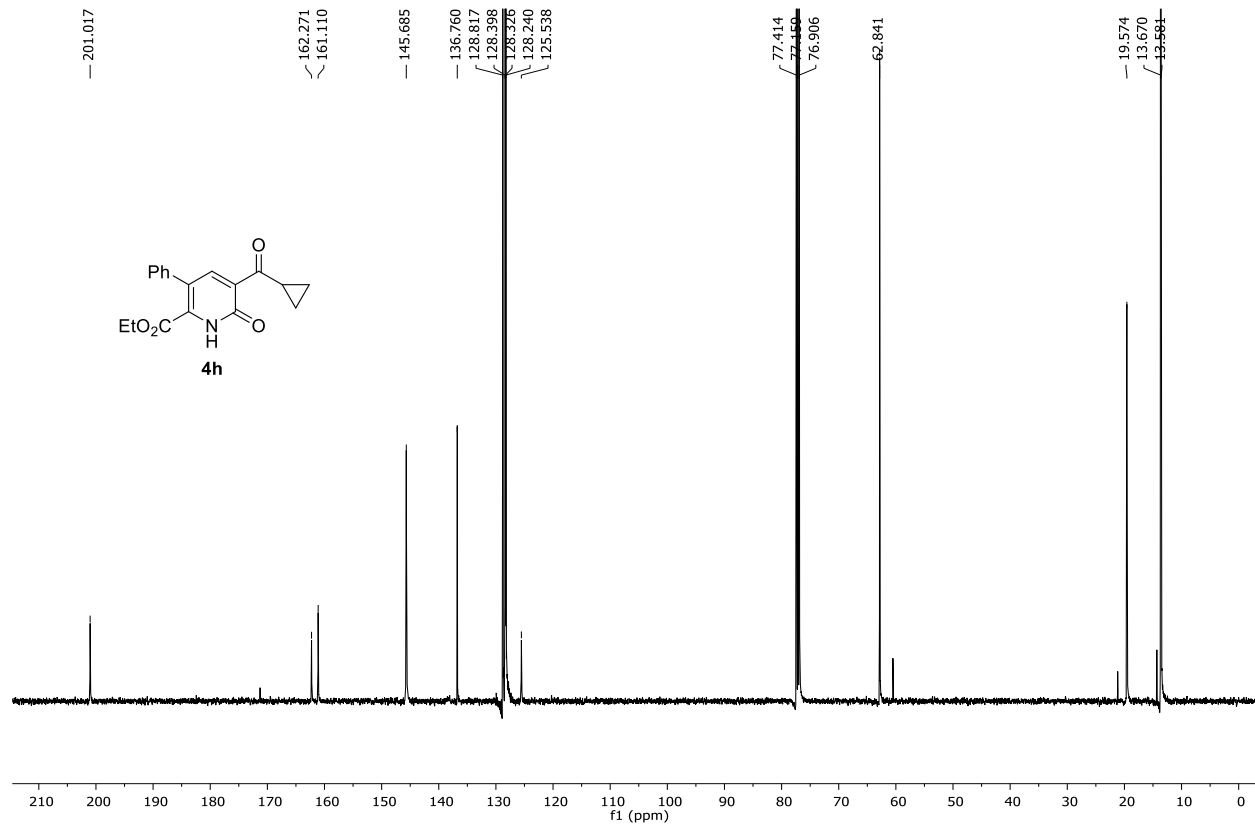
^{13}C -NMR (126 MHz, CDCl_3) of compound **4g**



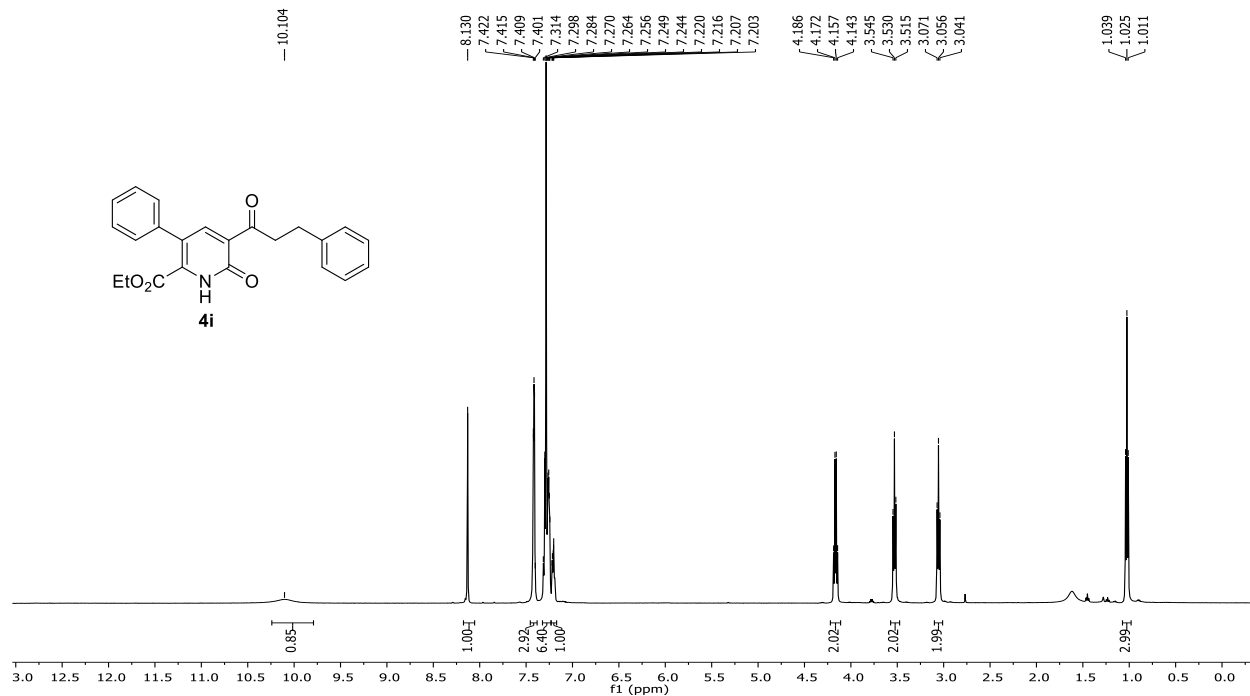
^1H -NMR (500 MHz, CDCl_3) of compound 4h



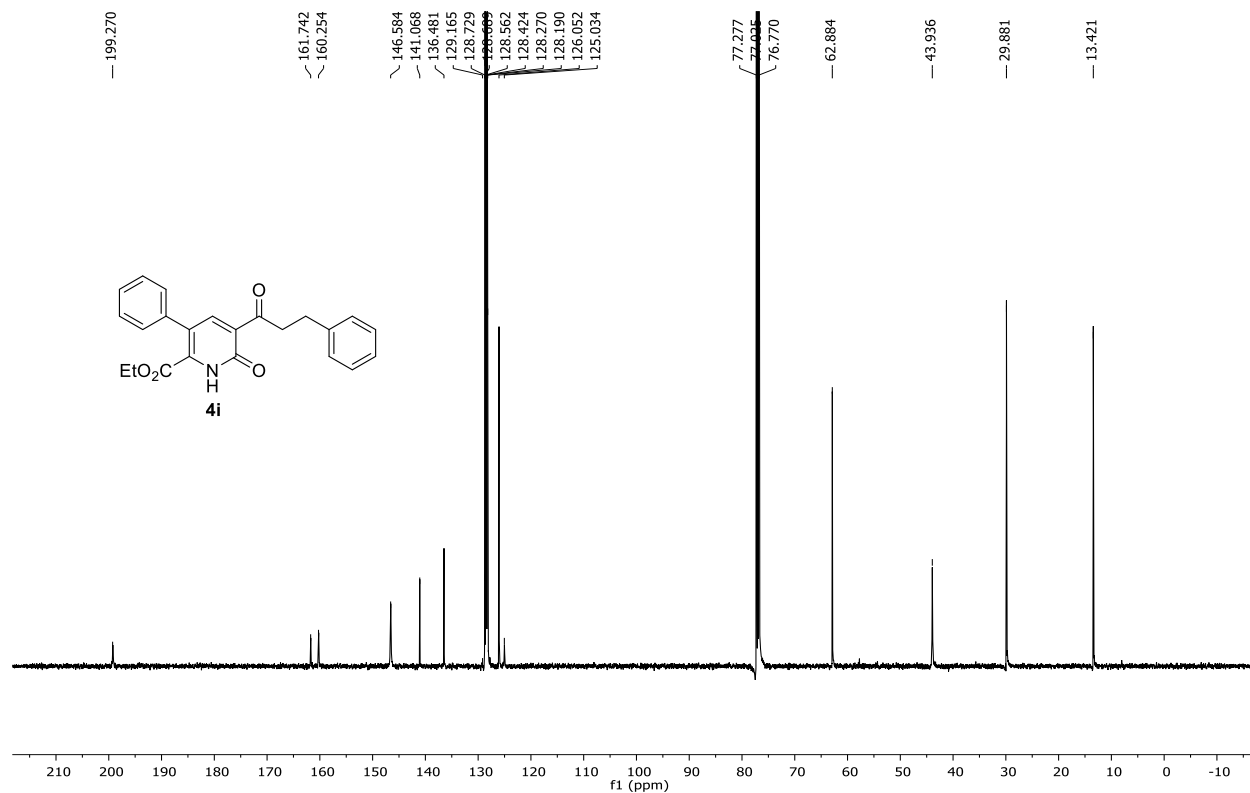
^{13}C -NMR (126 MHz, CDCl_3) of compound 4h



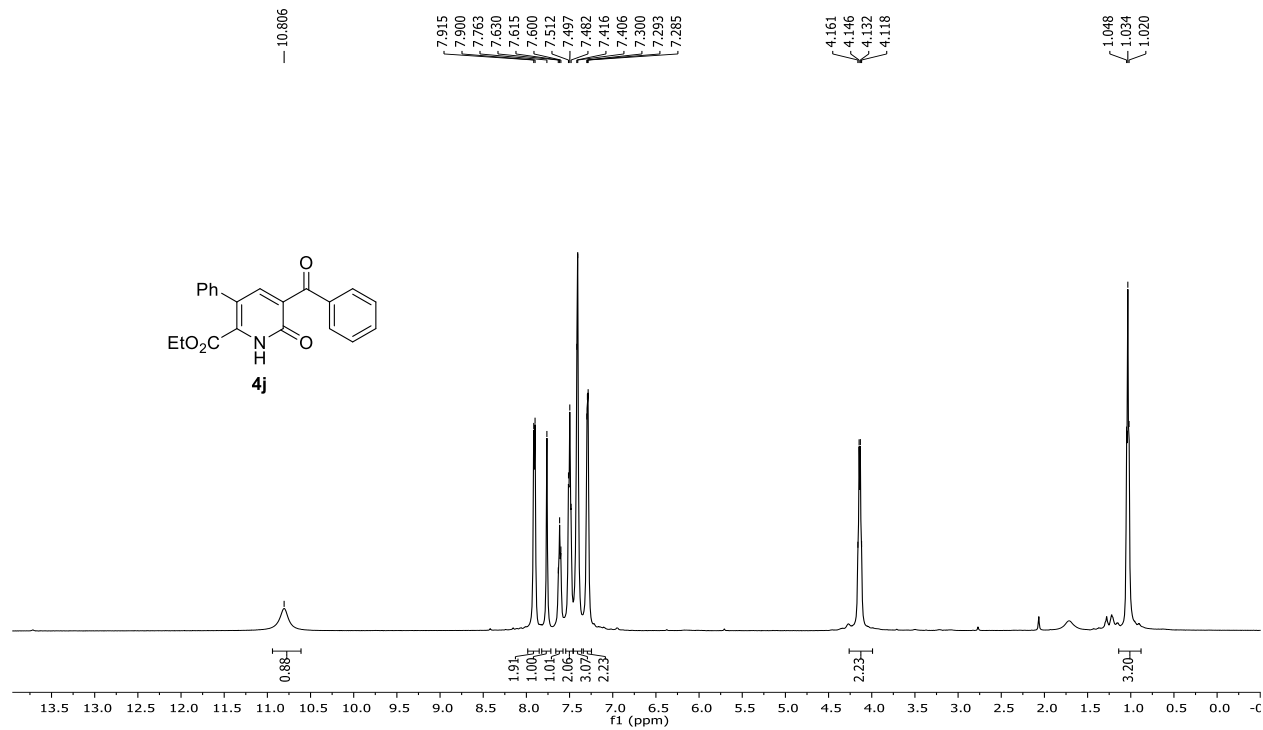
^1H -NMR (500 MHz, CDCl_3) of compound **4i**



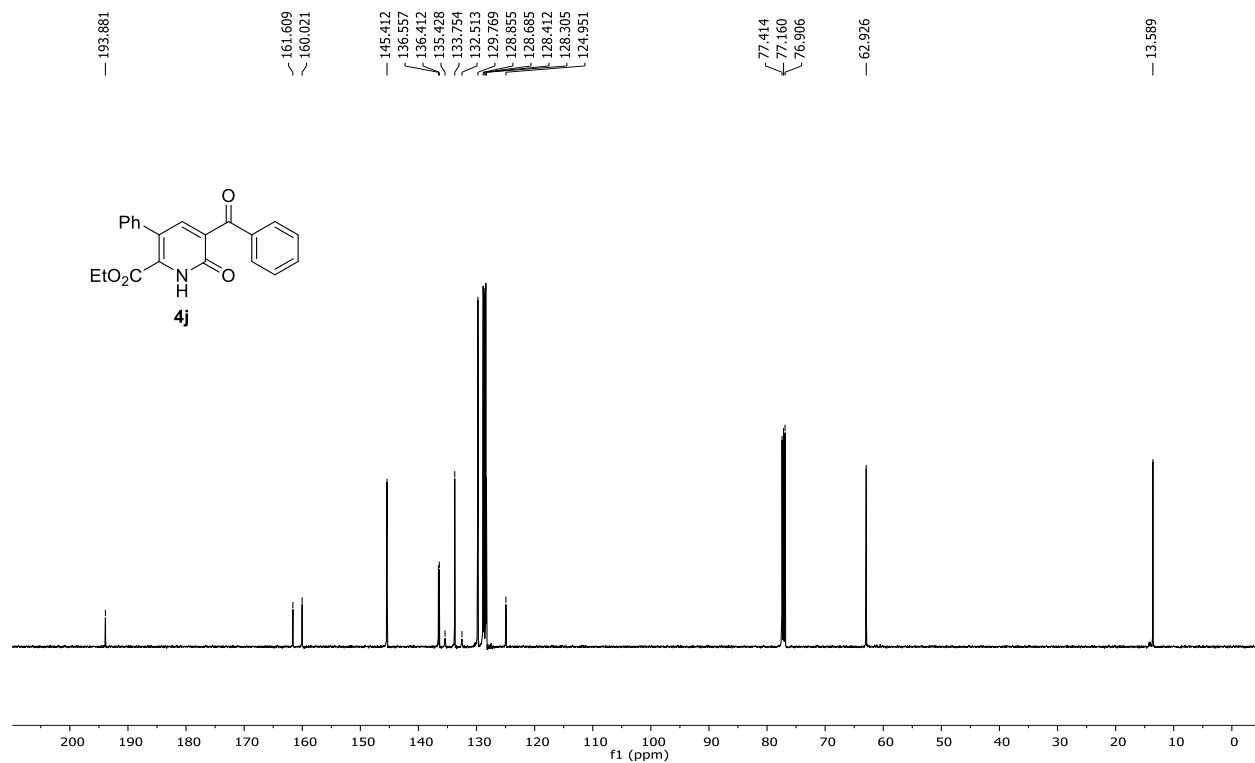
^{13}C -NMR (126 MHz, CDCl_3) of compound **4i**



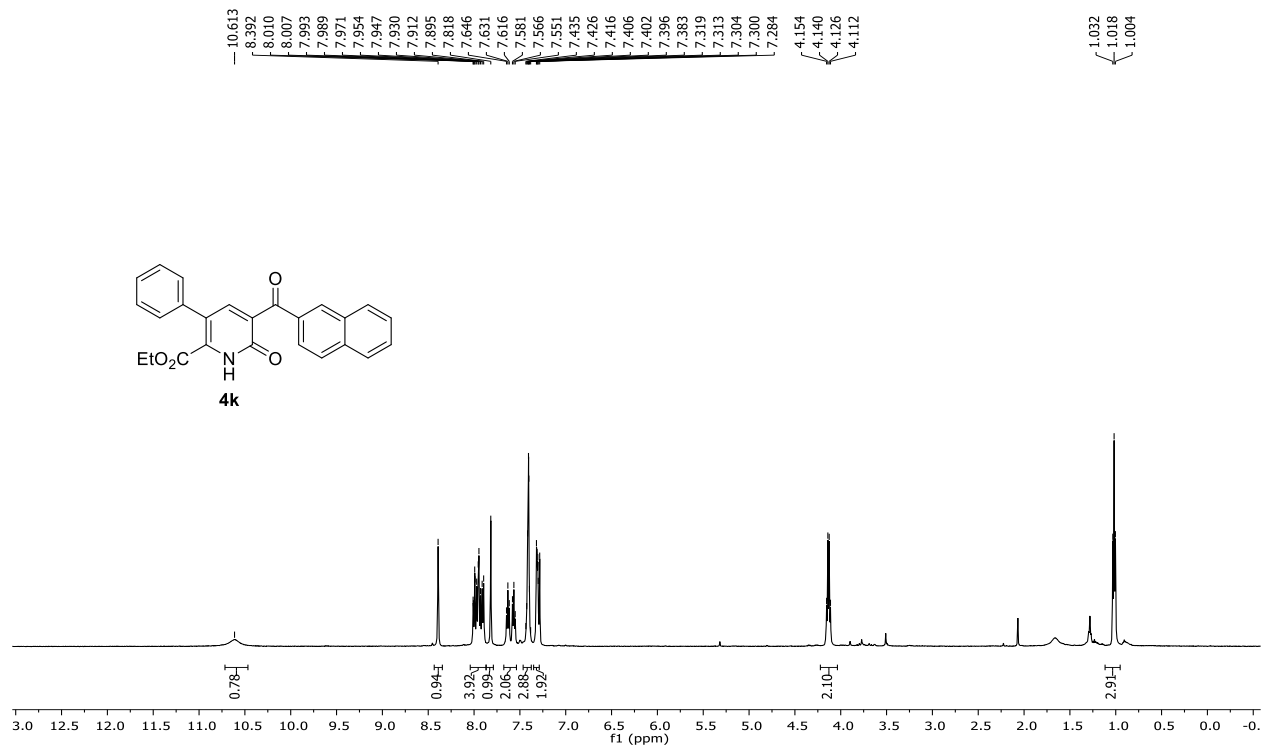
^1H -NMR (500 MHz, CDCl_3) of compound **4j**



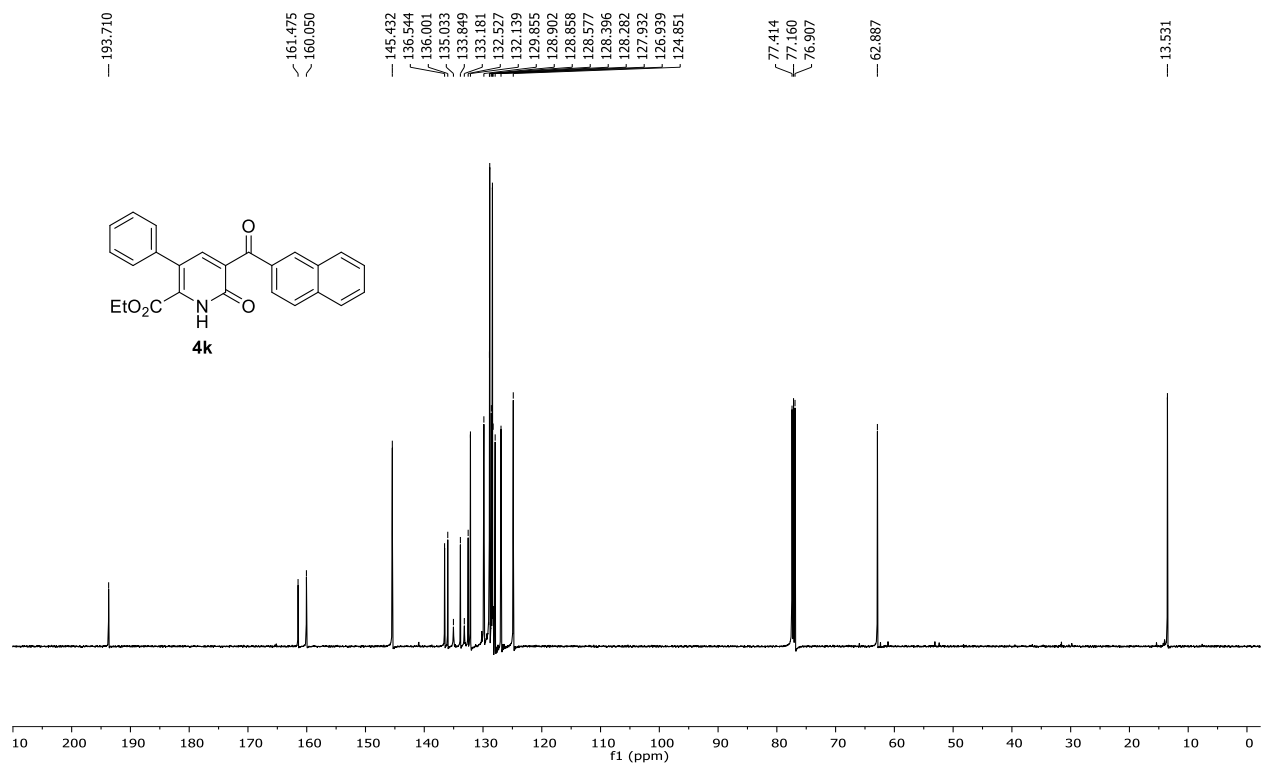
^{13}C -NMR (126 MHz, CDCl_3) of compound **4j**



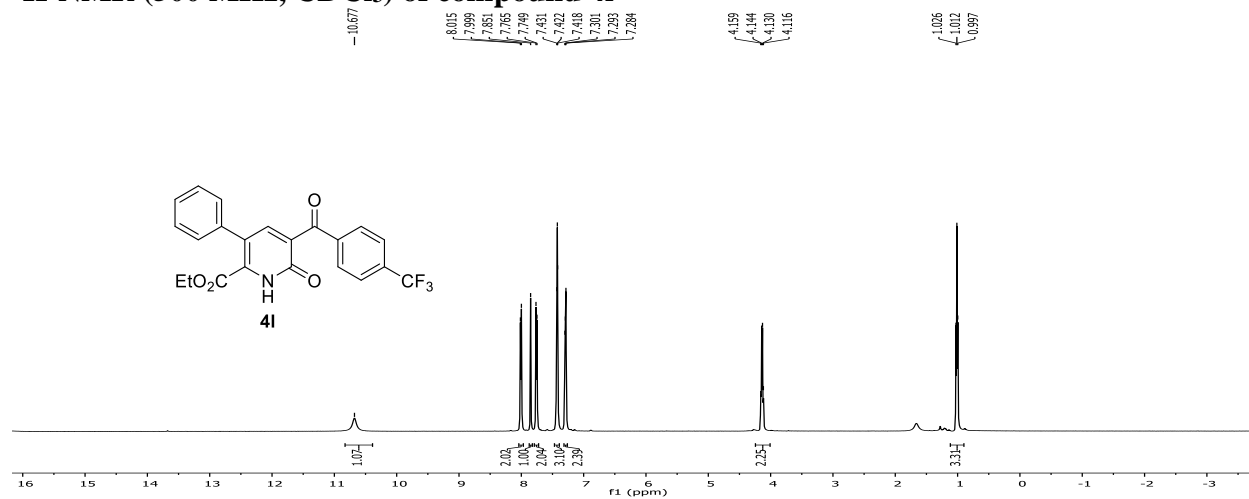
^1H -NMR (500 MHz, CDCl_3) of compound 4k



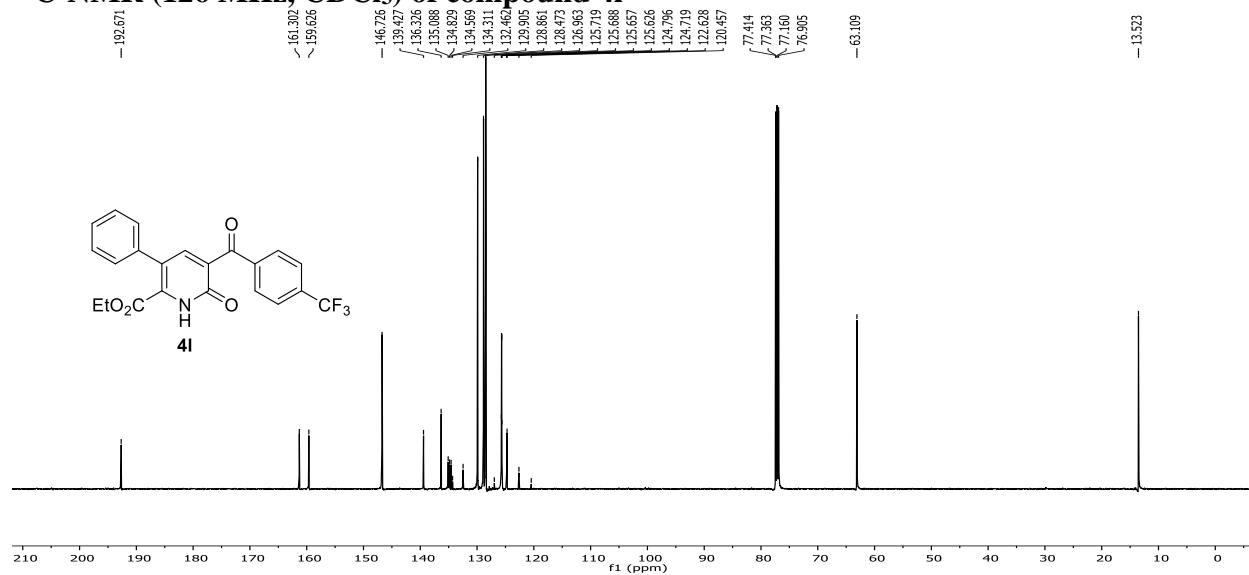
^{13}C -NMR (126 MHz, CDCl_3) of compound 4k



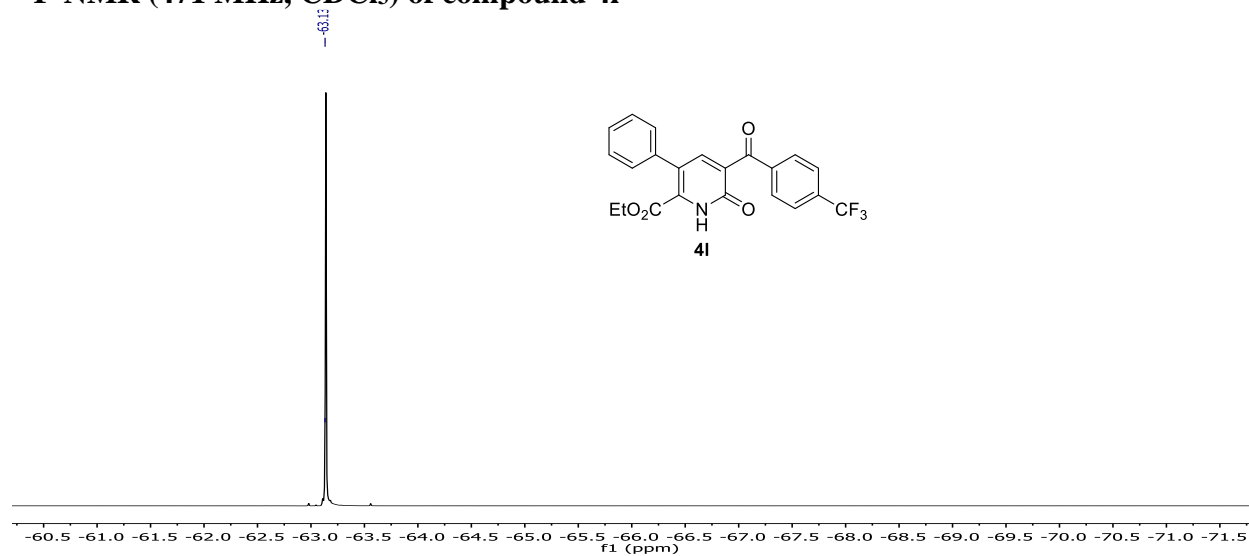
¹H-NMR (500 MHz, CDCl₃) of compound 4I



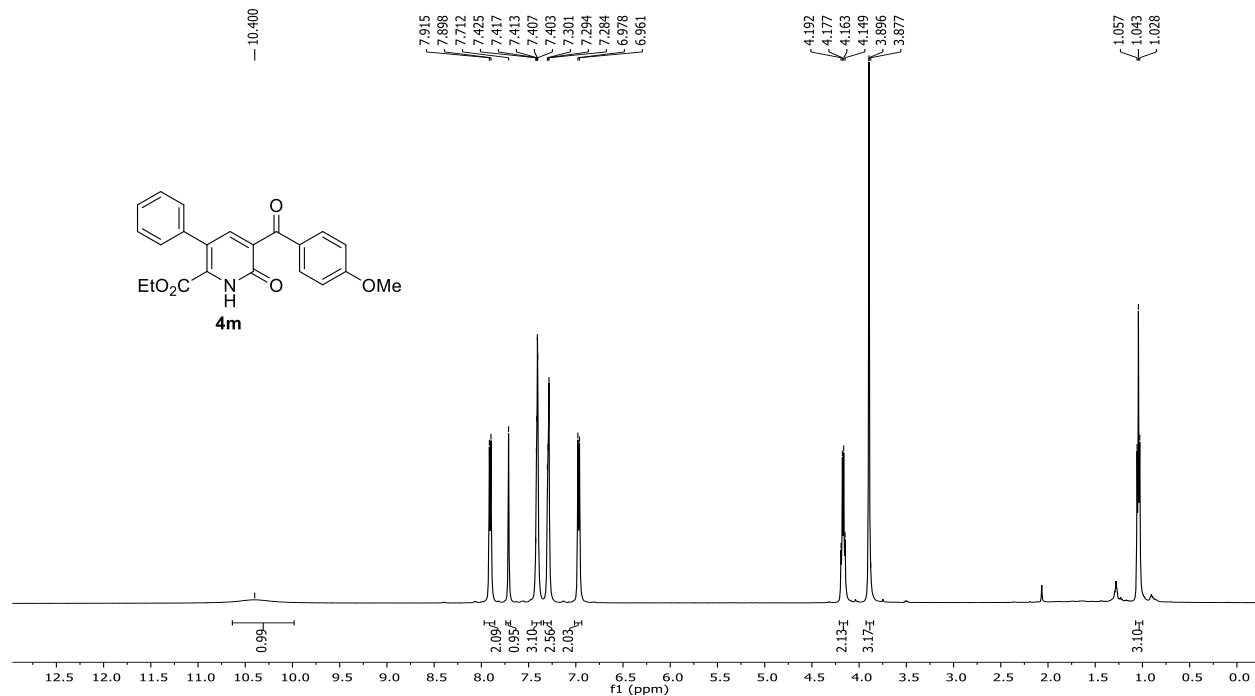
¹³C-NMR (126 MHz, CDCl₃) of compound 4I



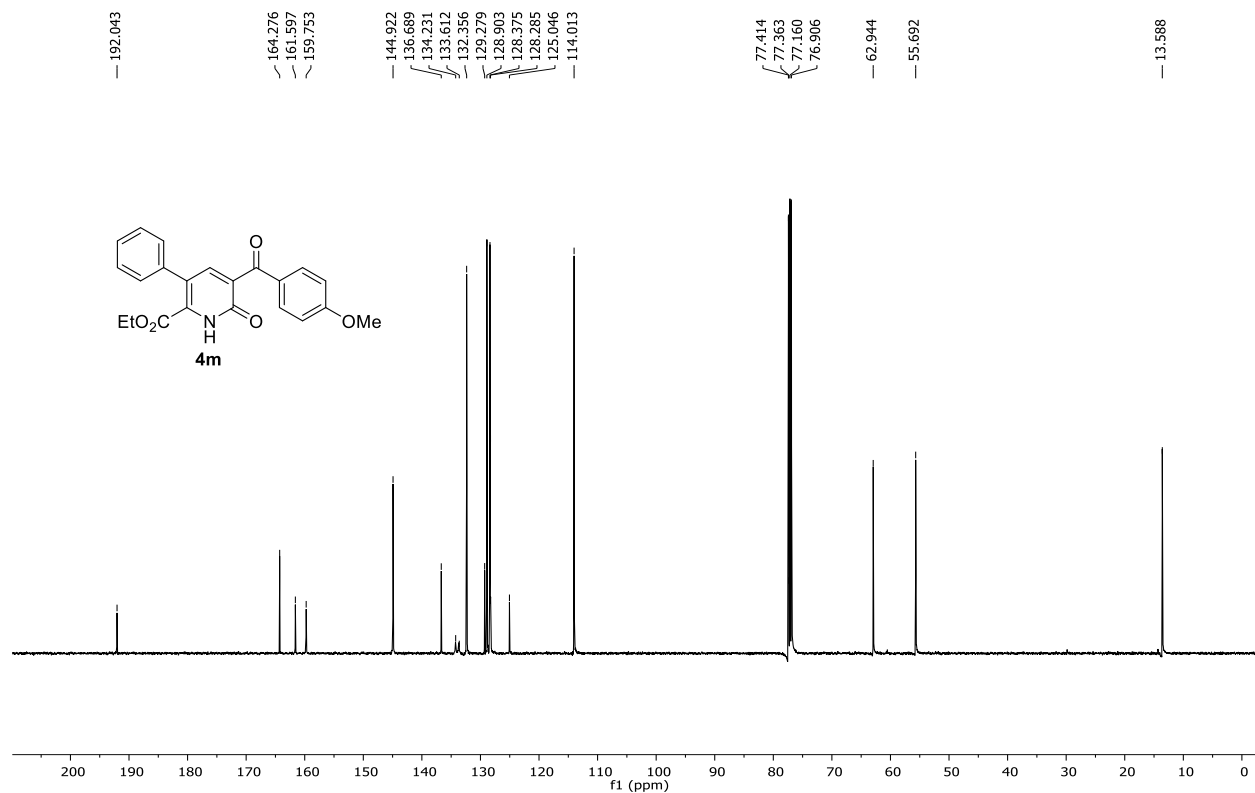
¹⁹F-NMR (471 MHz, CDCl₃) of compound 4I



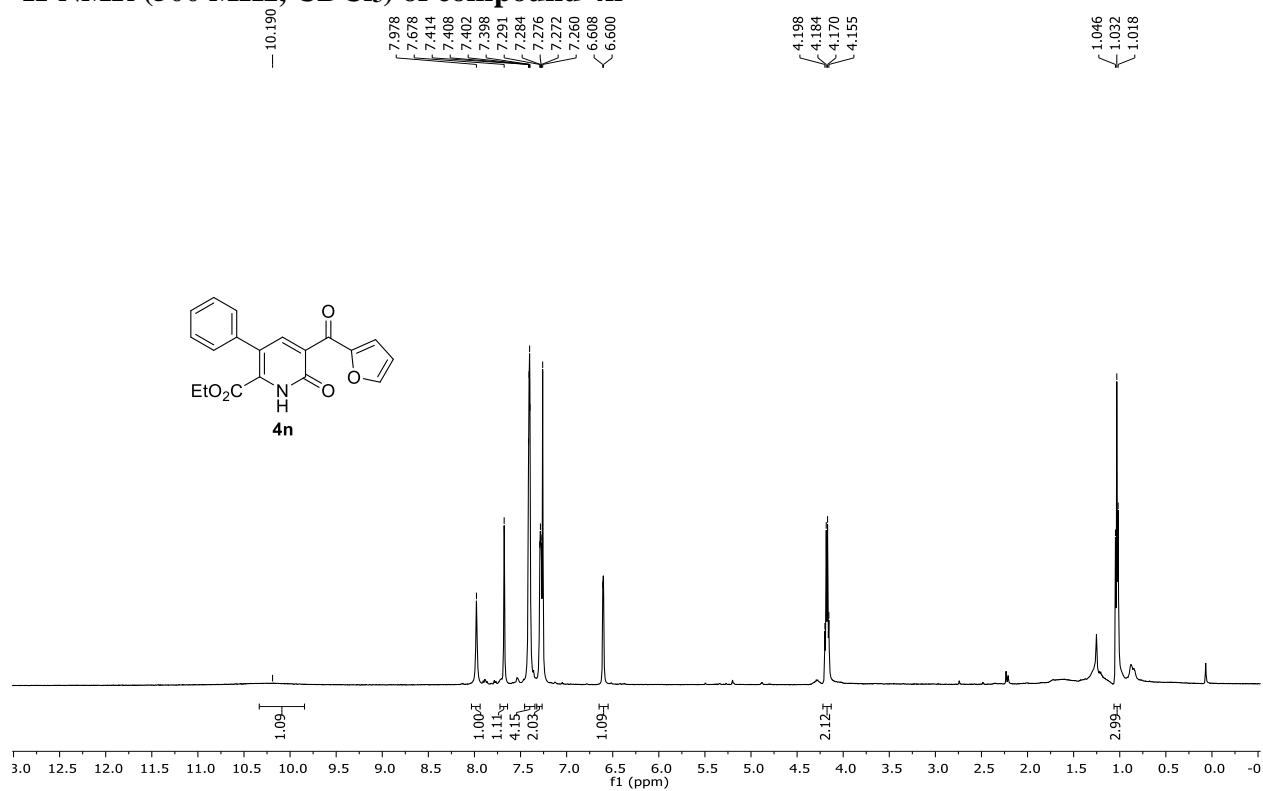
^1H -NMR (500 MHz, CDCl_3) of compound 4m



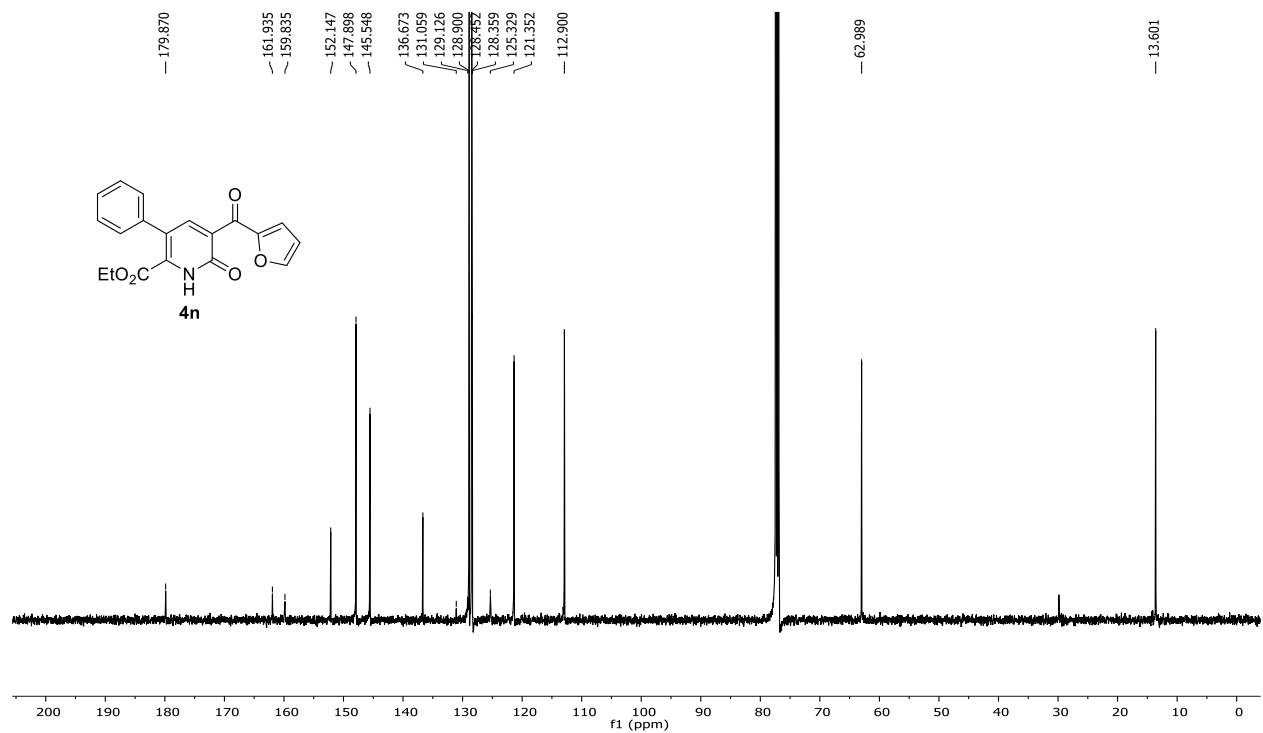
^{13}C -NMR (126 MHz, CDCl_3) of compound 4m



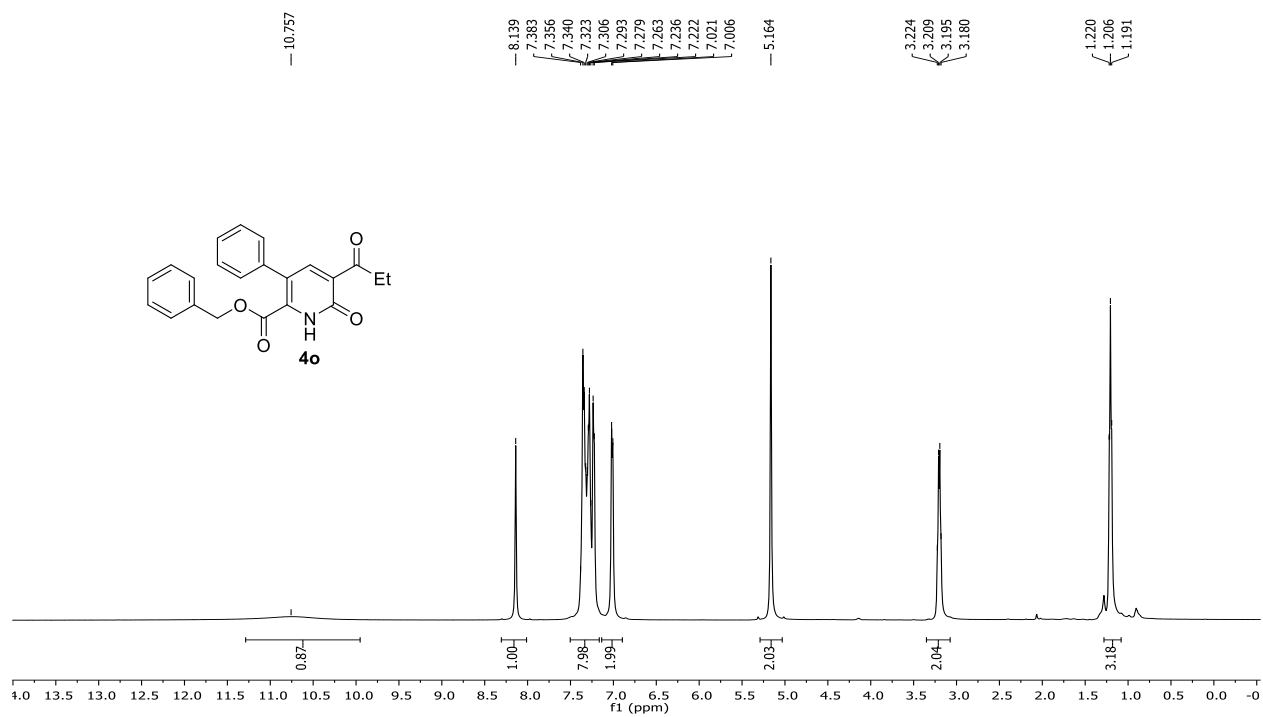
^1H -NMR (500 MHz, CDCl_3) of compound 4n



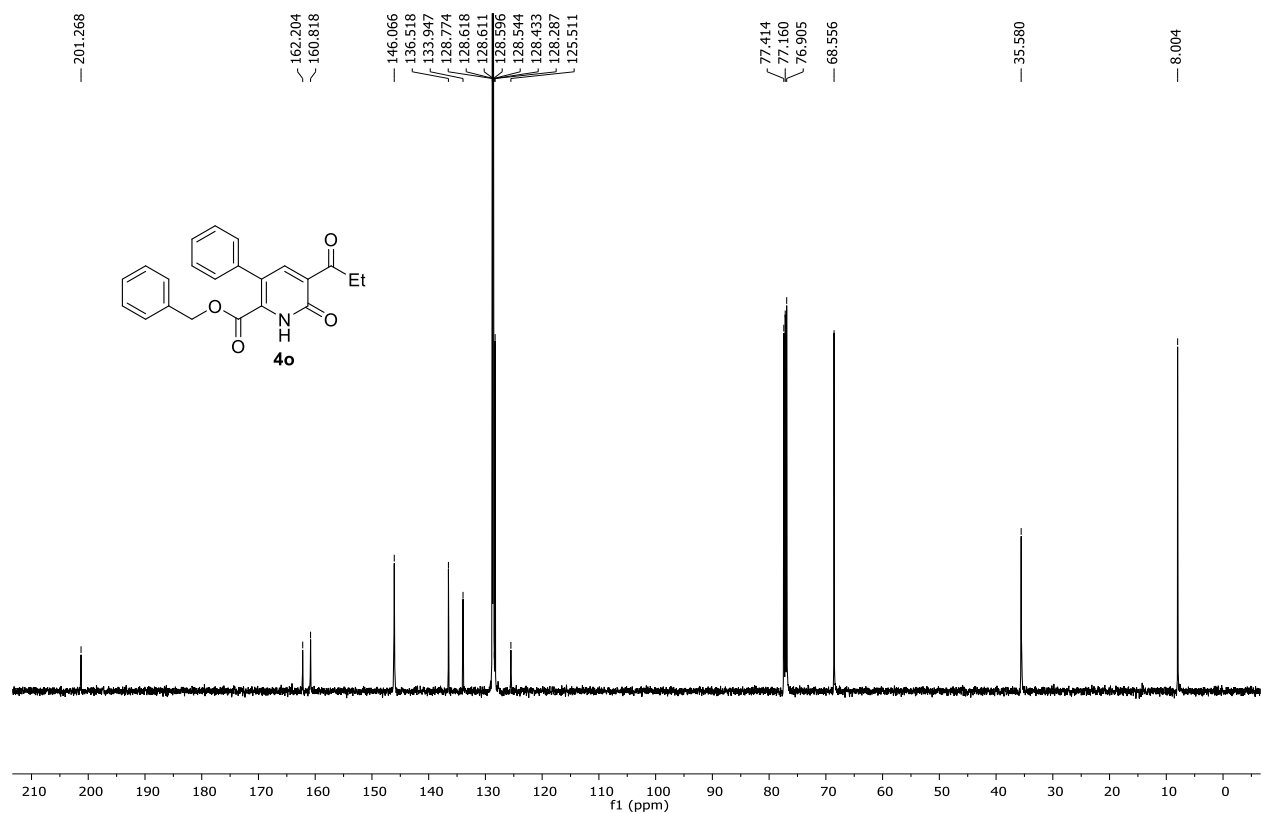
^{13}C -NMR (126 MHz, CDCl_3) of compound 4n



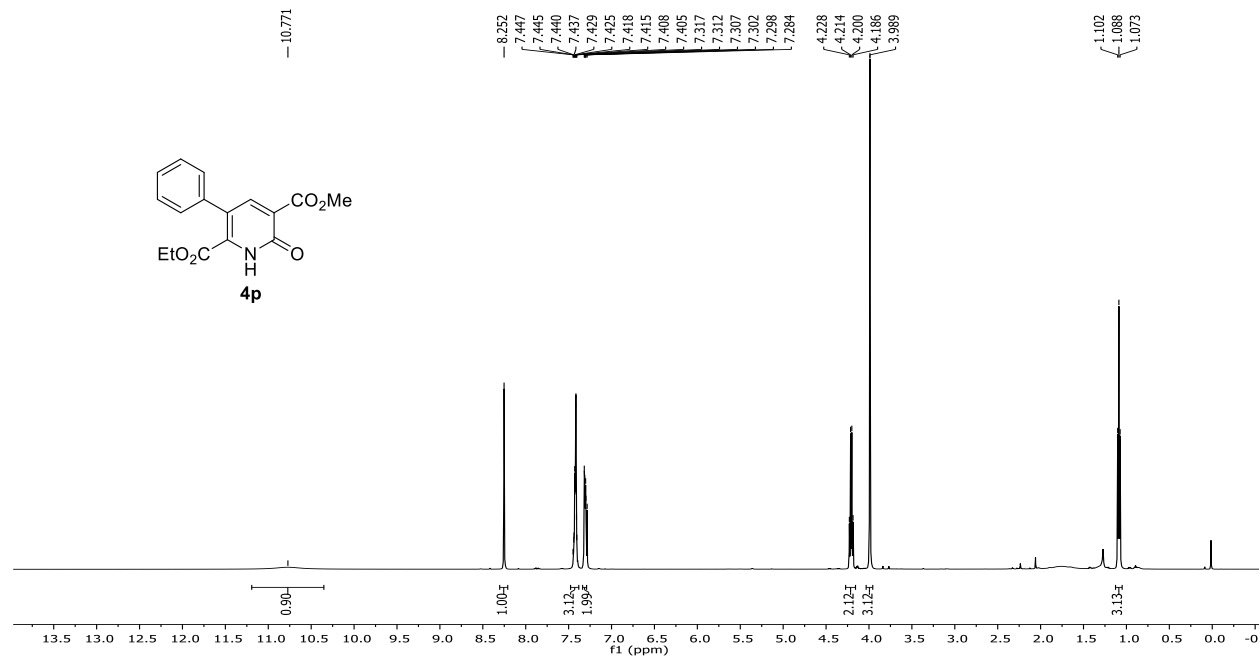
^1H -NMR (500 MHz, CDCl_3) of compound 4o



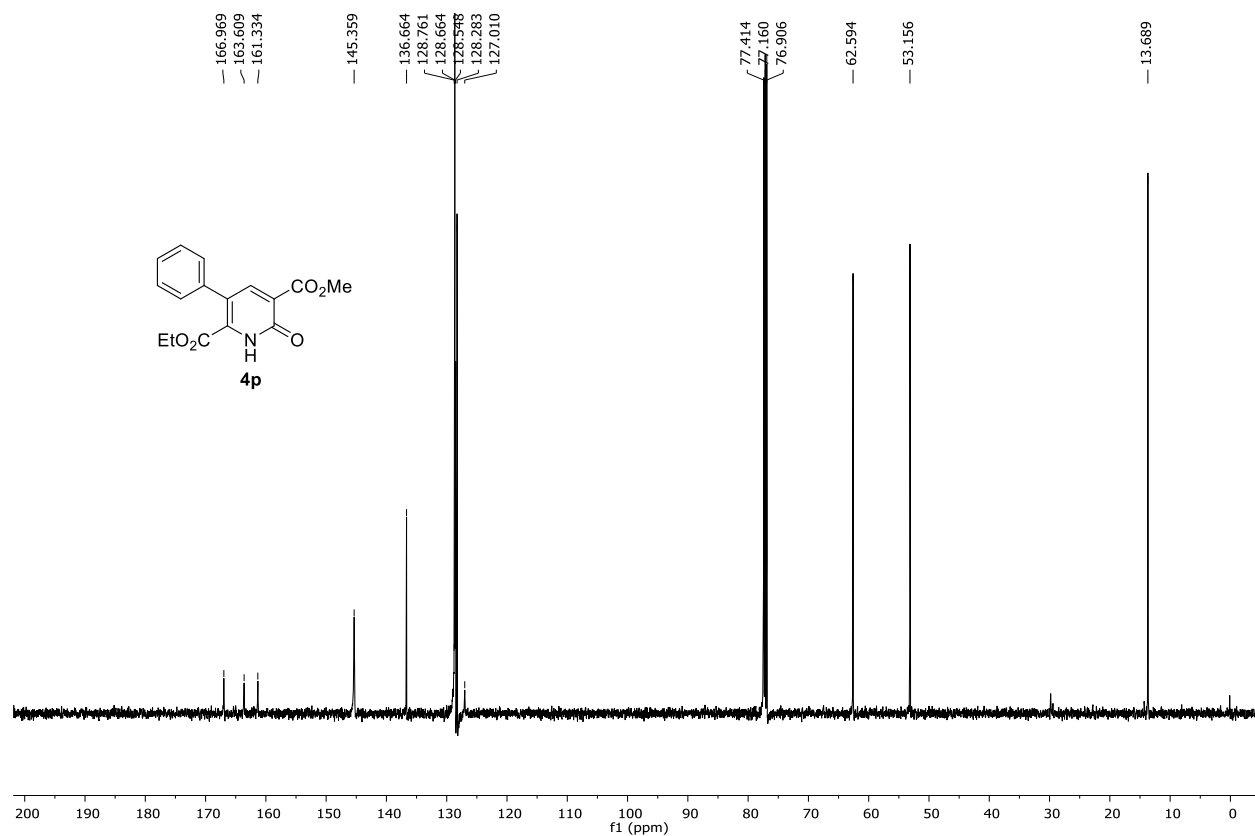
^{13}C -NMR (126 MHz, CDCl_3) of compound 4o



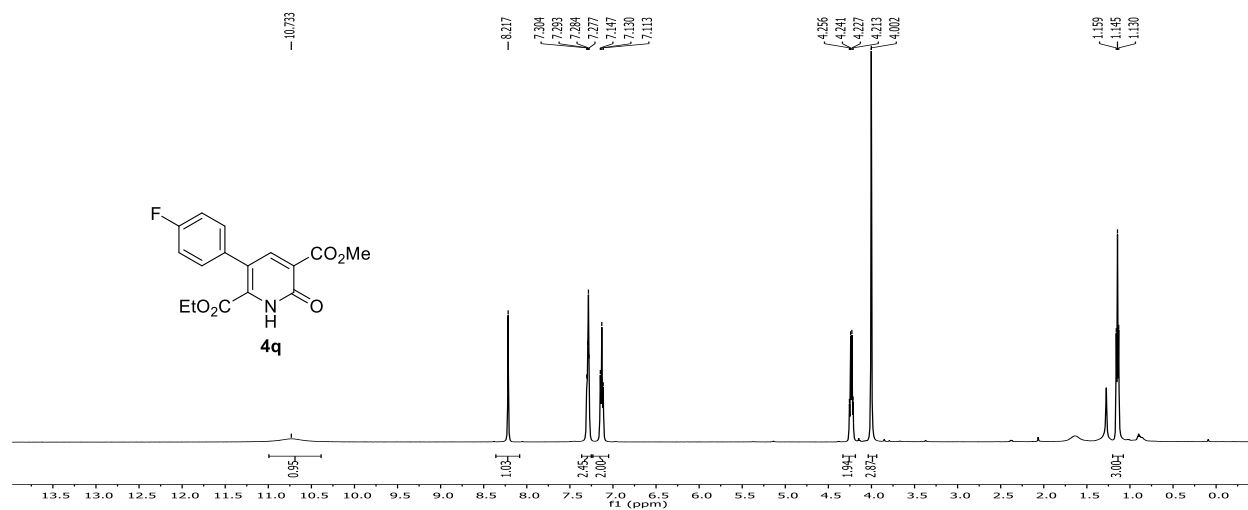
^1H -NMR (500 MHz, CDCl_3) of compound 4p



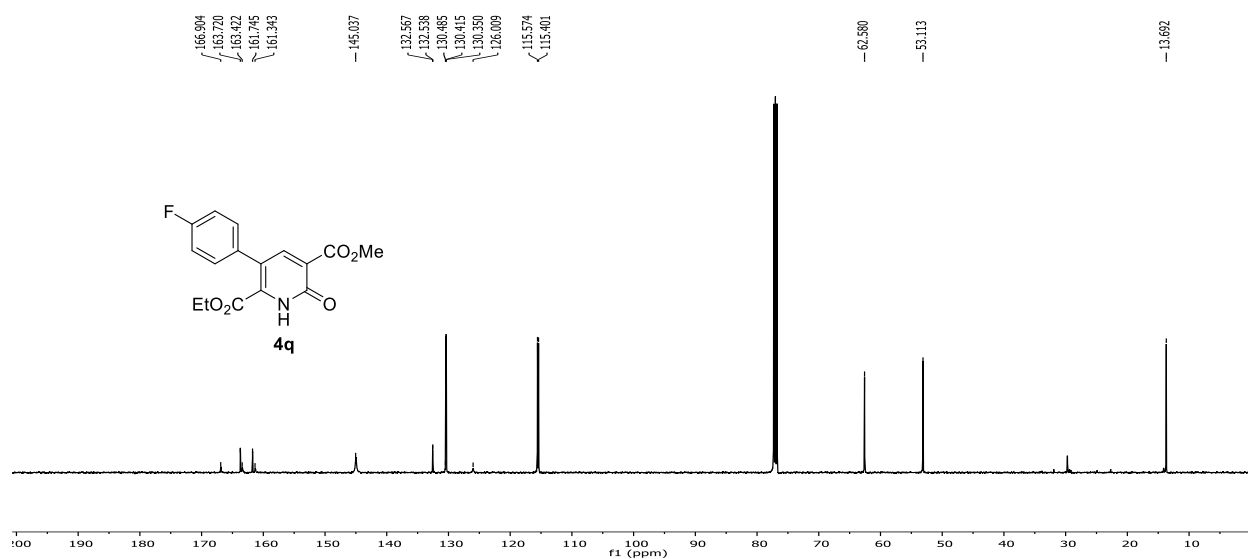
^{13}C -NMR (126 MHz, CDCl_3) of compound 4p



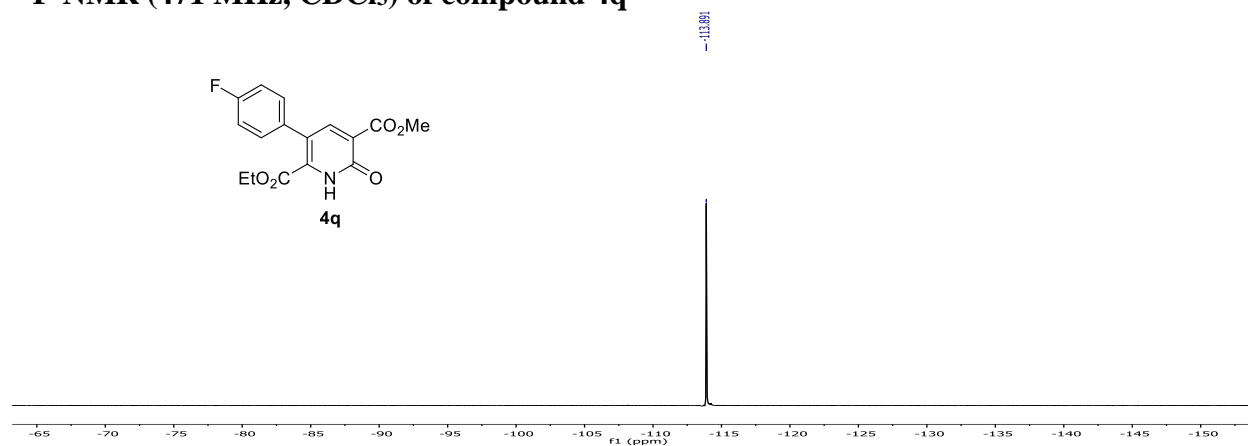
^1H -NMR (500 MHz, CDCl_3) of compound 4q



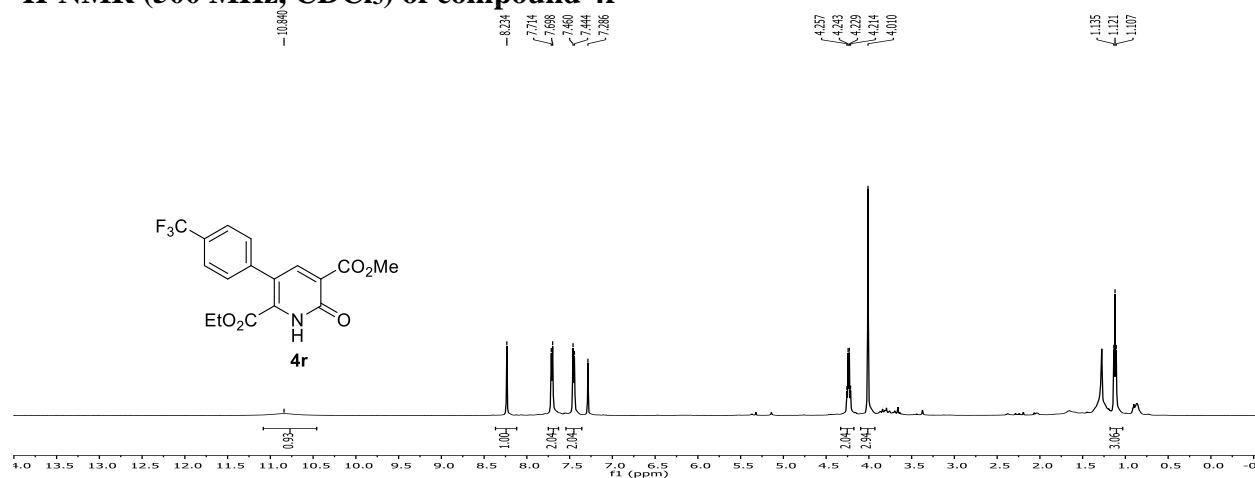
^{13}C -NMR (126 MHz, CDCl_3) of compound 4q



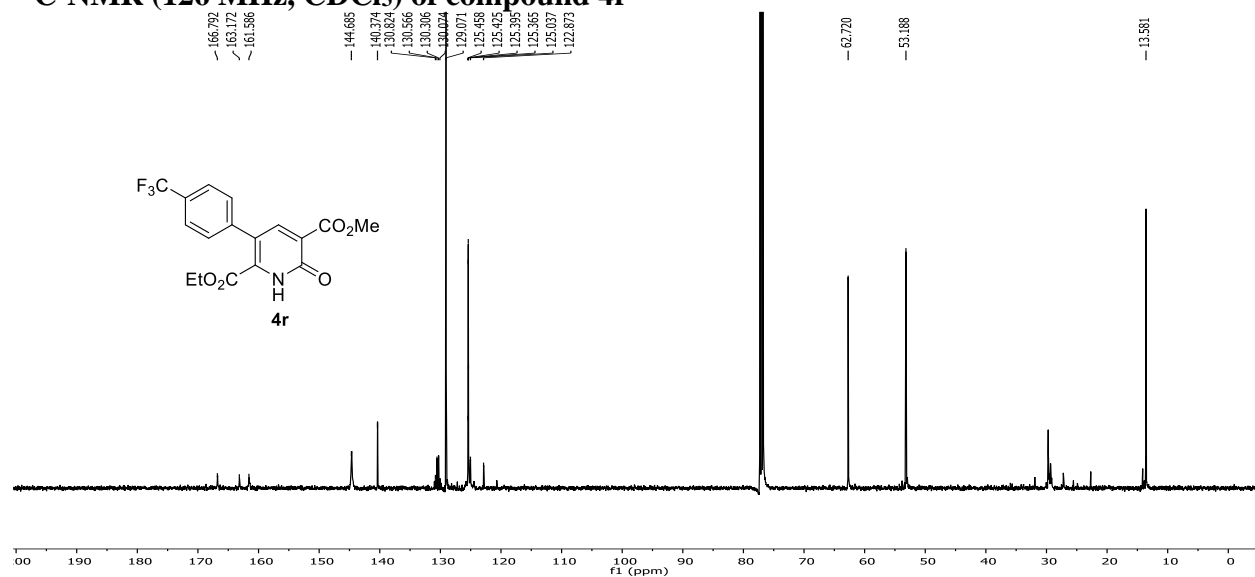
^{19}F -NMR (471 MHz, CDCl_3) of compound 4q



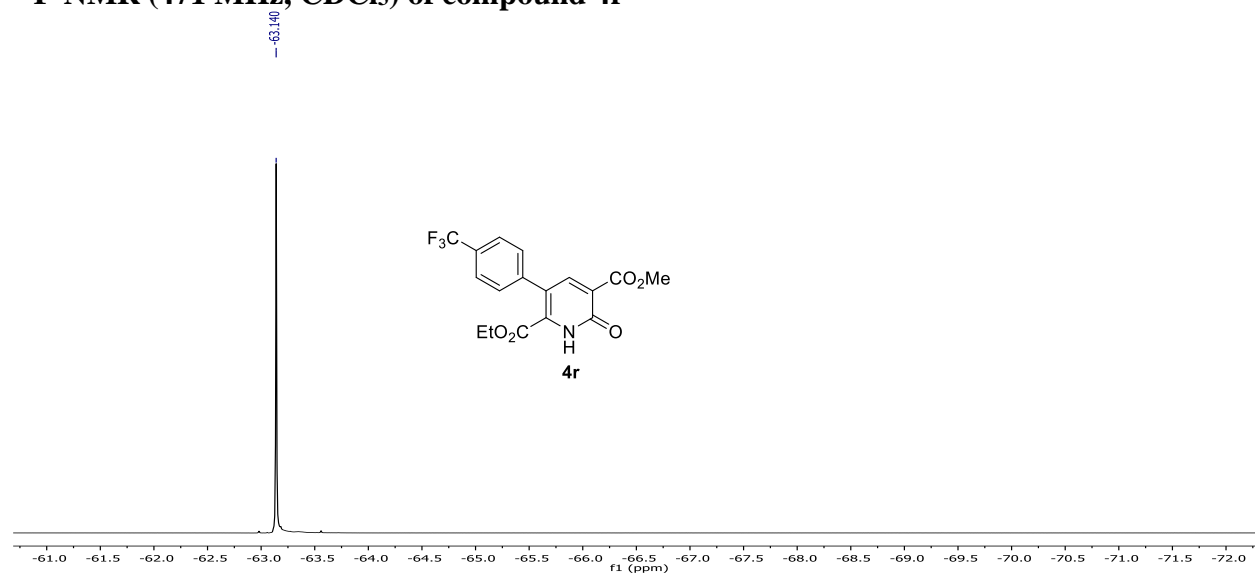
^1H -NMR (500 MHz, CDCl_3) of compound 4r



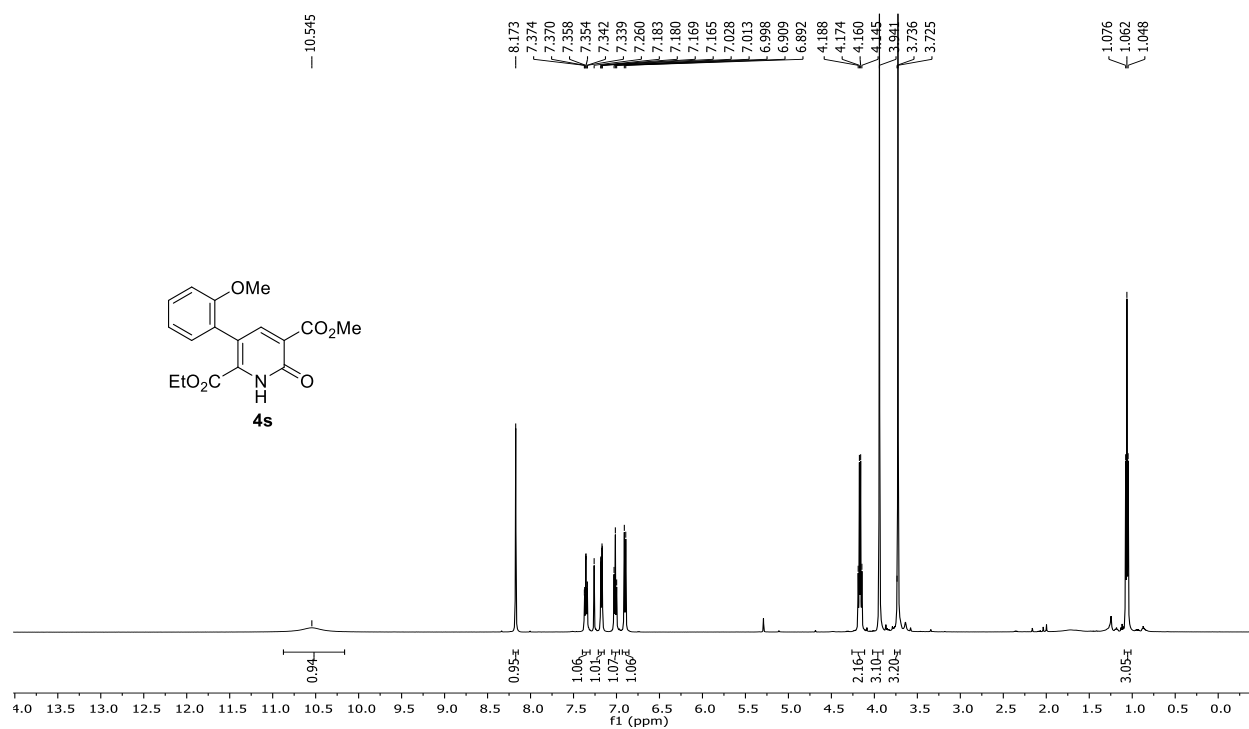
^{13}C -NMR (126 MHz, CDCl_3) of compound 4r



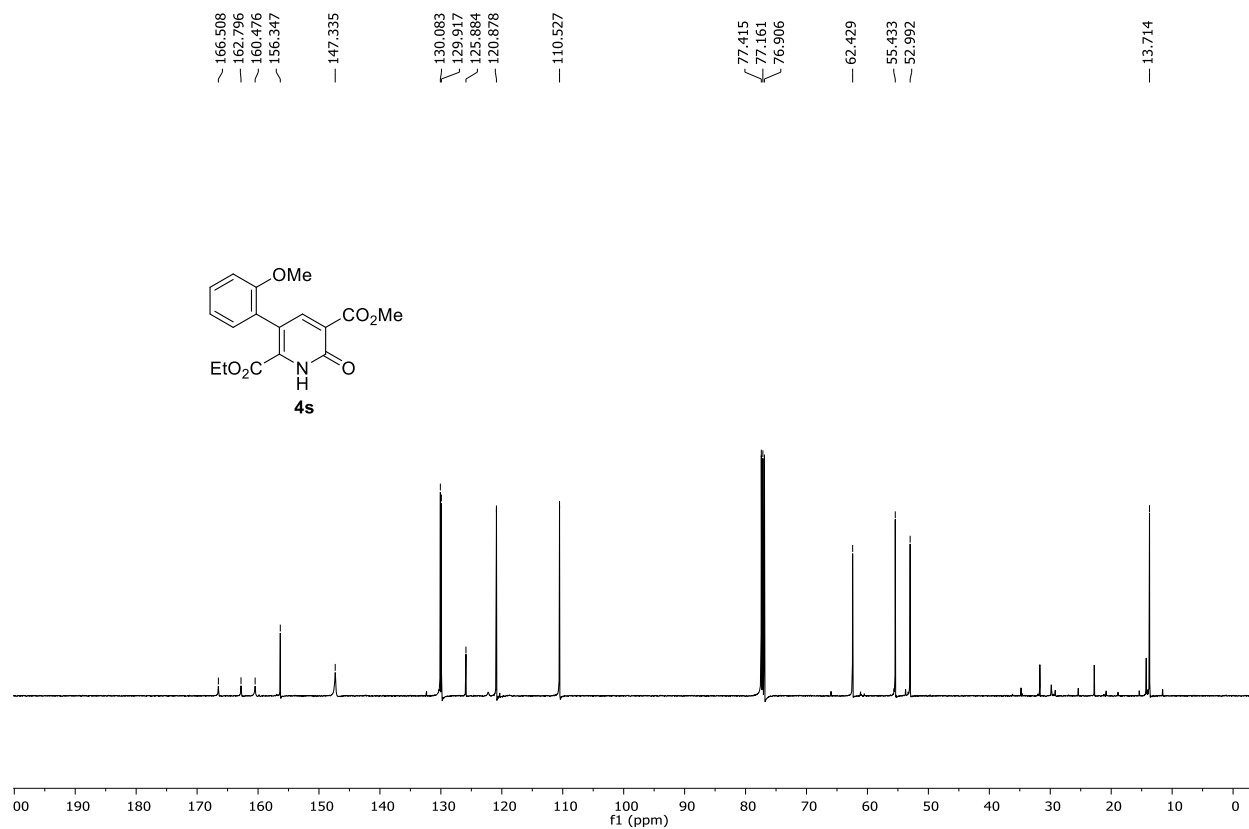
^{19}F -NMR (471 MHz, CDCl_3) of compound 4r



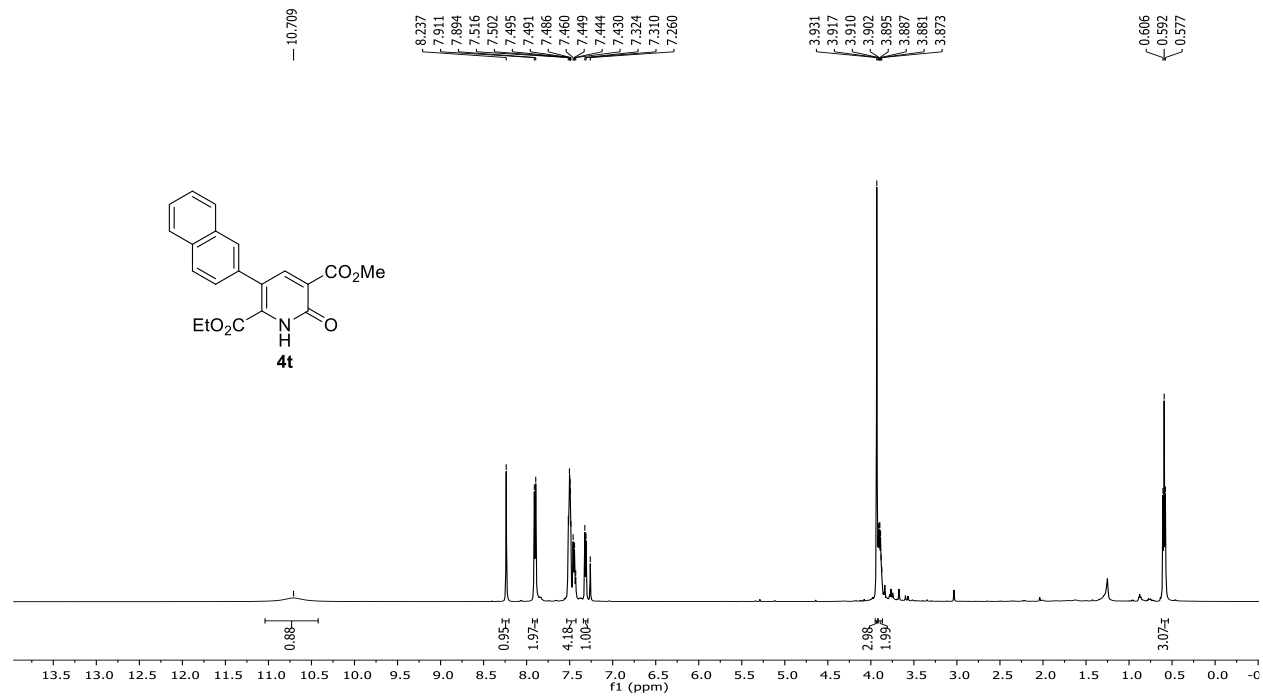
^1H -NMR (500 MHz, CDCl_3) of compound **4s**



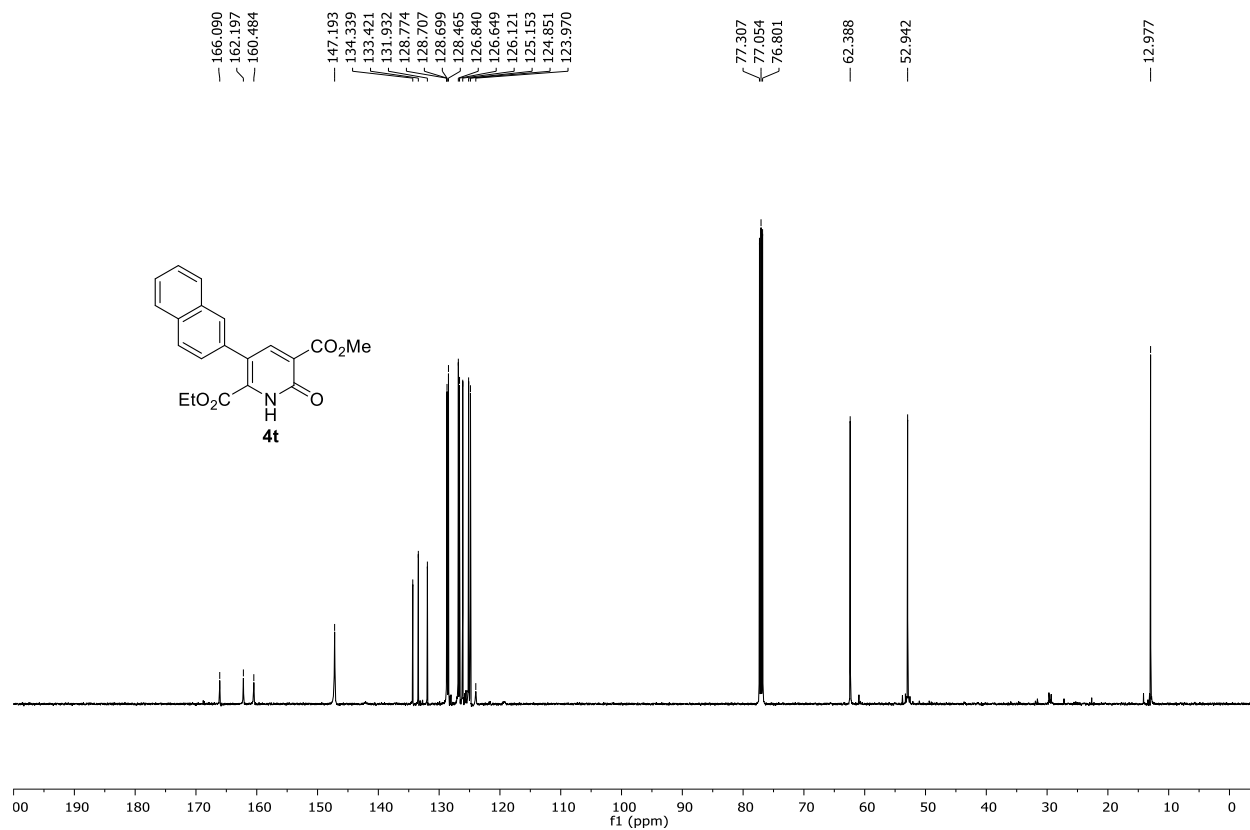
^{13}C -NMR (126 MHz, CDCl_3) of compound **4s**



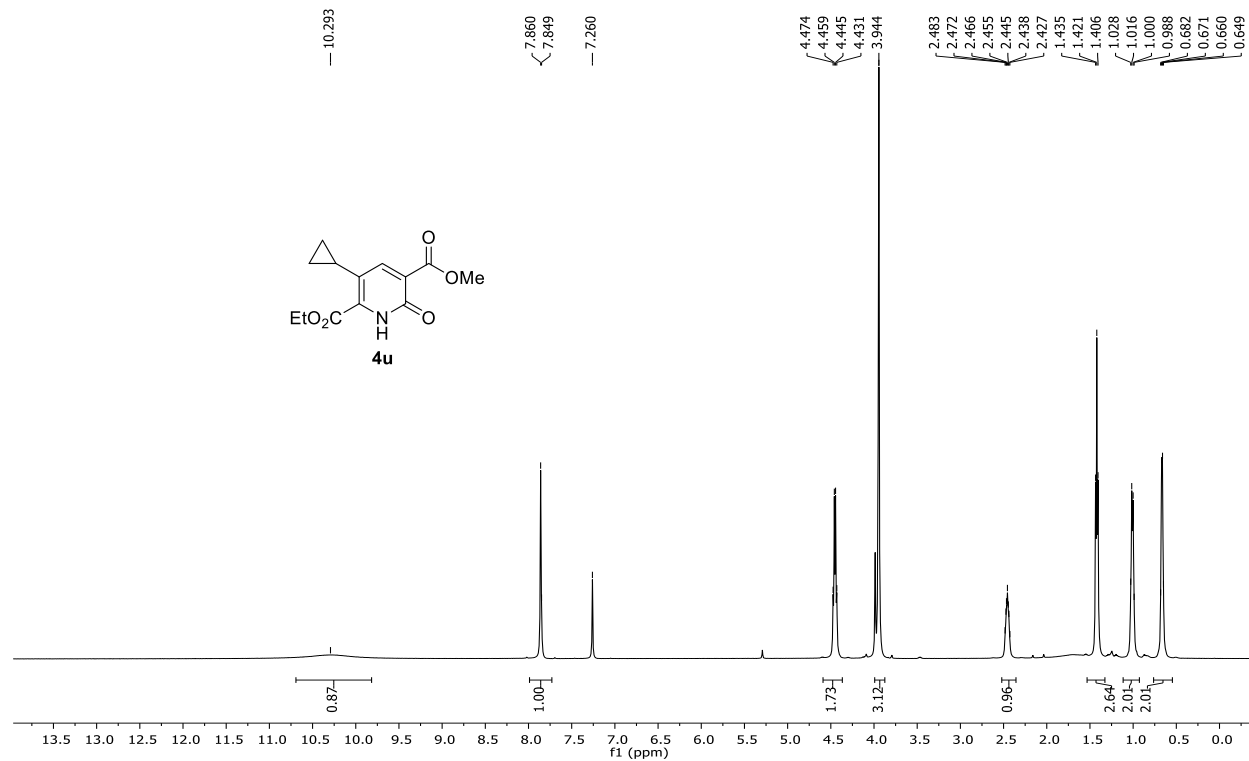
¹H-NMR (500 MHz, CDCl₃) of compound 4t



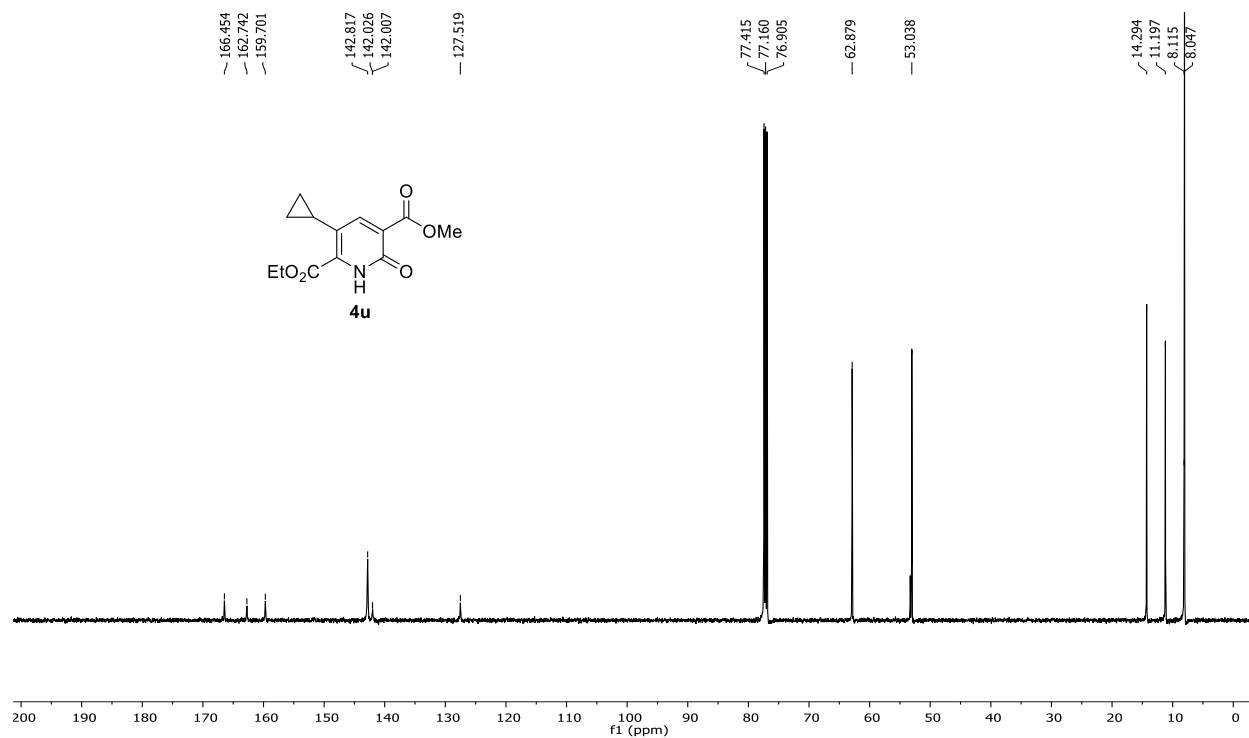
¹³C-NMR (126 MHz, CDCl₃) of compound 4t



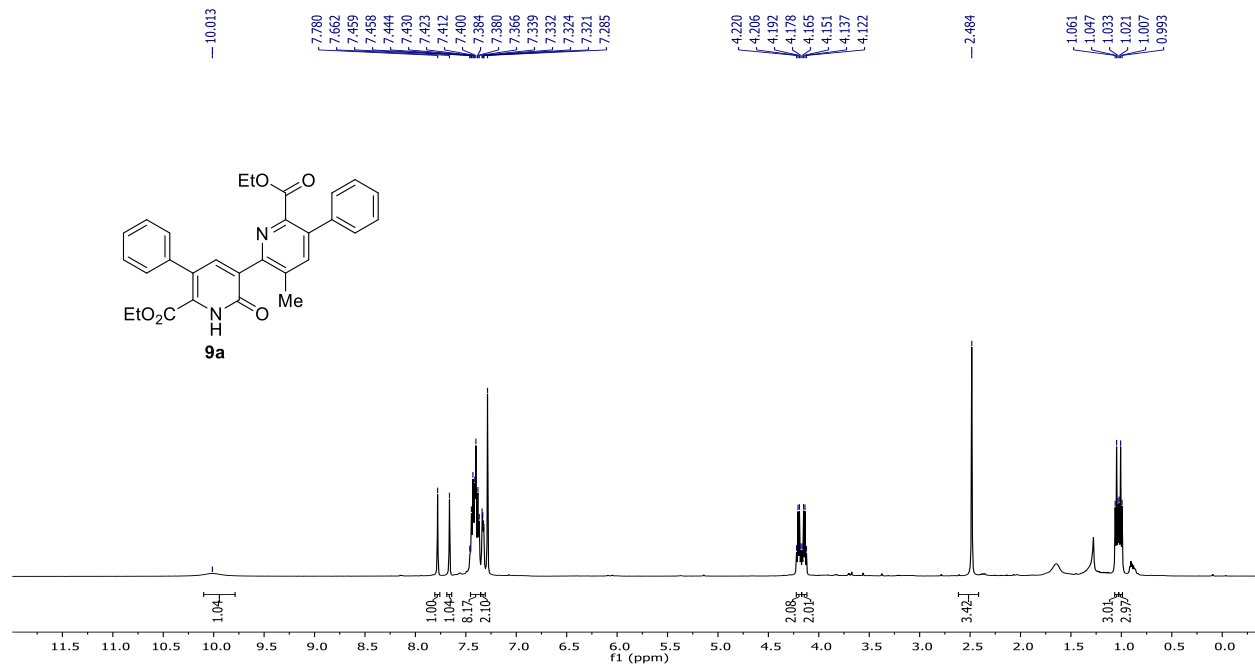
^1H -NMR (500 MHz, CDCl_3) of compound **4u**



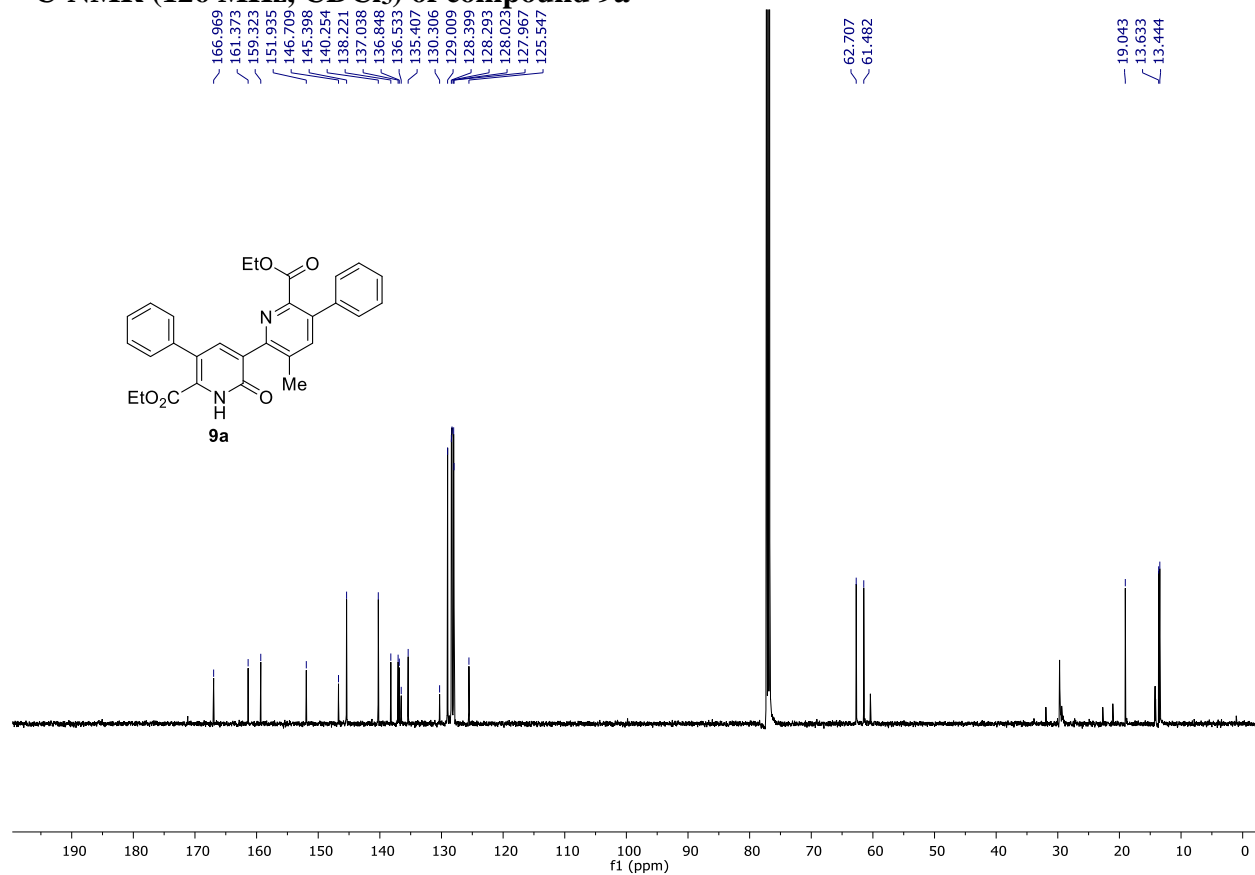
^{13}C -NMR (126 MHz, CDCl_3) of compound **4u**



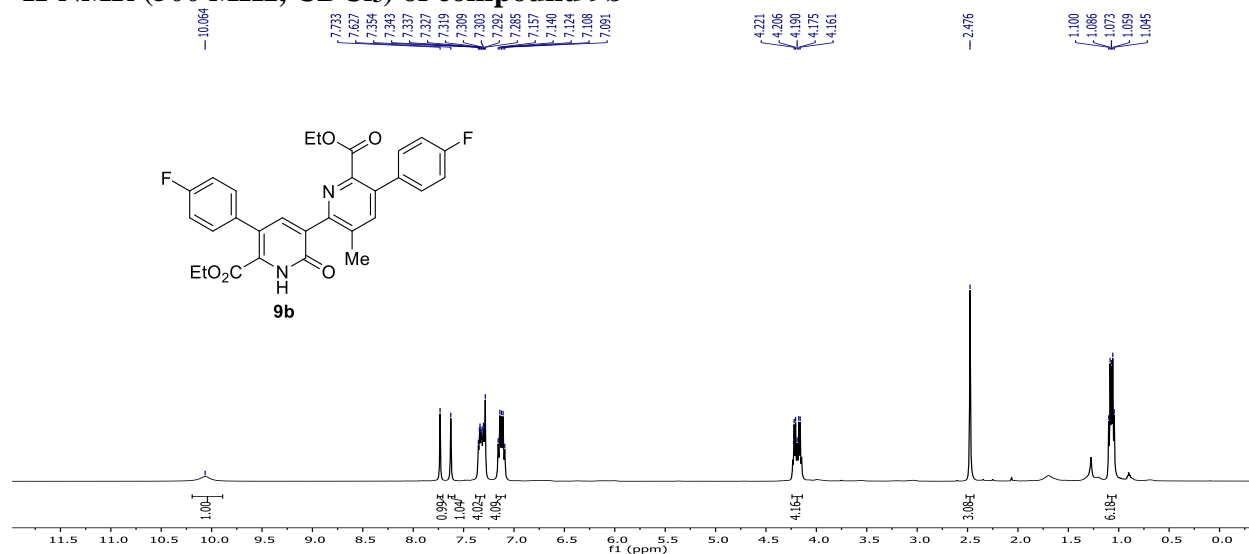
^1H -NMR (500 MHz, CDCl_3) of compound 9a



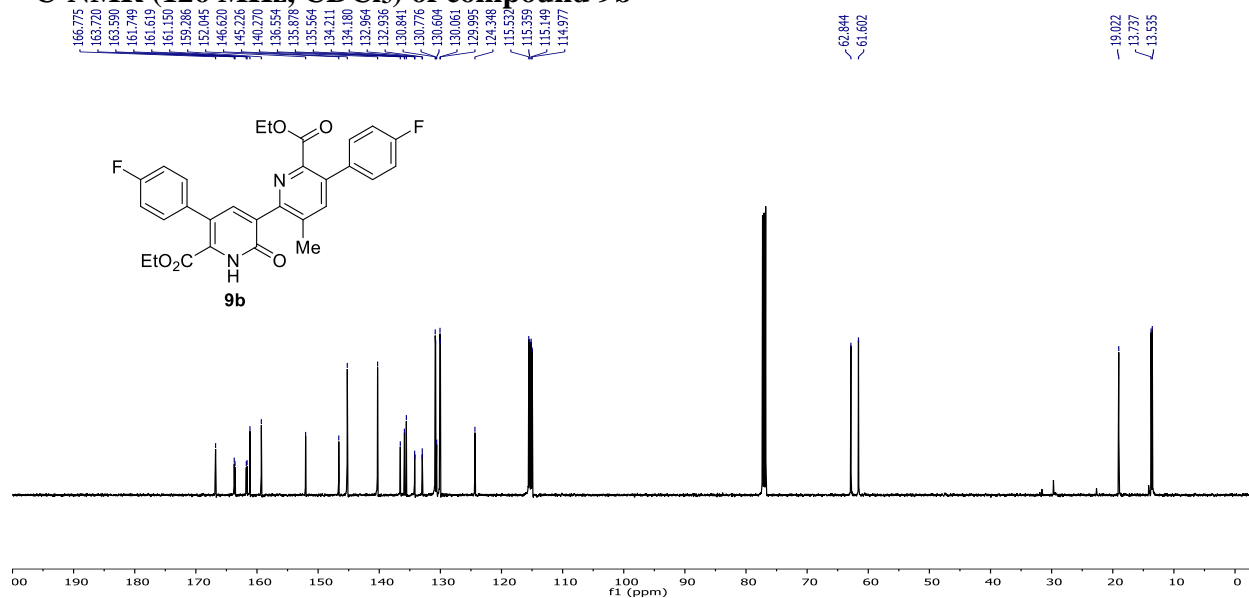
^{13}C -NMR (126 MHz, CDCl_3) of compound 9a



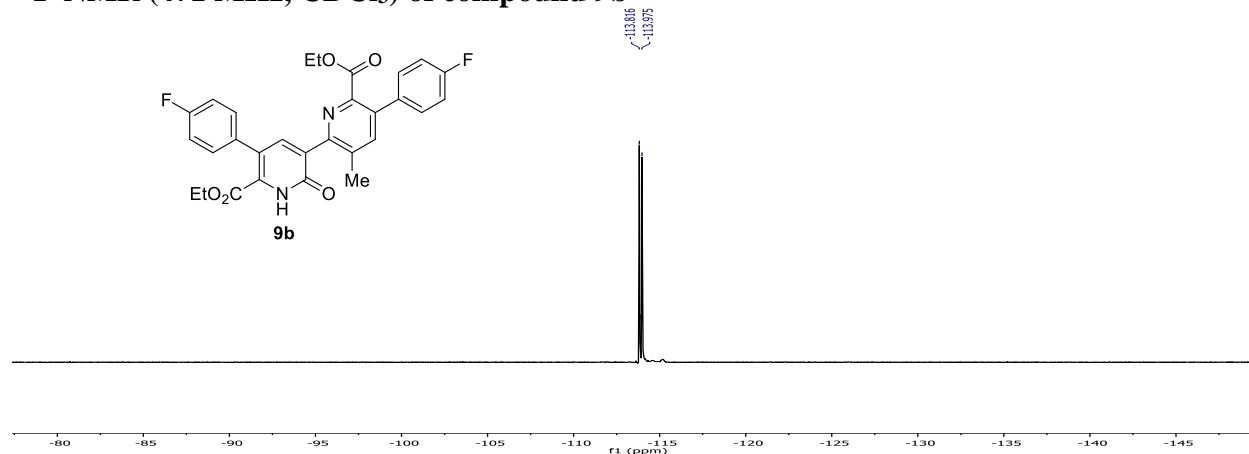
^1H -NMR (500 MHz, CDCl_3) of compound 9b



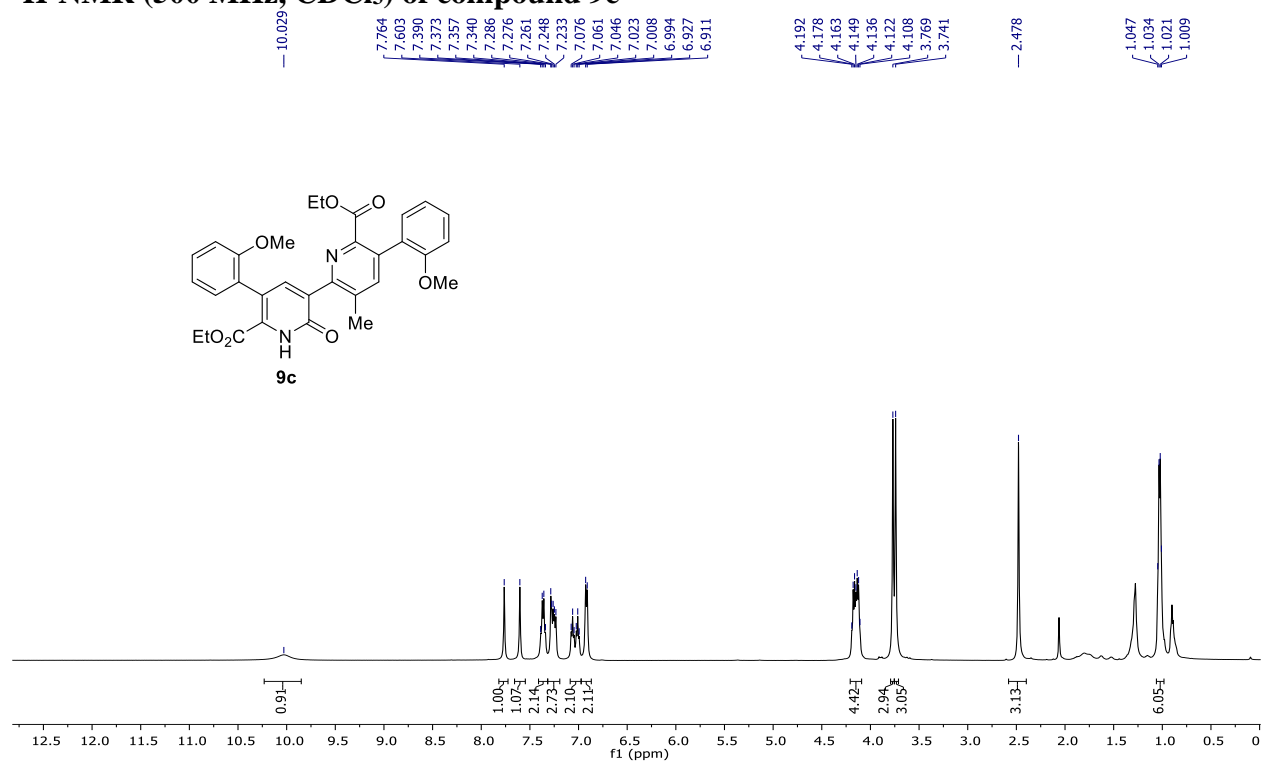
^{13}C -NMR (126 MHz, CDCl_3) of compound 9b



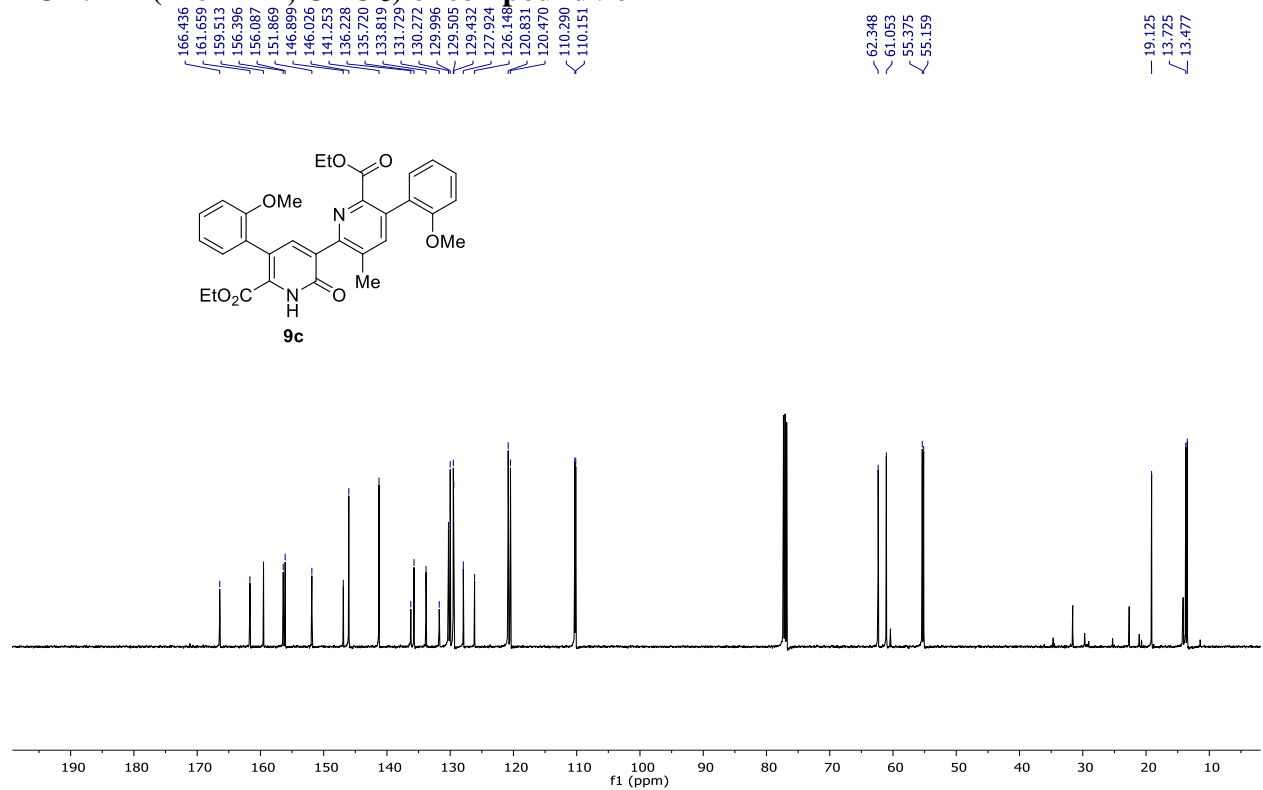
^{19}F -NMR (471 MHz, CDCl_3) of compound 9b



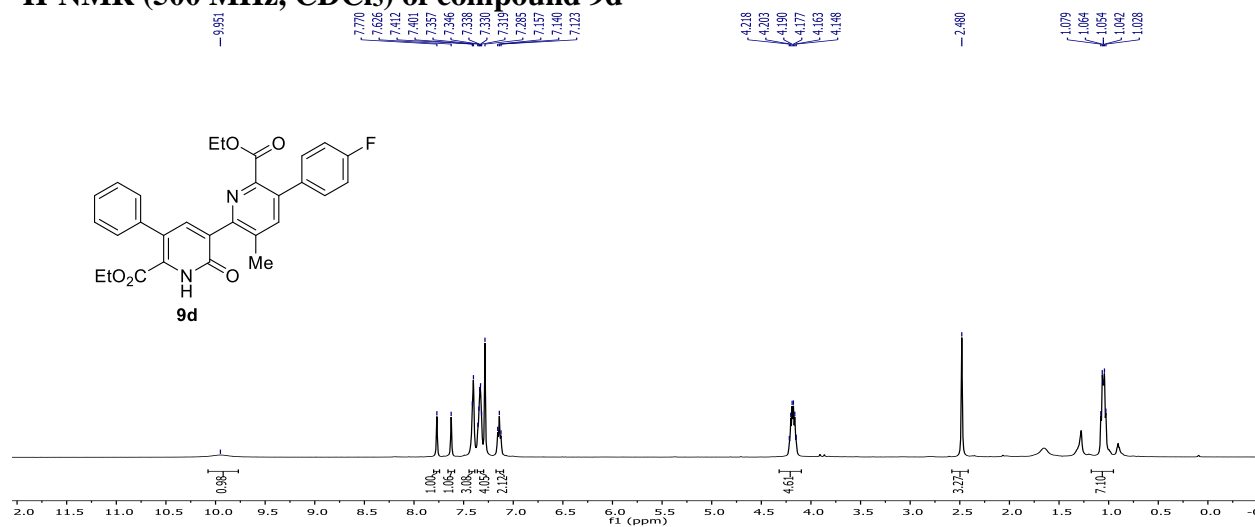
^1H -NMR (500 MHz, CDCl_3) of compound 9c



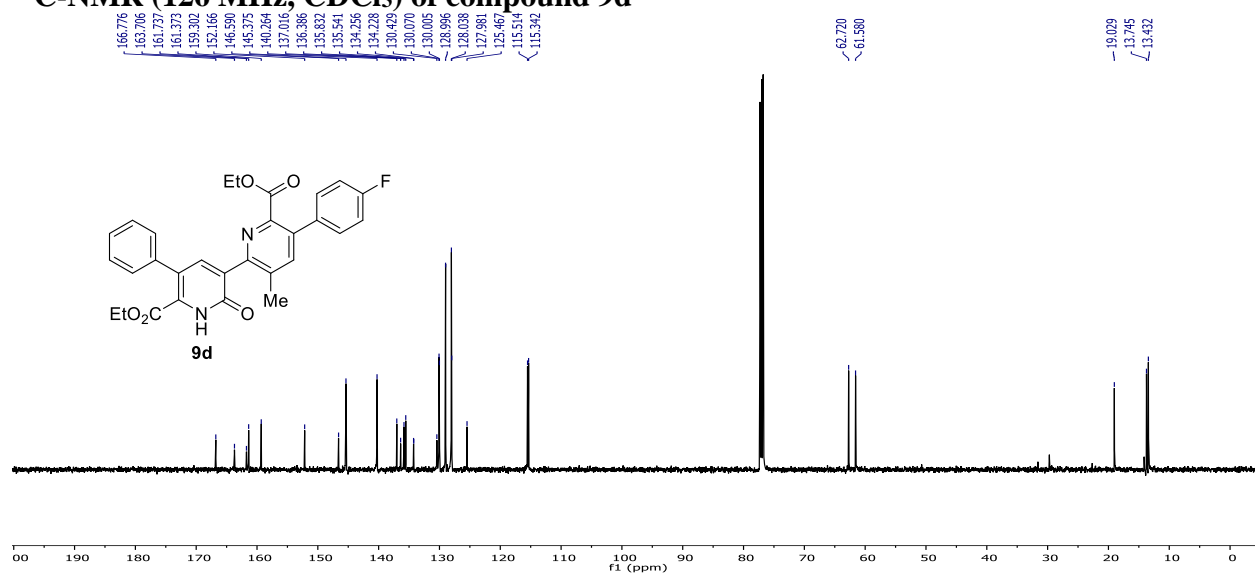
^{13}C -NMR (126 MHz, CDCl_3) of compound 9c



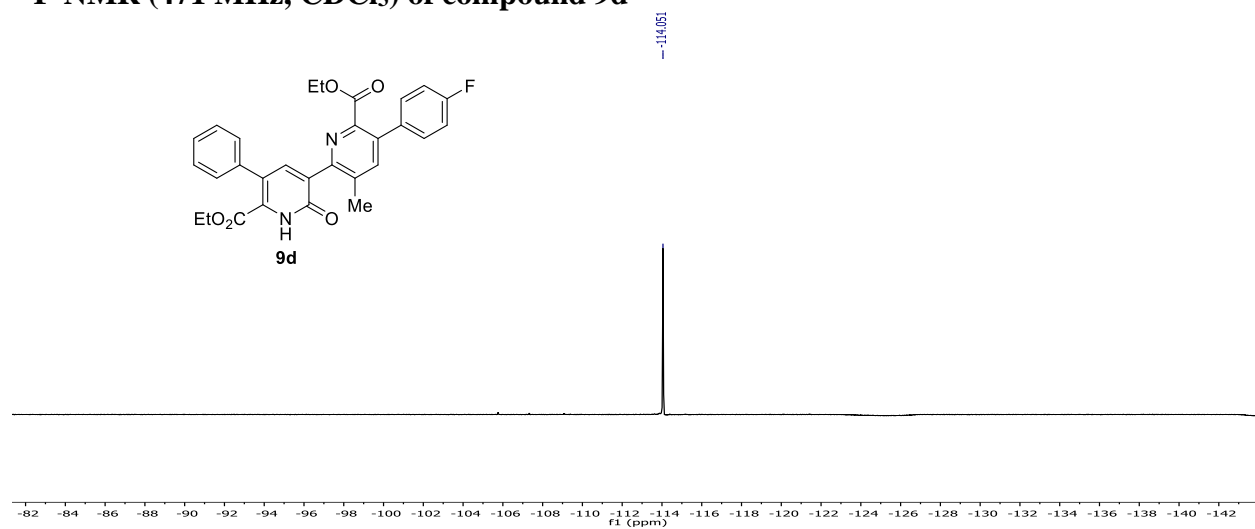
^1H -NMR (500 MHz, CDCl_3) of compound 9d



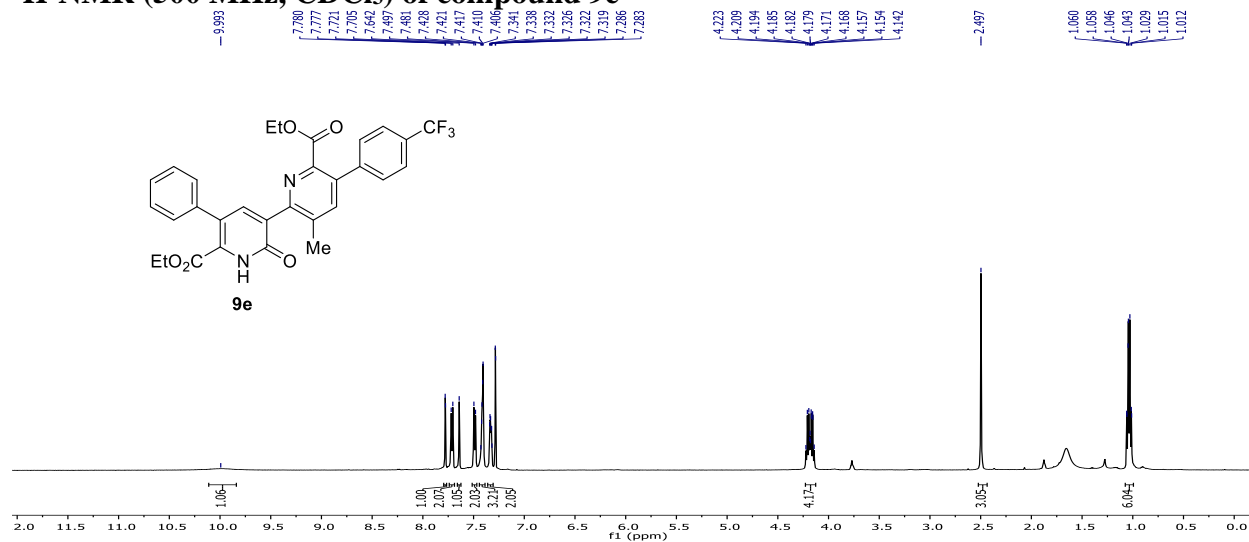
^{13}C -NMR (126 MHz, CDCl_3) of compound 9d



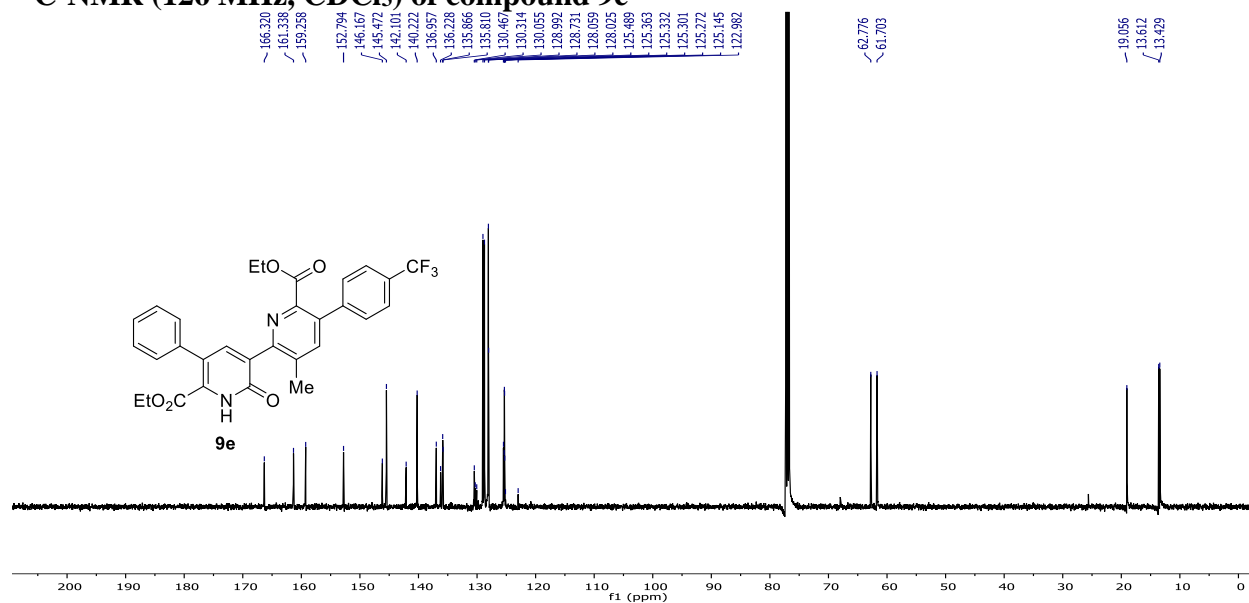
^{19}F -NMR (471 MHz, CDCl_3) of compound 9d



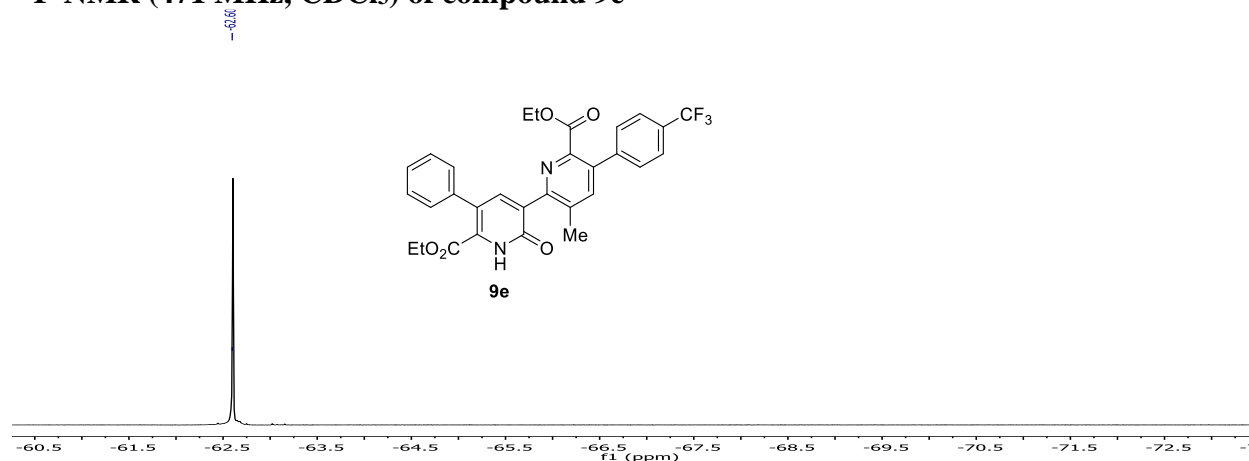
^1H -NMR (500 MHz, CDCl_3) of compound 9e



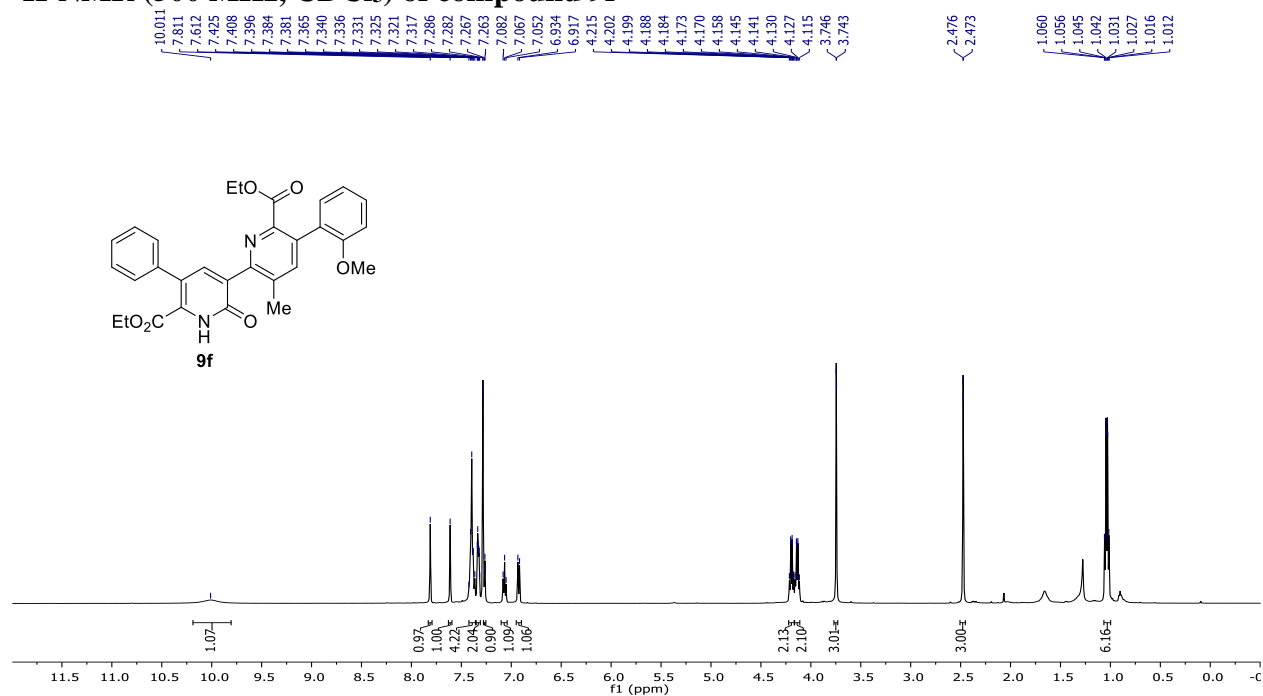
^{13}C -NMR (126 MHz, CDCl_3) of compound 9e



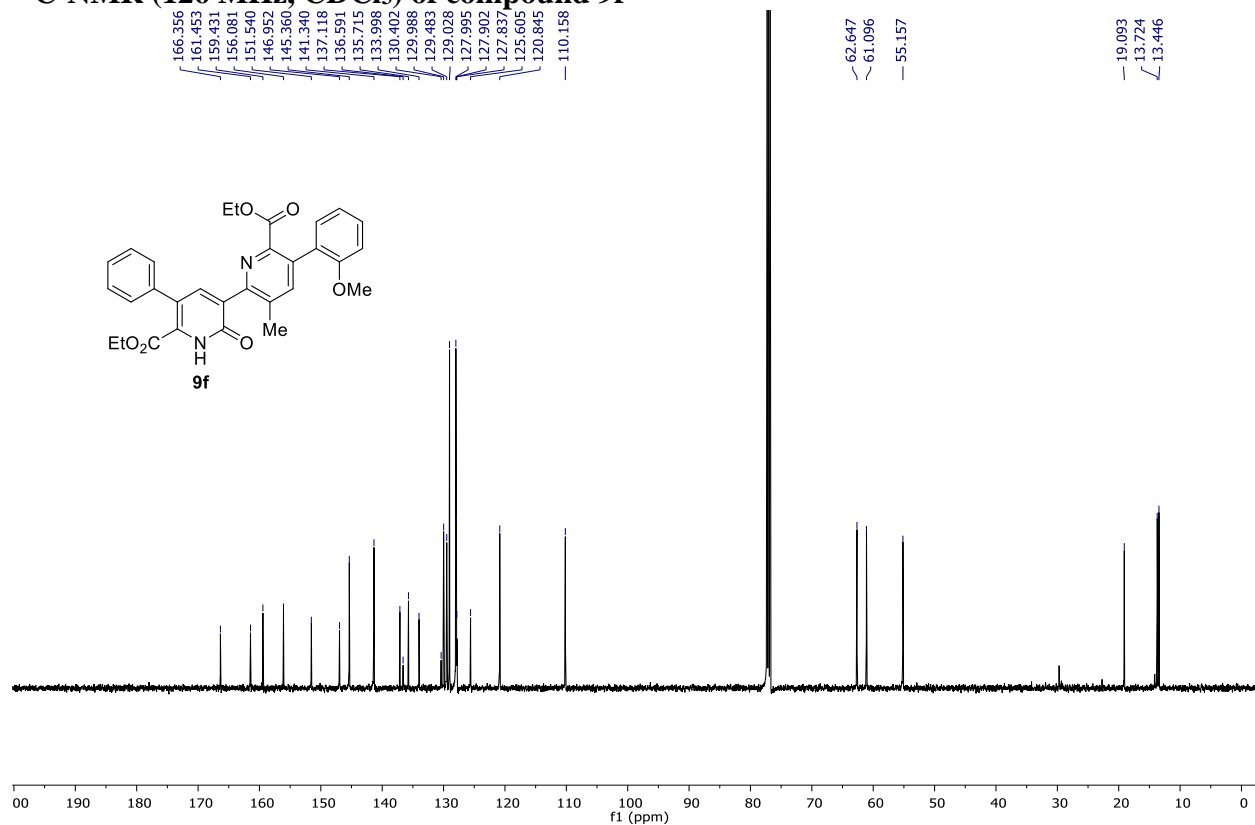
^{19}F -NMR (471 MHz, CDCl_3) of compound 9e



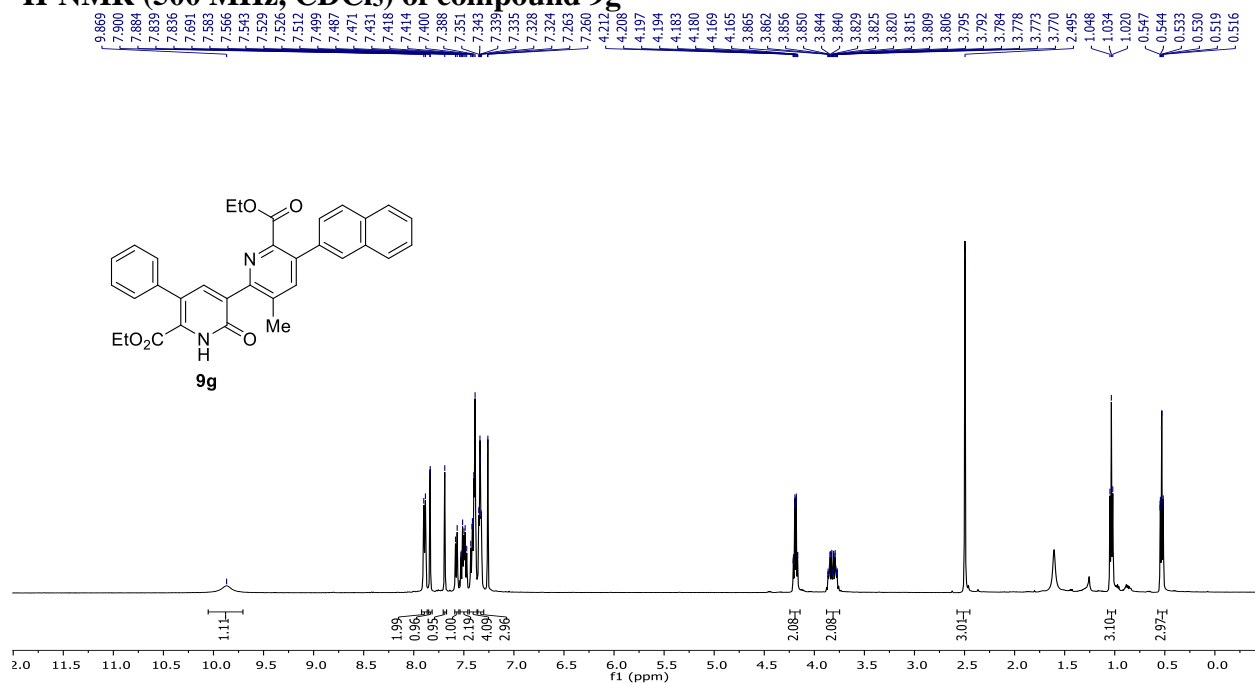
¹H-NMR (500 MHz, CDCl₃) of compound 9f



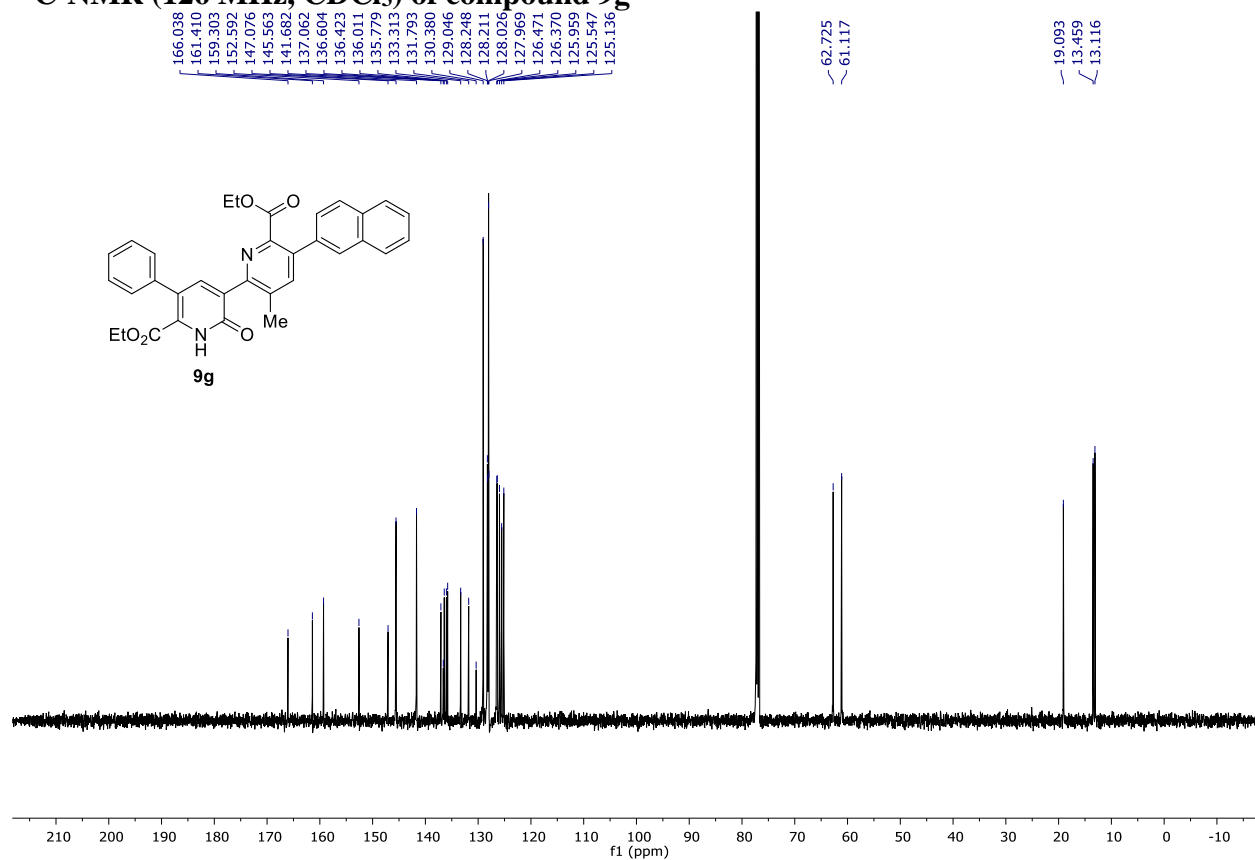
¹³C-NMR (126 MHz, CDCl₃) of compound 9f



$^1\text{H-NMR}$ (500 MHz, CDCl_3) of compound **9g**



$^{13}\text{C-NMR}$ (126 MHz, CDCl_3) of compound **9g**



¹H NMR (CDCl₃) spectrum of compound **9h**. The chemical structure of **9h** is shown above the spectrum. The spectrum displays peaks in the aromatic region (7.283–9.858 ppm) and aliphatic region (0.996–3.286 ppm). Integration values are provided below the baseline.

Chemical Shift (ppm)	Integration
9.858	1.07
7.283	1.00
7.380	0.98
7.332	8.10
7.316	2.10
4.154	2.15
4.151	2.09
2.836	2.09
1.064	3.32
1.050	3.08
1.036	3.09
1.024	
1.010	
0.996	

¹³C-NMR (126 MHz, CDCl₃) of compound 9h

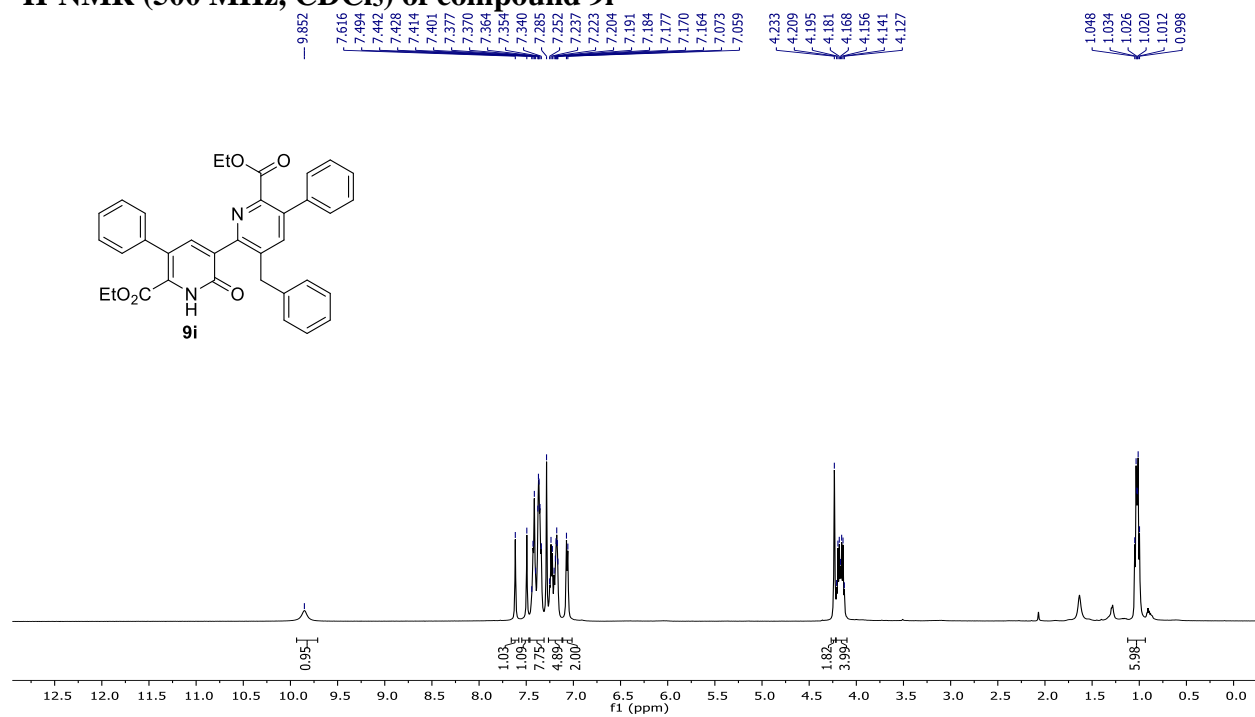
CCOC(=O)c1c(C(=O)Nc2cc(C(=O)OCC)cc2-c3ccccc3)cc(C(=O)OCC)c4ccccc14

Chemical structure of compound 9h is shown above the spectrum. The spectrum displays peaks corresponding to the carbon atoms in the molecule, with the following chemical shifts (ppm) labeled above the peaks:

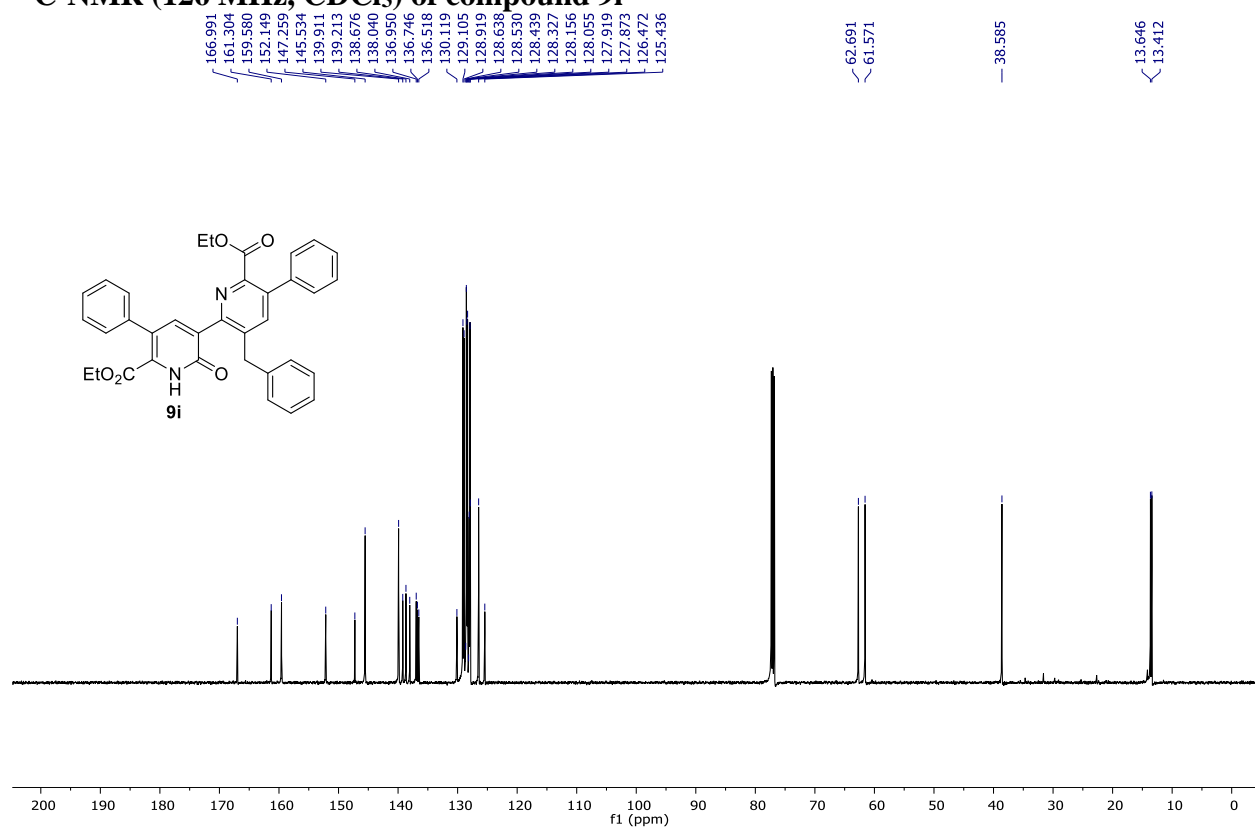
- 166.985, 161.344, 159.597, 151.559, 146.714, 145.291, 140.893, 138.417, 138.278, 137.060, 137.023, 136.754, 136.727, 130.126, 128.999, 128.412, 128.327, 128.023, 127.974, 125.539
- 62.705, 61.484
- 25.136
- 14.133, 13.632, 13.445

The x-axis is labeled f1 (ppm) and ranges from 200 to 0.

^1H -NMR (500 MHz, CDCl_3) of compound 9i



^{13}C -NMR (126 MHz, CDCl_3) of compound 9i



10. References

1. (a) A. Padwa, Y. S. Kulkarni and Z. J. Zhang, *J. Org. Chem.* 1990, **55**, 4144–4153; (b) H. M. L. Davis, P. W. Hougland and W. R. Cantrell Jr., *Synth Commun.* 1992, **22**, 971–978; (c) H. M. L. Davies, B. H. Hu, E. Saikali and P. R. Bruzinski, *J. Org. Chem.* 1994, **59**, 4535–4541; (d) M. P. Doyle, M. Yan and W. H. Hu, *J. Am. Chem. Soc.* 2003, **125**, 4692–4693; (e) V. V. Pagar, A. M. Jadhav and R. S. Liu, *J. Am. Chem. Soc.* 2011, **133**, 20728–2073; (f) H. F. Zheng, K. Y. Dong, D. Whertritt, H. Arman and M. P. Doyle, *Angew. Chem. Int. Ed.* **2020**, **59**, 13613–13617.
2. L. De Angelis, H. Zheng, M.T. Perz, H. Arman and M.P. Doyle, *Org. Lett.* 2021, **23**, 6542–6546.
3. CrysAlisPro 1.171.40.63a (Rigaku Oxford Diffraction, 2019).
4. SCALE3 ABSPACK - An Oxford Diffraction program (1.0.4,gui:1.0.3) (C) 2005 Oxford Diffraction Ltd.
5. O. V. Dolomanov, L. J. Bourhis, R. J. Gildea, J. A. K. Howard and H. Puschmann, *J. Appl. Cryst.* 2009, **42**, 339.
6. G. M. Sheldrick, *Acta Cryst.* 2015, **A71**, 3.
7. G. M. Sheldrick, *Acta Cryst.* 2008, **A64**, 112.
8. Gaussian 16, Revision A.03, M. J. Frisch, G. W. Trucks, H. B. Schlegel, G. E. Scuseria, M. A. Robb, J. R. Cheeseman, G. Scalmani, V. Barone, G. A. Petersson, H. Nakatsuji, X. Li, M. Caricato, A. V. Marenich, J. Bloino, B. G. Janesko, R. Gomperts, B. Mennucci, H. P. Hratchian, J. V. Ortiz, A. F. Izmaylov, J. L. Sonnenberg, D. Williams-Young, F. Ding, F. Lipparini, F. Egidi, J. Goings, B. Peng, A. Petrone, T. Henderson, D. Ranasinghe, V. G. Zakrzewski, J. Gao, N. Rega, G. Zheng, W. Liang, M. Hada, M. Ehara, K. Toyota, R. Fukuda, J. Hasegawa, M. Ishida, T. Nakajima, Y. Honda, O. Kitao, H. Nakai, T. Vreven, K. Throssell, J. A. Montgomery, Jr., J. E. Peralta, F. Ogliaro, M. J. Bearpark, J. J. Heyd, E. N. Brothers, K. N. Kudin, V. N. Staroverov, T. A. Keith, R. Kobayashi, J. Normand, K. Raghavachari, A. P. Rendell, J. C. Burant, S. S. Iyengar, J. Tomasi, M. Cossi, J. M. Millam, M. Klene, C. Adamo, R. Cammi, J. W. Ochterski, R. L. Martin, K. Morokuma, O. Farkas, J. B. Foresman and D. J. Fox, Gaussian, Inc., Wallingford CT, 2016.
9. S. Grimme, C. Bannwarth and P. Shushkov, *J Chem. Theory Comput.* 2017, **13**, 1989–2009.
10. CYLview, 1.0b, C. Y. Legault, Université de Sherbrooke, 2009 (<http://www.cylview.org>).
11. W. Humphrey, A. Dalke and K. Schulten, *J. Mol. Graph.* 1996, **14**, 33–38.
12. Chemcraft - graphical software for visualization of quantum chemistry computations. <https://www.chemcraftprog.com>
13. G. Luchini, J. V. Alegre-Requena, Y. Guan, I. Funes-Ardoiz and R. S. Paton, GoodVibes: GoodVibes v3.0.1 (2019).
14. <https://www.basissetexchange.org/>

15. S. Jin, G. C. Haug, R. Trevino, V. D. Nguyen, H. D. Arman and O. V. Larionov, *Chem. Sci.* 2021, **12**, 13914–13921.
16. F. M. Bickelhaupt and K. N. Houk, *Angew. Chem. Int. Ed.* 2017, **56**, 10070–10086.
- [17] I. Fernández, F. M. Bickelhaupt, F. P. Cossío, *Chem. Eur. J.* **2014**, *20*, 10791–10801.